Net Ecosystem Exchange of CO_2 and Energy Fluxes of Turf in the Denver Urban Ecosystem and an adjacent Tallgrass Prairie

Dissertation

zur Erlangung des

Doktorgrades der Naturwissenschaften (Dr. rer. nat.)

der

Naturwissenschaftlichen Fakultät III

Agrar- und Ernährungswissenschaften,

Geowissenschaften und Informatik

der Martin-Luther-Universität Halle-Wittenberg

vorgelegt von

Herrn Thomas S. Thienelt

Geb. am 20.04. 1979 in Halle/Saale

Gutachter:

1. Prof. Dr. Dr. h.c. Manfred Frühauf (Martin-Luther-Universität Halle-Wittenberg)
2. Prof. Dr. Georg Guggenberger (Leibniz Universität Hannover)
3. Dr. Dean E. Anderson (United States Geological Survey, Denver)

Tag der Verteidigung: 7. Mai 2015

Summary

The global trend of growing urban populations is characterized by a rapid expansion of urban areas into adjacent agricultural and natural ecosystems. The Denver metropolitan area in Colorado, USA, is a prime example of this pattern. The distinct change in land cover resulting from urban growth and the intensity of anthropogenic activities within urban areas are expected to significantly contribute to the rising concentrations of greenhouse gases in the atmosphere and to affect biogeochemical cycles. Vegetation within the urban environment, such as urban lawns, may modify the exchange of energy and greenhouse gases (e.g. CO_2) of urban ecosystems. This potential influence appears most relevant considering the spatial extent of turfgrass in the US.

The objectives of this study were to quantify carbon and energy exchange of turfgrass and natural grassland, identify important drivers that influence the diurnal and seasonal course of these exchanges, and assess the impact of land use change, i.e. urban sprawl, in a semi-arid climate on carbon, energy, and water budgets.

This study presents results of data obtained at two locations in the Denver metropolitan area between January 2011 and December 2012. Towers outfitted with equipment to conduct eddy covariance (EC) flux measurements were set up over a large lawn within Fort Logan National Cemetery south of downtown Denver, and over a xeric tallgrass prairie at Rocky Flats National Wildlife Refuge, approximately 30 km north-west of Fort Logan. Measurements taken at the sites included fluxes of CO_2, water vapor, and sensible heat as well as ancillary (meteorological) parameters. During the majority of the investigation period (Mar-Nov 2011, Mar-Dec 2012), data was collected simultaneously at the two sites. This allowed for a direct comparison of impacts of regional climate fluctuations, vegetation, and management practices on net ecosystem exchange (*NEE*) of CO_2 and energy fluxes.

The investigation found close links between seasonal vegetation development, energy fluxes, and *NEE* of CO_2. Irrigation of turfgrass led to discernible changes in energy and carbon fluxes and greatly contributed to the diurnal and seasonal differences observed between sites. Energy partitioning at the turfgrass site was characterized by

a distinct shift from sensible to latent heat energy in comparison to the tallgrass prairie, which directly affected site evapotranspiration (*ET*). Between April and October, cumulative *ET* of turfgrass exceeded that of the tallgrass prairie by a factor of more than 2.

NEE at the turfgrass site was characterized by a longer growing season showing higher daily net uptake of CO_2. Hence, cumulative *NEE* of turfgrass clearly exceeded that of the tallgrass prairie. Between April and October, the comparative sums were -173 g C m^{-2} vs. -81 g C m^{-2} in 2011 and -73 g C m^{-2} vs. -21 g C m^{-2} in 2012. Annual *NEE* at the urban site considerably changed when including carbon emissions due to turfgrass management. Temperature and water stress during the drought year 2012 greatly influenced the direction and magnitude of CO_2 flux at both research sites.

The results suggest that urban lawns in Denver can function as important carbon sinks within urban ecosystems but require considerable amounts of irrigation, particularly in semi-arid climates. The establishment of urban vegetation may therefore, under optimized resource allocation, conditionally contribute to the mitigation of carbon emissions in urban areas to a certain degree - directly by CO_2 sequestration and indirectly through effects of evaporative cooling on microclimate and energy use. These potential implications demand further study to improve our understanding of the interactions of urban ecosystems and the atmosphere and their impact on biogeochemical cycles.

Acknowledgements

To Professor Dr. M. Frühauf I would like to express my gratitude for his valuable support and for supervising this thesis.

I am very thankful to Dr. D. E. Anderson for his guidance and patience as mentor as I greatly benefitted from his extensive knowledge and experience in this field of research.

I would like to thank the management at Fort Logan National Cemetery and the US Fish and Wildlife Service at Rocky Flats for providing access to the measurement sites. Special thanks to “Hutch” at Fort Logan for sharing his knowledge on turfgrass management.

Appreciation is extended to the German Academic Exchange Service (DAAD) for its financial support, to the Max-Planck-Institute for Biogeochemistry for providing an online gap-filling tool which greatly helped in data processing, and to the customer support of Licor, Inc. and Campbell Scientific, Inc.

Special thanks to the USGS staff in Denver for a great work experience abroad (Cathy, Ed, Dave, Jim, Katherine, Rick) and to all the volunteers (Caitlin, Duncan, George, Joel, Julie, Kate, Laura, Mark, Taylor) for their contributions in the laboratory and in the field.

I am very grateful to my family for their advice and continuous encouragement.

Finally, I would like to thank Stefanie for her faith and support.

Table of Contents

List of Figures

List of Tables

List of Abbreviations

ABL	atmospheric boundary layer
AGC	automatic gain control
ALPM	actual liters per minute
a.s.l.	above sea level
CFC	chlorofluorocarbon
CO_2	Carbon Dioxide
CH_4	Methane
CP	Closed-Path Analyzer
cum.	cumulative
DLI	daily light integral
DOY	day of year
EBR	energy balance ratio
EC	eddy covariance (method)
ET	evapotranspiration
FL	Fort Logan
G	soil heat flux at the soil surface
H	sensible heat flux
ID	inner diameter
IRGA	Infrared Gas Analyzer
Irrig.	irrigation
LAI	Leaf Area Index
LE	latent heat flux
mod.	modeled
MST	Mountain Standard Time
N_2O	Nitrous Oxide
NEE	net ecosystem exchange (of CO_2)
NPP	net primary productivity
O_3	ozone
obs.	observed
OLS	ordinary least squares
OP	Open-Path Analyzer
PAR	photosynthetically-active radiation
RF	Rocky Flats
rH	relative humidity
p	atmospheric pressure
P	precipitation
Precip.	precipitation
R_n	net radiation
R_s	shortwave radiation
SD	standard deviation
SDT	South Denver Tower
SOC	soil organic carbon
T	air temperature
T_{soil}	soil temperature
TDR	time domain reflectrometry
u*	friction velocity
VWC	volumetric water content
WUE	water-use efficiency

1. Introduction

Over geologic time, Earth's climate has experienced large variations, but there is a growing consensus among the scientific community that the changes that have taken place since the start of the instrumental temperature record (ca. 1850) are at least in part due to anthropogenic activities *(Karl and Trenberth, 2003; Houghton, 2009; Shakun et al., 2012; IPCC, 2013).* The degree to which the current observations are influenced by humankind or natural climate variability is still subject of intense discussions *(Klein Tank et al., 2005; Moberg et al., 2005; Allen et al., 2006; Mann et al., 2008; Zorita et al.,2008; Swanson et al., 2009; Hunt, 2011*).

Nevertheless, increasing emissions of greenhouse gases (CO_2, CH_4, N_2O, CFCs, O_3) and aerosols since the industrial revolution have led to modifications of the atmosphere's chemical composition and Earth's radiation balance *(Houghton, 2009; Bond et al., 2013; IPCC, 2013).* From the 1950s to the 2000s, average land temperature has increased by 0.9 °C (*Rohde et al., 2012*). This trend of rising temperatures is considered evidence for a changing global climate with potentially serious consequences for man and biosphere *(King, 2004; Stern, 2007; Warren et al., 2011).* Thus, the investigation of climate, i.e. the complex interplay of atmosphere, hydrosphere, geosphere, biosphere, and solar irradiance, is critical to further our understanding of Earth's climate and the effects of human activities *(Kutzbach, 2006; Houghton, 2009, Mu et al. 2011).*

The role of terrestrial ecosystems in the exchange of energy, water, and greenhouse gases with the atmosphere and the resulting positive or negative feedbacks on regional and global climate and biogeochemical cycles has put them in the focus of science *(Heimann and Reichstein, 2008; Arneth et al., 2010).* However, despite the large volume of data on greenhouse gas emissions and accumulation rates in the atmosphere, the investigation of the terrestrial sink with regard to size, spatial distribution, and influencing parameters, remains a challenge fraught with some uncertainty. This uncertainty and the problems arising from it influence the accuracy of global and regional models and, in turn, model-derived scenarios about future climate development *(IPCC, 2013).* Thus, the accurate assessment of carbon budgets for individual ecosystems/land use systems is of great significance in understanding causes and consequences of (regional) climate change.

In this regard, the cycle of carbon dioxide (CO_2) and the processes that influence it are critical elements. The main anthropogenic sources of CO_2 include fossil fuel combustion, cement production, and land use change. These sources of CO_2 are reasonably well quantified, while the more diverse natural sinks of CO_2, which include the oceans and terrestrial vegetation, need more study (*Pacala et al. 2001; Clement, 2004; Canadell et al. 2007; Scholes et al. 2009; Warren et al., 2011).*

The connection between CO_2 and photosynthesis makes vegetation an important regulating parameter in the climate system with regard to CO_2-exchange but also the partitioning of available energy into latent and sensible heat. However, the uptake of CO_2 by vegetation varies spatially and temporally and is strongly influenced by management *(Oncley et al., 1997; Katul et al., 2001; Leuning et al., 2004; Ma et al., 2007; Baldocchi, 2008; Davis et al., 2010; Eugster et al., 2010).*

In this context, grassland ecosystems are of great significance since they cover approximately 25 % of the terrestrial surface and, as a category, include about 70 % of all agricultural lands. Moreover, grasslands contain about 20 % of the global carbon stocks and have the potential for further carbon sequestration *(Conant, 2010).*

The dominant natural grassland in North America is the prairie, part of the Great Plains which extends from Mexico into Canada and can be divided into three types running north-south, i.e. shortgrass, mixed grass, and tallgrass prairie. A precipitation gradient from drier West to wetter East is primarily responsible for this natural distribution. However, the grasslands of the Great Plains have been dramatically impacted by land use change, mostly due to agricultural production (*Suttie et al., 2005).*

Another phenomenon influencing grasslands is the conversion to urban land uses. A prime example of this is the Denver metropolitan area in Colorado, USA, which has been, and continues to be, one of the fastest growing urban areas in the United States (US) (*US Census, 2013*).

Although urban ecosystems cover only a relatively small fraction of the land surface in the US (1.4-5.2 %), they are expanding rapidly (*Alig et al., 2004; Elvidge et al., 2004+2007; Imhoff et al., 2004; Potere and Schneider, 2007; Nowak and Greenfield, 2012; United Nations, 2012)*. Combined with this growth, the intensity of multiple anthropogenic activities within urban areas contributes significantly to the rising concentrations of greenhouse gases in the atmosphere (*Pataki et al., 2006)*. But the heterogeneity of urban ecosystems and intensity of processes make it difficult to investigate basic ecosystem functions and to quantify greenhouse gas budgets, which could result in the exclusion of important sinks and sources necessary for accurate biogeochemical modeling (*Kaye et al., 2004; Pickett et al., 2011; Bulkeley, 2013*).

An important component of the urban environment in the US are urban lawns, which are ubiquitous and typically occur as monocultures in residential, recreational, and industrial settings. Estimates found urban lawns to be the largest irrigated crop of the United States (*Milesi et al., 2005*), often being subjected to management practices like fertilization and irrigation which may alter, for example, carbon cycling (*Kaye et al., 2004*).

As the transformation of (semi-)natural grassland ecosystems into urban use around Denver continues, potentially significantly changing regional carbon and water cycles, the need for a better understanding of the effects and impacts of these changes becomes apparent.

The general increase in ecosystem-level research on carbon cycle dynamics has coincided with a general improvement in micrometeorological measurement techniques since the 1980s. Technological advances have made it possible to directly measure the turbulent exchanges of greenhouse gases and energy by employing the eddy covariance (EC) method *(Baldocchi, 2003).* This method has several advantages including the implementation in the field without disturbing the ecosystem, the ability to measure continuously over long time frames, and the possibility to average small-scale variability of fluxes over a footprint that can range in size from hectares to square kilometers. Thus, the EC method enables scientists to identify and quantify fluxes of matter and energy and their environmental controls (*Clement, 2004; Baldocchi, 2008*). The EC method has been successfully applied in various ecosystem settings, including grasslands, to measure CO_2 and water vapor fluxes and assess the surface energy balance *(Verma et al., 1992; Ham and Knapp, 1998; Bremer and Ham, 1999+2010; Meyers, 2001; Owensby et al., 2006; Haslwanter et al., 2009; Peters and McFadden, 2012*). Moreover, during the last decade, networks for researchers using the EC method have been initiated (e.g. FLUXNET) in an effort to develop comprehensive datasets, coordinate the analysis of results gained from regional studies, and help develop bio-physical models which combine micrometeorological methods, remote sensing data as well as soil and (plant) physiological measurements (*Baldocchi et al. 2001*; *Clement, 2004; Friend et al., 2007).* As of October 2011, more than 500 sites had registered with FLUXNET, most of the stations located in North America and Europe. Among them are very few urban sites, only about 5 stations appear to be located within a truly (built-up) urban environment, while grassland sites are more numerous (78) (*FLUXNET, 2013*).

This study presents results of data obtained at two locations in the Denver area between January 2011 and December 2012. Instrument towers equipped to conduct EC measurements were set up at Fort Logan, a military cemetery south of downtown Denver, providing a large tract of urban lawn, and at Rocky Flats National Wildlife Refuge, a tallgrass prairie located approximately 30 km north-west of the urban site. Measurements taken at the sites included fluxes of CO_2, water vapor, and sensible heat as well as various ancillary (meteorological) parameters. During the majority of the investigation period (Mar-Nov 2011, Mar-Dec 2012), data was collected simultaneously at the two sites to allow for a direct comparison regarding the impact of regional climate/weather patterns and management practices on net ecosystem exchange (*NEE*) of CO_2 and energy fluxes.

The aim of this study is to contribute to our understanding of the interactions between natural ecosystems/urban land use systems and the atmosphere and to assess the impact of land use change in a semi-arid climate on carbon and water budgets.

Specifically, the main goals of this study are:

- Quantification of fluxes of matter (CO_2) and energy (latent and sensible heat) between urban lawn/prairie and the atmosphere at various times scales (hourly to yearly)
- Analysis of flux data regarding influencing parameters (climate, vegetation, management practices) and temporal variability
- Characterization of the partitioning of available energy at the investigation sites
- Quantification of cumulative sums of *NEE* and evapotranspiration (*ET*) for the investigation periods
- Estimation of an annual carbon budget for the investigated urban site including *NEE* as well as carbon emissions caused by turf management.

2. Investigation Area and Measurement Locations

2.1. Investigation Area

General

The two measurement locations, Fort Logan (urban) and Rocky Flats (prairie), are situated within the Denver metropolitan area in north-central Colorado, USA (Fig. 2.1). Colorado ranks eighth in size among the 50 States, covering an area of 270 000 km^2. Although famous for its Rocky Mountain landscape, the High Plains make up 40 % of Colorado's territory (*Doesken et al., 2003)*. Denver, the state capital on the border of the Great Plains and the Rocky Mountains, is approximately located at 39.5° N, 104.6° E. Bisected by the South Platte River, the "Mile-High-City", with an average elevation of 1655 m a.s.l., spreads over an area of 401 km^2.

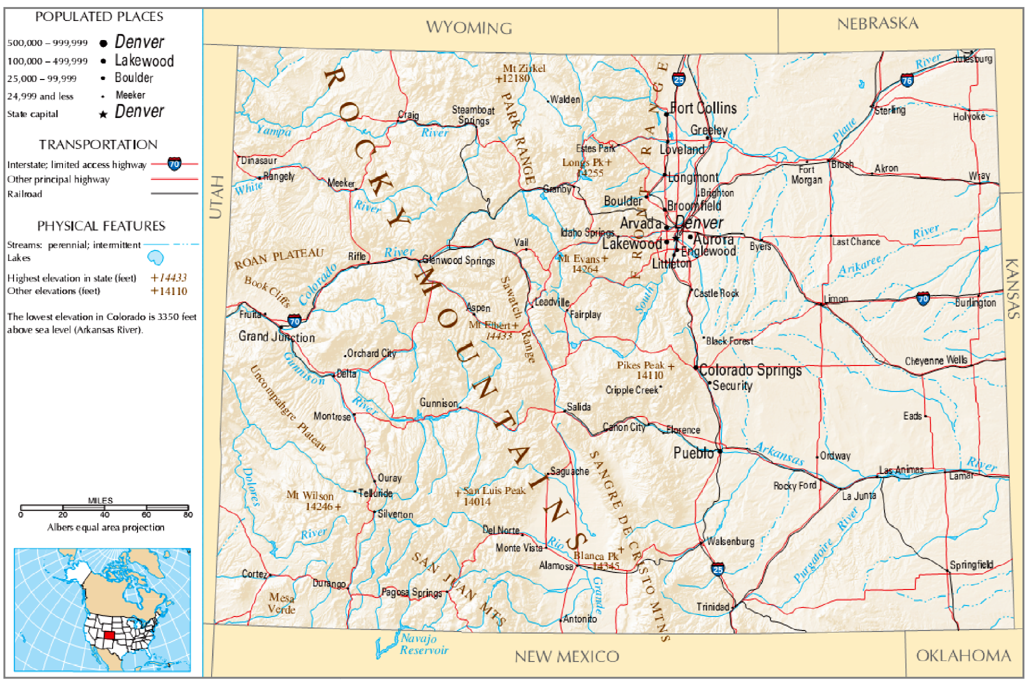

Fig. 2.1: Map of Colorado (*USGS, 2014;* modified)

The core of the Denver metropolitan area includes the city and county of Denver and 3 suburban counties (Adams, Arapahoe, Jefferson) containing a total population of about 2.2 million people (2011). Furthermore, the Denver metropolitan area is part of the larger Front Range urban corridor, which stretches from southern Wyoming (Cheyenne) into southern

Colorado (Pueblo) and has an estimated population of about 4.4 million people (*US Census, 2013)*.

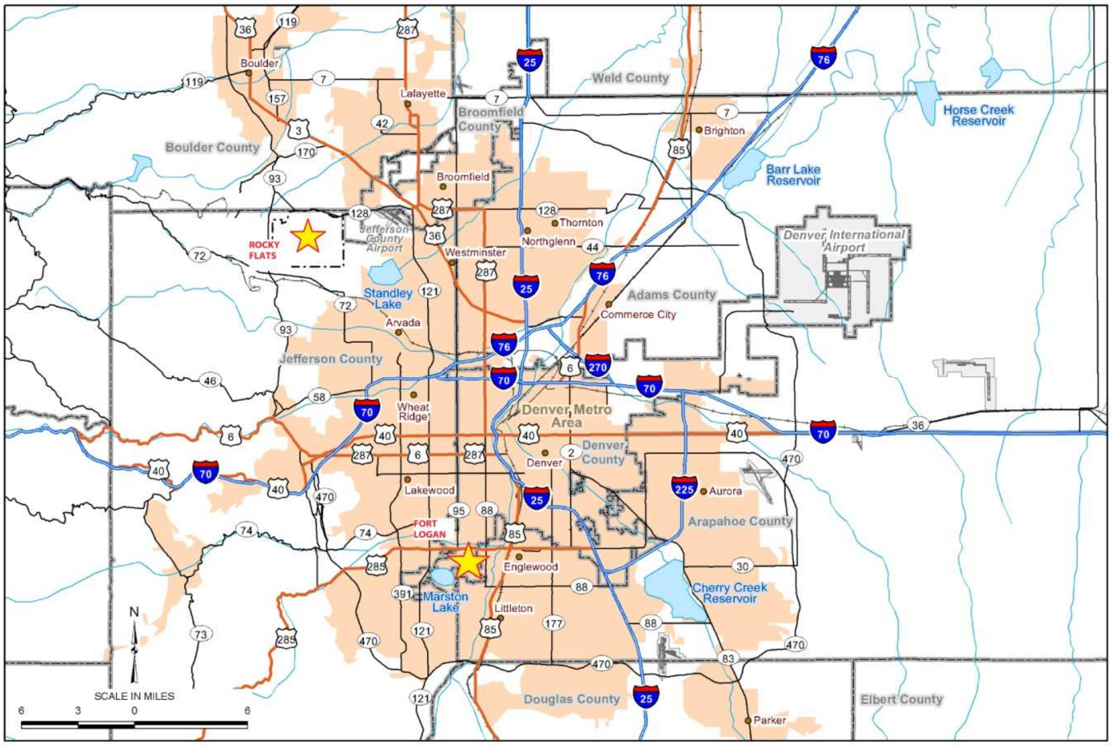

Fig. 2.2: Location of measurement sites ( ) within the Denver metropolitan area (*DOE, 2010*; modified)

Climate

Denver's combination of high elevation and mid-latitude, interior continental position results in a semi-arid climate with distinct seasons. The proximity of the Rocky Mountains (which rise up to 2500 m above the adjacent High Plains) is an important factor influencing the climate of the city and the surrounding area. Compared to the mountains to the west and the plains further east, Denver's climate near the foothills is characterized by smoother diurnal temperature changes, resulting in lower summer and higher winter temperatures. This generally milder climate and abundant sunshine (Denver experiences about 250 sunny days per year) is partly the reason why the majority of Colorado's population lives in this area today (*Doesken et al., 2003; NOAA, 2013b+c)*. The average temperature in Denver is 10.4°C with the warmest month being July (23.4°C) and the coldest December (-0.9°C) (*NOAA, 2013a*).

Due to Denver's distance from major sources of moisture (e.g. the Pacific Ocean or Gulf of Mexico) and the predominant westerly flows creating a rain shadow on the eastern slope of the mountains, precipitation is generally light and relative humidity low. Average precipitation in Denver is 381 mm (*Doesken et al., 2003; Paschke, 2011; NOAA, 2013a*).

Summer months can bring tropical moisture from the south-west to the city. This pattern, occasionally referred to as monsoon, leads to increased shower and thunderstorm frequency which provides a large portion of the year's precipitation. Winters in Denver are typically dry and mild. Again, rain shadow effects on the dominant westerly flow limit the amount of precipitation in form of rain or snow while storms moving in from the north usually carry little moisture but can potentially lead to blizzard conditions, i.e. drastic drops in temperature and heavy snow fall. Additionally, warm Chinook or Bora winds, the result of strong westerlies descending rapidly on the eastern slope, can bring sudden increases in temperature and rapid melting of snow cover. Average annual snowfall is 156 cm. The snow season usually lasts from mid-October to the end of April. March is the snowiest month with an average of almost 30 cm (*Doesken et al., 2003; NOAA, 2013b*).

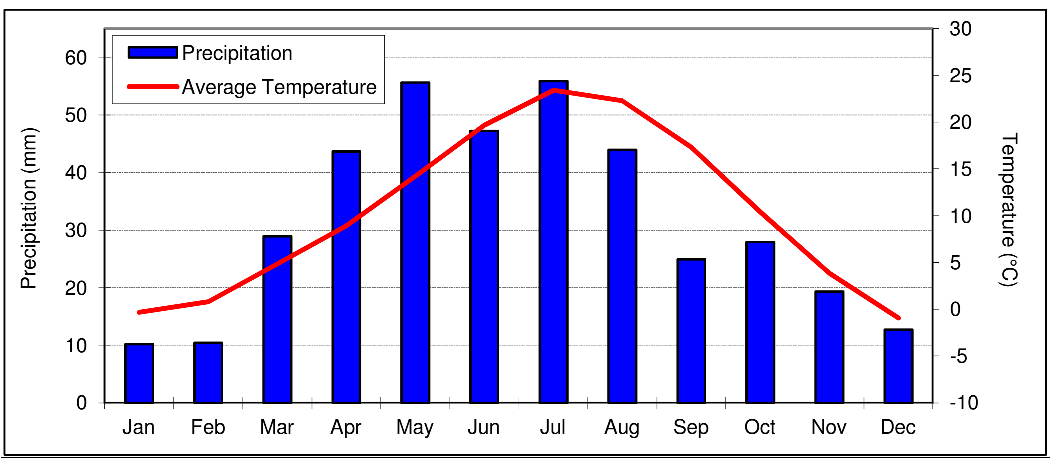

Fig. 2.3: Key climate variables for Denver (1981-2010) (*NOAA, 2013a*)

Geology

The urban measurement site, Fort Logan, is located on the Colorado Piedmont, a segment of stream-dissected terrain between the foothills of the Rocky Mountains and the true Great Plains to the east. The Denver Basin, the foreland basin of the Rocky Mountains, is filled with up to 3500 m of sedimentary rocks (mainly layers of limestone, shale and sandstone) and underlies the Colorado Piedmont. The top layer, the Denver Formation, is now being eroded by the South Platte River and its tributaries, which have sculptured the hilly Piedmont surface on which Denver sprawls (*Chronic, 1980; Paschke, 2011*).

The prairie investigation site Rocky Flats, part of the larger Rocky Flats National Wildlife Refuge, is located near the western margin of the Colorado Piedmont section, which coincides with the western limit of the Denver Basin. The investigation site is situated on the relatively flat Rocky Flats pediment, which gives way to several finger-like drainages that slope down to the rolling plains in the eastern portion of the site. Surficial deposits of this alluvial fan primarily include unconsolidated clastics (clayey and sandy gravels up to 30 m thick) of the Quaternary-age Rocky Flats Alluvium (*FWS, 2005; DOE, 2010*).

Soils

The natural soil distribution around the urban investigation site at Fort Logan is characterized by Mollisols and Aridisols (typical of arid and semi-arid climates) as well as Entisols (*USDA, 1971*; *Brady and Weil, 1999*). Due to the characteristics and dynamics of urban environments, specifically at the measurement site, these naturally occurring soils have been heavily influenced and/or modified by compaction, truncation, fertilization, and/or irrigation. Soil samples (n=29) collected from the top 5cm of soil at the site and analyzed for organic carbon yielded an average SOC content of 5.9(± 1.2) % (*Powell et al., 2011*).

Soils on the Rocky Flats pediments (the western half of Rocky Flats National Wildlife Refuge) have formed from alluvium and are dominated by Ustolls, a suborder of Mollisols. These soils consist of very cobbly to very stony, loamy surface soils and clayey subsoils and are usually deep and well drained (*FWS, 2005*). Average SOC content around the measurement site was more than double that of the urban site. Analysis revealed an average SOC content of 13.3(±2.4) % among the collected samples (n=18) (*Powell et al., 2011*).

Population

In 2010, Colorado's population totaled 5 million, the result of extraordinary population growth during the last 20 years. Between 1990 and 2010, the state's population increased by more than 50 % and the Denver metropolitan area gained around 900 000 people (Tab. 2.1). More than 50 % of Colorado's population (2.7 million) lives in Denver and the surrounding counties (Adams, Arapahoe, Boulder, Broomfield, Douglas, Jefferson).

	Metropolitan Denver								Colorado
Year	**Adams**	**Arapahoe**	**Boulder**	**Broomfield***	**Denver**	**Douglas**	**Jefferson**	**Metro Denver Total**	**State Total**
2020proj	544,258	672,230	332,107	71,211	686,613	373,308	571,753	3,252,481	5,999,989
2015proj	491,263	619,762	312,668	63,926	645,364	322,985	548,447	3,004,415	5,474,968
2010	441,603	572,003	294,567	55,889	600,158	285,465	534,543	2,784,228	5,029,196
2000	363,857	487,967	291,288		554,636	175,766	527,056	2,400,570	4,301,261
1990	265,038	391,511	225,339		467,610	60,391	438,430	1,848,319	3,294,394
1980	245,944	293,621	189,625		492,365	25,153	371,753	1,618,461	2,889,964
1970	185,789	162,142	131,889		514,678	8,407	233,031	1,235,936	2,207,259
1960	120,296	113,426	74,254		493,887	4,816	127,520	934,199	1,753,947
1950	40,234	52,125	48,296		415,786	3,507	55,687	615,635	1,325,089
1930	20,245	22,647	32,456		287,861	3,498	21,810	338,517	1,035,791
1920	14,430	13,768	31,881		256,491	3,517	14,400	334,487	939,191
1910	8,892	10,263	30,330		213,381	3,192	14,231	280,289	799,044

*Broomfield became its own city and county as of November 15, 2001. The former City of Broomfield was located in portions of Adams, Boulder and Jefferson counties. Thus, historical data comparisons for these counties are not possible.

Tab. 2.1: Population statistics of Denver, adjacent counties, and Colorado (*Metro Denver, 2013*)

The average annual population growth of 2.1 % (1990-2010) of metropolitan Denver was nearly double the national average of about 1.1 %. Accompanying this trend in population growth is a steady increase in the number of households. This is due to a decrease in housing density and the number of people per household which amplifies urban sprawl (e.g. in 1950 the average US household contained 3.4 people; this number has dropped to 2.6 in 2010; Colorado: 2.5) (*Metro Denver, 2013; US Census, 2013*).

2.2. Measurement Locations

2.2.1. Fort Logan

The urban investigation site is approximately located at 39.647° N, 105.039° W (elevation: 1640 m a.s.l.), within the boundaries of Fort Logan National Cemetery. Fort Logan, a former US Army installation, was founded in 1887 and is part of Denver County. After the Fort's closure in 1946, US Congress authorized the creation of Fort Logan National Cemetery in 1950. Originally about 64 hectares in size, the cemetery has expanded since then to about 86 hectares and currently contains nearly 100 000 graves (*VA, 2013*; *personal communication Charles Hutchison*).

Fig. 2.4: View of instrument setup at Fort Logan (May 2012)

The measurement site and its immediate surroundings are a relatively recent addition within the cemetery due to the continuing expansion and landscaping taking place at Fort Logan. Active lawn management for the studied area, i.e. the establishment of a mixed rye-bluegrass turf, began in 2005. Fertilization, irrigation, mowing, and seeding are managed by the Department of Veteran Affairs.

2.2.2. Rocky Flats

The adjacent prairie site is approximately located at 39.875° N, 105.218° W (elevation: 1860 m a.s.l.) and is part of the Rocky Flats National Wildlife Refuge, within viewing distance of downtown Denver, approximately 20 km to the southeast. The wildlife refuge comprises much of the former 2500-hectare Rocky Flats nuclear weapons plant which played an important role during the Cold War as a production facility of plutonium triggers. In 1992, the Rocky Flats plant was closed but the site's industrial legacy required cleanup actions prior to its transfer to the National Wildlife Refuge system in 2007. Since that time, the refuge has remained closed to the public due to a lack of funds for refuge management operations, but it continues to protect important natural resources. Many areas of Rocky Flats have remained relatively undisturbed for the past 30-50 years, allowing them to retain diverse natural habitat and associated wildlife.

Fig. 2.5: View of instrument setup at Rocky Flats (December 2012)

Some of the significant vegetation communities include the rare xeric tallgrass prairie which covers over 600 hectares on the Rocky Flats pediment tops, and is believed to be the largest example of this community remaining in Colorado and perhaps North America (*FWS, 2005+2013*).

2.2.3. Additional Stations

Two stations near the study investigation sites (one for each site) were chosen as data references in case of station failure at Fort Logan or Rocky Flats. This was done in order to create complete datasets with regard to meteorological parameters (i.e. air temperature, solar radiation, precipitation) and to aid gap-fill algorithms with regard to CO_2 and energy fluxes.

NREL Tower

Data from the NREL Tower (National Renewable Energy Laboratory) are derived from instruments mounted on or near an 82-m meteorological tower located at the NWTC site (National Wind Technology Center). The tower is located at 39.910° N, 105.235° W and an elevation of 1860 m a.s.l., about 4.2 km north of the Rocky Flats measurement site. Data from the NREL tower is publically accessible through the NREL website (*NREL, 2013*).

South Denver Tower

The South Denver Tower (SDT), a former radio antenna tower, is operated by the USGS (United States Geological Survey) and part of the Ameriflux network. It is located at 39.659° N, 105.013° W, and an elevation of 1620 m, approximately 2.7 km E-NE of the Fort Logan measurement site. The data is derived from instruments mounted on or near the 120-m tower and was made available to the investigator by the USGS.

3. Methods

3.1. Theoretical Background

3.1.1. Atmospheric Boundary Layer

The atmospheric boundary layer (ABL) forms the lower part of the troposphere. It is directly influenced by Earth's surface and reacts to these influences within a timescale of an hour or less. Among these influences are frictional drag, evapotranspiration, heat transfer, emission of pollutants, and terrain-induced flow modification. The vertical extent of the ABL varies spatially and temporally between a few hundred meters and a few kilometers. Within the ABL, turbulence is the dominant transport mechanism which can be imagined as irregular swirls of motion (eddies) of different sizes that together form a turbulence spectrum. Turbulence is created by convection or mechanical wind shear and as a transport mechanism is several orders more effective than molecular diffusion (*Stull, 1988*).

Above land surfaces, the ABL has a well-defined structure. Beginning at the surface is the *microlayer*, which extends only a few millimeters above the surface and within which molecular diffusion is the primary exchange mechanism. A shallow transition layer of approximately 1 cm extends between this and the *surface layer* above. From this layer and above, exchange processes are dominated by turbulence. The *surface layer* typically occupies the lower 10 % of the ABL. It is characterized by a logarithmic wind profile and fluxes that are nearly constant with height (constant flux layer) (*Stull, 1988; Foken, 2008a*).

As the surface layer deepens it extends into remnants of the *mixed or stable* layers developed during previous periods of the diurnal cycle. As a result, the vertical structure of the ABL also changes over the course of the day (Fig 3.1):

Given clear skies, convection induced by solar heating leads to the creation of a *mixed layer* above the surface shortly after sunrise (approximately ½ hour). This layer is characterized by intense vertical mixing and reaches its maximum depth by late afternoon, growing by "entraining" less turbulent air from above. The turbulent conditions within this layer create eddies that promote vertical mixing or transport of heat, moisture, and momentum. The *mixed layer* is capped by the entrainment zone, an inversion layer (*Stull, 1988*).

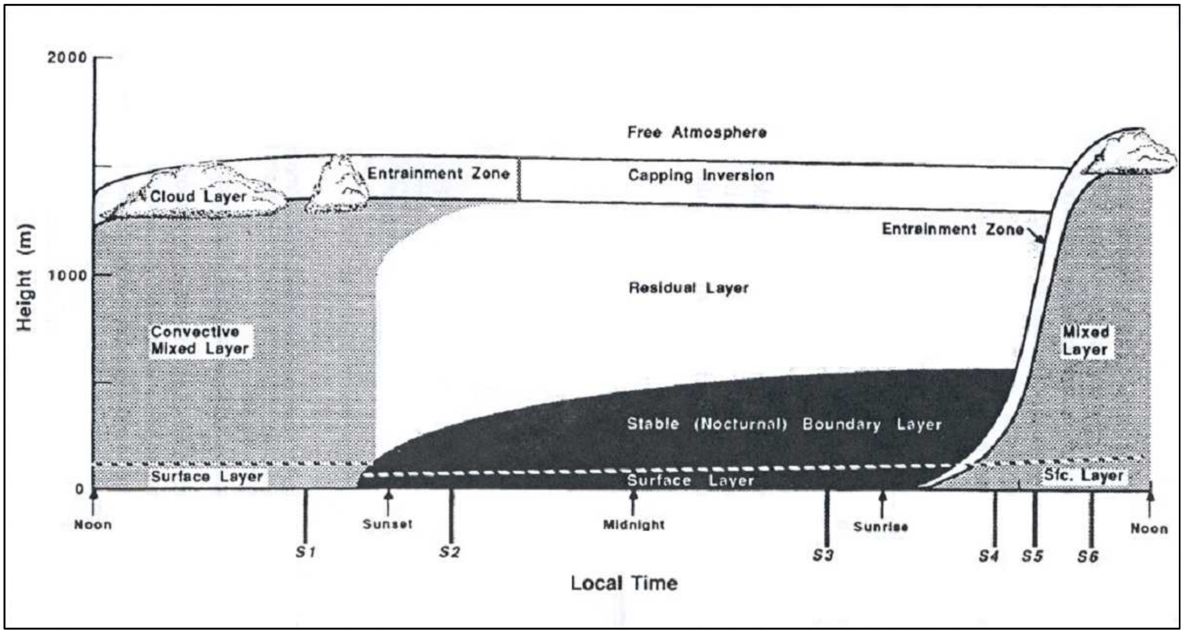

Fig. 3.1: Diurnal course of the vertical structure of the ABL in high pressure regions over land (*Stull, 1988*)

About ½ hour before sunset, convection ceases within the *mixed layer* and turbulence starts to decay. These modifications lead to the creation of the residual layer which initially shows similar characteristics (turbulence, concentration profiles) as the *mixed layer*. As the air in contact with the surface cools, a temperature inversion is created. Starting at the surface, a layer of stable stratification is formed which grows upward as the night progresses. This *stable nocturnal boundary layer* is characterized by decreased wind speeds and, typically, sporadic turbulence. However, nocturnal jets aloft can create wind shears and generate turbulence, which can cause intermittent turbulence and mixing throughout the *stable boundary layer*. Prior to sunrise, the *stable boundary layer* reaches its maximum vertical extent before solar radiation initiates the creation of the *mixed layer* again (*Stull, 1988; Foken, 2008a*).

3.1.2. Eddy Covariance Method

The eddy covariance (EC) method is based on the works of *Montgomery (1948), Swinbank (1951)*, and *Obukhov (1951)* and is the most direct meteorological method to quantify fluxes of energy and matter between the land surface and the atmosphere (see e.g. *Baldocchi, 2003; Foken, 2008a; Foken et al., 2012a* for more details on the historical development of the EC method). These fluxes can be imagined as the vertical transport of energy or matter across a horizontal plane per unit of time by means of turbulent air motions (eddies) of different spatial and temporal scales.

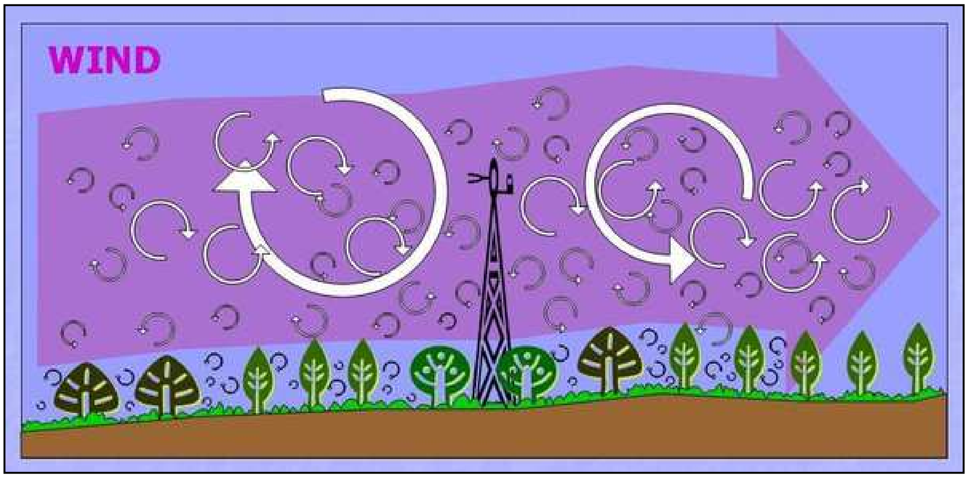

Fig. 3.2: Visual interpretation of horizontal flow in the ABL (*Burba and Anderson, 2010*)

The quantification of fluxes is based on the sampling of these turbulent motions within the ABL. The statistical analysis of the data obtained using the EC method requires the application of the Reynolds decomposition, i.e. the decomposition of time series data into a mean part and a fluctuating (turbulent) part (Fig 3.3) (*Foken, 2008a; Foken et al., 2012a*). This leads to a mean flux (*F*) averaged over a time span, defined as the covariance of the fluctuations of the vertical wind (*w*) and the scalar of interest (*s*), e.g. temperature, water vapor, or CO_2 (*Baldocchi, 2003*):

$$F = \overline{\rho_a} \cdot \overline{w's'} \tag{3.1}$$

(Overbars denote averages, primes denote fluctuations and ρ_a is dry air density).

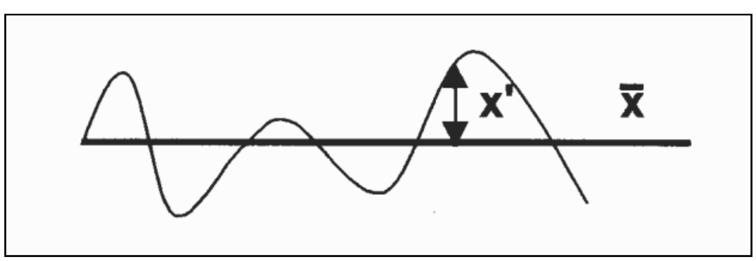

Fig. 3.3: Visual description of the Reynolds decomposition of the value *x* (*Foken, 2008a*)

The general form of the vertical flux equation (Eq. 3.1) may be modified into the equations for the calculation of sensible heat flux (*H*), latent heat flux (*LE*), and CO_2 flux (F_c) (*Burba, 2013*):

$$H = \overline{\rho_a} C_p \overline{w'T'} \tag{3.2}$$

$$LE = \lambda \frac{M_w/M_a}{P} \overline{\rho_a} \overline{w'e'} \tag{3.3}$$

$$F_c = \overline{\rho_a} \, \overline{w'c'} \tag{3.4}$$

where ρ_a is dry air density, C_p is specific heat, $\overline{w'T'}$ is the covariance between fluctuations in vertical wind and temperature, λ is the latent heat of vaporization, M_w/M_a is the ratio of molar masses of water vapor and dry air, P is ambient pressure, $\overline{w'e'}$ is the covariance between fluctuations in vertical wind and water vapor pressure, and $\overline{w'c'}$ is the covariance between fluctuations in vertical wind and mixing ratio of CO_2.

The mathematical derivation of the EC method, however, is based on a number of assumptions which need to be fulfilled in order to validate this approach (*Foken, 2008a*). These assumptions include steady atmospheric conditions, homogeneity of the surrounding environment, and level terrain. If these assumptions are violated, the measurements made may not represent the surface of interest. Moreover, since EC measurements are typically just of the vertical fluxes, additional measurements including storage change fluxes, flux divergence, or advection might become necessary at less than ideal sites where they are important flux terms (*Baldocchi, 2003*). Thus, application conditions and corrections have a major influence on results, more so than the presently available measuring technology. Experimental design and investigator expertise regarding atmospheric turbulence are also important prerequisites for a successful implementation of the EC method (*Foken, 2008a*).

Nonetheless, the EC method has several advantages for field research including the ability to quantify fluxes on the scale of entire ecosystems, to directly measure net exchange between land and atmosphere without disturbing the ecosystem, to sample an area (flux footprint) that can vary in size from a few hundred square meters to square kilometers, and to measure continuously over timescales from hours to years (*Baldocchi, 2003*).

3.1.3. Basic Equations

The theoretical basis of the EC method is given by the law of conservation of mass. For the scalar χ and the volume of height *h* and length *L*, it is defined by *Leuning et al. (2012)* as:

$$\overline{F} = \underbrace{\frac{1}{L^2}\int_0^L \int_0^L \int_0^h \overline{c_d}\,\overline{\frac{\partial \chi}{\partial t}}\,dx\,dy\,dz}_{\mathbf{I}}$$

$$+\underbrace{\frac{1}{L^2}\int_0^L \int_0^L \int_0^h \left[\overline{uc_d}\frac{\partial \overline{\chi}}{dx} + \overline{vc_d}\frac{\partial \overline{\chi}}{dy} + \overline{wc_d}\frac{\partial \overline{\chi}}{dz}\right] dx\,dy\,dz}_{\mathbf{II}}$$

$$+\underbrace{\frac{1}{L^2}\int_0^L \int_0^L \int_0^h \left[\frac{\partial c_d \overline{u'\chi'}}{dx} + \frac{\partial c_d \overline{v'\chi'}}{dy} + \frac{\partial c_d \overline{w'\chi'}}{dz}\right] dx\,dy\,dz}_{\mathbf{III}} \tag{3.5}$$

where $\overline{F}$ is the time- and space-averaged flux of scalar χ between surface and atmosphere, *u, v, w* correspond to the wind vector components in the *x,y,z* directions (orthogonal to the walls of the sample volume), *t* is time, and c_d is concentration of dry air.

Thus, for scalar χ (e.g. CO_2), it states that mean flux, $\overline{F}$, equals the rate of change of χ in the sample volume (I) plus the sum of mean horizontal and vertical advective fluxes (II) and the sum of eddy fluxes (III).

When neglecting horizontal eddy fluxes and assuming that the scalar χ measured at a single point is representative of the sampled volume, Eq. (3.5) becomes (*Leuning et al., 2012*):

$$\overline{F} = \underbrace{\overline{c_d}\,\overline{w'\chi'}}_{\mathbf{I}} + \underbrace{\int_0^h \overline{c_d}\,\frac{\overline{\partial\chi}}{\partial t}\,dz}_{\mathbf{II}} + \frac{1}{L^2}\int_0^L \int_0^L \int_0^h \left[\underbrace{\overline{uc_d}\,\frac{\partial\overline{\chi}}{dx}}_{\mathbf{III}} + \underbrace{\overline{vc_d}\,\frac{\partial\overline{\chi}}{dy}}_{\mathbf{IV}} + \underbrace{\overline{wc_d}\,\frac{\partial\overline{\chi}}{dz}}_{\mathbf{V}}\right] dx\,dy\,dz \qquad (3.6)$$

where (I) is eddy flux, (II) change in storage, and (III – V) are vertical and horizontal advective fluxes.

Furthermore, assuming ideal conditions, i.e. steady meteorological conditions, a horizontally homogeneous surface, and level terrain, the conservation equation can be simplified to (*Leuning et al., 2012*):

$$\overline{F} = \underbrace{\overline{c_d}\,\overline{w'\chi'}}_{\mathbf{I}} + \underbrace{\int_0^h \overline{c_d}\,\frac{\overline{\partial\chi}}{\partial t}\,dz}_{\mathbf{II}} \qquad (3.7)$$

which states that net flux $\overline{F}$ equals the sum of mean vertical flux (I) and the change in storage between soil and measurement height h (II).

Since the general EC equation (Eq. 3.1) is based on the assumptions of ideal terrain and well-developed turbulence, potential limits regarding its application exist during conditions when turbulence is not well developed or is intermittent, e.g. at night. Such conditions can lead in the case of CO_2 to substantial amounts of CO_2 generated below the height of the instruments not being detected, resulting in an underestimation of flux. Similarly, when turbulence resumes at sunrise and the stable stratification breaks up, venting of the stored CO_2 may lead to an overestimation of CO_2 flux. An analysis of diurnal cycles may therefore require a quantification of this storage of CO_2 (term II in Eq. 3.7) by correctly measuring changes in CO_2 concentration at several heights within and above the canopy (*Baldocchi, 2003*). Instrument towers at Fort Logan and Rocky Flats were not configured for storage flux measurements, which may have led to some uncertainties in flux estimation as just described.

3.1.4. Footprint

According to EC theory, fluxes measured at a point above and downwind of the source area represent the fluxes at the surface of the upwind area, provided that the assumptions of level terrain and homogeneous surface characteristics are met. The source area of the fluxes measured is called the flux *footprint*. However, influence on the measured flux is not equally distributed across this area. It can be described by a transfer function which defines the source area of a measured signal (Fig. 3.4) (*Foken, 2008a; Kordowski, 2009*) (see e.g. *Schmid (1994)* for further information on source areas of fluxes). Spatial extent of the footprint and spatial distribution of source area strength contributing to total flux are primarily influenced by instrument height, surface roughness, and thermal stability (*Burba, 2013*).

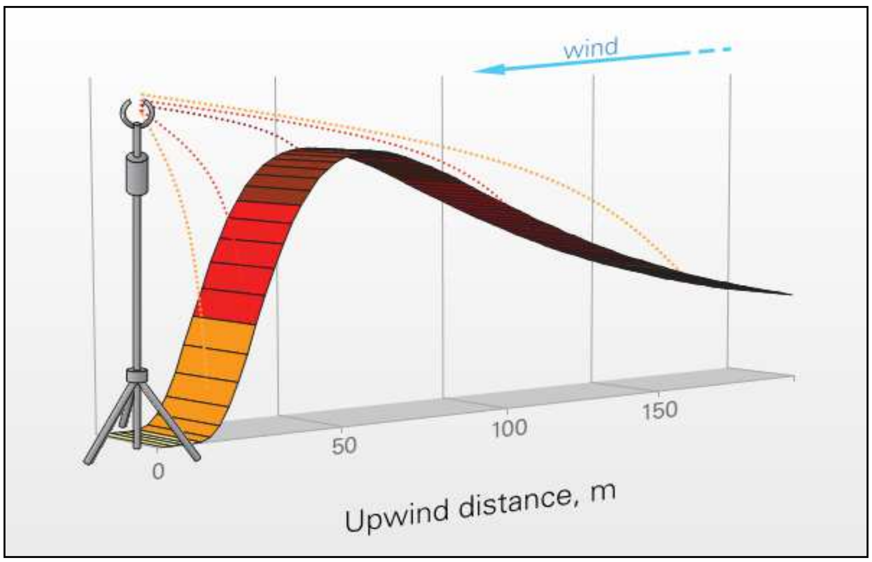

Fig. 3.4: Visualization of the footprint function: the darker the red tones – the larger the flux contribution, i.e. most of the contribution to total flux in this example does not come from very near (cm) or very far (km) away from the point of measurement (*Burba, 2013*)

3.1.5. Technical Requirements, Sampling Times, and Instrument Height

To ensure that all significant turbulent motions (eddies) contributing to CO_2 and other fluxes are sampled, it is necessary to measure at a high frequency and over sufficiently long enough periods. To capture the high-frequency portion of the flux, sampling rates of 10-20 Hz are widely used. Thus, the instruments used for measurements need to be capable of detecting high-frequency changes in wind and scalar quantities. Commonly used are sonic anemometers and infrared gas analyzers (IRGAs), either as closed-path (CP) or open-path

(OP) versions (see *Foken, 2008a* and *Burba, 2013* for technical details). The low-frequency portion, on the other hand, requires that sampling be long enough to capture all relevant motions of the boundary layer without being affected by diurnal changes. Sampling duration is also dependent on atmospheric stratification, wind velocity, and measurement height. Typical sampling intervals are 30 to 60 minutes long. Using shorter intervals increases the likelihood that low-frequency contributions to the flux might be missed, whereas longer sampling times are more likely to be influenced by diurnal trends and, therefore, may not fulfill the steady-state requirement (*Baldocchi, 2003; Foken, 2008a*).

With regard to measurement height, instruments should be located approximately 1.5-2 times canopy height above ground, within the constant flux layer (section 3.1.1.). When canopy height is low, i.e. less than 2-3 m, instruments should be placed at least 1.5-2 m above the canopy itself. If fluxes are measured at a lower height, they might not represent the turbulence developed over the surface of interest as the data becomes potentially falsified by the influence of local disturbances. Moreover, a low measurement height bears the risk of an increased impact of instrument path averaging and insufficient sampling frequency as the turbulence spectrum shifts to higher frequencies closer to the surface: As turbulent transport is increasingly accomplished by ever smaller eddies, there is a tendency for contributions to become spatially averaged out in the instrument path or not be detected at all due to a slow sampling frequency. Both effects would lead to an underestimation of flux. However, placing the instruments too high might place them in a layer decoupled from the constant flux layer and result in measurement of fluxes not representative of the surface of interest (*Burba, 2013*).

3.1.6. Corrections

Performance of the EC method is a function of sampling and atmospheric conditions but also of instrument characteristics and setup. The signals recorded can be influenced, for example, by low-pass filtering (an attenuation of high-frequency parts of the flux), high-pass filtering (an attenuation of low-frequency parts of the flux), or air density fluctuations, which can all lead to serious errors in flux calculations when no corrections are applied (*Baldocchi, 2003*). Listed below are some of the major corrections typically applied when the EC method is used:

Coordinate Rotation

Coordinate rotation is necessary for a correct calculation and interpretation of fluxes. The correction is needed due to limitations regarding anemometer setup: If the z-axis is not perfectly perpendicular to the surface, cross-contamination by the other wind components will occur and lead to tilt errors. This, in turn, influences flux calculations and by introducing a systematic error can seriously impact long-term budget estimates. To prevent this, the coordinate system is rotated so that the mean vertical wind becomes zero. A commonly used method, known as *double rotation*, includes the rotation of the z and y axes into the mean wind direction, thereby correcting for errors in the vertical and horizontal orientation of the anemometer. However, this method can potentially impact data quality (low wind speeds can result in large rotation angles) and lead to high-pass filtering (discontinuities in time series data), which is why alternative methods such as *planar fit* have been proposed (*Lee et al., 2004a; Rebmann et al., 2012*).

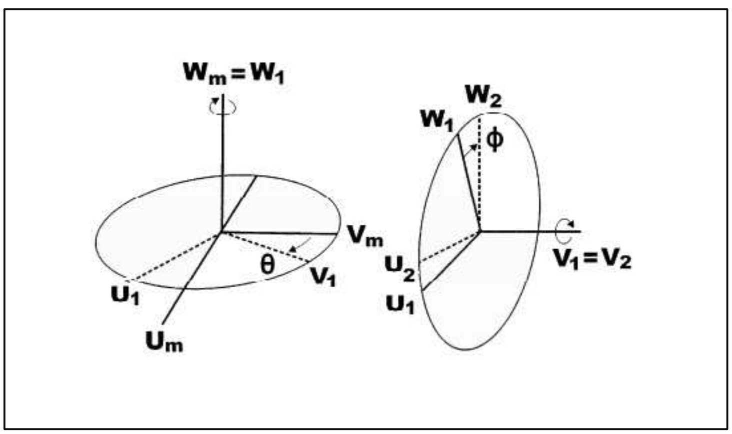

Fig. 3.5: Illustration of the two-step coordinate rotation: first rotation around the z-axis, second rotation around the new y-axis (*Foken, 2008a*; modified)

Spectral Corrections

Like any measuring instrument, sensors installed as part of an EC setup tend to dampen higher and undersample lower frequencies of a signal, i.e. they function as frequency filters (*Foken et al., 2012b*).

Low-pass filtering, a signal loss in the high-frequency part of the spectrum, is due to slow sensor response times, sensor path averaging, sampling rate, separation distance between the instruments, or too low measurement height (*Baldocchi, 2003*). The aim of the correction is to adjust this mismatch in spectral resolution of the installed instrument and an "ideal" measuring device using transfer functions (Fig. 3.6) (*Foken, 2008a*).

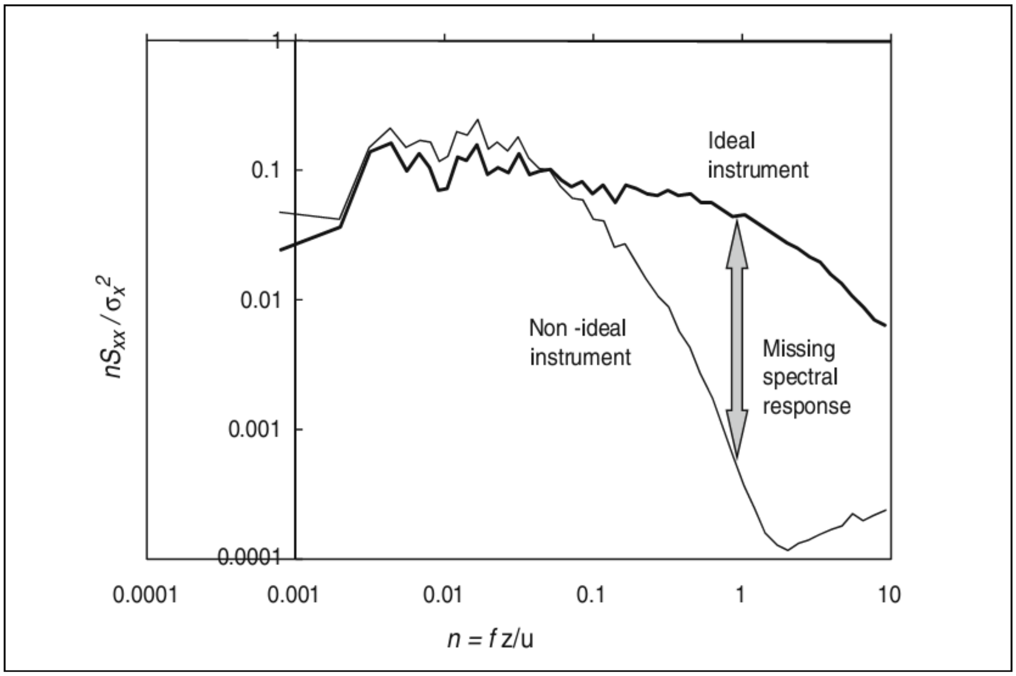

Fig. 3.6: Comparison of spectral resolution of an ideal and non-ideal instrument (n = normalized frequency, f = frequency, z = height, u = wind velocity, S_{xx} = density of scalar x, σ_x^2 = variance of scalar x) (*Foken et al., 2012b*)

High-pass filtering, a signal loss in the low-frequency part of the spectrum, can occur when the averaging method or the duration of the sampling interval is too short (*Baldocchi, 2003*). An extension of the sampling interval, on the other hand, bears the risk of introducing low frequency non-turbulent components. Whether the sampling interval needs to be modified can be determined with the help of an ogive analysis (*Foken, 2008a*). For more details on frequency response errors and related corrections see e.g. *Moore (1986).*

WPL-Correction

The WPL-correction, named after Webb, Pearman, and Leuning (*Webb et al., 1980*), is due to the occurrence of density fluctuations caused by changes in pressure, temperature, and water vapor content and the fact that the instruments used for measuring CO_2 and/or water vapor (IRGAs) typically measure (molecular or mass) densities and not mixing ratios (*Baldocchi, 2003*). As a result, density fluctuations may be recorded without any activity regarding uptake, release, or transport of the measured quantity (*Foken et al., 2012b*). Therefore, flux calculations (e.g. *NEE, LE*) need to be corrected for the influence of temperature, water vapor, and sensible heat flux on the density of air. The WPL-correction term can become large if the turbulent fluctuations of a scalar are relatively small in comparison to its mean concentration as, for example, in the case of CO_2 (Fig. 3.7) (*Foken, 2008a*). See *Fuehrer and Friehe (2002)* and *Liebethal and Foken (2003)* for a detailed review of this correction.

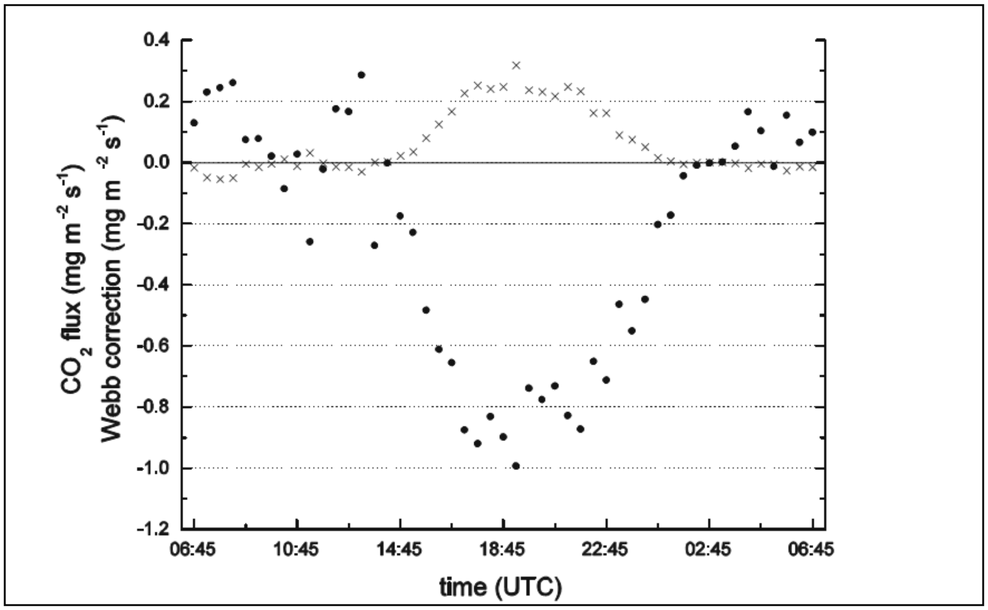

Fig 3.7: Uncorrected CO_2 flux (points) and corresponding WPL-correction terms (crosses) above an irrigated cotton field (from *Liebethal and Foken, 2003*, in *Foken et al., 2012b*)

3.1.7. Quality Control

Like the application of the corrections described above, quality control (QC) of EC data is essential to obtain correct results, i.e. ecosystem fluxes. This process includes the detection of data gaps and spikes, checks for plausibility of the data range as well as the exclusion of data collected during unfavorable meteorological conditions (*Foken, 2008a*). Moreover, it is necessary to carry out tests checking whether the assumptions the EC method is based on have been met, specifically with regard to steady-state conditions and developed turbulence. Such tests have been proposed and developed by *Foken and Wichura (1996)*, *Vickers and Mahrt (1997)*, and *Mauder and Foken (2006)*. Quality control during this study followed *Foken et al., (2004)* which is based on a combination of three tests (steady-state conditions, integral turbulence characteristics, horizontal inflow sector) producing an overall quality flag classified 1-9. Depending on data quality, the flag indicates whether the data can be used for basic research, the calculation of long-term flux sums, orientation only, or whether it should be discarded.

3.1.8. Gap-Filling

Gaps in the EC data series are unavoidable and are usually a result of data quality checks, instrument malfunction or maintenance, or the screening of data for unfavorable wind sectors or unwanted stationary sources of influence (*Baldocchi, 2003*). *Falge et al. (2001a)* found that average data coverage for EC studies is around 65 %. These data gaps need to be filled to obtain, for example, accurate annual flux sums. Different approaches exist including empirically derived algorithms, interpolation between adjacent periods, or data-binning by time and subsequent filling of gaps with a mean value (*Baldocchi, 2003; Moffat et al., 2007*).

3.2. Experimental Setup

3.2.1. Fort Logan

The urban EC array at Fort Logan National Cemetery (39.647° N, 105.039° W; elevation: 1640 m a.s.l.) was located on a level segment of turf within the eastern half of the cemetery grounds. Species composition of vegetation was dominated by Kentucky bluegrass, fescue, and ryegrass. Irrigation was active between May 9 and October 6 in 2011 and between April 23 and October 18 in 2012. Fertilizer application was recorded twice in 2011 (Jun 15, Oct 6) and once in 2012 (Jul 17) and amounted to approximately 49 kg N/ha per application. During the main growing season (Apr-Oct), grass was mown once a week and clippings were left at the site. The measuring setup consisted of a sonic anemometer (CSAT-3, Campbell Scientific) to quantify wind components, sonic temperature and an OP IRGA (LI-7500, Licor Inc., USA), measuring CO_2 and water vapor densities. Both instruments were mounted on a tripod 1.85 m above the ground. Orientation of the sonic anemometer was toward 180° True North to minimize flow disturbances from the dominant wind directions. Separation distance of the IRGA was 16 cm E (sonic anemometer = reference). Data from these fast response sensors was recorded at 10 Hz on a datalogger (CR-1000, Campbell Scientific, USA).

Furthermore, the setup included 2 soil heat flux plates at 5 cm soil depth (HFP-01, Campbell Scientific, USA) located 3.65 m southwest and 6.10 m southeast from the tripod center, 1 soil thermocouple located above the southwest soil heat flux plate, and 1 TDR-probe (CS-616, Campbell Scientific, USA) buried at a 45° angle 2.45 m south of the tripod center. Other aboveground instruments, mounted to the tripod, included a precipitation gage (Weathertronics, model 6010), a net radiometer (Q7.1 REBS, Campbell Scientific, USA) extending 1.2 m west on a boom from the tripod center at 1.85 m height, a pyranometer (LI-200 Licor Inc., USA) mounted to a platform 2.30 m above ground, and a temperature and humidity probe (HMP-45C, Campbell Scientific, USA) mounted to the tripod's center post.

Data from these slow response sensors listed above were also recorded on the datalogger (CR-1000, Campbell Scientific, USA) as 30-minute averages.

Power was supplied to the instrument setup via an 85-W solar panel connected to 2 12-V/ 90-Ah batteries.

LAI was measured by harvesting vegetation from 3 locations near the instrument tower. At each location, a circular plot of 58 cm^2 was sampled. Non-green components were removed from the samples and each sample was analyzed using a leaf area meter (LI-3100, Licor Inc., USA). The derived LAI values (3) were averaged for each sampling event (2011: n=29; 2012: n=34).

The station schedule included weekly checks and maintenance, including cleaning the sensors. Calibration of the IRGA was regularly checked and adjusted when substantial sensor drift had occurred.
Data at this station was collected in 2011 between March 16 and November 18 and in 2012 between March 12 and December 12. Restrictions imposed by the Fort Logan administration did not allow data collection between late November and early March.

3.2.2. Rocky Flats

The prairie EC site was located within the southwest section of Rocky Flats National Wildlife Refuge (39.875° N, 105.218° W, elevation: 1860 m a.s.l.). Local vegetation was classified as xeric tallgrass prairie (dominant species: bluestem, switchgrass, and blue grama). Measuring equipment consisted of a sonic anemometer (CSAT-3, Campbell Scientific) and a CP IRGA (LI-7200, Licor Inc., USA). Both instruments were mounted on a tower 3 m above the ground. Orientation of the sonic anemometer was 165° True North. Separation distance of the IRGA was 12 cm W and 12 cm N (sonic anemometer = reference). Sample air (IRGA) was drawn through a 1 m tube (ID = 7.7mm) at 19.5 ALPM using a flow module. Data from these fast response sensors was recorded at 10 Hz on a data logger (CR-3000, Campbell Scientific, USA).

The setup also included 2 soil heat flux plates at 5 cm soil depth (HFP-01, Campbell Scientific, USA) located 9.3 m southwest and 7.5 m east of the tower, 2 soil thermocouples located above each of the soil heat flux plates, and 2 TDR-probes (CS-616, Campbell Scientific, USA) buried at approximately 45° located 9.5 m southwest and 6.0 m east of the tower. Other instruments included a precipitation gage (Weathertronics, model 6010) located on the ground 10 m north of the tower, a net radiometer (Q7.1 REBS, Campbell Scientific, USA) extending 2.2 m east on a boom from the tower at 3 m height, a pyranometer (LI-200 Licor Inc., USA) and a quantum sensor (LI-190, Licor Inc., USA) mounted to a platform on the tower located 3.10 m above the ground, and a temperature and humidity probe (HMP-45C, Campbell Scientific, USA) mounted to the tower at 3 m height. Data from these slow response sensors listed above were also recorded on the datalogger (CR-3000, Campbell Scientific, USA) as 30-minute averages.

Power was supplied to the instrument setup via 3 135-W solar panels connected to 2 12-V/220-Ah batteries located 15 m north of the tower.

LAI was measured by harvesting vegetation from 3 locations near the instrument tower. At each location, a circular plot of 293 cm^2 was sampled. Non-green components were removed from the samples and each sample was analyzed using a leaf area meter (LI-3100, Licor Inc., USA). The derived LAI values (3) were averaged for each sampling event (2011: n=17; 2012: n=21).

The station schedule included weekly checks and maintenance, including cleaning the sensors. Calibration of the IRGA was regularly checked and adjusted when substantial sensor drift had occurred.

Data analyzed from this station included data collected in 2011 between January 01 and December 31 and in 2012 between January 01 and December 31, thus covering 2 full years.

3.2.3. South Denver Tower

Due to its proximity, meteorological data from the South Denver EC site (39.659° N, 105.013° W, elevation: 1620 m a.s.l.) was used to fill time series data of the urban site (Fort Logan). This data included shortwave radiation, air temperature and relative humidity. Radiation data was derived from a LI-200 pyranometer (Licor Inc., USA) installed on a roof 3 m above ground at the base of the tower, while air temperature and humidity were measured using a HMP-45C probe (Campbell Scientific, USA) mounted on the tower 60 m above ground. The data was recorded as 30-minute averages. Weekly checks were conducted on the station and the instruments to ensure proper function.

3.2.4. NREL Tower M2

Similar to the urban site, meteorological data from the NREL tower (39.910° N, 105.235° W, elevation: 1860 m a.s.l) was used to fill data gaps of the prairie site record (Rocky Flats). Fill data included shortwave radiation, air temperature, and relative humidity. Shortwave radiation was derived from a precision spectral pyranometer (Eppley Laboratory, Inc.). Air temperature was determined using a platinum resistance thermometer (PRT; Rosemount, USA) installed 2 m above ground. Relative humidity was calculated using measured dew point temperature and air temperature. The instruments mentioned above are calibrated annually. All data from the NREL tower is publically accessible through the NREL website (*NREL, 2013*).

3.3. Data Processing

The large volumes of data produced by EC measurements, the instruments involved as well as the restrictions imposed by the underlying EC theory require thorough data quality checks and the correct application of algorithms and corrections regarding the calculation of fluxes.

Fluxes (latent heat, sensible heat, CO_2, soil heat) and ancillary parameters were quantified for the time periods stated under sections 3.2.1. and 3.2.2. Time stamps for all data are given in Mountain Standard Time (MST, GMT -7). All values for wind direction are corrected for magnetic declination. Fluxes of CO_2, latent and sensible heat towards the atmosphere (away from the land surface) are positive; fluxes away from the atmosphere (towards the land surface) are negative. For example, a negative CO_2 flux would indicate uptake of CO_2 by the land surface for that specific time period. Fluxes of soil heat away from the soil surface towards the atmosphere are positive. Net radiation is positive when the sum of downward radiation (towards the land surface) exceeds the sum of reflected radiation and radiation emitted upward (towards the atmosphere).

3.3.1. Flux Calculation

Fluxes were calculated using EddyPro software (version 4.2; Licor, Inc., USA) which is based on the ECO_2S software project and was primarily chosen due to its free availability and its continuing development and support by Licor, Inc. Raw data consisted of binary files containing 1 hour of 10 Hz data which were being processed to output flux averages over 30-minute intervals. Prior to processing, the raw data was manually checked for gaps and signs indicating disturbances to the experimental setup (e.g. instrument diagnostics, implausible out-of-range values).

Raw data processing using EddyPro included the following steps:

- *Missing sample allowance* was set to 10 %. This acts as a first data quality check and prevents the processing of raw files which lack more than 10 % of the 10 Hz data record, i.e. 3,600 lines of data out of 36,000 lines (= 1 hour of 10 Hz data)
- Coordinate rotation of the measured wind components was calculated using *double rotation* as explained under section 3.1.6.
- Turbulent fluctuations of the measured wind components, sonic temperature, CO_2, and water vapor were quantified by using the *block average* method, which calculates the mean of a variable over the averaging period and subsequently quantifies turbulent fluctuations as deviations from the mean
- Uncorrected *fluxes* for CO_2, sensible heat, and latent heat were calculated as described under section 3.1.2. and equations 3.2-3.4
- Time lag compensation correcting for sensor separation and possible tube delay (LI-7200 at Rocky Flats) was calculated using *covariance maximization with default.* This method instructs EddyPro to check whether the calculated time lag lies within a pre-

defined plausibility window (of minimum and maximum time lag). If not, EddyPro will use the pre-defined nominal time lag. For the urban site (Fort Logan) nominal time lag was set to 0 (zero) seconds (LI-7500, OP IRGA). For the prairie site (Rocky Flats) nominal time lag was set to 0.3 seconds for CO_2 and 0.4 seconds for water vapor (LI-7200, CP IRGA).

- *Spectral corrections* for high-pass and low-pass filtering effects were applied following *Moncrieff et al. (2004)* and *Moncrieff et al. (1997)*, respectively.
- *Compensation of density fluctuations* followed *Webb et al. (1980)* for the urban site (section 3.1.6.). Instrumentation at the prairie site, i.e. the CP IRGA (LI-7200), allowed for a conversion from density to mixing ratio (water vapor and CO_2 values), which made similar density corrections unnecessary.
- *Quality control* followed the scheme suggested by *Foken et al. (2004)* (section 3.1.7.).
- *Footprint estimation*, i.e. the analysis of the source area and its contribution to total flux, was done in accordance with *Kormann and Meixner (2001)*.
- *Output* files included all calculated fluxes, statistics, and data quality flags for every 30-minute averaging interval processed.

To determine soil heat flux at the soil surface, fluxes measured at 5 cm soil depth were corrected for changes in soil heat storage in the soil layers above the heat flux plates (Appendix A1).

3.3.2. Quality Control

Quality control of the output data obtained through Eddy Pro 4.2 started with a plausibility test of the parameters measured by the IRGA (CO_2, water vapor) and anemometer (wind components, sonic temperature). Records which contained data outside the range specified by the manufacturer were deleted. Data was further screened for instrument diagnostics given by the IRGA and anemometer. If the count of diagnostic flags exceeded 10 % (i.e. 1,800 out 18,000) for any half-hour record, the record was deleted. The IRGAs were further checked for high AGC (Automatic Gain Control) values indicating an obstruction in the optical path of the instrument. The normal AGC value was 56 or lower. When this value exceeded 75, the record was deleted. Records displaying diagnostic values between 0 and 1,800 for instrument flag or between 56 and 75 for AGC were evaluated for plausibility, cross-checked against other diagnostics and logbook entries, compared to the present diurnal trend, and if deemed necessary deleted.

Raw data was statistically screened following *Vickers and Mahrt (1997)* which included tests on amplitude resolution, dropouts, absolute limits, skewness and kurtosis, discontinuities as well as count and removal of spikes. If any half-hour record was hard-flagged for *w* (vertical wind component), CO_2, water vapor, or sonic temperature, the record was evaluated for plausibility, cross-checked against other diagnostics and logbook entries, compared to the present diurnal trend, and if deemed necessary deleted.

Processed data was filtered for periods of insufficient turbulence, i.e. low friction velocity (u^*). The thresholds for filtering were derived from the MPI-Gap-filling tool (*MPI, 2013*). Records when u^* was less than 0.05 m s^{-1} at the urban site or less than 0.11 m s^{-1} at the prairie site were removed.

Outliers in the data regarding fluxes of CO_2, latent and sensible heat were detected as follows: Monthly data was first split into day and night ($R_s < 10$ W/m^2) parts. Next, 5 and 95 % percentiles were calculated for these day and night datasets. Data that occurred below or above these percentile thresholds was excluded. The remaining data was averaged for day- and nighttime, respectively. If a record occurred outside this mean ± 3σ, the record was deleted.

3.3.3. Gap-Filling

Gaps in the ancillary (meteorological) data such as temperature, radiation, and relative humidity were filled depending on the length of the data gap: shorter gaps (up to one hour) were filled using interpolation, while longer gaps and missing precipitation data were filled using data recorded at the South Denver Tower and NREL Tower M2 for gaps at Fort Logan and Rocky Flats, respectively. Longer soil temperature gaps were filled using a regression between air temperature and soil temperature. Missing soil heat flux records were filled using a regression between net radiation and soil heat flux. Gaps in the soil moisture or wind record were not filled.

Gaps in the flux data were filled using an algorithm suggested by *Reichstein et al. (2005)*, which bears similarities to the methods used by *Falge et al. (2001a+b)*, but additionally considers the covariation of the calculated fluxes with meteorological parameters (incoming shortwave radiation, air temperature, VPD) and the temporal auto-correlation of these fluxes. The algorithm analyzes the dataset for the type of missing data (e.g. only flux data is missing, meteorological data is missing) and fills the gaps accordingly using, for example, averages under comparable meteorological conditions or values derived from the mean diurnal variation of the missing parameter. Depending on the filling method and/or the size of the time window used (i.e. ± days before/after the gap), the quality of the fill data is classified as A, B, or C. Application of this gap-fill algorithm is convenient, since the MPI has provided an online tool which provides easy upload, documentation, visualization, and downloadable results (*MPI, 2013*).

4. Results

4.1. Meteorological Conditions

4.1.1. Fort Logan 2011

Meteorological and soil conditions, i.e. air temperature, relative humidity, barometric pressure, precipitation as well as soil moisture and soil temperature for the 2011 season at Fort Logan are presented below. The raw data consisted of 30-minute averages (11,808 records; Mar 17-Nov 17; 246 days). Data coverage was 95.2 % for air temperature and relative humidity, 93.1 % for soil temperature and soil moisture, and 95.8 % for precipitation.

Average air temperature over the investigated period in 2011 was 14.9(± 7.3)°C, with daily means ranging from a minimum of -3.2°C on November 2 to a maximum of 26.9°C on July 4 and 31 (Fig. 4.1 A). The lowest 30-minute average was recorded on November 16 at -9.6°C and the highest on July 4 at 35.2°C. Large variations in temperature were not only observed between seasons but also between individual days, especially in spring and fall. For example, average daily air temperature dropped from 19.3°C on May 9 to 3.4°C on May 11 and from 15.2°C on October 24 to -1.7°C on October 26.

Monthly averages for the 2011 investigation period at Fort Logan were generally in good agreement with long-term averages for Denver (1981-2010) (*NOAA, 2013a*). Notable differences between the two records did occur in March (+3.1 K) and May (-2.8 K) (Tab 4.1). Temperature data for Denver in 2011 also showed noticeable deviations (> 1 K) for March (+1.5 K) and May (-2.5 K) but also August (+2.7 K), thereby confirming the observations made at Fort Logan during that year (Tab 4.1).

	Mar	**Apr**	**May**	**Jun**	**Jul**	**Aug**	**Sep**	**Oct**	**Nov**
FL 2011	7.9*	8.9	11.4	19.9	23.4	23.2	16.5	10.5	3.8**
Denver 1981-2010	4.8	8.9	14.2	19.7	23.4	22.3	17.3	10.4	3.8
Denver 2011	6.3	9.1	11.7	20.1	24.4	25.0	17.9	11.4	4.2

Tab. 4.1: Comparison of mean monthly air temperature (°C) at Fort Logan in 2011; *monthly mean derived from data of Mar 17-31 2011; **monthly mean derived from data of Nov 1-17 2011

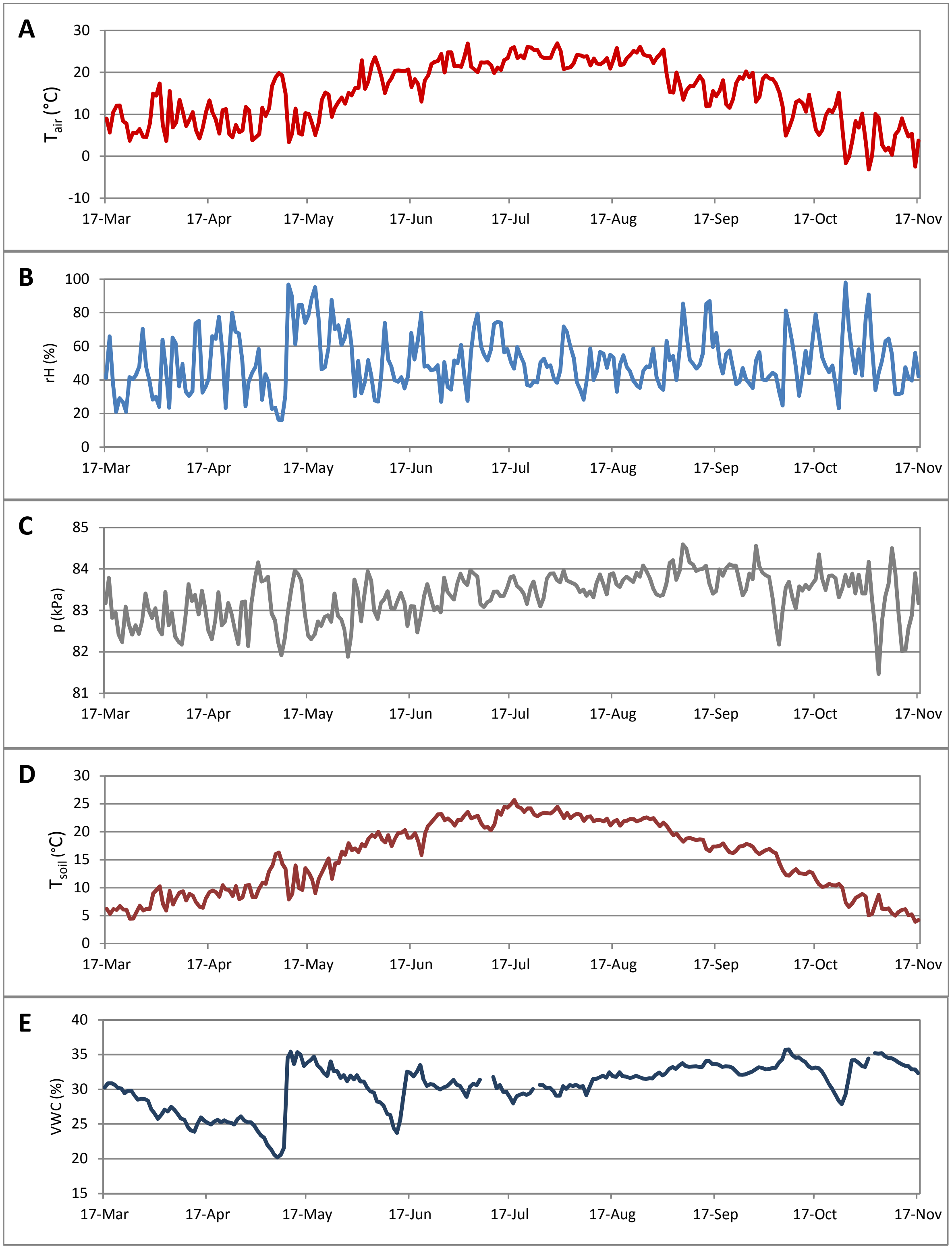

Fig. 4.1: Meteorological and soil conditions at Fort Logan in 2011: (**A**) Average daily air temperature (°C), (**B**) Average daily relative humidity (%), (**C**) Average daily barometric pressure (kPa), (**D**) Average daily soil temperature (°C), (**E**) Average daily soil moisture (VWC, %)

Daily means for relative humidity (rH) varied between 16.2 % (May 9) and 98.0 % (October 26) with an overall average (2011) of 50.7(±16.6) % (Fig. 4.1 B). Minimum relative humidity for a single 30-minute averaging period was recorded on May 8 at 5.6 %. Relative humidity typically showed a diurnal pattern with maximum values near sunrise and minimum values in the afternoon. Moreover, the data clearly showed the influence of precipitation events and, more importantly at this urban site, irrigation.

Barometric pressure ranged between daily means of 81.47 kPa and 84.60 kPa, showing the greatest variability in spring and fall (Fig. 4.1 C). The overall average for the 2011 season was 83.34 (±0.57) kPa.

The seasonal course of soil temperature closely followed that of air temperature, though the amplitude of fluctuations was smaller. There was no marked delay between changes in air temperature and soil temperature. Daily means for soil temperature varied between 3.9°C (Nov 16) and 25.7 °C (Jul 18) with an overall average of 15.3(±6.3)°C (Fig. 4.1 D). Minimum soil temperature for a single 30-minute averaging period was recorded on March 29 at -1.3°C, while maximum soil temperature was reached on July 18 at 33.3°C. Soil frost occurred on 3 nights in 2011 (Mar 24-26).

Daily means for soil moisture (volumetric water content, VWC) varied between 20.2 % and 35.7 % with an overall average of 30.5(±3.3) % (Fig. 4.1 E). Variations in the seasonal course of soil moisture were strongly influenced by precipitation/irrigation events. For example, the lowest (15.8 %, May 8) and highest (36.7 %, May 11) 30-minute mean record are only 3 days apart, but are separated by the start of irrigation (May 9) and a late snowfall event (May 10).

Precipitation and irrigation (May 9 - Oct 6 2011) at Fort Logan in 2011 totaled to more than 1000 mm with the wettest month being August at 271 mm (Fig. 4.2). Data from the South Denver Tower indicates that precipitation varied considerably from March through November compared to the monthly averages of Denver (1981-2010). March and August displayed the largest deviations: -26.5 mm and -41.5 mm from the long-term average for Denver (negative values indicating below the mean) (Fig. 4.3).

Moreover, the impact of irrigation on the amount of available water per month becomes apparent when comparing the annual average of Denver (1981-2010: 381 mm) and the amount of precipitation recorded at the South Denver Tower (Mar 17-Nov 17: 342 mm) to the total water input (precipitation and irrigation) at Fort Logan (Mar 17-Nov 17: 1062 mm).

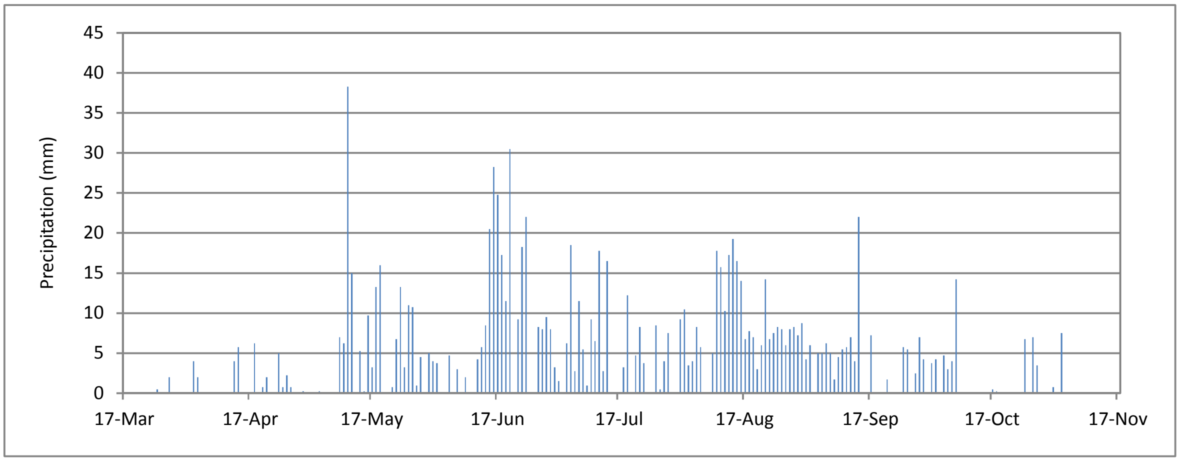

Fig. 4.2: Total daily precipitation (mm; including irrigation) at Fort Logan in 2011

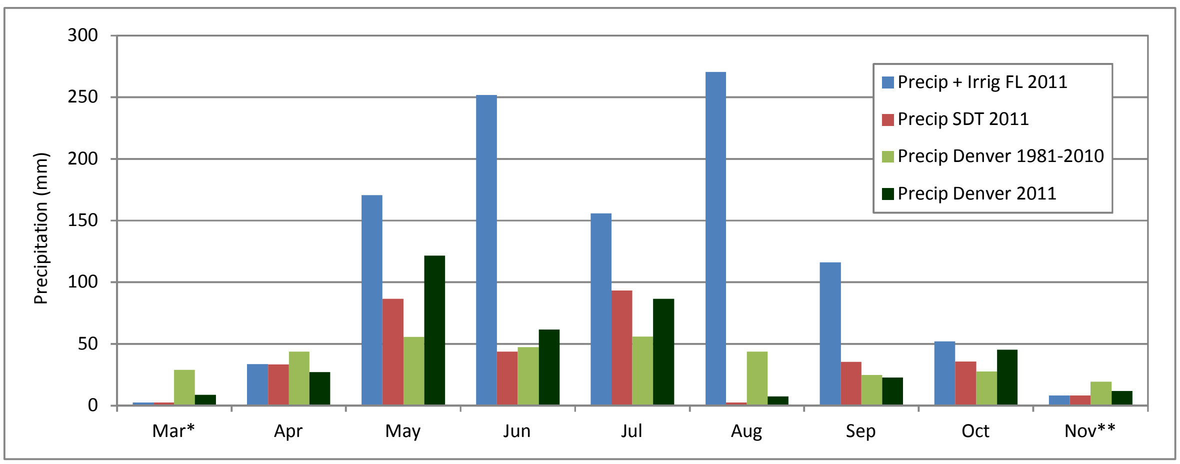

Fig. 4.3: Comparison of monthly precipitation at Fort Logan in 2011 (mm; including irrigation); *monthly total for Fort Logan (FL) and South Denver Tower (SDT) derived from data of March 17-31 2011; **monthly total for Fort Logan and South Denver Tower derived from data of November 1-17 2011

4.1.2. Fort Logan 2012

Data for meteorological and soil parameters for the 2012 season at Fort Logan are presented below. The raw data consisted of 30-minute averages (13,152 records; Mar 13 – Dec 11; 274 days). Data coverage for air temperature, relative humidity, barometric pressure, soil temperature and soil moisture, and precipitation was 99.7 %.

Air temperature over the investigated period in 2012 averaged to 15.1(± 7.6)°C and was therefore slightly higher in comparison to 2011, even though measurements in 2012 extended into December. Daily means also indicated a greater temperature variation ranging from a minimum of -7.7°C on December 9 to a maximum of 28.0°C on June 25 (Fig. 4.4 A). These 2 days also hold the records for the lowest and highest 30-minute average recorded during the 2012 investigation period, i.e. -14.0°C and 37.2°C, respectively. As in 2011, large variations in temperature occurred not only over the span of the investigated period but also between individual days, for example between April 1-3 (18.7°C to 0.6°C) and December 5-9 (11.9°C to -7.7°C).

Monthly means for air temperature at Fort Logan showed more deviations from the long-term mean of Denver (1981-2010) in 2012 than in 2011. Notable differences occurred in March (+6.1 K), April (+3.1 K), June (+ 2.6 K), and December (+3.8 K). Similarly, data for Denver for 2012 showed clear deviations (> 1 K) for March (+4.8 K), April (+2.9 K), May (+1.6 K), June (+4.2 K), July (+ 2.7 K), September (+1.7 K), and November (+2.6 K) (Tab 4.2).

	Mar	**Apr**	**May**	**Jun**	**Jul**	**Aug**	**Sep**	**Oct**	**Nov**	**Dec**
FL 2012	11.9*	12.0	15.3	22.3	23.7	22.2	17.5	9.0	5.3	2.9**
Denver 1981-2010	4.8	8.9	14.2	19.7	23.4	22.3	17.3	10.4	3.8	-0.9
Denver 2012	9.6	11.8	15.8	23.9	26.1	23.9	19.1	9.4	6.4	-0.4

Tab. 4.2: Comparison of mean monthly air temperature (°C) at Fort Logan in 2012; *monthly mean derived from data of Mar 13-31 2012; **monthly mean derived from data of Dec 1-12 2012

Statistical parameters and diurnal patterns for relative humidity in 2012 were similar to 2011. Daily means varied between 17.1 % (Apr 1) and 97.0 % (Apr 3) with an average of 46.6(±15.5) %, about 4 % lower than in 2011 (Fig. 4.4 B). Minimum relative humidity for a single 30-minute averaging period was recorded on April 6 at 5.1 %.

Daily means of barometric pressure ranged between 81.77 kPa and 84.69 kPa (Fig. 4.4 C), while the seasonal average amounted to 83.47(±0.51) kPa, thus showing very similar statistics compared to 2011.

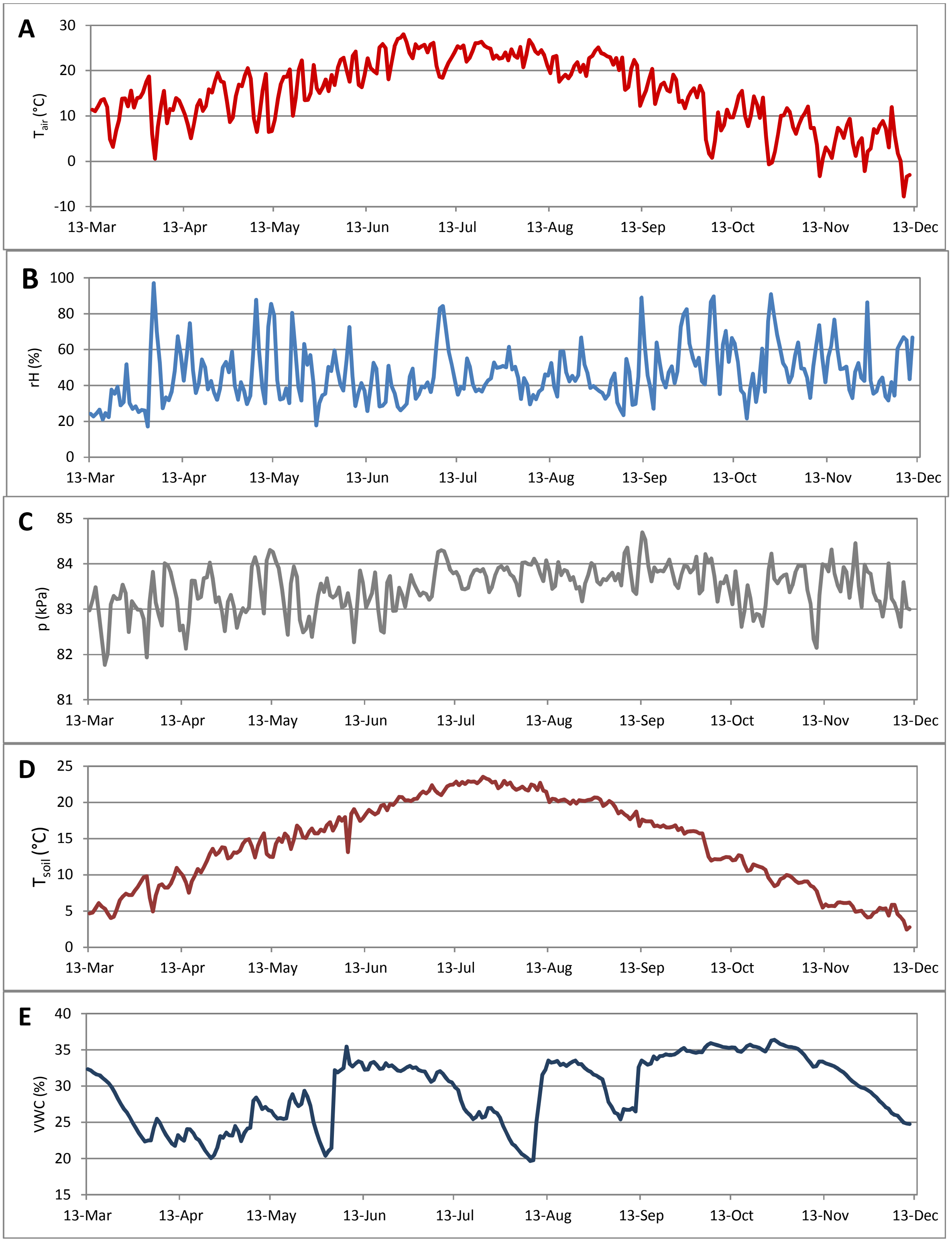

Fig. 4.4: Meteorological and soil conditions at Fort Logan in 2012: (**A**) Average daily air temperature (°C), (**B**) Average daily relative humidity (%), (**C**) Average daily barometric pressure (kPa), (**D**) Average daily soil temperature (°C), (**E**) Average daily soil moisture (VWC, %)

Soil temperature varied between daily averages of 2.4°C (Dec 10) and 23.5°C (Jul 22) with an overall average of 14.3(±5.9)°C (Fig. 4.4 D). Minimum soil temperature (30-minute average) was recorded on March 21 at 0.7°C, while the maximum was reached on July 22 at 28.4°C. There was no recorded occurrence of soil frost during the investigated period in 2012.

Daily averages of soil moisture varied between 19.7 % and 36.4 % with an overall average of 29.4(±4.6) % and thus showed a similar extent and average compared to 2011. However, variations in the seasonal course of soil moisture were visibly influenced by regional drought conditions, especially in July and August, which led to clearly identifiable low points in the record (Fig. 4.4 E). The minimum 30-minute average for soil moisture occurred on August 8 at 18.2 %, while the maximum was on June 6 at 37.9 %.

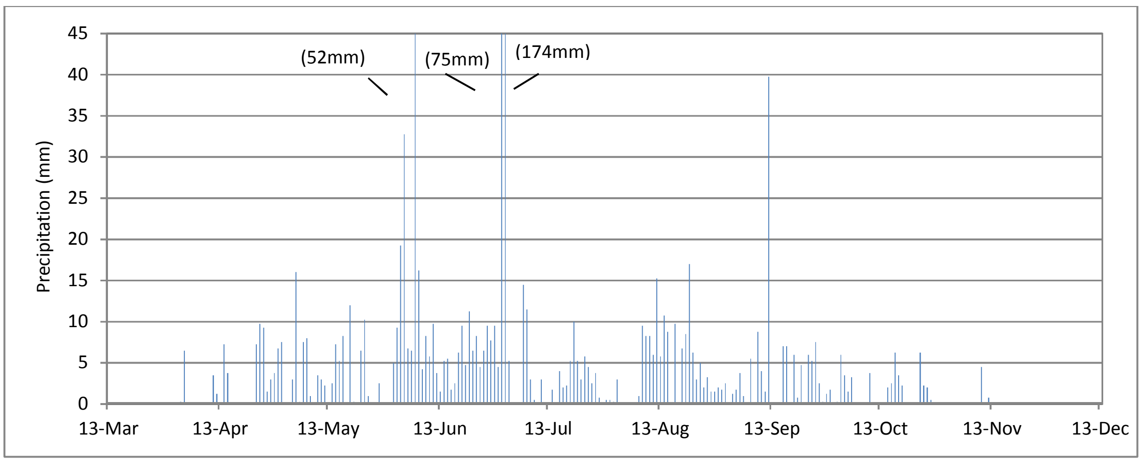

Fig. 4.5: Total daily precipitation (mm; including irrigation) at Fort Logan in 2012

Precipitation totaled 1111 mm during the investigation period (including irrigation between April 23 and October 18), with the wettest month being June (355 mm) (Fig. 4.5). However, precipitation excluding irrigation (as derived from SDT data) showed that the measured amount of precipitation (Mar 13-Dec 11: 232 mm) was noticeably less compared to 2011 (342 mm) and the long-term record of Denver (1981-2010: 381 mm). June, July, and August were months of very little precipitation (Fig. 4.6). This lack of precipitation and restrictions on irrigation led to periods of dramatically reduced water availability, despite the total seasonal amount of precipitation and irrigation being comparable to 2011.

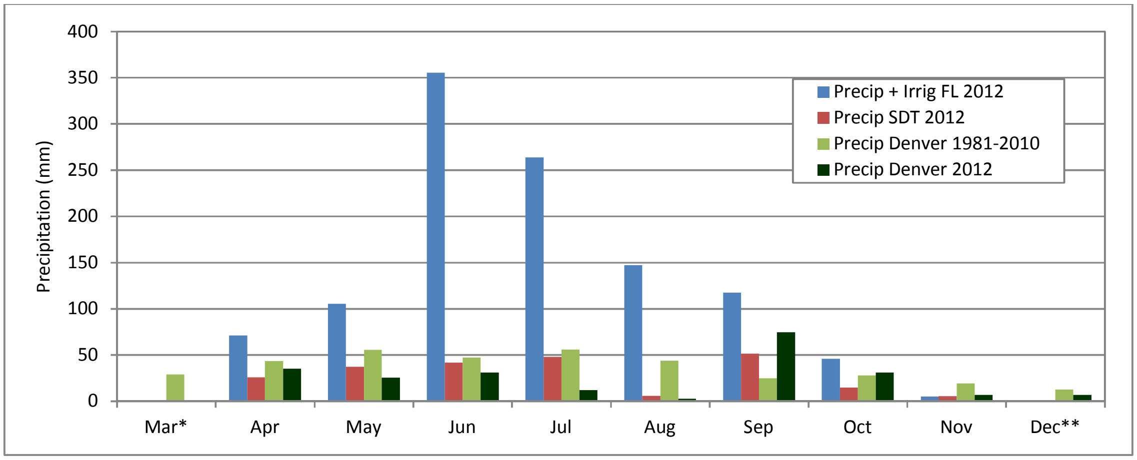

Fig. 4.6: Comparison of monthly precipitation at Fort Logan in 2012 (mm; including irrigation); *monthly total for Fort Logan (FL) and South Denver Tower (SDT) derived from data of March 13-31 2012; **monthly total for Fort Logan and South Denver Tower derived from data of December 1-11 2011

4.1.3. Rocky Flats 2011

Meteorological and soil conditions, i.e. air temperature, relative humidity, barometric pressure, soil temperature, soil moisture, and precipitation at Rocky Flats in 2011 are presented below. The raw data consisted of 30-minute averages (17,520 records; Jan 1 – Dec 31; 365 days). Data coverage for the parameters mentioned above was 98.5 %.

Average air temperature in 2011 was 9.9(± 9.8)°C, with daily means ranging from a minimum of -23.2°C on February 1 to a maximum of 27.3°C on August 23 (Fig. 4.7 A). Over the same period of time as the investigated period at Ft Logan (Mar 17- Nov 17 2011), air temperature averaged to 14.3(±7.6)°C and was therefore 0.6 K lower at Rocky Flats in comparison to the urban site. The lowest 30-minute average occurred on February 2 at -29.2°C and the highest on August 18 at 33.2°C. Similar to the temperature record at Fort Logan (2011), significant temperature fluctuations occurred between May 9-11 and October 24-26, but also between January 28-February 1 (11.1°C to -23.3°C) and between November 28 - December 5 (10.5°C to -16.1°C).

The comparison of monthly averages for 2011 of Rocky Flats with the long-term record for Denver (1981-2010) showed notable differences for February (-2.1 K), April (-1.5 K), May (-4.0 K), and November (+1.2 K) (Tab 4.3). Moreover, Rocky Flats showed similar deviations compared to Fort Logan, i.e. a slightly warmer March and a cooler May. However, when comparing Rocky Flats data (temperature) to data of Denver, it is important to recognize the horizontal separation (ca. 20 km) and vertical difference (approx. 200 m) between these locations.

	Jan	Feb	Mar	Apr	May	Jun	Jul	Aug	Sep	Oct	Nov	Dec
RF 2011	0.4	-1.3	5.8	7.4	10.2	18.9	22.5	23.2	16.7	11.0	5.0	-1.4
Denver 1981-2010	-0.3	0.8	4.8	8.9	14.2	19.7	23.4	22.3	17.3	10.4	3.8	-0.9
Denver 2011	-1.2	-1.6	6.3	9.1	11.7	20.1	24.4	25.0	17.9	11.4	4.2	-3.0

Tab. 4.3: Comparison of mean monthly air temperature (°C) at Rocky Flats in 2011

Daily means for relative humidity varied between 7.6 % (Nov 10) and 96.8 % (May 11), with an annual average of 46.3(±21.0) % (Fig. 4.7 B). Minimum relative humidity for a single 30-minute averaging period was recorded on November 11 at 1.8 %. Large fluctuations occurred throughout the year and, as for Fort Logan, relative humidity at Rocky Flats typically showed a diurnal pattern with maximum values near sunrise and minimum values in the afternoon.

Barometric pressure ranged between daily averages of 79.33 kPa and 82.14 kPa, showing the greatest variability in spring and fall (Fig. 4.7 C). The overall average for 2011 was 80.99(±0.51) kPa.

Similar to Fort Logan, soil temperature followed the seasonal course of air temperature though the amplitude of fluctuations was smaller. The two soil sensors deployed compared well. Daily means for soil temperature varied between -2.5°C (Jan 1) and 27.8°C (Aug 25) for soil sensor “1” and between -3.9°C (Jan 6) and 26.8°C (Aug 25) for soil sensor “2”. The annual average was 11.9(±8.7)°C and 11.4(±8.6)°C for soil sensor “1” and “2”, respectively (Fig. 4.7 D). Soil temperature between March 17 - November 17 (FL 2011) was 16.3(±7.0)°C for sensor “1” and 15.8(±6.8)°C for sensor “2” and therefore 1.0 K and 0.5 K higher in comparison to Fort Logan. Minimum soil temperature for a single 30-minute averaging period was recorded on January 26 at -10.0 °C, while maximum soil temperature was reached on August 25 at 47.0 °C, both at soil sensor “1”. Soil frost occurred on 46 days in 2011, mostly in January and February, but also in March, November, and December.

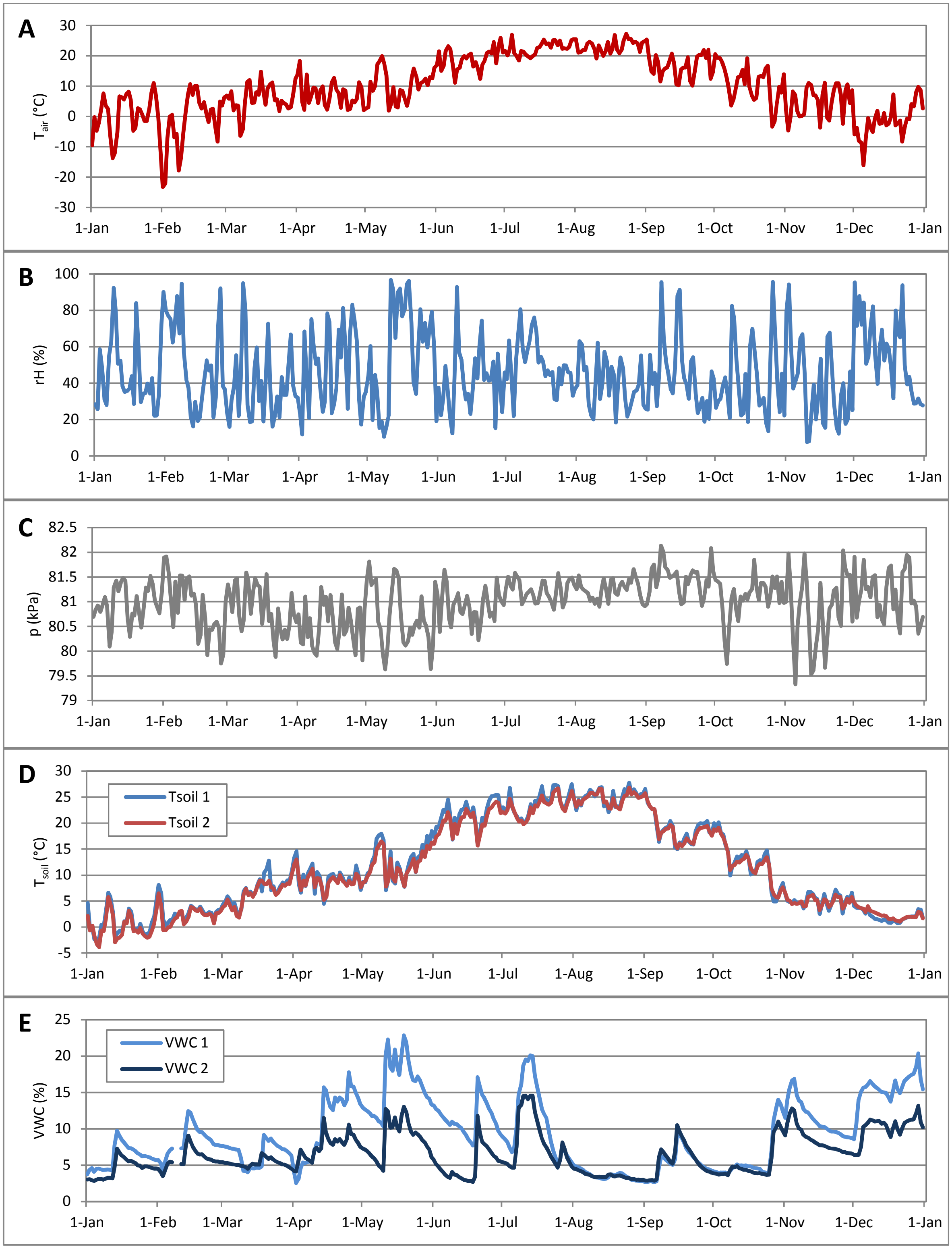

Fig. 4.7: Meteorological and soil conditions at Rocky Flats in 2011: (**A**) Average daily air temperature (°C), (**B**) Average daily relative humidity (%), (**C**) Average daily barometric pressure (kPa), (**D**) Average daily soil temperature (°C) , (**E**) Average daily soil moisture (VWC, %)

Daily means for soil moisture varied between 2.6 % and 22.8 % for soil sensor "1" and between 2.7 % and 14.6 % for soil sensor "2" (Fig. 4.7 E). The annual average was 9.3(±4.8) % and 6.5(±2.8) % for soil sensor "1" and "2", respectively. Variations in the seasonal course of soil moisture were strongly influenced by precipitation events. The lowest (1.8 %, soil sensor "2") and highest 30-minute average (25.5 %, soil sensor "1") were recorded on June 18 and May 18, respectively.

Recorded precipitation at Rocky Flats in 2011 summed up to 454 mm (Denver 1981-2010: 381 mm), with the wettest month being May at 113 mm (Fig. 4.8). Precipitation in May, June, and July accounted for more than 50 % of total annual precipitation and was mainly associated with thunderstorm activity.

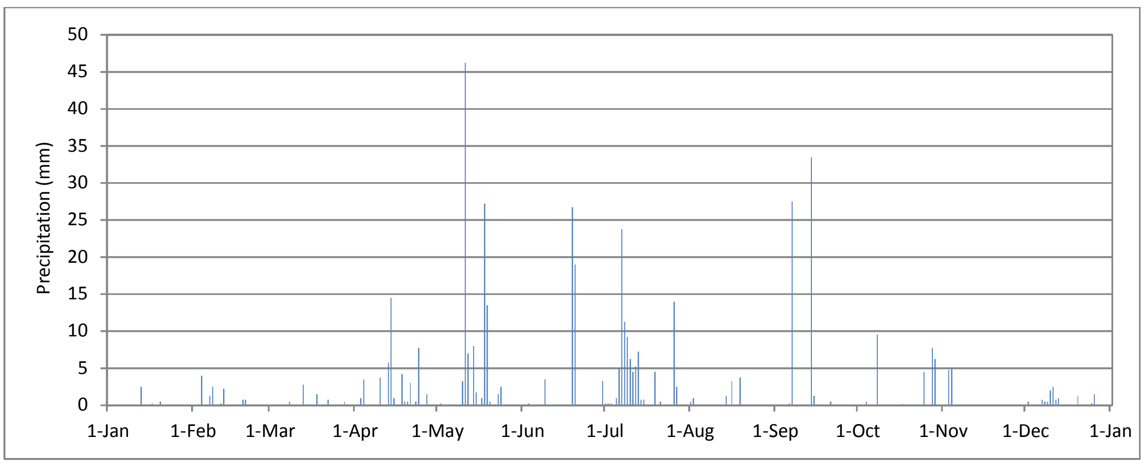

Fig. 4.8: Total daily precipitation (mm) at Rocky Flats in 2011

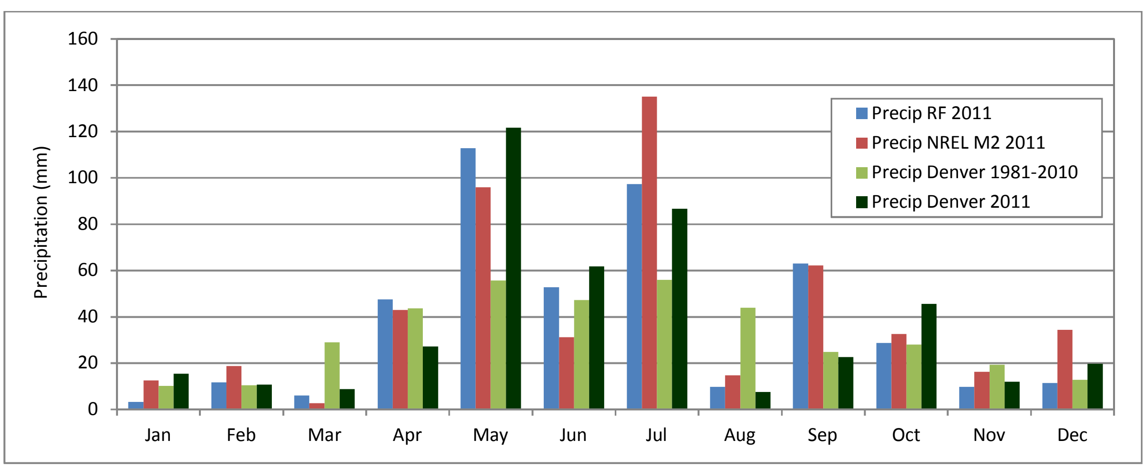

Fig. 4.9: Comparison of monthly precipitation (mm) at Rocky Flats in 2011

Comparing monthly precipitation sums (RF 2011) with monthly means of Denver (1981-2010) revealed that noticeable deviations from the long-term record occurred in March (-23.0 mm), May (+57.1 mm), July (+41.3 mm), and August (-34.1 mm), with the precipitation record for Denver (2011) showing a similar trend (Fig. 4.9). Larger differences between Rocky Flats and data from the NREL Tower M2 occurred in December and January, which may be due to the use of a non-heated precipitation gage at Rocky Flats. Differences in May, June, and July could be the result of localized thunderstorms.

4.1.4. Rocky Flats 2012

Data for meteorological and soil parameters at Rocky Flats in 2012 are presented below. The raw data consisted of 30-minute averages (17,568 records; Jan 1 – Dec 31; 366 days). Data coverage for the parameters mentioned above exceeded 99 %, except for soil moisture sensor "1", where data coverage was 91.1 %.

For 2012, average annual air temperature was 11.7(± 9.6)°C and thus nearly 2 K higher than in 2011. Daily means ranged from a minimum of -13.4°C on December 25 to a maximum of 29.7°C on June 23 (Fig. 4.10 A). Between March 13 and December 11 (FL 2012), average air temperature was 15.3(±7.6)°C, 0.2 K higher than at the urban site. December 25 marked the lowest 30-minute average recorded at -17.7°C, June 25 the highest at 36.6°C. As for Fort Logan, large temperature fluctuations occurred between April 1-3 and between December 5-9, but also, for example, between January 17-19 (-8.2°C to 11.3°C) and October 2-6 (19.4°C to -1.1°C).

Monthly averages of air temperature for 2012 showed notable differences for January (+3.6 K), February (-2.4 K), March (+4.5 K), April (+2.1 K), Jun (+2.9 K), November (+3.6 K), and December (+1.3 K) when compared to the long-term record for Denver (1981-2010) (Tab 4.4). Thus, Rocky Flats showed similar deviations as Fort Logan, i.e. a warmer March, April, and June. Again, it is important to recognize the horizontal and vertical separation between these locations when comparing Rocky Flats data to data of Denver.

	Jan	Feb	Mar	Apr	May	Jun	Jul	Aug	Sep	Oct	Nov	Dec
RF 2012	3.3	-1.6	9.3	11.0	14.2	22.6	23.2	22.4	17.8	9.5	7.4	0.4
Denver 1981-2010	-0.3	0.8	4.8	8.9	14.2	19.7	23.4	22.3	17.3	10.4	3.8	-0.9
Denver 2012	2.2	-2.0	9.6	11.8	15.8	23.9	26.1	23.9	19.1	9.4	6.4	-0.4

Tab. 4.4: Comparison of mean monthly air temperature (°C) at Rocky Flats in 2012

Relative humidity averaged to 41.3(±21.1) % in 2012, 5 % lower than in 2011. Daily means varied between 9.9 % and 99.4 % (June 18/23 and October 25, respectively) (Fig. 4.10 B). The lowest value for relative humidity was recorded on April 6 at 2.6 %.

Statistical parameters for barometric pressure were very similar in 2012 compared to 2011: The annual average amounted to 80.97(±0.54) kPa, while daily means ranged between 79.37 kPa and 82.21 kPa (Fig. 4.10 C).

Daily averages for soil temperature varied between -2.9°C (Dec 29) and 29.1°C (Jun 23) for soil sensor “1” and between -1.5°C (Dec 31) and 29.5°C (Jun 25) for soil sensor “2”. Thus, both sensors showed a slightly increased temperature span compared to 2011. Annual averages were 12.5(±8.8)°C and 12.7(±9.0)°C for soil sensor “1” and “2”, respectively (Fig. 4.10 D). Soil temperature between March 13 - December 11 (FL 2012) averaged to 16.0(±7.2)°C for sensor “1” and 16.4(±7.4)°C sensor “2”. These values were 1.7 K and 2.1 K higher in comparison to the urban site. Minimum soil temperature was recorded on December 29 at -5.9°C, while a maximum was reached on June 23 at 44.5°C (both values for soil sensor “1”). Soil frost occurred on 47 days in 2012, mostly in January and December.

Soil moisture varied over the course of the year between 2.7 % and 20.7 % for soil sensor “1” and between 2.4 % and 13.7 % for soil sensor “2” (Fig. 4.10 E). Annual averages were slightly lower than in 2011 at 8.1(±3.7) % and 5.6(±2.5) % for soil sensor “1” and “2”, respectively. In the absence of irrigation, variations were again strongly influenced by precipitation events. The minimum (1.7 %, soil sensor “2”) and maximum values (24.0 %, soil sensor “1”) were recorded on September 10 and February 22, respectively.

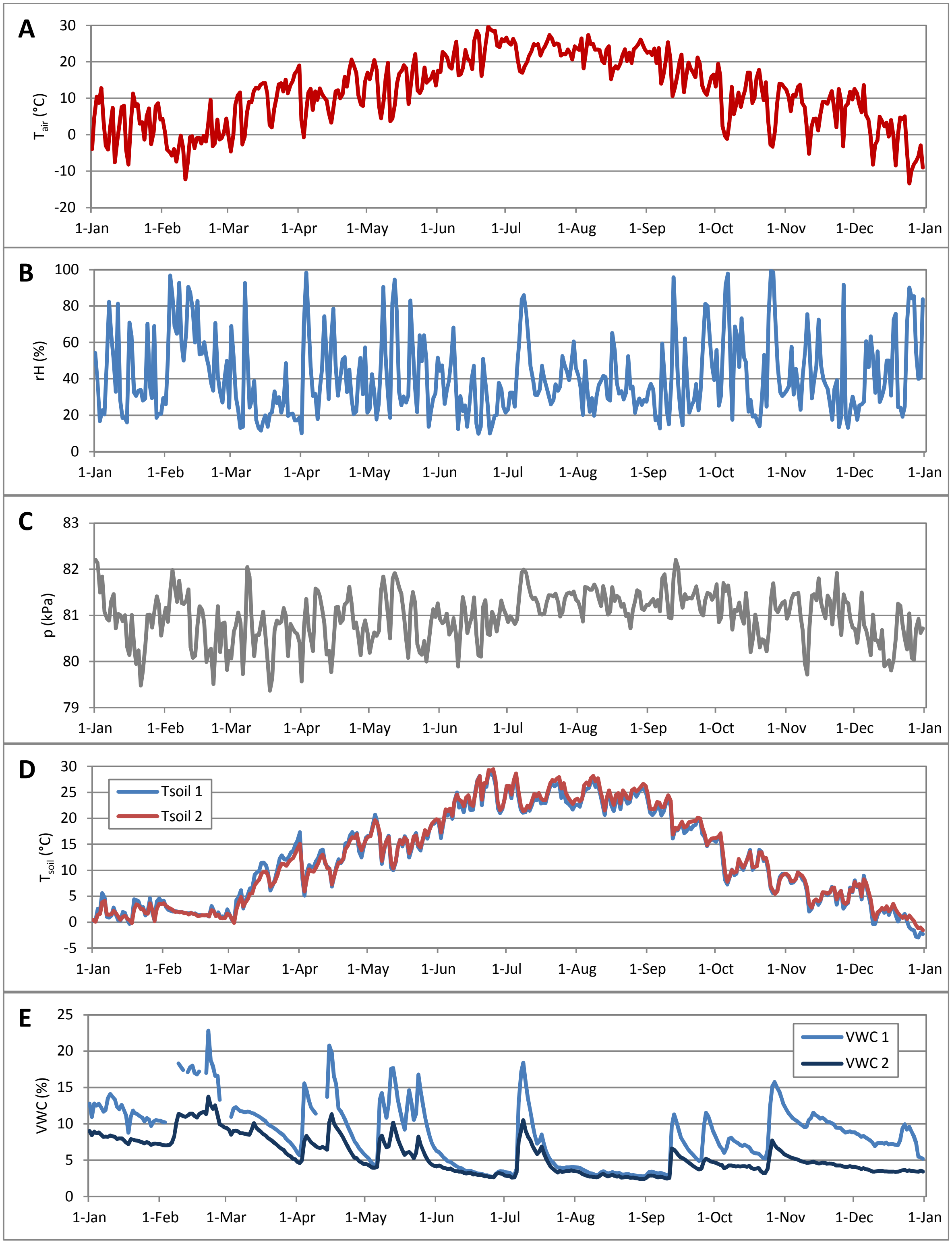

Fig. 4.10: Meteorological and soil conditions at Rocky Flats in 2012: (**A**) Average daily air temperature (°C), (**B**) Average daily relative humidity (%), (**C**) Average daily barometric pressure (kPa), (**D**) Average daily soil temperature (°C) , (**E**) Average daily soil moisture (VWC, %)

Precipitation in 2012 summed to 269 mm with the wettest month being July at 68 mm (Fig. 4.11). The annual total was 29 % below the 1981-2010 climatic mean for Denver. Noticeable deviations from the long-term average occurred especially during the summer months (Fig. 4.12).

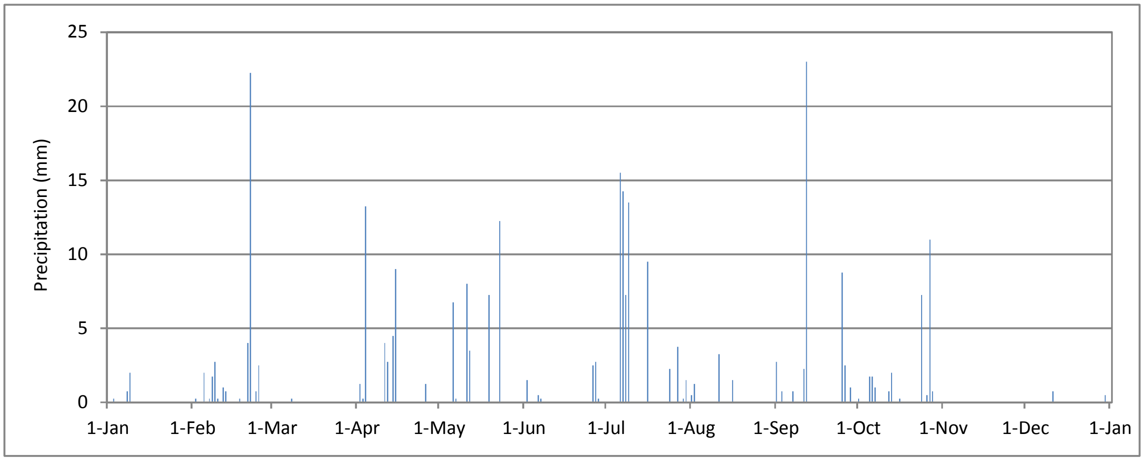

Fig. 4.11: Total daily precipitation (mm) at Rocky Flats in 2012

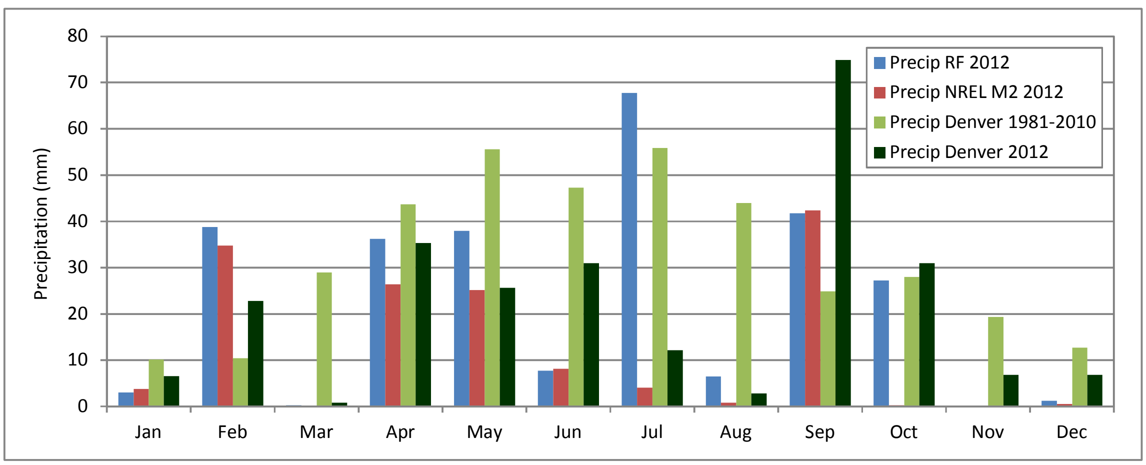

Fig. 4.12: Comparison of monthly precipitation (mm) at Rocky Flats in 2012

4.1.5. Comparison of Air and Soil Temperatures at Fort Logan and Rocky Flats

Monthly averages of air and soil temperature at Fort Logan and Rocky Flats in 2011 and 2012 are shown in Fig. 4.13. For reasons of comparability, only full months based on the shortest investigation period, i.e. Fort Logan 2011, are presented.

As described in the previous sections, monthly air temperatures at Fort Logan and Rocky Flats deviated at times from the long-term means of Denver (1981-2010), most notably in spring and early summer, which also resulted in differences between the investigated years. As illustrated in Fig. 4.13 A, April through June showed the largest differences between years at both sites, with 2012 being the warmer year. At Fort Logan, these differences between April and June amounted to +3.1 K, +3.9 K, and +2.4 K, respectively, when comparing 2012 to 2011. Rocky Flats displayed even slightly larger differences at +3.6 K, +4.0 K, and +3.7 K, although temperature averages during these months were generally lower compared to Fort Logan. Differences in July through September were less pronounced and usually less than 1 K at both sites. In contrast to the warmer April-June of 2012, October 2012 was cooler at both sites compared to 2011, deviating by -1.5 K from the previous year. The average temperature between April and October at Fort Logan was 16.3°C in 2011 and 17.4°C in 2012. For Rocky Flats, the respective values are 15.7°C and 17.3°C.

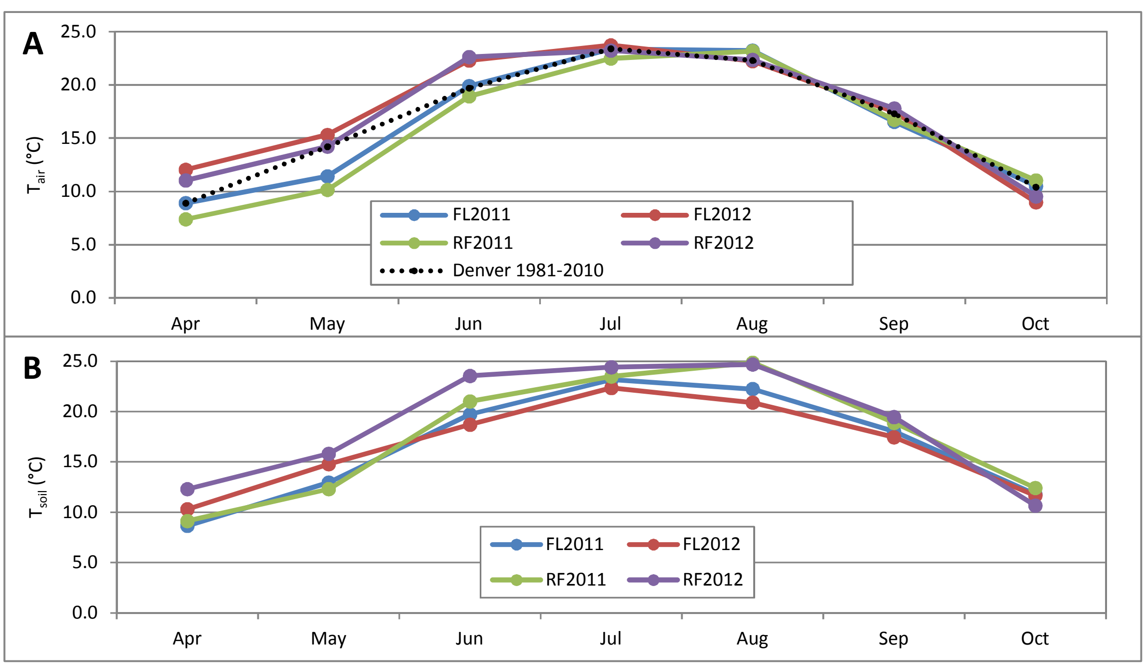

Fig. 4.13: Comparison of monthly averages of (**A**) air temperature (°C) and (**B**) soil temperature (°C) at Fort Logan and Rocky Flats in 2011 and 2012

Comparing soil temperatures at Rocky Flats between years showed a similar pattern as air temperature (Fig. 4.13 B). Here, monthly averages were +3.2 K, +3.5 K, and +2.5 K higher in April-June of 2012 than in 2011. Also, similar to air temperature, October 2012 was cooler by -1.7 K compared to the previous year. At Fort Logan, differences in soil temperature between years were smaller than at Rocky Flats, reaching +1.6 K and +1.8 K in April and May of 2012 compared to 2011. Monthly soil temperatures in June and August were slightly cooler in 2012 (-1.0 K and -1.3 K) than in 2011, while the remaining months showed differences of less than 1 K. Moreover, Fort Logan usually showed slightly lower soil temperatures compared to Rocky Flats. The overall average of soil temperature between April and October at Fort Logan figured to 16.7°C in 2011 and 16.6°C in 2012. The respective values for Rocky Flats are 17.4°C and 18.7°C.

4.2. Wind and Turbulence Conditions

4.2.1. Fort Logan

Data on wind and turbulence conditions (i.e. frequency of wind direction, wind speed by wind sector as well as seasonal course of wind speed, friction velocity, and average fetch) for the 2011 and 2012 seasons at Fort Logan are presented below. Raw data consisted of 30-minute averages (2011: 11,808 records; 2012: 13,152 records) and covers the time between March 17 and November 17 2011, and between March 13 and December 11 2012. Gaps in the wind data record were not filled. Data coverage was 92.5 % and 95.8 % in 2011 and 2012, respectively.

In 2011, wind frequency distribution by quadrants was as follows: NE (0°-90°): 22.4 %, SE (90°-180°): 17.9 %, SW (180°-270°): 39.2 %, and NW (270°-360°): 20.4 %. Thus, winds from the southwest dominated during the investigated period. Especially prevalent were winds between 180°-230° which made up 25.4 % of all valid records (Fig. 4.14 A).

Analysis of wind speed by sector showed that the highest values were observed for winds coming from the north, i.e. the NE-quadrant (2.0 m s^{-1}) and the NW-quadrant (2.2 m s^{-1}). Winds from the SE-quadrant averaged to 1.7 m s^{-1}, while winds from the SW, the most dominant direction, were the lightest at 1.4 m s^{-1} (Fig. 4.14 B).

Wind frequency distribution in 2012 showed a similar pattern compared to 2011, with a clear dominance of winds from the southwest. In detail, winds from the NE-quadrant occurred 21.2 %, SE 18.4 %, SW 42.7 %, and from the NW-quadrant 17.7 % of the time. Compared to 2011, the share of southwest winds had increased (+3.5 %), while the proportion of winds from the NW had decreased (-2.7%). Winds of the sectors 180°-230° occurred more than a quarter of the investigated time frame (27.8%). Extending this range to 180°-240° increased the share to nearly one-third (32.8 %) (Fig. 4.14 C).

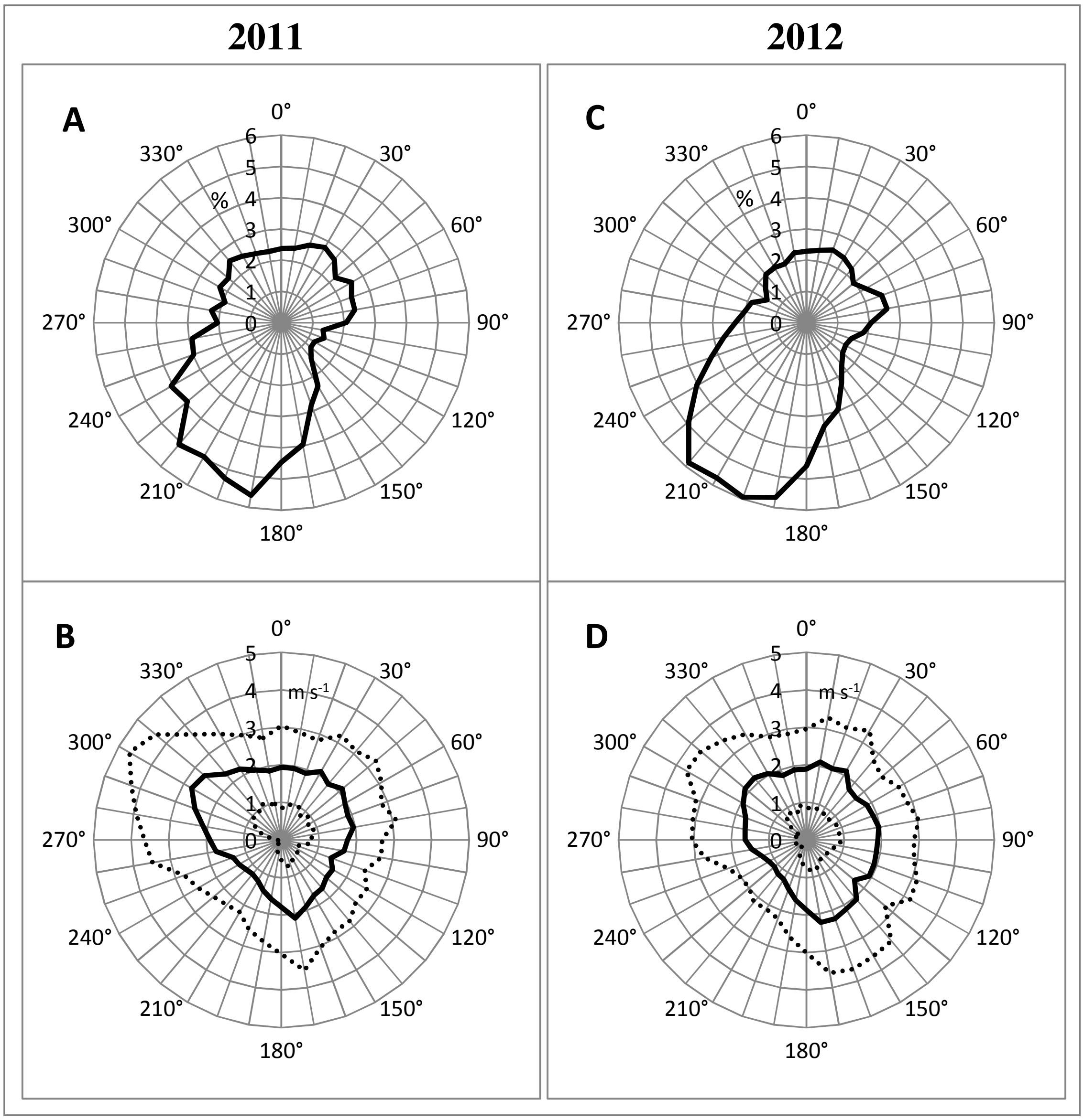

Fig. 4.14: Wind conditions at Fort Logan in 2011 and 2012: (**A+C**) Radar plots of frequency of wind direction (%) and (**B+D**) wind speed (m s^{-1}); solid line represents 10°-sector averages, dotted lines represent ±1 SD

Sectoral wind speeds in 2012 closely resembled conditions observed in 2011. Winds from the NE and NW-quadrants both averaged to 1.9 m s^{-1}, while winds from the SE-quadrant were slightly higher than in 2011 at 2.0 m s^{-1}. The lightest winds on average came, again, from the southwest at 1.4 m s^{-1} (Fig. 4.14 D).

Over the course of the investigated period, wind speeds averaged to 1.8(±1.3) m s^{-1} in 2011. Noteworthy calm periods (less-than-average wind speeds) occurred in the July, August, and September, while the spring and autumn months of March, April, October, and November showed higher wind speeds and greater variability (Fig. 4.15 A).

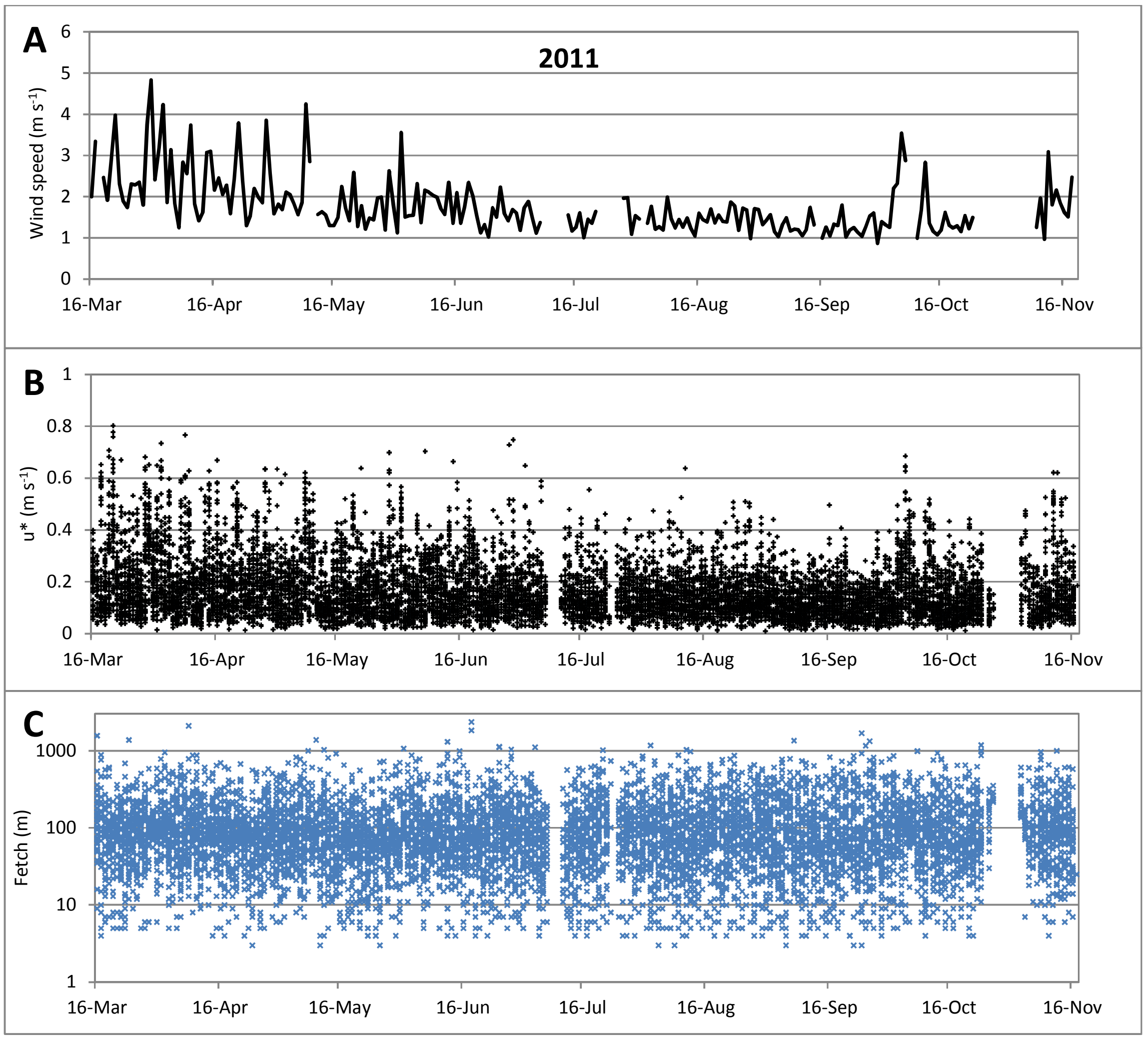

Fig. 4.15: Wind speed, friction velocity $u*$, and fetch at Fort Logan in 2011: (**A**) Daily averages of wind speed (m s^{-1}), (**B**) 30-minute averages of $u*$ (m s^{-1}) and (**C**) 30-minute averages of fetch (m) (70% flux contribution; $u* > 0.05$ m s^{-1}); days with more than 10 % missing/invalid data were omitted from the calculation of daily averages

Friction velocity (u*) averaged to 0.17(±0.11) m s^{-1} in 2011 with a range of 0.01-1.27 m s^{-1} (Fig. 4.15 B). Averaging periods of low turbulence (u*<0.05 m s^{-1}) made up 6.2 % of all valid data. These periods occurred mainly at night and were excluded from further analysis (Fig. 4.17 A). Fetch (70 % flux contribution; u*>0.05 m s^{-1}) averaged to 117(±136) m (Fig. 4.15 C).

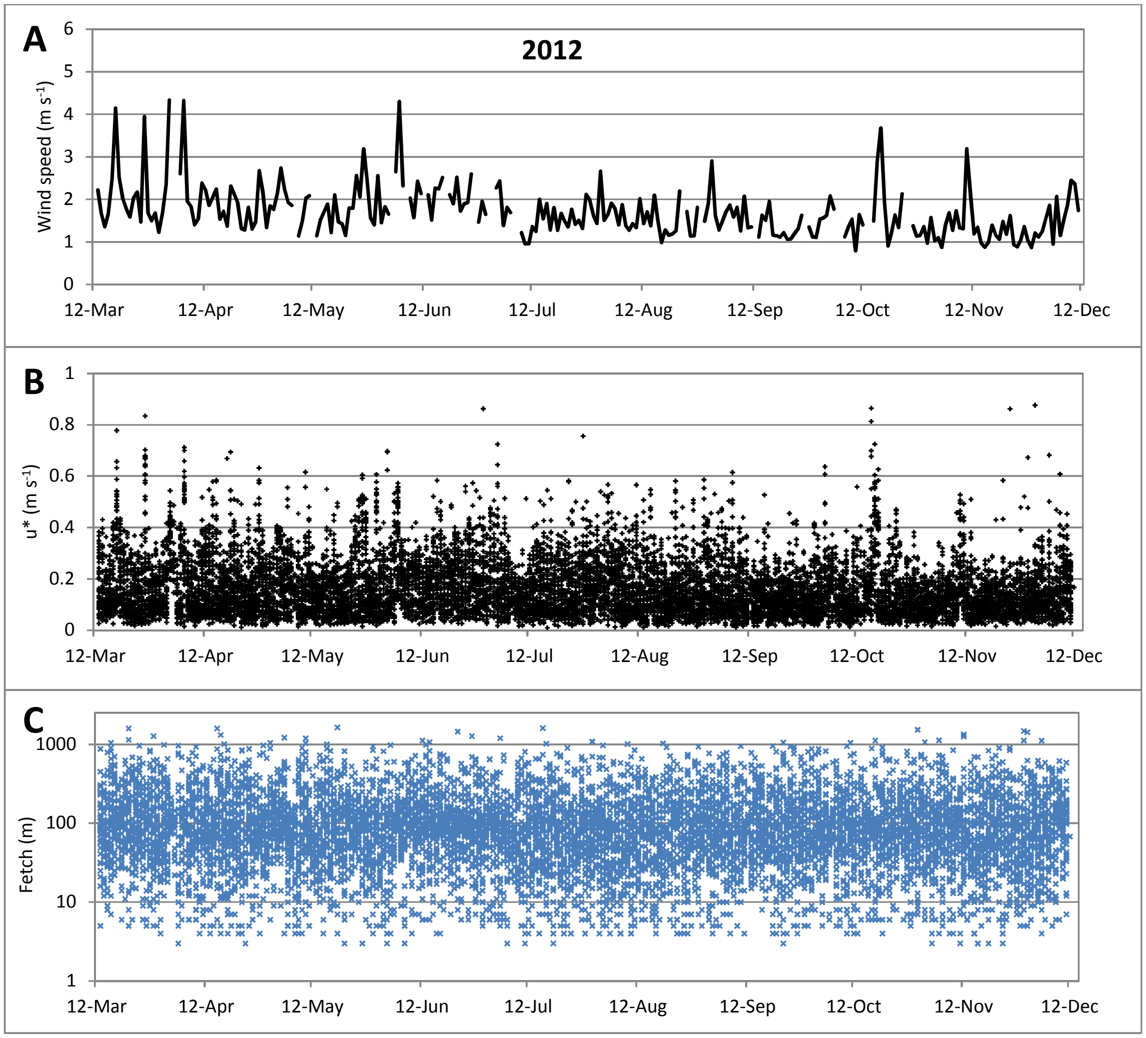

Fig. 4.16: Wind speed, u*, and fetch at Fort Logan in 2012: (**A**) Daily averages of wind speed (m s^{-1}), (**B**) 30-minute averages of u* (m s^{-1}) and (**C**) 30-minute averages of fetch (m) (70% flux contribution; u* > 0.05 m s^{-1}); days with more than 10 % missing/invalid data were omitted from the calculation of daily averages

Wind speeds in 2012 closely resembled conditions in 2011 by averaging to 1.7(±1.2) m s^{-1} and showing similar "calm periods" during the summer months (Fig. 4.16 A). Friction velocity averaged to 0.16(±0.11) m s^{-1} in 2012 with a range of 0.01-1.24 m s^{-1} (Fig. 4.16 B).

Averaging periods of low turbulence (u*<0.05 m s^{-1}) made up 8.7 % of all valid data in 2012. Fetch (70 % flux contribution; u*>0.05 m s^{-1}) averaged to 124(±147) m (Fig. 4.16 C).

Figure 4.17 (A) displays the diurnal course of *u** at Fort Logan. Friction velocity was, on average, highest in the early afternoon (13:30-14:30) at 0.25(±0.12) m s^{-1} and lowest before sunrise (5:00-6:00) at 0.12(±0.08) m s^{-1}. This pattern corresponded well with wind speed, where highest values were reached between 14:30-15:30 at 2.5(±1.5) m s^{-1} and lowest between 5:30-6:30 at 1.1(±0.9) m s^{-1}, and confirmed the strong relation found between wind speed and *u** (Fig. 4.17 B).

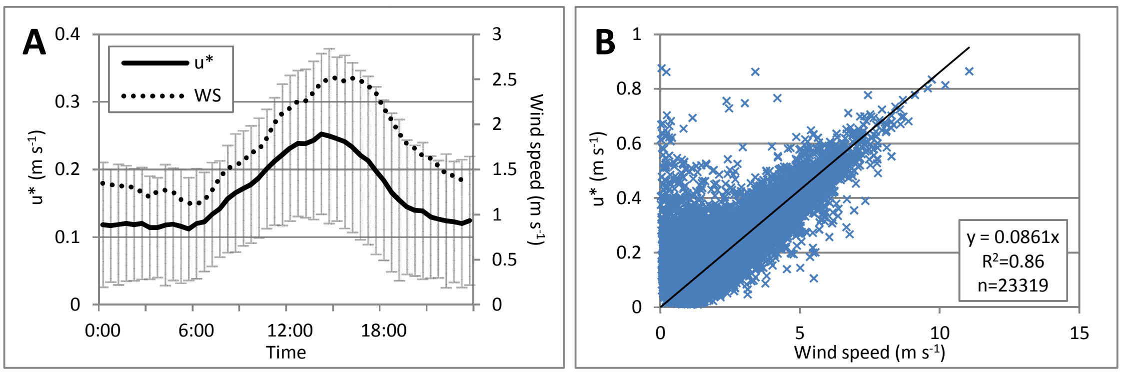

Fig. 4.17: (**A**) Diurnal trends of *u** (m s^{-1}) and wind speed (m s^{-1}) (error bars ±1 SD) and (**B**) relation between wind speed (m s^{-1}) and *u** (m s^{-1}) at Fort Logan (data: Fort Logan 2011+2012)

The diurnal course of fetch at Fort Logan is shown in Fig. 4.18 (A). Fetch was longest between 20:30-22:30 at 200(±214) m and shortest between 9:30-10:30 at 47(±34) m. Figure 4.18 (B), displaying the relation between *u** and fetch, illustrates the effect of *u**-filtering: By excluding data when *u** was smaller than 0.05 m s^{-1}, fluxes potentially originating outside the investigated area or recorded during times of insufficiently developed turbulence were excluded from further analysis.

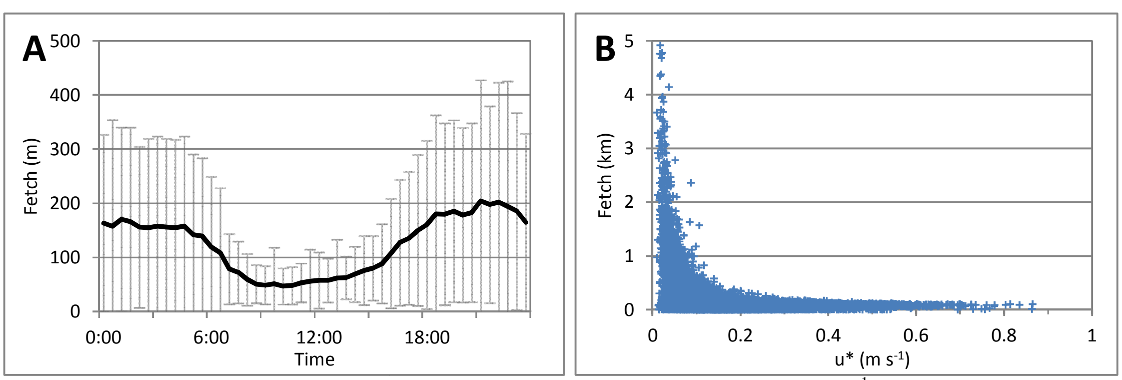

Fig. 4.18: (**A**) Diurnal trends of fetch (m) (70% flux contribution; u*>0.05 m s^{-1}; error bars ±1 SD) and (**B**) relation between *u** (m s^{-1}) and fetch (km) at Fort Logan (data: Fort Logan 2011+2012)

4.2.2. Rocky Flats

Data on wind and turbulence conditions for 2011 and 2012 at Rocky Flats are presented below. Raw data consisted of 30-minute averages (2011: 17,520 records, 2012: 17,568 records). Gaps in the wind data record were not filled. Data coverage was 93.9 % and 95.6 % in 2011 and 2012, respectively.

Wind frequency distribution in 2011 by quadrants was as follows: NE (0°-90°): 16.5 %, SE (90°-180°): 17.3 %, SW (180°-270°): 27.3 %, and NW (270°-360°): 39.0 %. Winds from westerly directions clearly dominated in 2011, in particular winds between 260°-290° which made up 23.1 % of all valid records (Fig 4.19 A).

Analysis of wind speed by sector showed that the highest values were observed for winds coming from westerly directions, i.e. the NW-quadrant (3.3 m s^{-1}) and the SW-quadrant (2.7 m s^{-1}). Winds from the SE and NE-quadrants averaged to 2.1 m s^{-1} and 2.2 m s^{-1}, respectively (Fig. 4.19 B).

In 2012, wind frequency distribution showed a pattern comparable to 2011 with a clear dominance of winds from the west. In detail, winds from the NE-quadrant occurred 15.5 %, SE 18.5 %, SW 29.2 %, and from the NW-quadrant 36.7 % of the time. Similar to 2011, winds of the sector 250°-280° made up 24.5 % of the data. (Fig. 4.19 C).

Wind speeds by quadrants in 2012 closely resembled conditions observed in 2011. Winds from the NW and SW-quadrants were highest at 2.9 m s^{-1} and 2.8 m s^{-1}, respectively, while winds from the SE-quadrant were slightly higher than in 2011 at 2.5 m s^{-1}. The lightest winds on average came from the northeast at 2.3 m s^{-1} (Fig. 4.19 D).

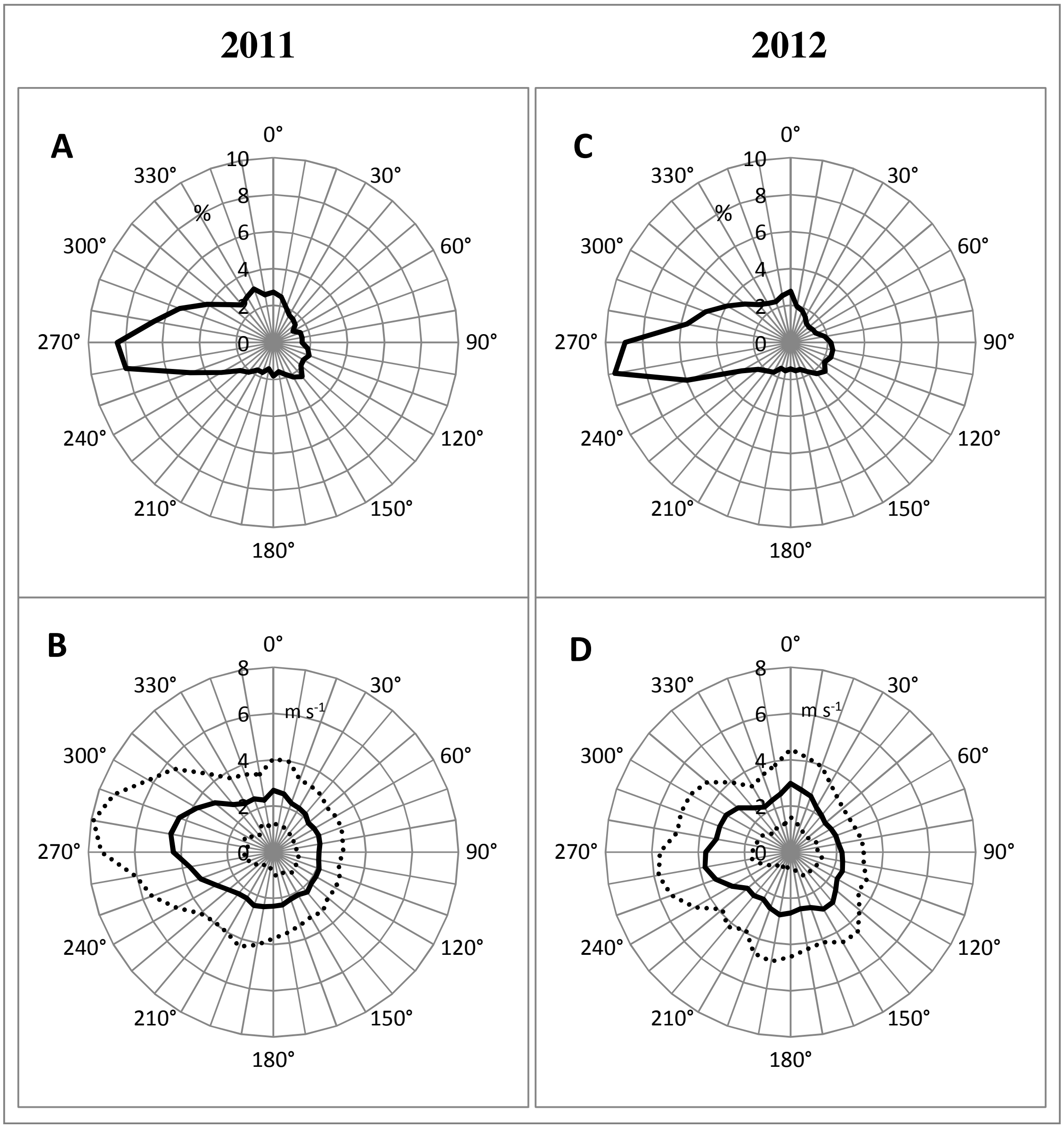

Fig. 4.19: Wind conditions at Rocky Flats in 2011 and 2012: (**A+C**) Radar plots of frequency of wind direction (%) and (**B+D**) wind speed (m s^{-1}) at Rocky Flats in 2011 and 2012; solid line represents 10°-sector averages, dotted lines represent ±1 SD

Over the course of the year, wind speeds averaged to 3.0(±2.2) m s^{-1} in 2011 and (similar to Fort Logan) showed a period of calmer conditions in July through September. In contrast, January through April was characterized by higher wind speeds and greater variability due to seasonal weather patterns (Fig. 4.20A).

Friction velocity at Rocky Flats averaged to 0.26(±0.19) m s^{-1} in 2011 with a range of 0.01-1.30 m s^{-1} (Fig. 4.20 B). Periods of low turbulence ($u^*<0.11$ m s^{-1}) made up 18.0 % of all valid data. Again, these periods occurred mainly at night when winds were light and were excluded from further analysis (Fig. 4.22 A). Fetch (70 % flux contribution; u*>0.11 m s^{-1}) averaged to 162(±171) m (Fig. 4.20 C).

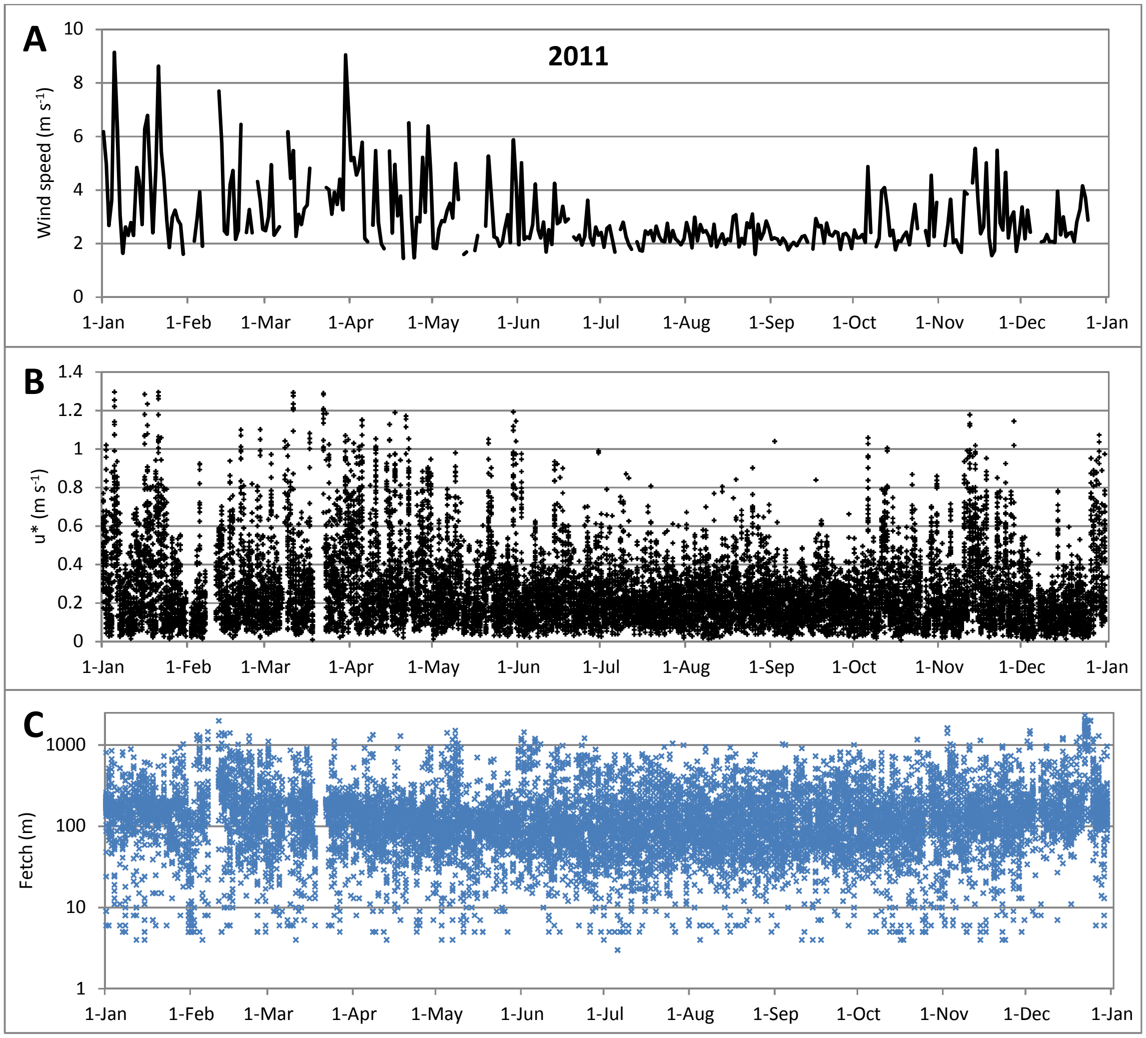

Fig. 4.20: Wind speed, *u**, and fetch at Rocky Flats in 2011: (**A**) Daily averages of wind speed (m s^{-1}), (**B**) 30-minute averages of *u** (m s^{-1}) and (**C**) 30-minute averages of fetch (m) (70% flux contribution; u* > 0.11 m s^{-1}); days with more than 10 % missing/invalid data were omitted from the calculation of daily averages

Mean wind speed in 2012 was 2.9(±1.7) m s^{-1}, very similar to the previous year but showing slightly less variability (Fig. 4.21 A). This holds also true for *u** which averaged to 0.25(±0.16) m s^{-1} in 2012 with a range of 0.01-1.30 m s^{-1} (Fig. 4.21 B). Periods of low turbulence (u*<0.11 m s^{-1}) made up 16.2 % of all valid data and were, again, omitted from further analysis. Fetch (70 % flux contribution; u*>0.11 m s^{-1}) averaged to 165(±162) m (Fig. 4.21 C).

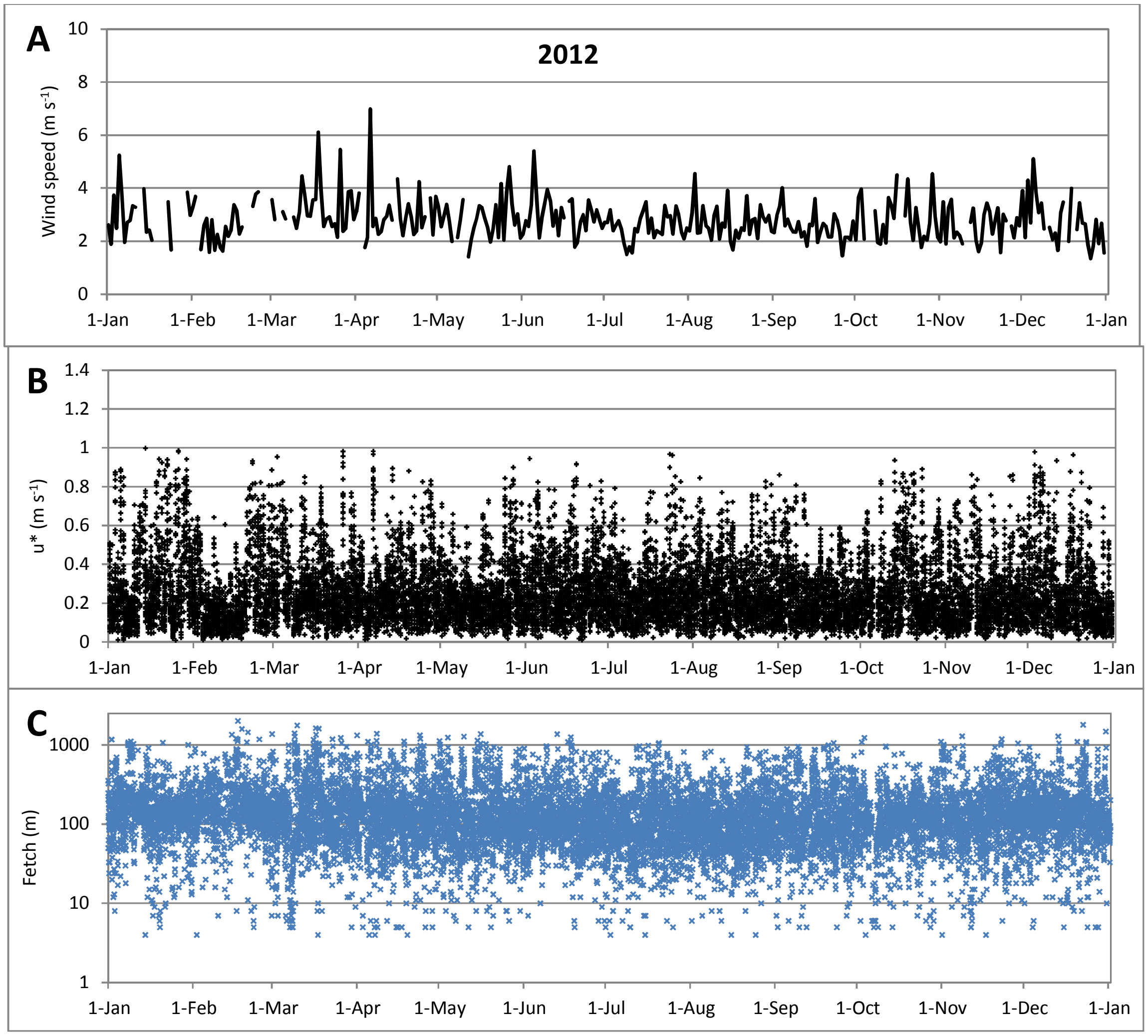

Fig. 4.21: Wind speed, *u**, and fetch at Rocky Flats in 2012: (**A**) Daily averages of wind speed (m s^{-1}), (**B**) 30-minute averages of *u** (m s^{-1}) and (**C**) 30-minute averages of fetch (m) (70% flux contribution; u* > 0.11 m s^{-1}); days with more than 10 % missing/invalid data were omitted from the calculation of daily averages

The diurnal course of *u** at Rocky Flats is shown in Fig. 4.22 (A). Highest values for *u** occurred, on average, in the early afternoon (13:30-14:30) at 0.32(±0.18) m s^{-1} and lowest before sunrise (5:00-6:00) at 0.21(±0.17) m s^{-1}. Similar to Fort Logan, *u** showed a clear relation to wind speed (Fig, 4.22 B), where highest values were reached, on average, between 15:30-16:30 at 3.4(±2.3) m s^{-1} and lowest between 6:00-7:00 at 2.6(±2.0) m s^{-1}.

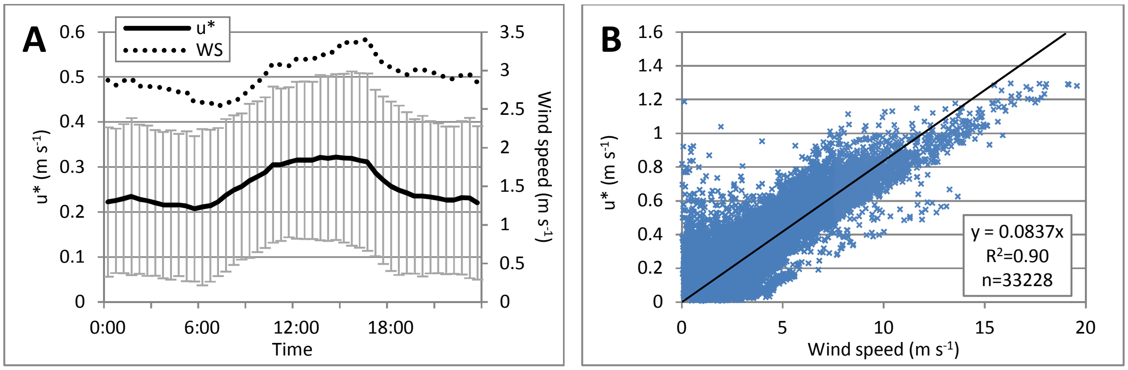

Fig. 4.22: (**A**) Diurnal trends of *u** (m s^{-1}) and wind speed (m s^{-1}) (error bars ±1 SD) and (**B**) relation between wind speed (m s^{-1}) and *u** (m s^{-1}) at Rocky Flats (data: Rocky Flats 2011+2012)

Analysis of the diurnal course of fetch at Rocky Flats showed that, on average, fetch was longest between 21:00-22:00 at 250 (±208) m and shortest between 10:30-11:30 at 80 (±59) m (Fig 4.23 A).

The relation between *u** and fetch at Rocky Flats is illustrated in Fig. 4.23 (B). Similar to Fort Logan, the Rocky Flats dataset was u*-filtered, i.e. data when *u** was smaller than 0.11 m s^{-1} was excluded. This eliminated flux data potentially originating from outside the investigated area or derived during times of insufficiently developed turbulence.

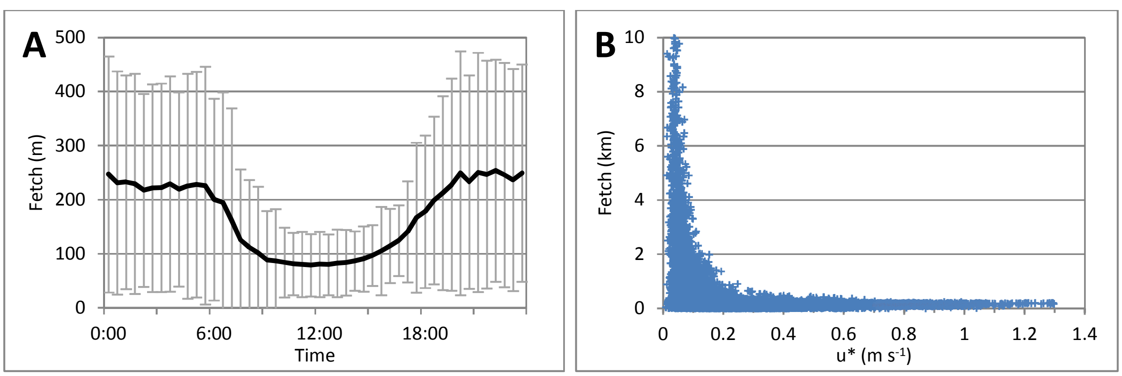

Fig. 4.23: (**A**) Diurnal trends of fetch (m) (70% flux contribution; u*>0.11 m s^{-1}; error bars ±1 SD) and (**B**) relation between *u** (m s^{-1}) and fetch (km) at Rocky Flats (data: Rocky Flats 2011+2012)

4.3. Energy Fluxes

4.3.1. Fort Logan 2011

Energy fluxes (shortwave radiation R_s, net radiation R_n, soil heat flux G, sensible heat flux H, and latent heat flux LE) for the 2011 season at Fort Logan are presented below. The raw data consisted of 30-minute averages (11,850 records; Mar 16 – Nov 18). Valid data for R_s, R_n, and G covered 95.2 %, 95.1 %, and 93.1 % of the investigation period, respectively. Gaps in the data for turbulent fluxes amounted to 25.2 % for H and 32.2 % for LE.

Data for R_s at Fort Logan in 2011 are shown in Figure 4.24 (A) and indicate the prevalence of generally sunny conditions. Instances of prolonged low solar radiation were few, with the most notable periods occurring in mid-May and early September. Peak values averaged to 900(±44) W m^{-2} in March, 1013(±85) W m^{-2} in June, and 948(±71) W m^{-2} in August. During the fall months of September through November, averages for daily maxima gradually declined from 783(±170) W m^{-2} to 670(±146) W m^{-2}, and finally to 553(±56) W m^{-2}.

Net radiation showed its greatest diurnal variation in June and July, when daytime values reached peaks of, on average, 573(±124) W m^{-2} and 545(±106) W m^{-2}, respectively, while nighttime values showed lowest averages of around -37(±11) W m^{-2}. Highest R_n was measured in May and June, when values exceeded 700 W m^{-2} at times. Parallel to R_s, R_n gradually declined between September and November, from average daytime peaks of 432(±137) W m^{-2} to 242(±73) W m^{-2}. Snowfall events (May 11, Oct 25, Nov 2), i.e. fresh snow cover, clearly impacted the regular diurnal pattern of R_n, resulting in reduced daytime and increased nighttime values (Fig. 4.24 B, Fig. 4.25).

Soil heat flux (upward fluxes away from the soil surface towards the atmosphere are positive) showed a strong relation to R_n, almost mirroring its seasonal course. In March, the average diurnal range spanned from -116(±47) W m^{-2} in mid-morning to 52(±26) W m^{-2} in early evening. By June, this span had widened to -172(±50) W m^{-2} and 62(±16) W m^{-2}, respectively. Past the summer solstice, the magnitude of fluxes declined again, reaching the overall lowest diurnal variation (of 2011) in November, when, on average, daytime values peaked at -28(±13) W m^{-2} and nighttime values at 22(±5) W m^{-2} (Fig. 4.24 C, Fig. 4.25).

Diurnal variation for H was greatest in March with daytime averages as high as 174(±50) W m^{-2}, clearly exceeding LE. Nighttime means in March were as low as -36 (±20) W m^{-2}. In

April, *H* had about the same magnitude as *LE* during the day, peaking at about 130 (±63) W m^{-2}. Early May, coinciding with the start of irrigation, displayed a notable drop in daytime values for *H*. From then on, values did rarely exceed 100 W m^{-2} until the end of the investigated period in November. Lowest diurnal averages during the day were observed in July and August at 27(±21) W m^{-2}. After irrigation had stopped in early October, daytime values increased again to a diurnal average of about 50 W m^{-2} (Fig. 4.24 D, Fig. 4.25).

Daytime values for *LE* showed a nearly opposite seasonal course to *H*, while nighttime values always trended towards zero. Average peak values in March and April were 93(±21) W m^{-2} and 128(±61) W m^{-2}, respectively. Following the start of irrigation in May, daytime peaks displayed a marked step-up in values to, on average, 195(±120) W m^{-2}. Hereafter, daytime maxima steadily increased until reaching a climax in August at an average of 366(±89) W m^{-2}. Strong *LE* during the day in July and August often coincided with negative *H*. By September, midday values had decreased to 256(±89) W m^{-2}, and following the end of irrigation in October, quickly declined further to about 100(±35) W m^{-2} in November (Fig. 4.24 E, Fig. 4.25).

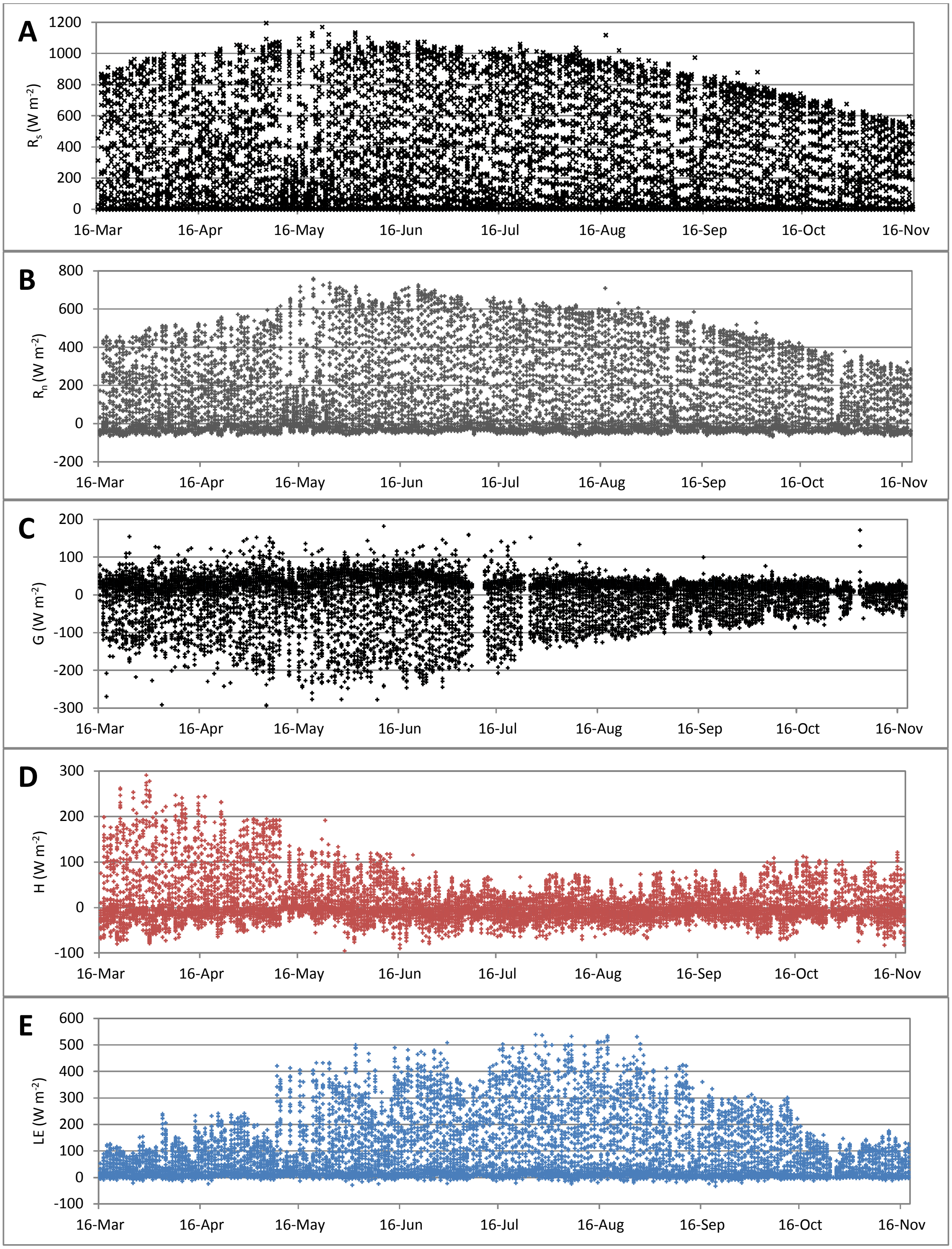

Fig. 4.24: Energy fluxes (30-minute averages) at Fort Logan in 2011: (**A**) shortwave radiation (R_s , W m^{-2}), (**B**) net radiation (R_n , W m^{-2}) , (**C**) average soil heat flux (G, W m^{-2}) , (**D**) sensible heat flux (H, W m^{-2}) , and (**E**) latent heat flux (LE, W m^{-2})

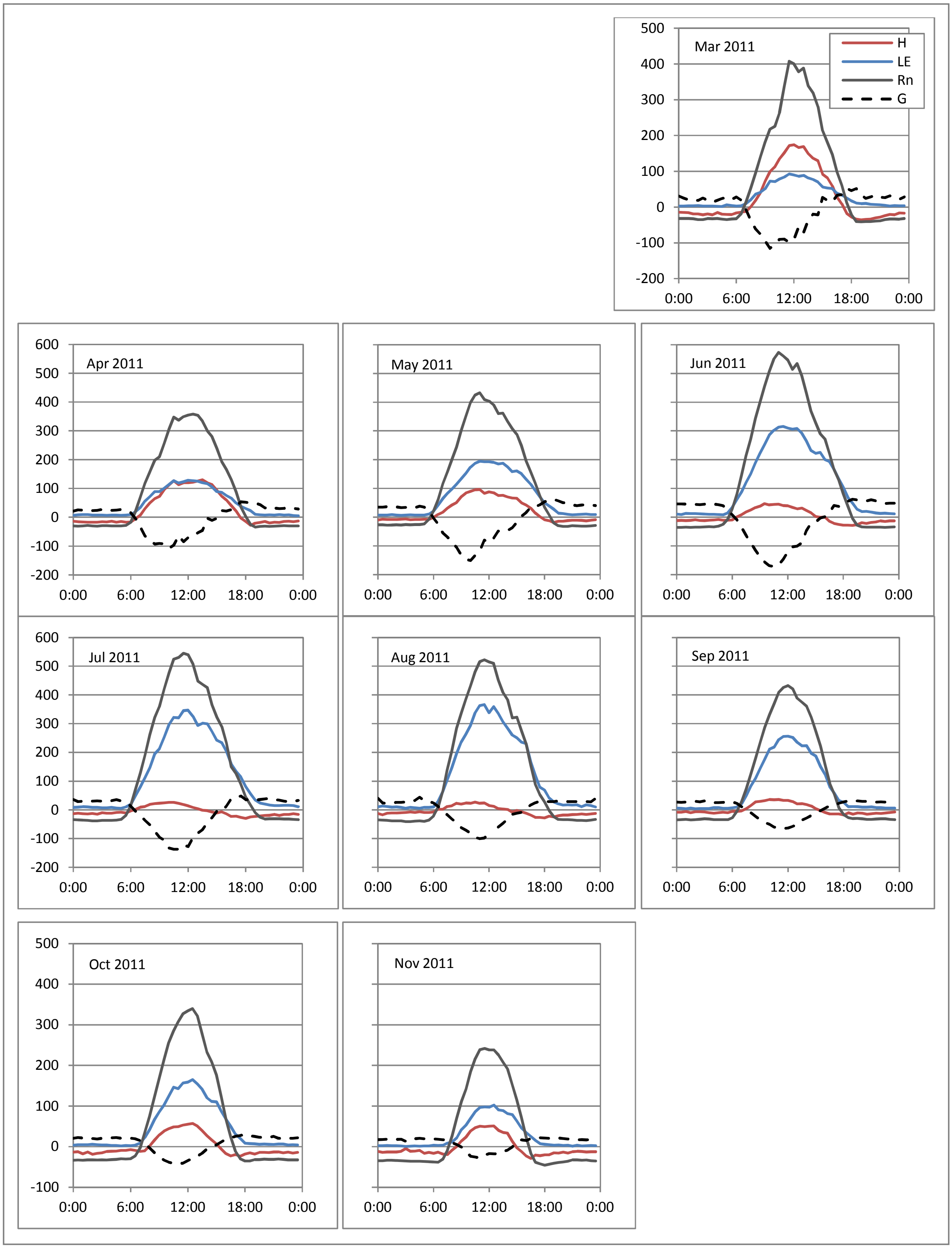

Fig. 4.25: Average diurnal course of energy fluxes at Fort Logan in 2011: net radiation (R_n , W m^{-2}), sensible heat flux (H, W m^{-2}), latent heat flux (LE, W m^{-2}), and average soil heat flux (G, W m^{-2})

4.3.2. Fort Logan 2012

Energy fluxes for the 2012 season at Fort Logan are presented below. The raw data consisted of 30-minute averages (13,199 records; Mar 12 – Dec 12). Data coverage for R_s and G exceeded 99 %, while for R_n 98.2 % of the data was available. Gaps in the data record of H and LE amounted to 19.7 % and 23.6 %, respectively.

Data for R_s at Fort Logan in 2012 is given in Figure 4.26 (A). Values for the average maxima were slightly higher than in 2011, increasing from 883(±50) W m^{-2} in March to 1034(±68) W m^{-2} in June, and declining again until averaging to 449(±92) W m^{-2} in December.

Daytime peaks for R_n had averages of 438(±24) W m^{-2} in March and kept increasing until reaching the greatest diurnal range, similar to 2011, in June and July with daytime peaks at 551(±178) W m^{-2} and 548(±117) W m^{-2}, respectively (nighttime minima between -44(±9) W m^{-2} and -36(±14) W m^{-2}). August values at midday had already decreased by about 100 W m^{-2} on average and by December had reached 181(±76) W m^{-2}. Minimum nightly values for those months ranged between -40(±11) W m^{-2} and -36(±8) W m^{-2}. Rare snowfall events (e.g. Apr 2-3) led to a noticeable dampening of the diurnal amplitude (Fig 4.26 B, Fig. 4.27).

Maximum variation for G in 2012 occurred in June, when peak values at midday averaged to -78(±30) W m^{-2} and nightly minima to 28(±10) W m^{-2}. This clearly represented a diminished diurnal amplitude in comparison to 2011. Past the summer solstice, peak values gradually declined from daytime maxima of -55(±18) W m^{-2} and nighttime minima of 23(±8) W m^{-2} in August to values of -27(±6) W m^{-2} and 14(±2) W m^{-2}, respectively, in November (Fig 4.26 C, Fig. 4.27).

Values for H displayed again greatest diurnal variation in March (range: 165(±32) W m^{-2} to -39(±21) W m^{-2}). The beginning of irrigation (Apr 23), albeit earlier than in 2011, did not impact fluxes as markedly as the year before, although diurnal averages for April showed that LE exceeded H at midday by about 60 W m^{-2}. Midday values in May averaged to 73(±41) W m^{-2}. During the last week of the month (May 23-31), however, a lack of water input coincided with daytime measurements reaching up to 160 W m^{-2} again. June displayed the lowest daytime maxima on average at 37(±38) W m^{-2}, while July and August showed an increasing trend again with values at 57(±41) W m^{-2} and 71(±42) W m^{-2}, respectively. Diurnal minima for those 3 months varied between -40(±26) W m^{-2}, -29(±17) W m^{-2} and

-26(±15) W m^{-2}, respectively. By November, midday averages had decreased again to 47(±29) W m^{-2} (Fig. 4.26 D, Fig. 4.27).

Diurnal maxima for *LE* in March were similar to the previous year, averaging to 98(±15) W m^{-2}. Values in April, when first measurable precipitation occurred and irrigation started, had already doubled to an average of 182(±79) W m^{-2} and continued to increase, amounting to 264(±117) W m^{-2} in May. Late May and early June showed a notable decline in peak values, corresponding to the peak in *H* described above. Nonetheless, June also displayed the highest measurements for *LE* of the season, exceeding 500 W m^{-2}. However, the period of highest fluxes was significantly narrower and occurred earlier than in 2011, when it extended from about mid-July to the end of August. Diurnal maxima for July had already decreased by about 90 W m^{-2}. The beginning of August was characterized by another low point of the seasonal course, corresponding again to a spike in *H*. Although *LE* temporarily increased again during the remaining month of August, averages for midday maxima steadily declined from September (208(±63) W m^{-2}) to December (38(±13) W m^{-2}) (Fig. 4.26 E, Fig. 4.27).

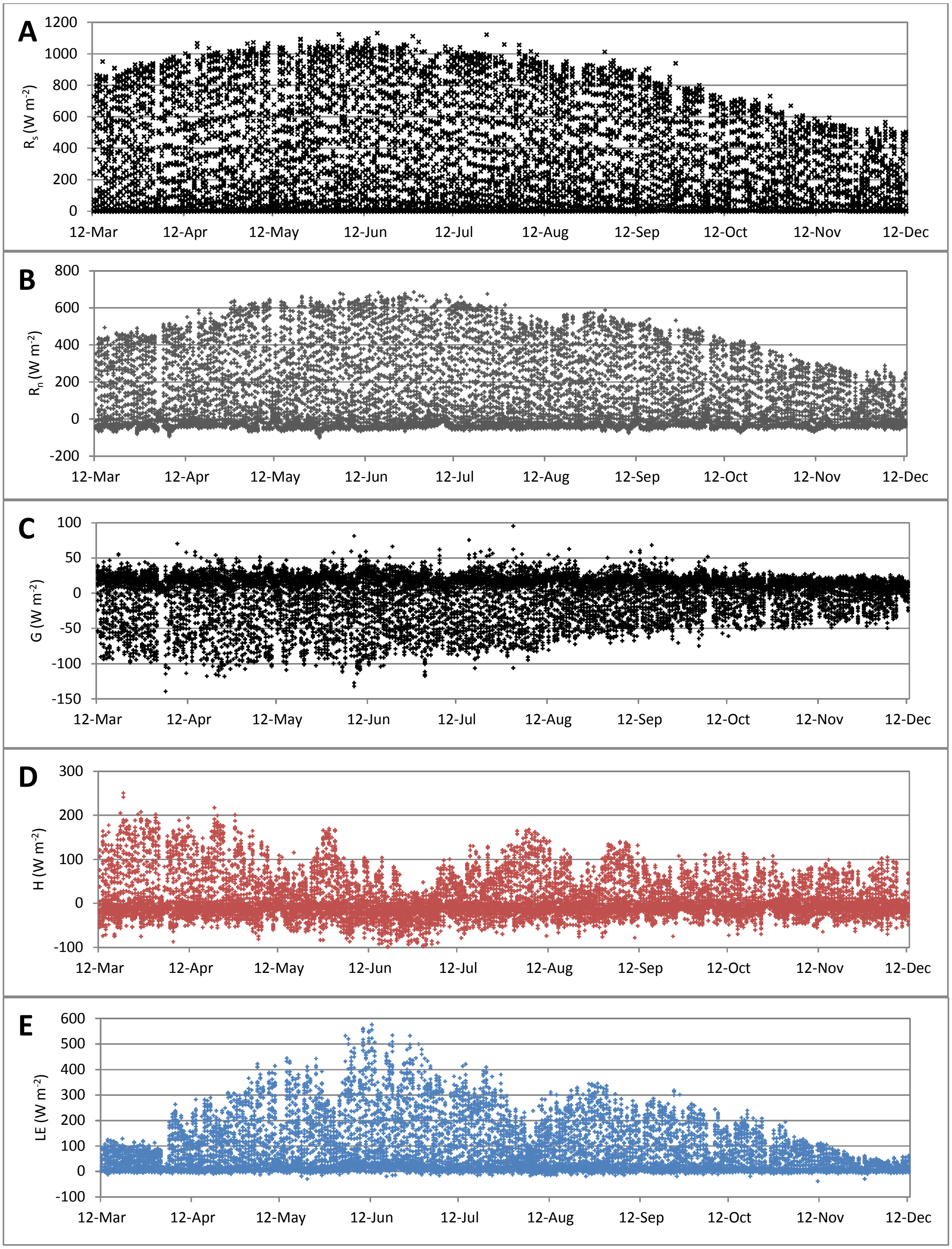

Fig. 4.26: Energy fluxes (30-minute averages) at Fort Logan in 2012: (**A**) shortwave radiation (R_s , W m^{-2}), (**B**) net radiation (R_n , W m^{-2}) , (**C**) average soil heat flux (G, W m^{-2}) , (**D**) sensible heat flux (H, W m^{-2}) , and (**E**) latent heat flux (LE, W m^{-2})

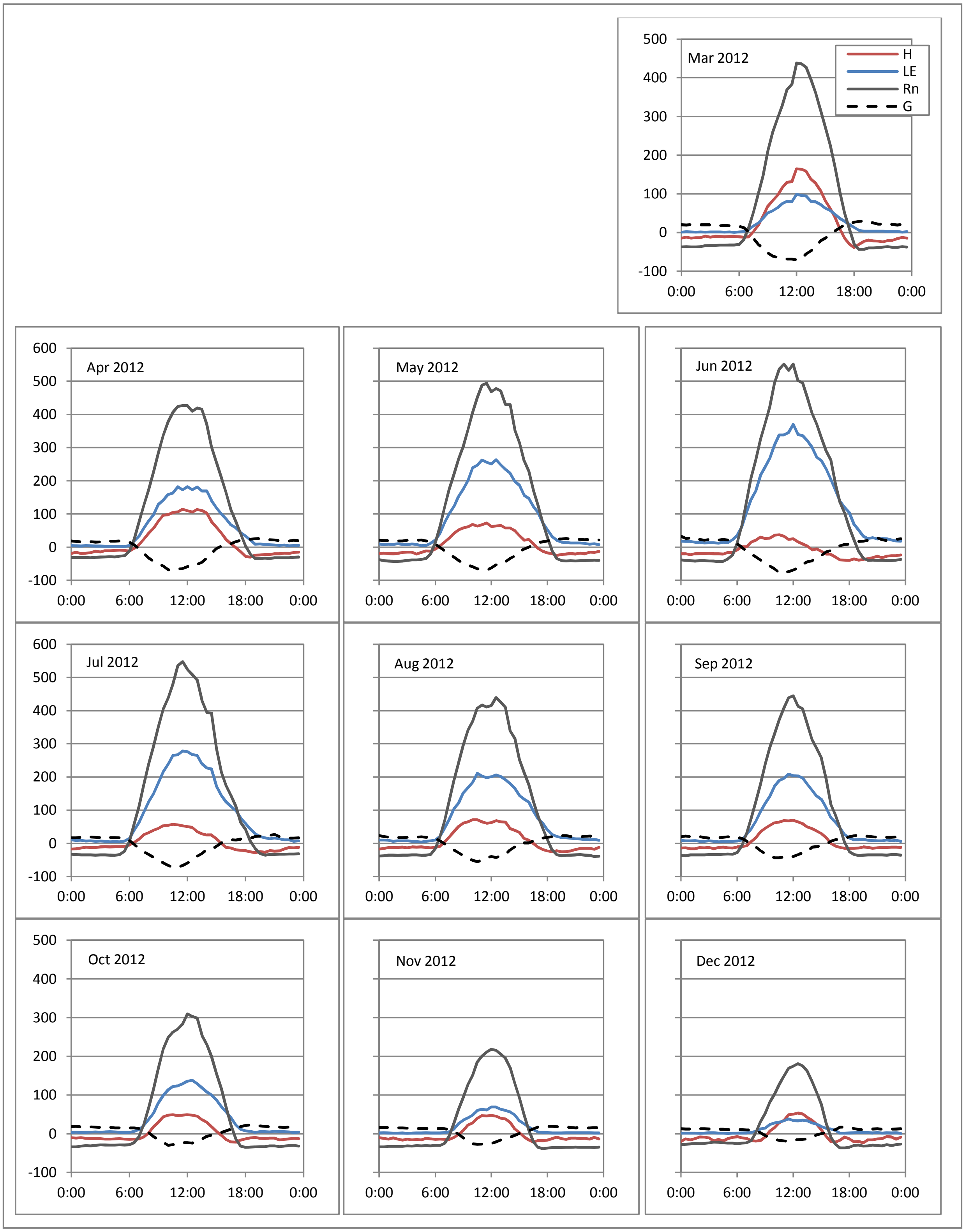

Fig. 4.27: Average diurnal course of energy fluxes at Fort Logan in 2012: net radiation (R_n , W m^{-2}), sensible heat flux (H, W m^{-2}), latent heat flux (LE, W m^{-2}), and average soil heat flux (G, W m^{-2})

4.3.3. Rocky Flats 2011

Energy fluxes at Rocky Flats in 2011 are presented below. The raw data consisted of 30-minute averages (17,520 records; Jan 1 – Dec 31). Data coverage for R_s was 97.8 %, for R_n 98.2 % and for *G* 98.5 %. Gaps in the data record for *H* and *LE* amounted to 28.7 % and 33.6 %, respectively.

The annual course of R_s observed at Rocky Flats in 2011 is shown in Figure 4.28 (A). Due to its relative proximity to Fort Logan, Rocky Flats experienced very similar solar conditions between March and November in 2011, albeit absolute values were slightly lower. Average maximum values started off in January at 466(±99) W m^{-2}, peaked in June at 933(±81) W m^{-2}, and steadily declined again to 445(±78) W m^{-2} in December.

Average values for R_n gradually increased January through July from 180(±95) W m^{-2} to 567(±128) W m^{-2} during the day. Nighttime means varied less, showing lowest diurnal averages at -40(±16) W m^{-2}. The remainder of the year then showed a declining trend with daytime peak values in August reaching on average 502(±131) W m^{-2} and in November only 237(±95) W m^{-2}. Minimum averages for nighttime values during those months amounted to -49(±14) W m^{-2}. Longer periods of snow cover clearly impacted values in December by buffering daily amplitudes of R_n. Here, midday values reached only 73(±85) W m^{-2}, while lowest night values averaged to -37(±17) W m^{-2} (Fig. 4.28 B, Fig. 4.29).

Soil heat flux showed an average diurnal span in January ranging between -24(±42) W m^{-2} and 32(±23) W m^{-2}. Daytime values steadily increased to an average of -114(±39) W m^{-2} in July, while changes in nighttime values were smaller, peaking on average at 53(±50) W m^{-2}. From August to November, daytime maxima for *G* decreased from an average of -99(±49) W m^{-2} to -44(±32) W m^{-2}, whereas nighttime peaks remained almost constant. Values in December were clearly influenced by snow cover leading to average daytime maxima of -5(±15) W m^{-2} and nighttime average lows of 14(±6) W m^{-2} (Fig. 4.28 C, Fig. 4.29).

Diurnal values for *H* reached daytime maxima of 87(±61) W m^{-2} and 120(±94) W m^{-2} in January and February, and minima of -46(±26) W m^{-2} and -41(±38) W m^{-2} at night. In March, daytime peak averages had basically doubled in value, amounting to 247(±96) W m^{-2}, and the end of the month displayed the highest absolute values measured in 2011, near 400 W m^{-2}.

Throughout June, midday averages stayed above 200 W m^{-2}. However, in July, diurnal averages showed a decline in flux and were exceeded by those of *LE*. This relation had already reversed again in August, when midday fluxes slightly increased to 189(±44) W m^{-2} from 148(±52) W m^{-2} in July. November displayed midday averages of 125(±73) W m^{-2} and by December, with extended periods of snow cover, peak averages were only 13(±37) W m^{-2} (Fig 4.28 D, Fig. 4.29).

The seasonal course of *LE* was characterized by a very distinct one-peak maximum in the month of July when recorded measurements were near 400 W m^{-2}. In contrast, the first 3 months of the year showed small fluxes that rarely exceeded 50 W m^{-2} during the day (Jan-Mar). Diurnal averages for midday peaks were 69(±43) W m^{-2}, 125(±50) W m^{-2}, and 253(±63) W m^{-2} for May, June, and July, respectively. After the peak in July, daytime maxima dropped again by nearly half to 134(±45) W m^{-2} in August. Coinciding with stronger precipitation events at the beginning of September, values for *LE* temporarily increased again but showed a generally declining trend in the following months up to the year's end. November and, again, December were characterized by weak fluxes of 26(±13) W m^{-2} and 14(±10) W m^{-2}, respectively (Fig. 4.28 E, Fig. 4.29).

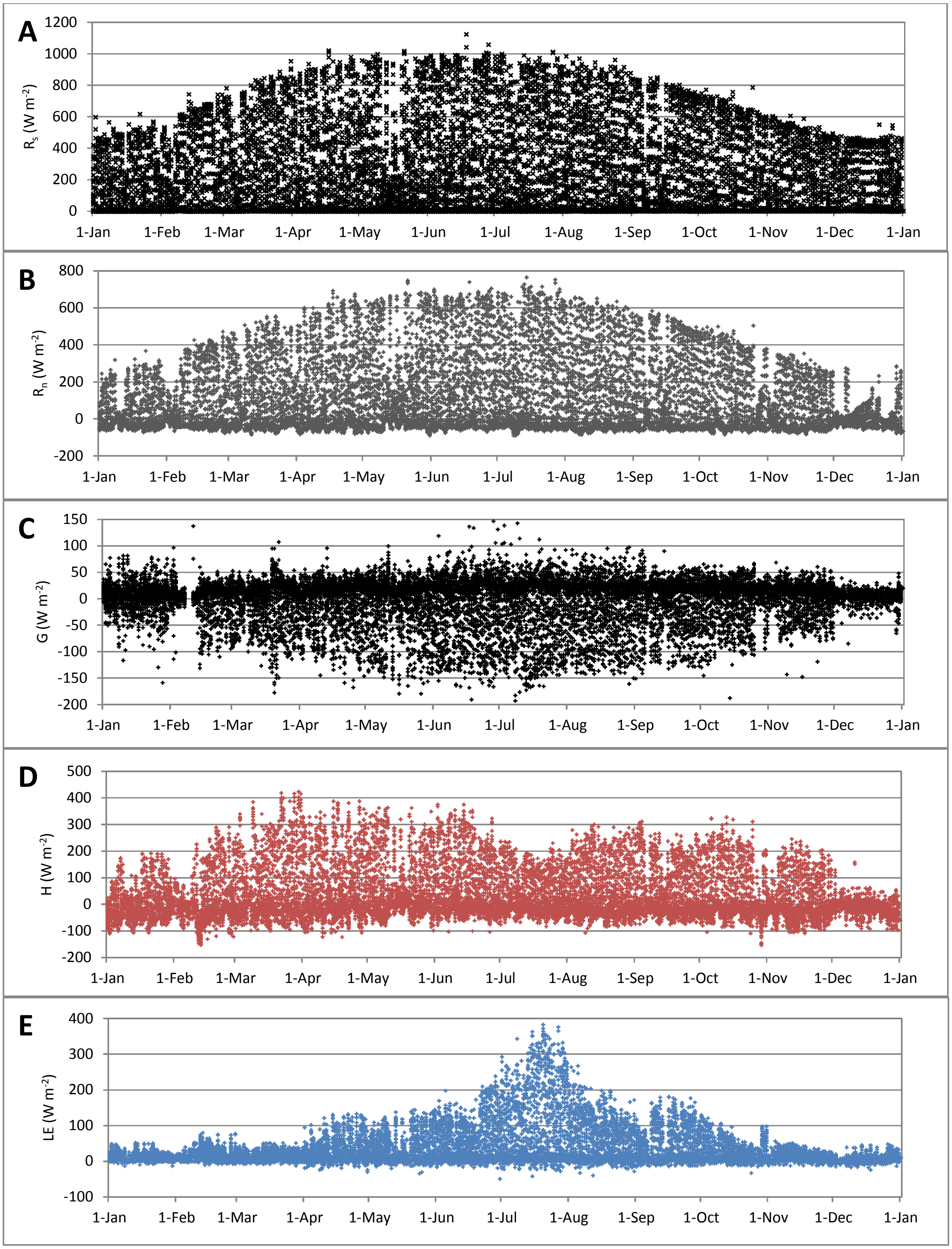

Fig. 4.28: Energy fluxes (30-minute averages) at Rocky Flats in 2011: (**A**) shortwave radiation (R_s, W m^{-2}), (**B**) net radiation (R_n , W m^{-2}) , (**C**) average soil heat flux (G, W m^{-2}) , (**D**) sensible heat flux (H, W m^{-2}) , and (**E**) latent heat flux (LE, W m^{-2})

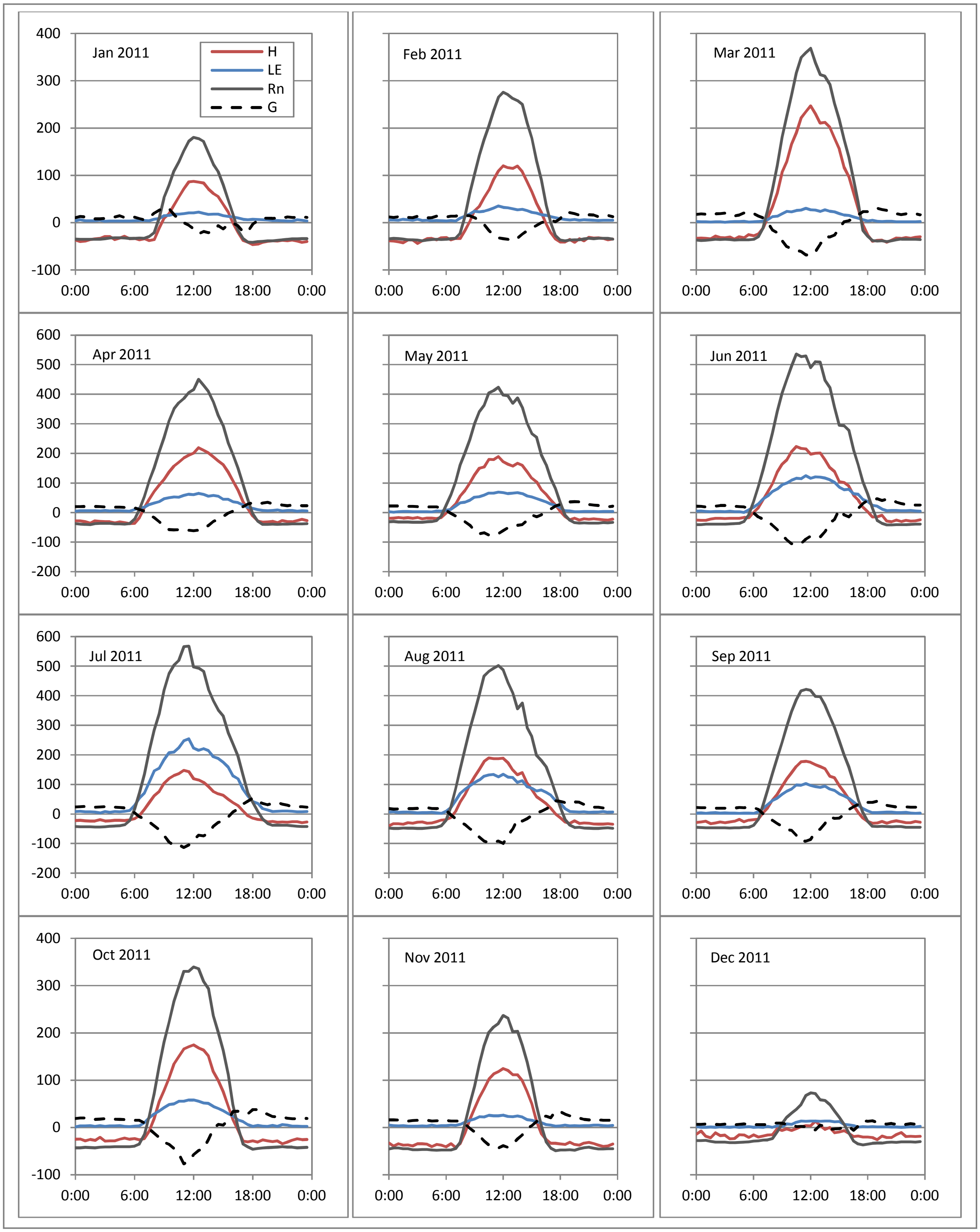

Fig. 4.29: Average diurnal course of energy fluxes at Rocky Flats in 2011: net radiation (R_n , W m^{-2}), sensible heat flux (H, W m^{-2}), latent heat flux (LE, W m^{-2}), and average soil heat flux (G, W m^{-2})

4.3.4. Rocky Flats 2012

Energy fluxes at Rocky Flats in 2012 are presented below. The raw data consisted of 30-minute averages (17,568 records; Jan 1 – Dec 31). Data coverage for R_s and G exceeded 99 %. For R_n, 97.1 % of the data was available. Gaps for H and LE amounted to 26.5 % and 30.9 %, respectively.

Figure 4.30 (A) shows data for R_s recorded at Rocky Flats in 2012. Conditions in 2012 closely resembled those of 2011 with regard to average maximum and minimum values. In January, R_s peaked, on average, at 460(±105) W m^{-2}, while June and July showed the highest peak averages at 911(±86) W m^{-2} and 933(±91) W m^{-2}, respectively. Following this summer maximum, values declined until the end of the year, reaching only 417(±83) W m^{-2} in December.

Diurnal maxima for R_n steadily increased January through June from 196(±90) W m^{-2} to 545(±74) W m^{-2}, while nighttime minima were -50(±11) W m^{-2} and -44(±15) W m^{-2}, respectively. An exception to this increasing trend towards the summer months was February, which, following a blizzard event on February 2-3, was characterized by continuous snow cover for nearly the entire month. Midday maxima in February reached only 140(±151) W m^{-2} before sharply increasing to 446(±99) W m^{-2} in March. Past the peak in June, values gradually declined, reaching on average 453(±170) W m^{-2} in August and only 234(±105) W m^{-2} in November. Minimum nighttime averages in those months differed little at -49(±11) W m^{-2} and -48(±13) W m^{-2}, respectively (Fig. 4.30 B, Fig. 4.31).

Soil heat flux in early 2012 (January) showed a similar diurnal range (-24(±28) W m^{-2} to 23(±12) W m^{-2}) as in the previous year. Values in February were clearly influenced by the existing snow cover (approximately between February 3-24), when the diurnal range of G narrowed to -12(±26) to 13(±10) W m^{-2} on average. From March to July, diurnal maxima changed only little, moving between -77(±34) W m^{-2} to -87(±23) W m^{-2}, while for the same months diurnal minima were 41(±17) W m^{-2} and 35(±12) W m^{-2}, respectively. Thus, G displayed a slightly reduced diurnal span compared to the previous year. From August to December daytime maxima moved from an average of -79(±29) W m^{-2} to -29(±17) W m^{-2}, while diurnal minima in those months amounted to 38(±14) W m^{-2} and 30(±15) W m^{-2}, respectively (Fig. 4.30 C, Fig. 4.31).

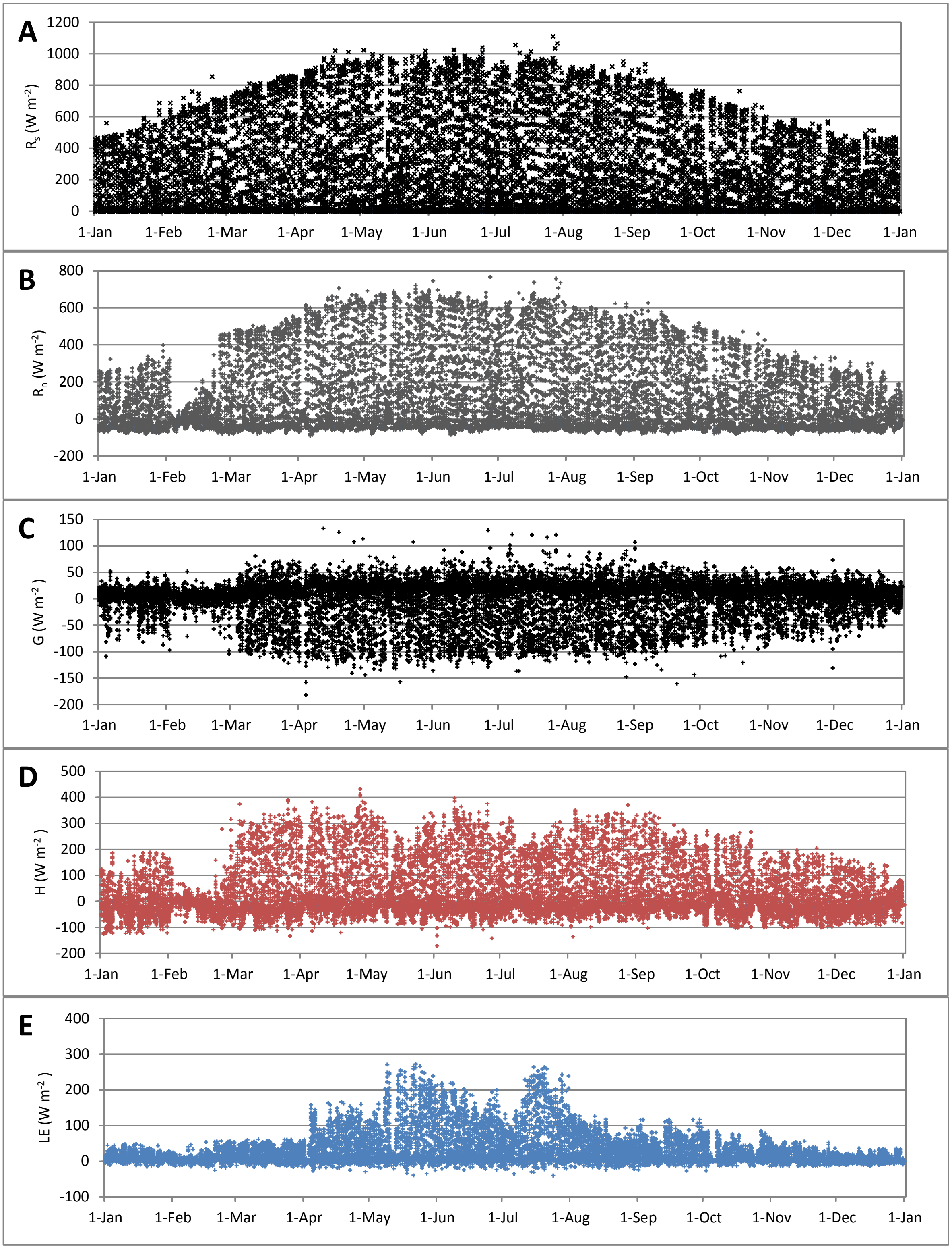

Fig. 4.30: Energy fluxes (30-minute averages) at Rocky Flats in 2012: (**A**) shortwave radiation (R_s , W m^{-2}), (**B**) net radiation (R_n , W m^{-2}) , (**C**) average soil heat flux (G, W m^{-2}) , (**D**) sensible heat flux (H, W m^{-2}) , and (**E**) latent heat flux (LE, W m^{-2})

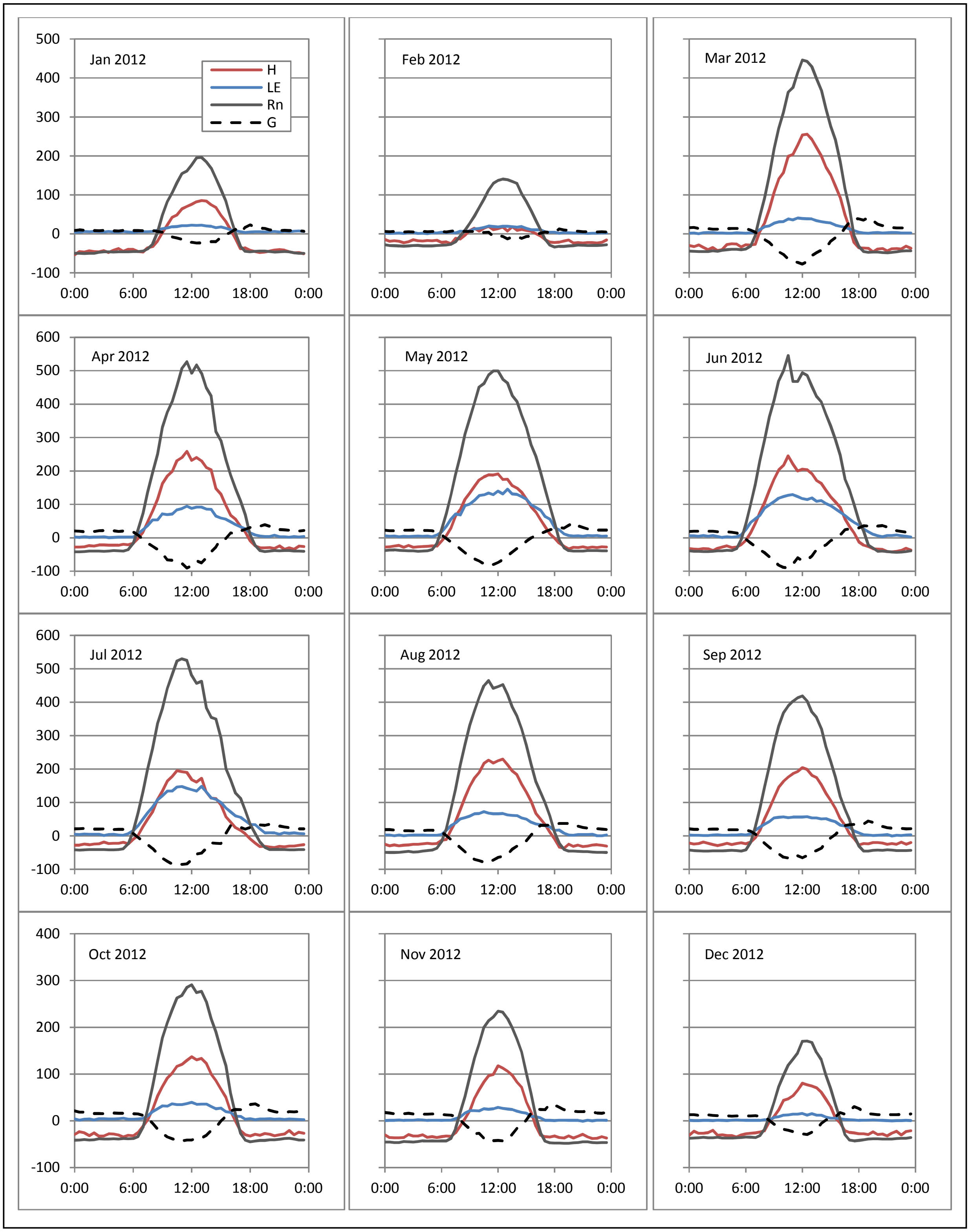

Fig. 4.31: Average diurnal course of energy fluxes at Rocky Flats in 2012: net radiation (R_n , W m^{-2}), sensible heat flux (H, W m^{-2}), latent heat flux (LE, W m^{-2}), and average soil heat flux (G, W m^{-2})

The diurnal span for H ranged from 85(±63) W m^{-2} to -53(±34) W m^{-2} in January. Snowy February displayed a narrower range at 17(±64) to -24(±25) W m^{-2}. From March through September, midday peaks remained high, varying between 256(±82) W m^{-2} and 204(±80) W m^{-2} on average (minima: -43(±25) to -26(±16) W m^{-2}). Only in May and July did the seasonal trend deviate from this high level, where lower values coincided with periods of stronger precipitation. Between October and December, maximum averages gradually declined from 137(±80) W m^{-2} to 80(±49) W m^{-2} (Fig. 4.30 D, Fig. 4.31).

Values for LE rarely exceeded 60 W m^{-2} during the first 3 months of 2012 (peak average: 20-40 W m^{-2}). As April brought first measurable precipitation since February, the average maximum increased to 94(±38) W m^{-2}. Values exceeded 250 W m^{-2} in May (peak average: 145(±75) W m^{-2}) but decreased thereafter until the end of June (peak average: 129(±45) W m^{-2}), before another peak appeared during the second half of July (peak average: 148(±77) W m^{-2}). By August (73(±30) W m^{-2}), average daytime maxima were about 50 % lower in comparison to the previous month and to August of 2011. September through December was characterized by continuously smaller fluxes, declining from 58(±26) W m^{-2} to 29(±14) W m^{-2}, respectively (Fig. 4.30 E, Fig. 4.31).

4.4. Energy partitioning

Average daily sums of energy fluxes, i.e. the main components of the energy balance (LE, H, G, R_n, and energy residual), are depicted for Fort Logan and Rocky Flats in Fig. 4.32. The data shown includes 2011 and 2012. For reasons of comparability, only full months based on the shortest investigation period, i.e. Fort Logan 2011, are presented.

At Fort Logan, R_n was primarily converted into LE but H still contributed moderately in the spring of both years. In April and May of 2011, the daily sum for H amounted to 2.5 and 2.0 MJ d^{-1} m^{-2}, respectively. This translates to a relative share of 31 % and 19 % of R_n in the respective months. In 2012, daily sums in April and May were 1.9 and 0.9 MJ d^{-1} m^{-2}, while the relative shares were 19 % and 8 %, respectively. By June in both years, LE clearly dominated. Daily sums amounted to 10.3 MJ d^{-1} m^{-2} in 2011 and 11.3 MJ d^{-1} m^{-2} in 2012. The relative shares of R_n were 72 % and 86 % in 2011 and 2012, respectively. Latent heat fluxes continued to be strong at Fort Logan throughout both summers. In August 2011, LE

amounted to 91 % of R_n. However, one year later, this relative share was down to 67 %, coinciding with severe drought conditions and intermittent irrigation. Moreover, *H* started to make again a small but measurable contribution. The daily sums of *G* in both years ranged between near zero and 0.9 MJ d^{-1} m^{-2} (Apr-Aug), resulting in shares of 4 – 6 % of R_n at maximum. In September and October, daily sums became negative and soils turned into a net energy source. The energy balance residual, i.e. the difference unaccounted for by the measured components, ranged between 11-35 % of R_n in 2011 and between 16-37 % in 2012.

Rocky Flats clearly differed from Fort Logan with regard to energy partitioning, showing generally a more balanced distribution between *H* and *LE*. Daily sums for *H* in April and May of 2011 were 3.8 MJ d^{-1} m^{-2} and 3.9 MJ d^{-1} m^{-2}, respectively, representing a 42 % and 38 % share of R_n. During those same months, daily sums for *LE* amounted to 2.1 MJ d^{-1} m^{-2} and 2.2 MJ d^{-1} m^{-2}, corresponding to shares of R_n of 23 % and 22 %. By June 2011, *H* and *LE* were almost of same magnitude, totaling to 4.6 MJ d^{-1} m^{-2} and 4.4 MJ d^{-1} m^{-2}, respectively. In July 2011, *LE* clearly dominated, summing up to 7.4 MJ d^{-1} m^{-2} and a relative share of 58 %, while *H* decreased to 2.1 MJ d^{-1} m^{-2} and 16 %, respectively. The daily sum of *LE* in August was still larger than *H* (4.3 MJ d^{-1} m^{-2} vs. 2.9 MJ d^{-1} m^{-2}; relative share of R_n: 41 % vs. 28 %) but by September, daily sums were almost equalized. Sensible heat in 2012 summed up to 4.6, 3.7, and 4.3 MJ d^{-1} m^{-2} in April, May, and June, respectively. The corresponding shares of R_n were 30 %, 30%, and 33 %. The daily sums for *LE* increased from 2.7 MJ d^{-1} m^{-2} in April (relative share of R_n: 25 %) to 4.6 MJ d^{-1} m^{-2} in May (38 %). After a minor decline in June, values for *LE* in July of 2012 had increased to a similar magnitude as in May. By August, however, coinciding with the peak of drought conditions (similar to Fort Logan), this relation had almost reversed again, when *H* summed to 4.2 MJ d^{-1} m^{-2} (43 %) and *LE* to only 2.3 MJ d^{-1} m^{-2} (23 %). Relative shares of R_n remained nearly unchanged, before in October, daily totals of *H* and *LE* were practically equal. Daily sums for *G* ranged between near zero and 0.7 MJ d^{-1} m^{-2} (April-August), resulting in a relative share of R_n between 1 – 5 %. As at Fort Logan, totals for *G* became negative in September and October, turning soils into a net energy source. Energy balance residuals ranged between 21-36 % of R_n in 2011 and between 30-50 % in 2012.

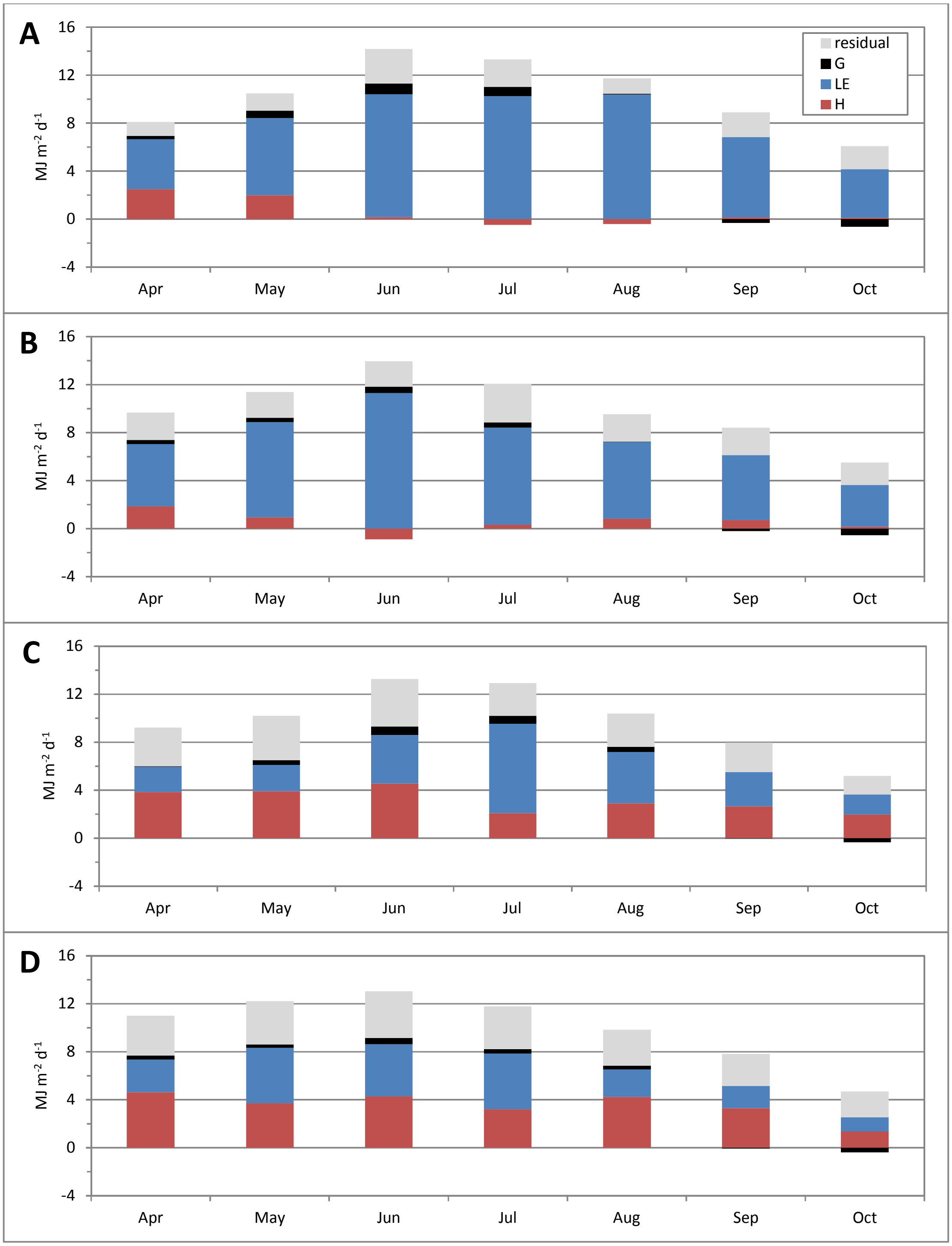

Fig. 4.32: Average daily sums of energy fluxes at Fort Logan and Rocky Flats in 2011 and 2012: sensible heat flux (H, MJ m^{-2} d^{-1}), latent heat flux (LE, MJ m^{-2} d^{-1}), average soil heat flux (G, MJ m^{-2} d^{-1}), and energy balance residual (residual, MJ m^{-2} d^{-1}). Net radiation (R_n, MJ m^{-2} d^{-1}) is given by the sum of H, LE, G, and residual. Positive daily sums indicate net sinks of available energy, negative daily sums indicate net sources.
(**A**) Fort Logan 2011, (**B**) Fort Logan 2012, (**C**) Rocky Flats 2011, (**D**) Rocky Flats 2012

4.5. Energy Balance Closure

The analysis of energy balance closure using linear regression (OLS) between the sum of R_n and G vs. the sum of LE and H is illustrated in Fig. 4.33. Data included 2011 and 2012 for Fort Logan and Rocky Flats, but only non-gapfill data that passed QC criteria was used in analyses.

Statistical analysis indicated a general lack of closure. Greatest discrepancies in energy balance (absolute values) at both sites were usually found between midday and early afternoon, the time of greatest magnitude with regard to relevant fluxes. Including storage change in G generally increased slopes of the derived regression lines by 0.04-0.07 points, whereas r^2 remained nearly unchanged (decrease of 0.01 points, except Fort Logan 2011 – decrease of 0.04 points).

For Fort Logan 2011, regression analysis yielded a slope, intercept, and r^2 of 0.84, -2.3, and 0.90, respectively. The energy balance ratio (EBR = $\Sigma(LE+H) / \Sigma(R_n+G)$) amounted to 0.82. Both results indicate a lack of closure. The average energy balance residual was calculated at 24(±50) W m^{-2}. In 2012, the slope of the regression line had decreased, the overall goodness of fit, however, had improved. The respective regression coefficients for slope and intercept were 0.73 and 3.1, while r^2 equaled 0.94. The EBR was calculated to be 0.76. The average residual amounted to 30(±56) W m^{-2}.

Regression analysis for Rocky Flats resulted in very similar results for 2011 and 2012. For the first year of investigation, slope, intercept, and r^2 were 0.79, -11.4, and 0.94, respectively. In 2012, the coefficients of regression showed only little change when slope, intercept, and r^2 amounted to 0.77, -10.9, and 0.95. The respective EBRs for 2011 and 2012 were 0.69 and 0.67. As for Fort Logan, the calculated statistics indicate a lack of closure, amounting to average 34(±47) W m^{-2} and 35(±48) W m^{-2} in 2011 and 2012, respectively.

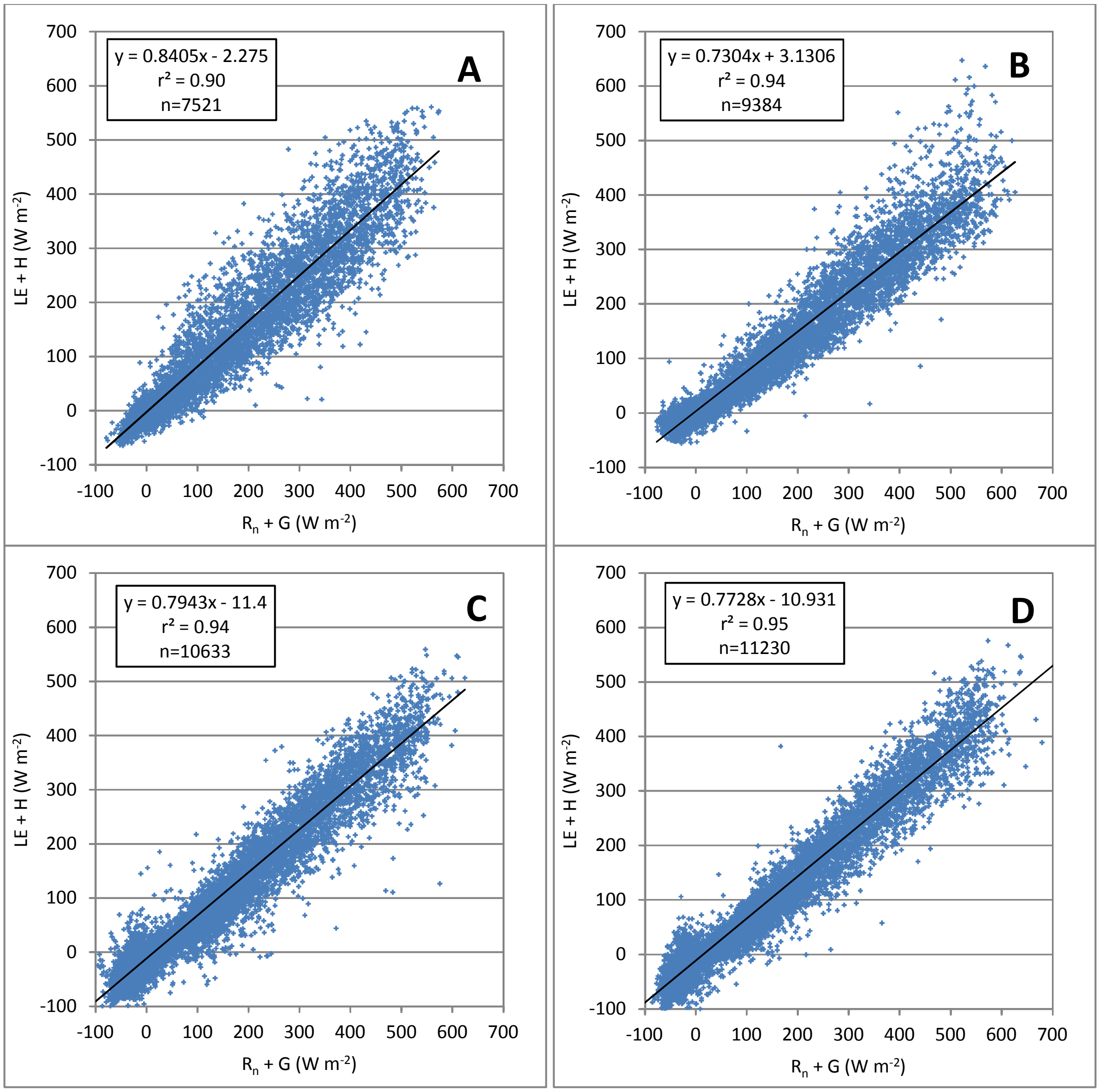

Fig. 4.33: Comparison of energy balance closure for Fort Logan and Rocky Flats (2011 + 2012). Valid data of net radiation (R_n; W m^{-2}) and soil heat flux at the soil surface (G; W m^{-2}) is plotted against latent (LE; W m^{-2}) and sensible heat (H; W m^{-2}) flux. Black line represents the regression line (OLS). (**A**) Fort Logan 2011, (**B**) Fort Logan 2012, (**C**) Rocky Flats 2011, (**D**) Rocky Flats 2012

4.6. Carbon Dioxide Fluxes

4.6.1. Fort Logan 2011

Data for carbon dioxide fluxes, i.e. net ecosystem exchange (*NEE*), for the 2011 season at Fort Logan, are presented below. The raw data consisted of 30-minute averages (11,850 records; Mar 16 – Nov 18). Data coverage was 67.0 %.

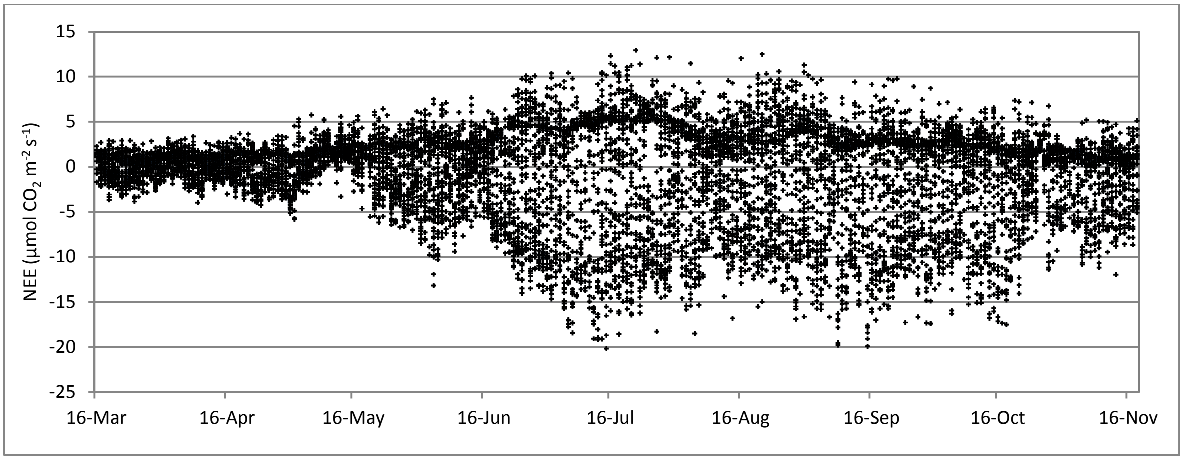

Fig. 4.34: NEE at Fort Logan in 2011(30-minute averages; µmol CO_2 m^{-2} s^{-1})

The diurnal range of *NEE* in March and April was very similar (Fig 4.35). Maximum net uptake during the day averaged to -1.6(±0.7) µmol CO_2 m^{-2} s^{-1} and -1.5(±1.2) µmol CO_2 m^{-2} s^{-1}, respectively, while highest net release of CO_2 in early evening was on average 1.3(±0.9) µmol CO_2 m^{-2} s^{-1} and 1.5(±0.7) µmol CO_2 m^{-2} s^{-1}. The beginning of May witnessed a shift towards net release, whereas following the onset of irrigation (May 9), CO_2 uptake increased again in magnitude (Fig. 4.34). In June, net uptake reached maxima of -6.6(±3.5) µmol CO_2 m^{-2} s^{-1} on average. July, August, and September were the strongest months regarding net uptake with maximum diurnal averages of -13.3(±2.8), -10.1(±3.1), and -11.8(±3.7) µmol CO_2 m^{-2} s^{-1}, respectively. However, net release of CO_2 during those months was also large: highest diurnal averages figured to 6.6(±2.0), 5.7(±2.5), and 4.0(±2.2) µmol CO_2 m^{-2} s^{-1}. The remaining months of the investigation season showed a declining trend with regard to net uptake of CO_2: values reached maxima of -9.0(±4.7) µmol CO_2 m^{-2} s^{-1} in October and -6.7(±2.0) µmol CO_2 m^{-2} s^{-1} in November. Net release showed values comparable to the start of the data record, when diurnal averages reached 2.6(±1.8) µmol CO_2 m^{-2} s^{-1} and 1.5(±1.5) µmol CO_2 m^{-2} s^{-1} in October and November, respectively.

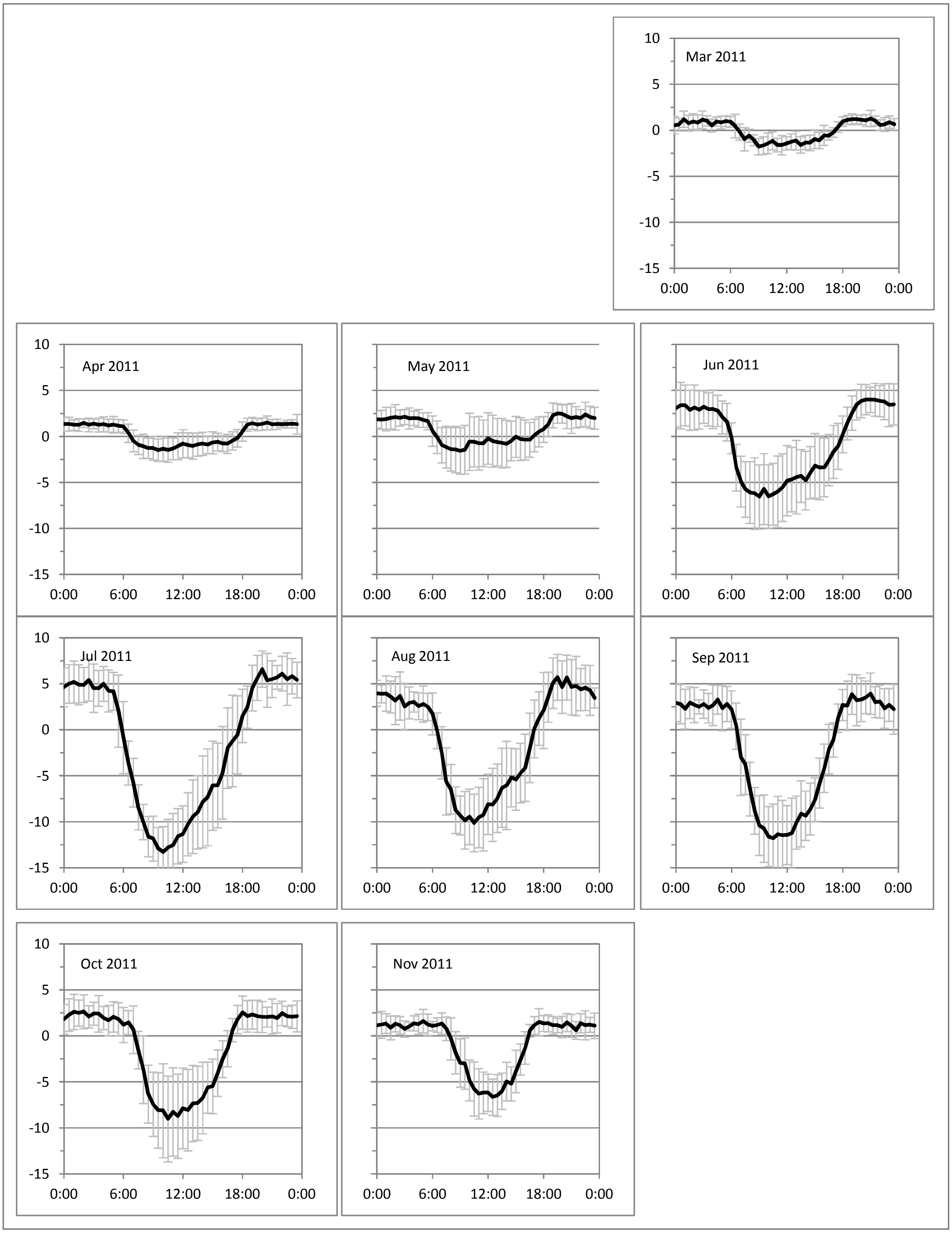

Fig. 4.35: Average diurnal course of NEE (µmol CO_2 m^{-2} s^{-1}) at Fort Logan in 2011 (error bars represent ±1 SD)

4.6.2. Fort Logan 2012

Carbon dioxide fluxes for the 2012 season at Fort Logan are presented below. The raw data consisted of 30-minute averages (13,199 records; Mar 12 – Dec 12). Data coverage was 74.1 %.

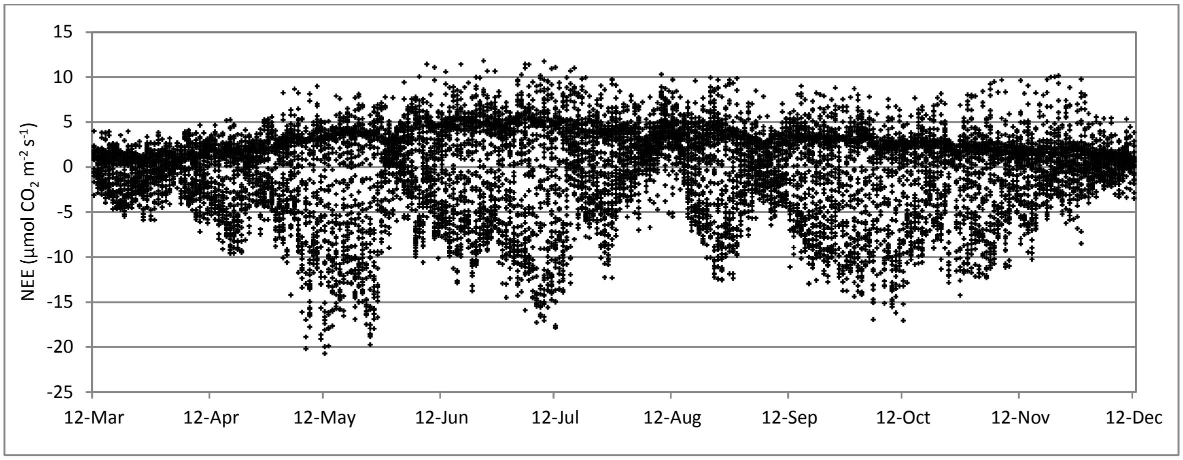

Fig. 4.36: NEE at Fort Logan in 2012 (30-minute averages; µmol CO_2 m^{-2} s^{-1})

Values for *NEE* in March and April of 2012 showed distinct differences compared to the previous investigation period. Diurnal maxima for net uptake in March averaged to -3.3(±1.0) µmol CO_2 m^{-2} s^{-1}, more than double in comparison to March 2011 (Fig. 4.37). Differences to 2011 were even more pronounced in April, when peak uptake values averaged to -4.9 (±2.2) µmol CO_2 m^{-2} s^{-1}. Maxima of net release during these months were on average 1.6(±0.5) µmol CO_2 m^{-2} s^{-1} and 2.3 (±0.7) µmol CO_2 m^{-2} s^{-1}, respectively. In May, maxima for net CO_2 uptake increased in magnitude to -10.6(±6.0) µmol CO_2 m^{-2} s^{-1}. In contrast, June saw a weakening of net CO_2 uptake (average: -6.5(±2.9) µmol CO_2 m^{-2} s^{-1}) and strong net CO_2 release (average: 5.8(±2.3) µmol CO_2 m^{-2} s^{-1}). During July, net uptake increased slightly, resulting in a peak diurnal average of -8.0(±3.8) µmol CO_2 m^{-2} s^{-1}, while maxima for net release remained nearly unchanged. Late July witnessed a weakening of net uptake and in August peak uptake had changed to an average of -2.9(±5.4) µmol CO_2 m^{-2} s^{-1}, while the average maximum for net release was 4.4(±2.1) µmol CO_2 m^{-2} s^{-1}. September through November experienced higher net uptake values again, peaking in October (average: -8.6(±3.2) µmol CO_2 m^{-2} s^{-1}), before in December, the diurnal amplitude of *NEE* was significantly dampened.

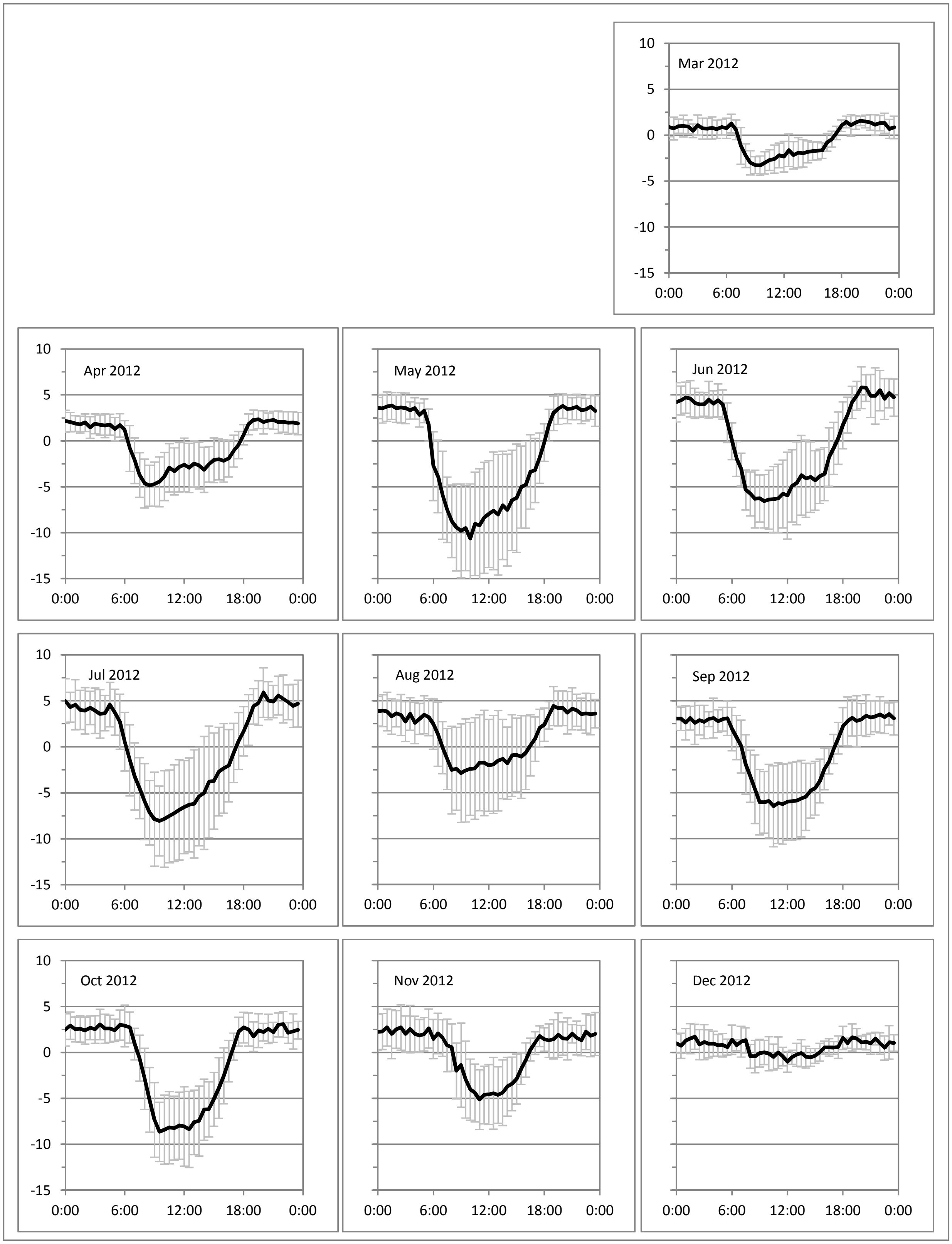

Fig. 4.37: Average diurnal course of NEE (µmol CO_2 m^{-2} s^{-1}) at Fort Logan in 2012 (error bars represent ±1 SD)

4.6.3. Rocky Flats 2011

Carbon dioxide fluxes for 2011 at Rocky Flats are presented below. The raw data consisted of 30-minute averages (17,520 records; Jan 1 – Dec 31). Data coverage was 64.3 %.

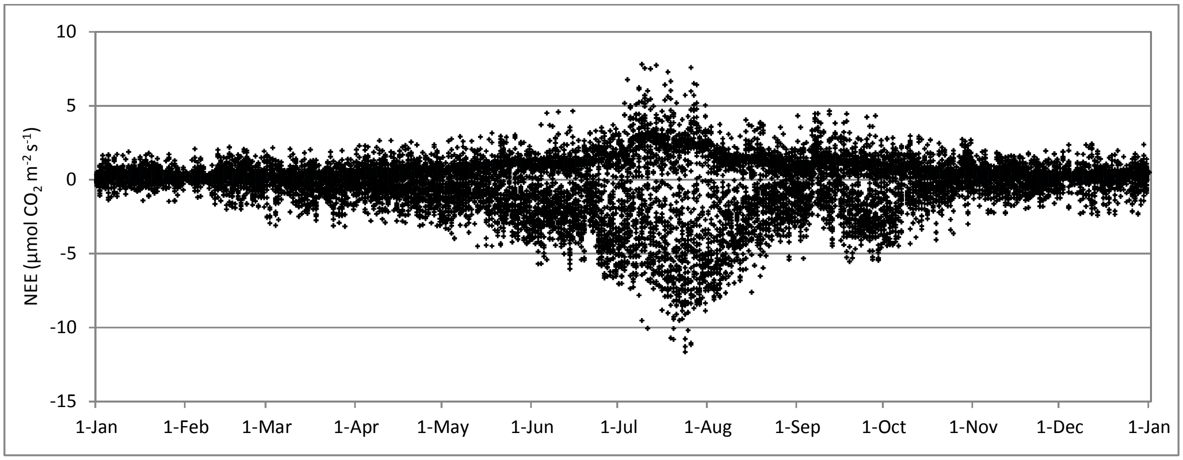

Fig. 4.38: NEE at Rocky Flats in 2011 (30-minute averages; µmol CO_2 m^{-2} s^{-1})

Diurnal variation of *NEE* was negligible in January and February, but March showed first discernible signs of CO_2 uptake, when diurnal maxima amounted to approximately -0.9(±1.2) µmol CO_2 m^{-2} s^{-1} (Fig. 4.39). April showed an already more distinct diurnal cycle and by May, peak values for net CO_2 uptake had reached -1.8(±1.2) µmol CO_2 m^{-2} s^{-1} while averages for net release of CO_2 were highest at 1.2(±0.6) µmol CO_2 m^{-2} s^{-1}. Diurnal variation of *NEE* kept increasing throughout June and July. Here, averages of net uptake reached -3.6(±1.5) µmol CO_2 m^{-2} s^{-1} in June and doubled to -6.3(±2.1) µmol CO_2 m^{-2} s^{-1} in July. The same doubling in magnitude took place with regard to net release of CO_2, when diurnal maxima averaged to 1.6(±1.3) µmol CO_2 m^{-2} s^{-1} and 3.1(±2.0) µmol CO_2 m^{-2} s^{-1} in June and July, respectively. Values for net uptake in August already showed a declining trend again which, with a temporary exception in late September, continued until the end of the year (Fig. 4.38). For net uptake, the respective maxima in August, September, and October were -4.4(±1.9), -2.3(±1.4), and -1.4(±1.6) µmol CO_2 m^{-2} s^{-1}. The corresponding diurnal maxima of net release amounted to 1.5(±0.6), 1.7(±0.9), and 1.0(±0.6) µmol CO_2 m^{-2} s^{-1}. Similar to the first two months of the year, diurnal variation in November and December was minor.

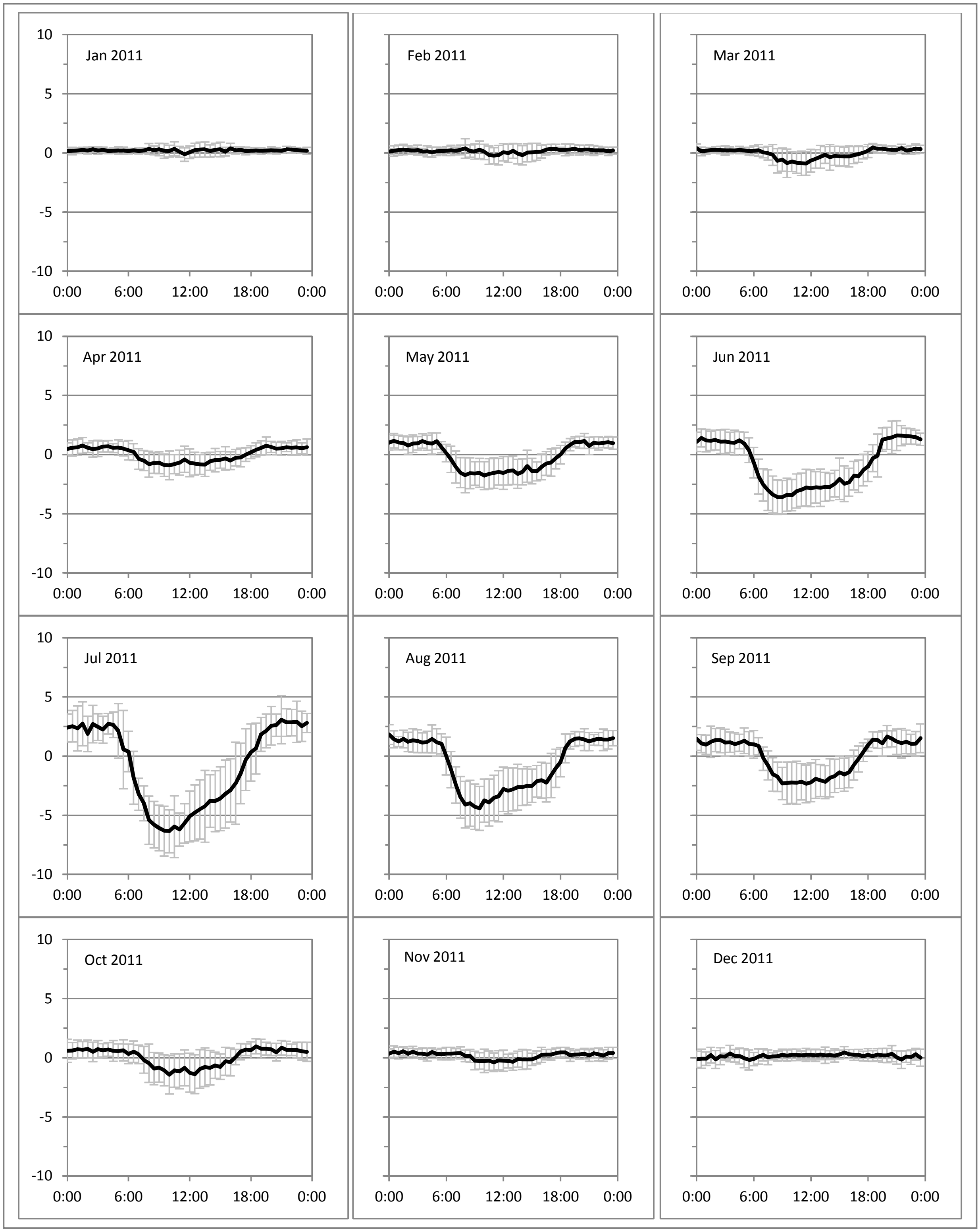

Fig. 4.39: Average diurnal course of NEE (µmol CO_2 m^{-2} s^{-1}) at Rocky Flats in 2011 (error bars represent ±1 SD)

4.6.4. Rocky Flats 2012

Carbon dioxide fluxes for 2012 at Rocky Flats are presented below. The raw data consisted of 30-minute averages (17,568 records; Jan 1 – Dec 31). Data coverage was 66.8 %.

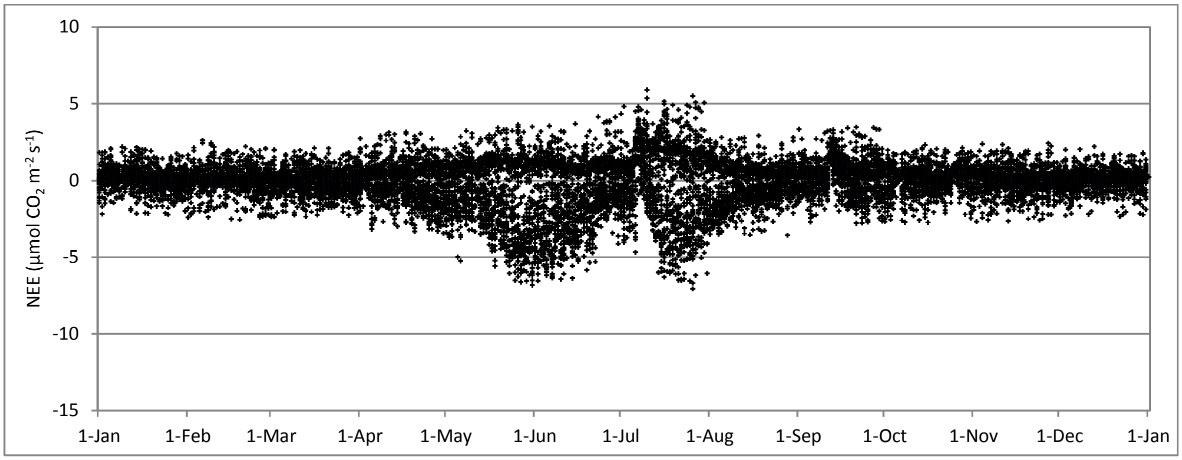

Fig. 4.40: NEE at Rocky Flats in 2012 (30-minute averages; µmol CO_2 m^{-2} s^{-1})

Similar to 2011, diurnal variation of *NEE* was very small in January and February. March showed, again, first signs of weak CO_2 uptake during the day (Fig. 4.41). By April, average peak values for net CO_2 uptake had reached -1.1(±0.9) µmol CO_2 m^{-2} s^{-1} and for net release 0.9(±0.7) µmol CO_2 m^{-2} s^{-1}. May, June, and July showed the highest diurnal averages for net uptake in 2012 averaging to -2.9(±1.7), -3.3(±1.8), and -3.2(±2.1) µmol CO_2 m^{-2} s^{-1}, respectively. Averages for net release during these months figured to 1.5(±0.8), 1.5(±0.6), and 2.3(±1.3) µmol CO_2 m^{-2} s^{-1}. Values for net uptake decreased significantly in August, averaging then to -1.6(±1.1) µmol CO_2 m^{-2} s^{-1}, whereas maximum net release was at 1.2(±0.6) µmol CO_2 m^{-2} s^{-1}. September witnessed a further drop in net uptake values (average: -0.6(±1.1) µmol CO_2 m^{-2} s^{-1}) while the peak average for values of net release remained nearly unchanged. By October, the diurnal amplitude of *NEE* had further dampened (when peaks of net uptake and release averaged to -0.6(±1.2) µmol CO_2 m^{-2} s^{-1} and 0.6(±0.4) µmol CO_2 m^{-2} s^{-1}, respectively), and became negligible in November and December.

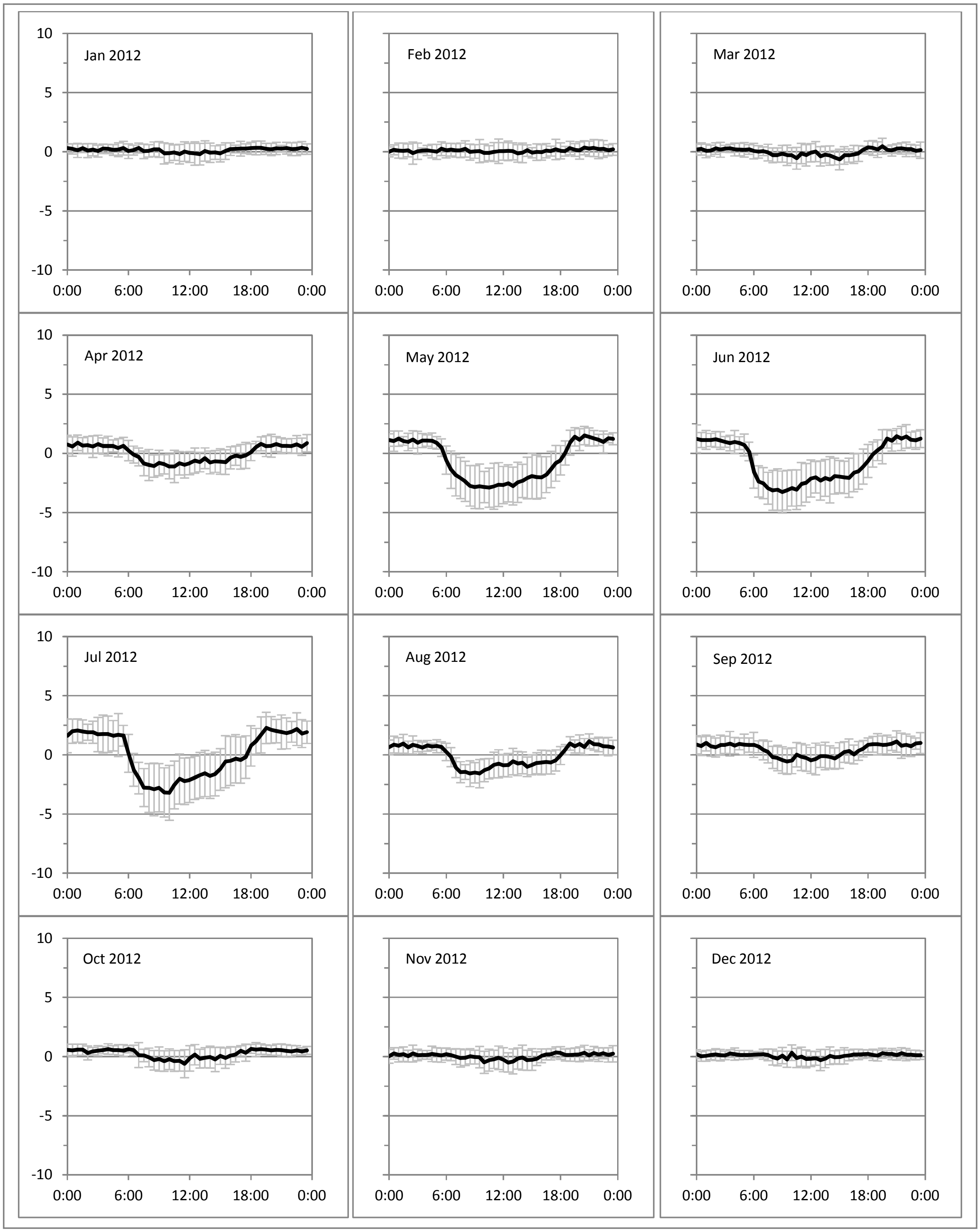

Fig. 4.41: Average diurnal course of NEE (µmol CO_2 m^{-2} s^{-1}) at Rocky Flats in 2012 (error bars represent ±1 SD)

4.7. Seasonal Course of Net Ecosystem Exchange of CO_2 and Evapotranspiration

4.7.1. Fort Logan

Figure 4.42 and Fig. 4.43 (A + B) depict daily sums and cumulative trends of seasonal *ET* and *NEE* as well as cumulative water input over the course of the 2011 and 2012 investigation periods. Panels C through E of Fig. 4.42 and Fig. 4.43 contain data of ancillary measurements that may significantly influence *ET* and *NEE*, including precipitation (+irrigation), soil moisture, soil temperature, daily sums of PAR (daily light integral, DLI), leaf area index (LAI), and vapor pressure deficit (VPD).

ET

As detailed in sections 4.3.1. and 4.3.3., *ET* (i.e. latent heat flux) showed distinct seasonal courses. Starting off in March, daily *ET* was similar for both years, averaging to 1.0(±0.3) mm d^{-1} and 0.9(±0.2) mm d^{-1}, respectively. Values continued to increase steadily, however, showing a slightly stronger monthly increase in the spring of 2012, which had shown above-average temperatures in March-May (section 4.1.2.), higher monthly averages for VPD, and an earlier start of irrigation. In June, average daily *ET* amounted to 4.1(±1.2) mm d^{-1} in 2011 and 4.5(±1.3) mm d^{-1} in 2012, coinciding with high water input and high values for VPD. By the end of the month, total *ET* figured to approximately 265 mm in 2011 and 315 mm in 2012, while water input up to this point had amounted to 450 mm and 465 mm, respectively. Average values for total *ET* per day remained high at around 4 mm d^{-1} throughout July and August in 2011, while in 2012 the respective monthly averages declined to 3.2(±0.8) mm d^{-1} in July and 2.6(±0.7) mm d^{-1} by August. This decrease in 2012 is paralleled by a decline in soil moisture and LAI until mid-August as well as generally lower, intermittently applied amounts of irrigation in comparison to the previous year. By the end of September, cumulative *ET* had approximately doubled in both years compared to the values at the end of June, summing to 555 mm in 2011 and 605 mm in 2012 (respective water input: 1000 mm and 1050 mm). In October, daily *ET* was nearly identical in both years at 1.6(±0.8) mm d^{-1} and 1.4(±0.6) mm d^{-1}, and shortly after irrigation had stopped, values dropped to about 1 mm d^{-1} or less for the remaining investigation periods. Overall, cumulative *ET* in 2011 amounted to approximately 670 mm, while water input summed to 1070 mm (including 340 mm of precipitation)(ET/P = 0.63). In 2012, cumulative *ET* was 625 mm and water input amounted to 1100 mm (including 230 mm of precipitation) (ET/P = 0.57).

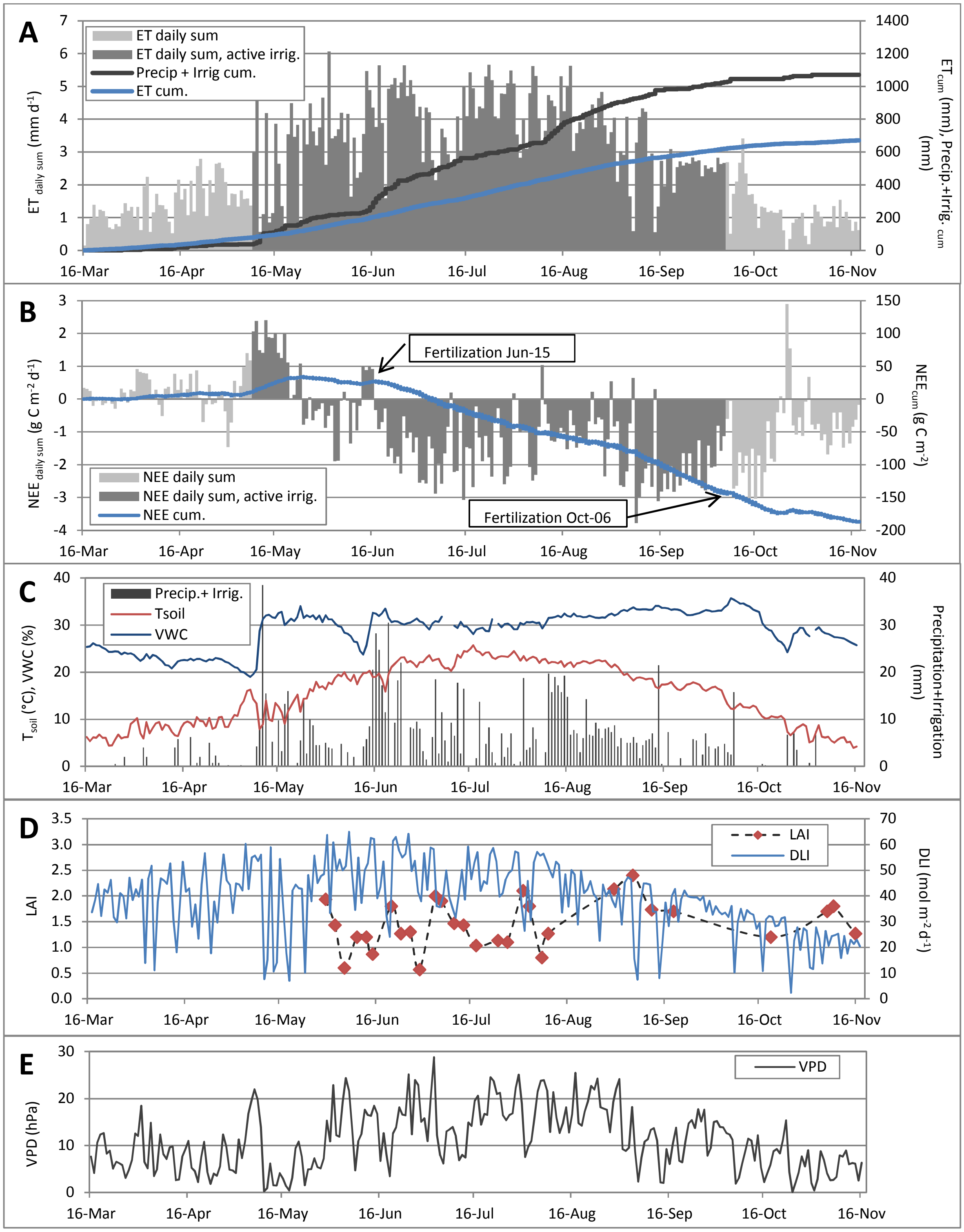

Fig. 4.42: Seasonal course of ET, NEE, and ancillary measurements at Fort Logan in 2011: (**A**) Daily sums of ET (mm d^{-1}) and cumulative ET and cumulative precipitation+irrigation (mm) (**B**) Daily sums of NEE (g C m^{-2} d^{-1}) and cumulative NEE (g C m^{-2}), (**C**) daily averages of T_{soil} (°C), VWC (%), and daily sums of water input (precipitation + irrigation) (mm), (**D**) DLI (mol m^{-2} d^{-1}) and LAI sample average, (**E**) daily averages of VPD (hPa)

NEE

As described in section 4.7.1., the diurnal magnitudes of uptake and release of CO_2 in March were very small, resulting in a cumulative loss of carbon of less than +1 g C m^{-2}. In April, daily sums of *NEE* (April average: +0.3(±0.4) g C m^{-2} d^{-1}) tended to be mainly positive, indicating net release of CO_2. Early May (May 10-24) witnessed a distinct increase in daily sums of *NEE* following a marked peak in soil temperature, the onset of irrigation and coinciding with several lows of DLI. During this period, daily *NEE* approached and exceeded at times +2 g C m^{-2} d^{-1} (May average: +0.7(±1.0) g C m^{-2} d^{-1}), before net uptake of CO_2 dominated daily sums for the remaining month. Until the end of May, cumulative *NEE* had amounted to +32 g C m^{-2}, i.e. a loss of carbon. Daily *NEE* sums turned temporarily positive again around mid-June following another strong pulse of irrigation. However, shortly after fertilization on June 15, net uptake started to dominate, resulting in a monthly average for daily *NEE* sums in June of -0.7(±0.9) g C m^{-2} d^{-1}. Sequestration of CO_2 continued in July, and as a result, cumulative *NEE* turned negative around July 5, i.e. urban lawns at Fort Logan became a net sink for CO_2. Moreover, daily sums of *NEE* showed a first seasonal peak near the middle of the month when values were close to -3 g C m^{-2} d^{-1} (July average: -1.6(±0.9) g C m^{-2} d^{-1}). Net accumulation of carbon slowed in August as the daily sum average of *NEE* decreased to -0.9(±0.8) g C m^{-2} d^{-1}. August also showed the highest monthly average for VPD which potentially affected stomata and therefore photosynthetic flux. By the end of the month, cumulative *NEE* stood at -69 g C m^{-2}. Sequestration grew stronger again in September, coinciding with the highest seasonal sample averages for LAI, and remained high throughout the month as daily sums of *NEE* frequently exceeded -2 g C m^{-2} d^{-1} (September average: -2.1(±1.0) g C m^{-2} d^{-1}). Net uptake of CO_2 continued steadily until about October 23 when a short cold spell temporarily interrupted sequestration, marked by a distinct positive deviation in daily *NEE* sums. Nonetheless, as urban lawns remained vital (high LAI), daily sums of *NEE* during the first half of November indicated further uptake of CO_2 (November average: -0.8(±0.6) g C m^{-2} d^{-1}). Overall, cumulative *NEE* between March 16 and November 18 amounted to -187 g C m^{-2}.

In contrast to 2011, March and April of 2012 already showed discernible net uptake of CO_2, when daily sums of *NEE* averaged to -0.3(±0.4) g C m^{-2} d^{-1} and -0.4(±0.9) g C m^{-2} d^{-1}, respectively (Fig. 4.43 B). As a result, cumulative *NEE* figured to -16 g C m^{-2} by the end of April. This trend of sequestration grew stronger in May, paralleled by increasing LAI. Nearly the entire month of May was characterized by negative daily sums of *NEE* indicating net uptake (May average: -1.9(±1.7) g C m^{-2} d^{-1}). However, during the last week of May, daily sums of *NEE* became positive, following and overlapping with a period of practically no water input and declining soil moisture. Cumulative *NEE* showed almost no change in June as daily sums of *NEE* nearly balanced over the course of the month (June average: +0.1(±0.9) g C m^{-2} d^{-1}). June also showed an increasing trend with regard to VPD as well as the highest absolute values and highest monthly average of all summer months. Net uptake dominated again in the first half of July and brought cumulative *NEE* to -94 g C m^{-2}, the largest cumulative uptake recorded in 2012. During the remaining month, however, daily sums of *NEE* were mainly positive again and led to an overall loss of carbon. This pattern coincided with intermittent irrigation, declining soil moisture, high soil temperature, and a noticeable drop in LAI, all of which lasted into early August. Until mid-August, daily sums of *NEE* were exclusively positive, at times exceeding 4 g C m^{-2} d^{-1} (August average: +1.3(±1.7) g C m^{-2} d^{-1}). Within these three weeks of severe drought conditions (late July to mid-August), approximately 50 g C m^{-2} were released, bringing cumulative *NEE* to -36 g C m^{-2}. Irrigation resumed around August 8 and *NEE* stabilized about one week later. As another cutback in irrigation occurred at the end of August, daily sums of *NEE* became positive again and led to loss of carbon lasting into early September. When LAI recovered and strong precipitation around September 12 increased soil moisture, net uptake of CO_2 started to dominate again and continued throughout October (October average: -0.9(±1.0) g C m^{-2} d^{-1}) until mid-November. This period of sequestration balanced the carbon lost in late July/mid-August. However, after a temporary period of stagnation with regard to cumulative *NEE*, daily *NEE* turned positive again and remained so until the end of the investigation period in December. Summed over the entire measurement period in 2012, cumulative *NEE* amounted to -70 g C m^{-2}.

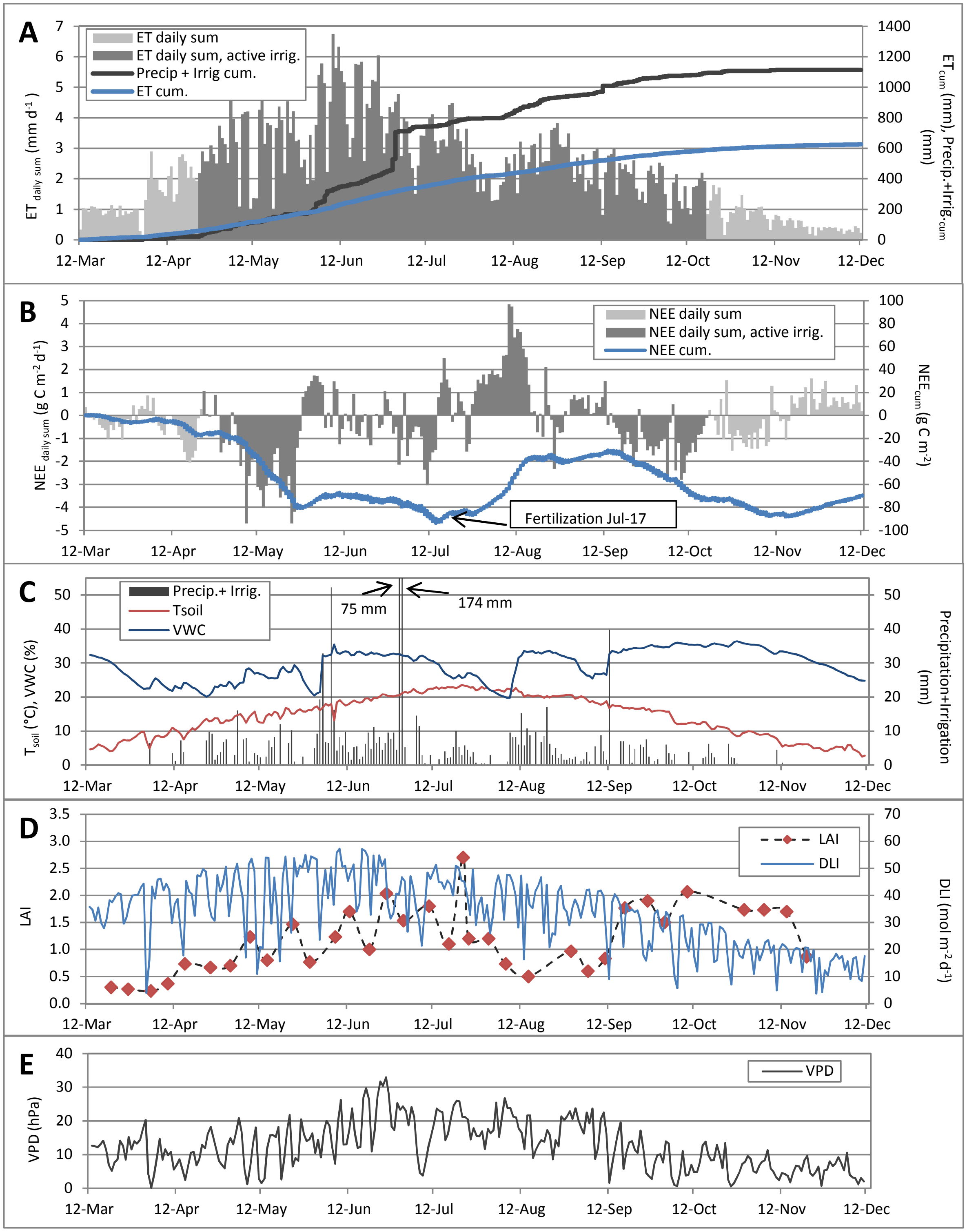

Fig. 4.43: Seasonal course of ET, NEE, and ancillary measurements at Fort Logan in 2012 (**A**) Daily sums of ET (mm d^{-1}) and cumulative ET and cumulative precipitation+irrigation (mm) (**B**) Daily sums of NEE (g C m^{-2} d^{-1}) and cumulative NEE (g C m^{-2}), (**C**) daily averages of T_{soil} (°C), VWC (%), and daily sums of water input (precipitation + irrigation) (mm), (**D**) DLI (mol m^{-2} d^{-1}) and LAI sample average, (**E**) daily averages of VPD (hPa)

4.7.2. Rocky Flats

Figure 4.44 and Fig. 4.45 (A + B) depict daily sums and cumulative trends of seasonal *ET* and *NEE* as well as cumulative precipitation in 2011 and 2012. Panels C through E of Fig. 4.44 and Fig. 4.45 contain data of ancillary measurements that may significantly influence *ET* and *NEE*, including precipitation, soil moisture, soil temperature, daily sums of PAR (DLI), leaf area index (LAI), and vapor pressure deficit (VPD).

ET

In 2011 and 2012, average sums for daily *ET* did not exceed 0.5 mm d^{-1} until March. By May, values had increased to 0.9(±0.5) mm d^{-1} in 2011 and to 1.8(±0.9) mm d^{-1} in 2012. Higher *ET* rates at Rocky Flats in spring of 2012, especially during April and May, overlapped with above-average temperatures and higher monthly averages of VPD compared to the previous year. Daily *ET* sums continued to increase in 2011, reaching a peak in July when daily sums averaged to 3.0(±0.7) mm d^{-1}. This trend was paralleled by noticeably higher monthly averages for VPD as well episodical strong precipitation events leading to distinct peaks in soil moisture. In contrast, daily sums in June 2012 showed a declining trend as soil moisture gradually decreased due to a lack of precipitation. This trend continued into the first week of July 2012 when daily *ET* dropped to less than 1 mm d^{-1}. Following strong precipitation events, daily sums temporarily increased to values between 2 and 3 mm d^{-1}, coinciding with some of the highest seasonal values for LAI. Until the end of June, total *ET* amounted to approximately 130 mm in 2011 and 170 mm in 2012, while measured precipitation had been 230 mm and 120 mm, respectively. In August, averages for daily ET (2011: 1.7(±0.4) mm d^{-1}; 2012: 0.9(±0.3) mm d^{-1}) had approximately halved in comparison to July as during both years monthly precipitation was sparse, soil moisture low, and VPD values remained high. Above-average precipitation in September temporarily enhanced *ET*, more so in 2011 than in 2012 as precipitation sums and LAI were higher and VPD lower. By the end of that month, cumulative *ET* figured to 310 mm in 2011 and 280 mm in 2012 (respective cumulative precipitation: 400 mm and 240 mm). Until November, average sums for daily *ET* had decreased to values of less than 0.5 mm d^{-1} and remained so until the end of the year. Annual cumulative *ET* in 2011 amounted to approximately 350 mm and precipitation summed to 450 mm (ET/P = 0.78), while in 2012 total *ET* and precipitation were 310 mm and 270 mm, respectively (ET/P = 1.15).

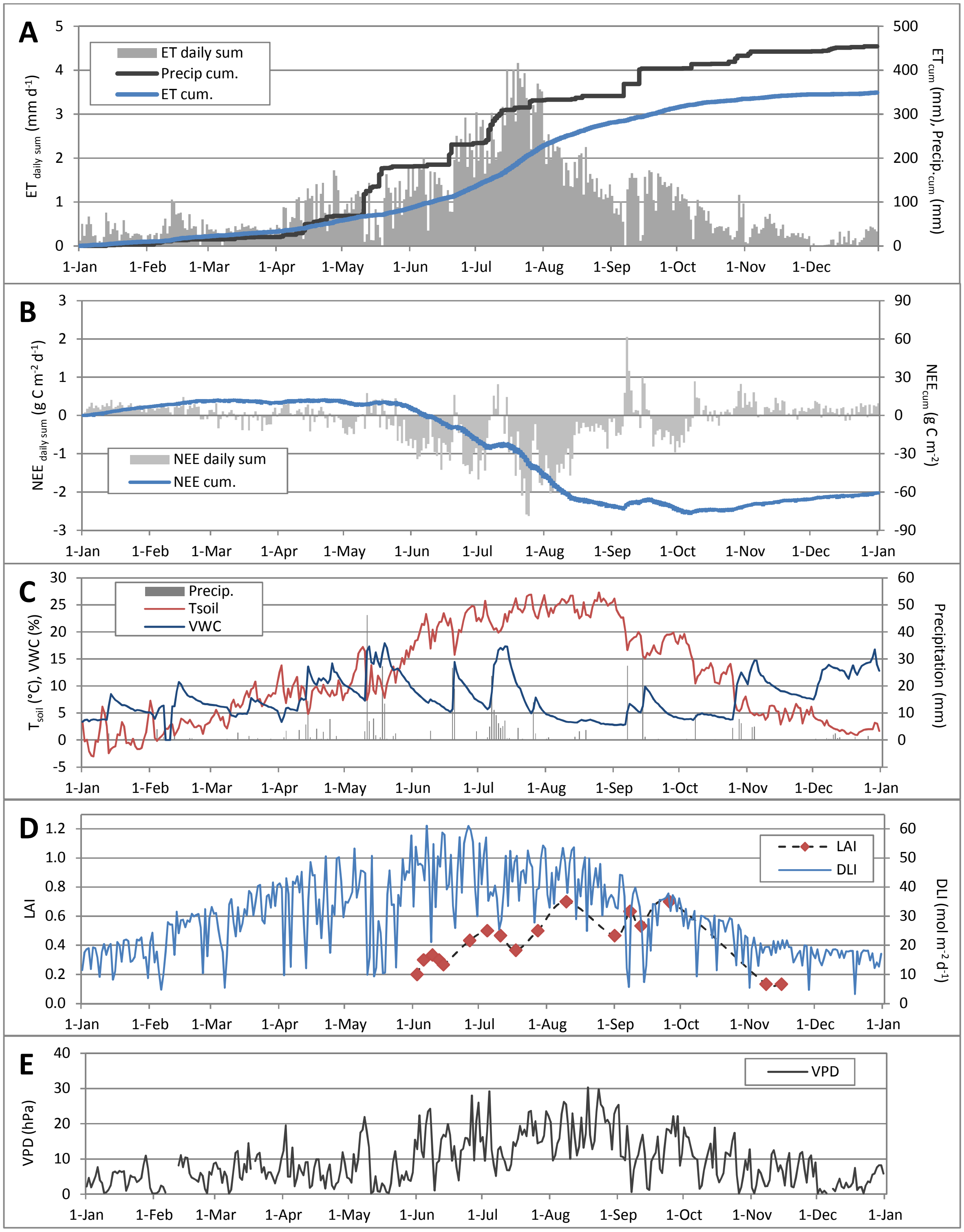

Fig. 4.44: Seasonal course of ET, NEE, and ancillary measurements at Rocky Flats in 2011 (**A**) Daily sums of ET (mm d^{-1}) and cumulative ET and cumulative precipitation (mm) (**B**) Daily sums of NEE (g C m^{-2} d^{-1}) and cumulative NEE (g C m^{-2}), (**C**) daily averages of T_{soil} (°C), VWC (%), and daily sums of precipitation (mm), (**D**) DLI (mol m^{-2} d^{-1}) and LAI sample average, (**E**) daily averages of VPD (hPa)

NEE

January and February of 2011 showed very small daily sums of *NEE* which were predominantly positive and averaged in both months to +0.2(±0.1) g C m^{-2} d^{-1}. March and April witnessed a mostly balanced distribution of daily *NEE* resulting in only marginal changes to the overall cumulative sum, and by the end of April seasonal *NEE* totaled to +11 g C m^{-2}. In May, daily *NEE* became increasingly stronger, especially during the second half of the month, averaging to -0.2(±0.4) g C m^{-2} d^{-1}. This trend of greater net uptake continued into June (June average: -0.8(±0.5) g C m^{-2} d^{-1}) and around June 8 the prairie at Rocky Flats had become a net sink for CO_2 in 2011. Highest daily accumulation of carbon was observed in late July (July average: -0.9 (±0.9) g C m^{-2} d^{-1}), when daily sums for *NEE* were near -2.5 g C m^{-2} d^{-1}. The summer months of June, July, and August were generally characterized by net uptake, paralleled by increasing values for LAI. However, net uptake was occasionally interrupted after strong precipitation events, which were followed by peaks of net release of CO_2 before uptake resumed again. This sequence of events is most notable around June 20, July 7, but also later around September 6. Net uptake slowed during the second half of August as daily averages for VPD peaked, LAI declined, and precipitation was scarce. By the end of August cumulative *NEE* reached -70 g C m^{-2}. After strong individual precipitation events had led to net emission of CO_2 in early September, net uptake dominated again for the remaining month. The maximum of -76 g C m^{-2} in the seasonal cumulative carbon flux occurred in early October (October average: +0.1(±0.4) g C m^{-2} d^{-1}). For the remaining year, daily sums of *NEE* were mostly positive and stayed below +0.5 g C m^{-2} d^{-1}, resulting in a moderate but steady loss of carbon. For 2011, annual cumulative *NEE* summed to -61 g C m^{-2}.

The first quarter of 2012 was very similar to 2011 with regard to *NEE*: January and February showed very small, primarily positive, daily sums. This pattern continued into March, paralleled by nearly constantly increasing soil temperature and declining soil moisture. Early April recorded the first significant precipitation since late February and by mid-April net uptake of CO_2 dominated daily sums of *NEE*. Nonetheless, cumulative *NEE* at the end of April (+8 g C m^{-2}) differed only slightly from the previous year. Uptake in May became increasingly stronger, coinciding with increasing values of LAI and almost regular precipitation events. Late May showed the highest daily uptake sums which approached -1.8 g C m^{-2} d^{-1}, while the monthly average amounted to -0.6 g C m^{-2} d^{-1}. This stronger net uptake continued into June (June average: -0.7(±0.6) g C m^{-2} d^{-1}) but became continuously weaker as the month progressed, concurring with rising soil temperature, increasing VPD, and declining soil moisture. As already observed in 2011, occasional heavy precipitation events interrupted net uptake during the height of the growing season and were coincident with periods of net release of CO_2. Examples of these occurrences were around June 27 and a more pronounced event around July 6. During the latter event, approximately 10 g C m^{-2} were released from the ecosystem reducing cumulative *NEE* to -25 g C m^{-2}. The second half of July was characterized by net uptake again, nearly offsetting the loss of carbon at the beginning of the month. August witnessed further net uptake but daily sums were usually small. Around August 26, cumulative *NEE* had reached a maximum for the season at -36 g C m^{-2}. Thereafter, daily net loss of CO_2 was common for the remaining months of the season, at times accelerated by precipitation events such as those in mid- and late September and late October. Averages for daily sums of *NEE* were +0.4(±0.4) g C m^{-2} d^{-1} and +0.3(±0.2) g C m^{-2} d^{-1} in September and October, respectively. The remaining months of 2012 witnessed small daily sums of *NEE* and, as a result, almost no change concerning cumulative *NEE* which, in 2012, summed to -9 g C m^{-2}.

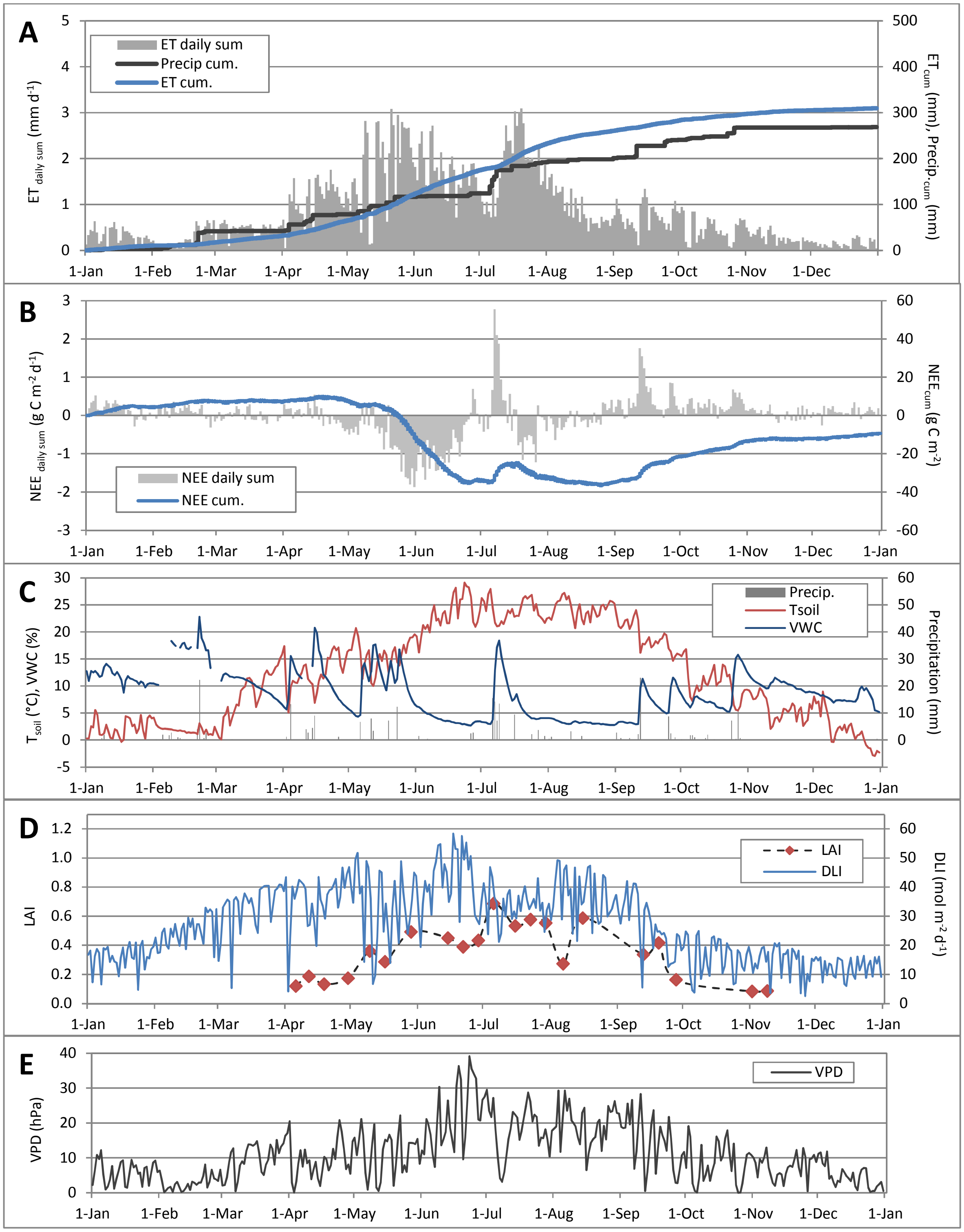

Fig. 4.45: Seasonal course of ET, NEE, and ancillary measurements at Rocky Flats in 2012 (**A**) Daily sums of ET (mm d^{-1}) and cumulative ET and cumulative precipitation (mm) (**B**) Daily sums of NEE (g C m^{-2} d^{-1}) and cumulative NEE (g C m^{-2}), (**C**) daily averages of T_{soil} (°C), VWC (%), and daily sums of precipitation (mm), (**D**) DLI (mol m^{-2} d^{-1}) and LAI sample average, (**E**) daily averages of VPD (hPa)

4.8. Comparison of Evapotranspiration and Water Input

Figure 4.46 and Fig. 4.47 depict a comparison of monthly sums of water input and *ET* as well as cumulative *ET* for Fort Logan and Rocky Flats in 2011 and 2012. For reasons of comparability, only full months based on the shortest investigation period, i.e. Fort Logan 2011, are presented.

In April 2011, measured water input at Fort Logan was 34 mm. One year later, the amount recorded had doubled to 68 mm, largely due to an earlier start of irrigation contributing about 42 mm of water. At Rocky Flats, measured precipitation in April was 48 mm in 2011 and 36 mm in 2012. The monthly sums for *ET* at Fort Logan in 2011 and 2012 were 50 mm and 62 mm, respectively, while values at Rocky Flats were approximately half at 25 mm and 33 mm. Above-average precipitation and the start of irrigation at Fort Logan in May 2011 increased monthly water input to 171 mm, nearly half of this amount coming from irrigation. Precipitation in May of 2012 stayed below average, totaling only 38 mm at Fort Logan. However, total water input amounted to 110 mm, thus, two-thirds of available water came from irrigation. Precipitation totals at Rocky Flats summed to 113 mm in May 2011 and only 38 mm in May 2012. Totals for *ET* in May summed to 80 mm and 99 mm at Fort Logan and to 27 mm and 57 mm at Rocky Flats in 2011 and 2012, respectively.

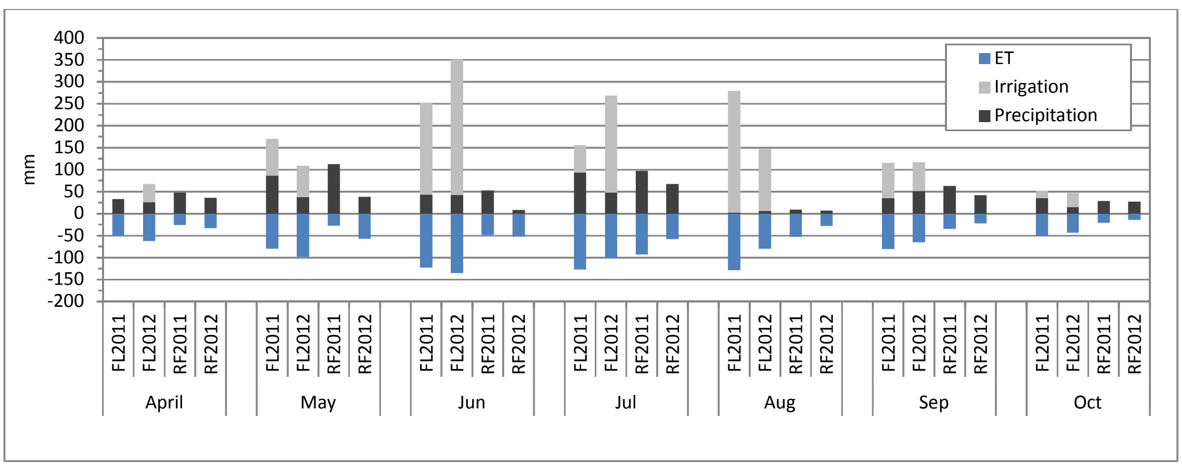

Fig. 4.46: Monthly sums of precipitation, irrigation, and ET between April and October at Fort Logan and Rocky Flats (2011 + 2012). Positive values for precipitation and irrigation indicate water input. Negative values for ET indicate water loss to the atmosphere.

At the start of June, notable differences became apparent with regard to cumulative *ET* when comparing years as well as sites (Fig. 4.47). Values tended to be higher at this point in 2012 than in 2011 and Fort Logan showed generally higher *ET* sums than Rocky Flats. In detail, cumulative *ET* up to June 1 amounted to 130 mm and 160 mm at Fort Logan and to 53 mm and 90 mm at Rocky Flats in 2011 and 2012, respectively. June also witnessed a further increase in total water input at Fort Logan. Precipitation amounted to 44 mm in 2011 and 42 mm in 2012. However, irrigation input summed up to 208 mm and 308 mm, bringing the monthly total up to 252 mm and 350 mm in June 2011 and June 2012, respectively. In contrast, Rocky Flats received 53 mm in June 2011 and only 8 mm of precipitation in June 2012. Data for August showed this to be the driest month in both years with regard to precipitation at Fort Logan as well as Rocky Flats. Monthly totals were only 3 mm (2011) and 6 mm (2012) at Fort Logan, while Rocky Flats received 10 mm and 7 mm, respectively. Similar to July, however, strong irrigation increased available water at Fort Logan to 280 mm in 2011 and 147 mm in 2012. Moreover, as the direct comparison in Fig. 4.47 illustrates, values for cumulative *ET* in 2011 and 2012 had equalized in early August for Fort Logan and Rocky Flats, respectively. While approximately 208 mm had been consumed by *ET* so far at Rocky Flats, Fort Logan showed a total of nearly double this amount at 408 mm. From this point on, cumulative *ET* for 2011 stayed above values of 2012 at Fort Logan and Rocky Flats. When irrigation was stopped in October at Fort Logan, water input dropped to 52 mm in 2011 and 47 mm in 2012. Rocky Flats received 29 mm and 27 mm of precipitation in the respective years. Monthly sums of *ET* were also the lowest since April, summing to 50 mm and 43 mm at Fort Logan in 2011 and 2012, respectively, while *ET* sums at Rocky Flats were 20 mm and 15 mm.

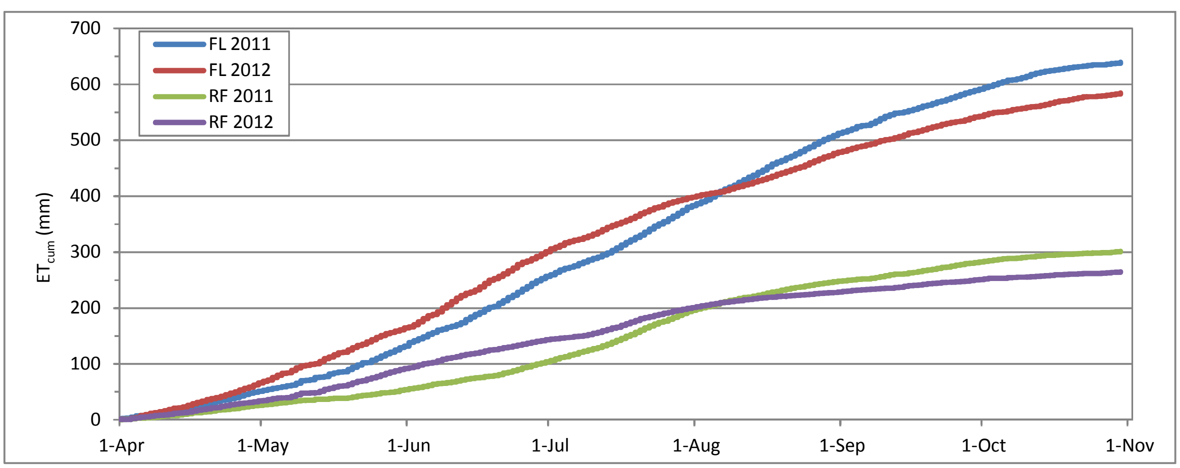

Fig. 4.47: Cumulative ET (mm) between April and October at Fort Logan and Rocky Flats (2011 + 2012)

Overall, cumulative *ET* between April and October totaled to 639 mm (2011; ET/P = 0.60) and 584 mm (2012; ET/P = 0.53) at Fort Logan, more than twice the amount of water consumed by *ET* compared to Rocky Flats. Here, the respective values for 2011 and 2012 were 302 mm (ET/P = 0.73) and 265 mm (ET/P = 1.18).

4.9. Comparison of Monthly Carbon Fluxes

Figure 4.48 and Fig. 4.49 represent a comparison of monthly sums of *NEE* for Fort Logan and Rocky Flats in 2011 and 2012. For reasons of comparability, only full months based on the shortest investigation period, i.e. Fort Logan 2011, are presented.

As shown in Fig. 4.48, notable differences between years as well as between sites become already apparent in April with regard to monthly sums of *NEE*: While Rocky Flats showed no significant *NEE* activity in April of 2011 or 2012, Fort Logan was estimated to have had a loss of approximately +8 g C m^{-2} in 2011. In contrast, net sequestration of CO_2 in 2012 amounted to -12 g C m^{-2}. This contrast between years at Fort Logan grew stronger in May when the respective monthly *NEE* sums were +23 g C m^{-2} and -58 g C m^{-2}. As a result, cumulative *NEE* for Fort Logan at the end of May summed to +31 g C m^{-2} in 2011 and -70 g C m^{-2} in 2012. Rocky Flats, on the other hand, was estimated to have had net sequestration in both years in May, about -5 g C m^{-2} in 2011 and -19 g C m^{-2} in 2012. In June, monthly sums of about -20 g C m^{-2} indicated sequestration at Fort Logan in 2011 and Rocky Flats in 2011 and 2012, whereas Fort Logan in 2012 showed a small net release. Net sequestration grew stronger in July at Fort Logan and Rocky Flats in 2011, whereas as in 2012, Fort Logan and Rocky Flats showed only small monthly uptake and release, respectively. Moreover, cumulative *NEE* for Rocky Flats showed that by early July approximately -34 g C m^{-2} had been sequestered in both years since April 1 (Fig. 4.49).

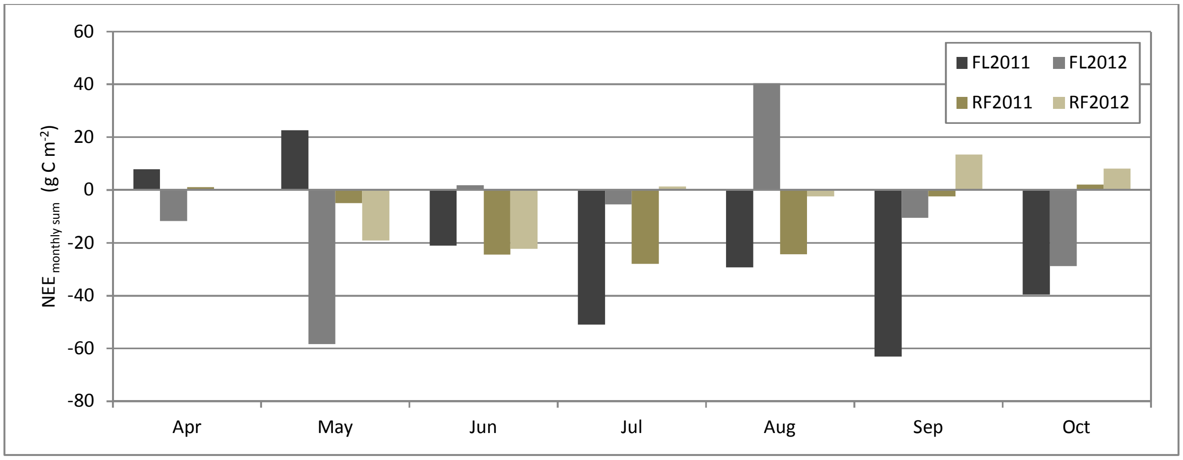

4.48: Monthly sums of NEE (g C m^{-2}) between April and October at Fort Logan and Rocky Flats (2011 + 2012)

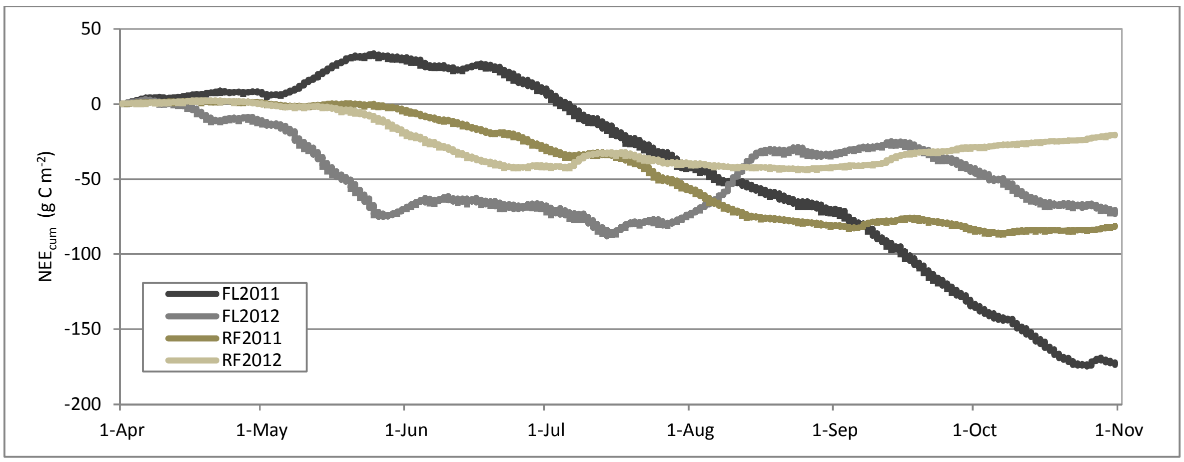

4.49: Cumulative NEE (g C m^{-2}) between April and October at Fort Logan and Rocky Flats (2011 + 2012)

The following months, however, showed a widening gap between the two years. In August of 2011, Fort Logan and Rocky Flats still showed net uptake, albeit slightly less than in July. Fort Logan in August 2012, however, displayed a major net release of CO_2 amounting to +40 g C m^{-2}. As a result, cumulative *NEE* by the end of August was -71 g C m^{-2} in 2011 but only -33 g C m^{-2} in 2012 for the urban lawns. Strong net uptake continued at Fort Logan in 2011 throughout October, with September showing the highest monthly sum overall (-63 g C m^{-2}). In September of 2012, following the large net loss of carbon at Fort Logan in August, sequestration resumed and intensified in October, with cumulative carbon flux reaching -29 g C m^{-2}. There was very little *NEE* activity at Rocky Flats in September and October of 2011, while in 2012 a net loss of CO_2 was measured in these months totaling to +13 g C m^{-2} and +8 g C m^{-2}, respectively.

Overall, cumulative *NEE* carbon flux between April 1 and October 31 at Fort Logan was -173 g C m^{-2} in 2011 and -73 g C m^{-2} in 2012. The respective sums for Rocky Flats were -81 g C m^{-2} and -21 g C m^{-2}.

4.10. Annual Carbon Budgets for Fort Logan and Rocky Flats

Annual *NEE* for Rocky Flats was calculated based on the gap-filled data presented in sections 4.6.3. and 4.6.4. At Fort Logan, the calculation of annual *NEE* required filling data gaps prior and past the investigation periods of 2011 and 2012. Missing days in March 2011/2012, November 2011, and December 2012 were filled using the MPI-Gapfill-Tool (after *Reichstein et al., 2005*). The remaining missing months (i.e. January and February 2011/2012; December 2011) were filled using a soil temperature/soil respiration regression (Appendix A2) assuming that CO_2-uptake, i.e. photosynthesis, was negligible. The required data for soil temperature was derived using a regression between soil temperature at Rocky Flats and soil temperature at Fort Logan (Appendix A2). Estimates for carbon emissions related to lawn management are based on findings published in *Townsend-Small and Czimzcik (2010)*.

Figure 4.50 displays annual sums of *NEE* and carbon emissions deduced from management activities such as general maintenance, irrigation, and fertilization at Fort Logan and Rocky Flats in 2011 and 2012. Since no active management was carried out at the prairie site, related carbon emissions were zero.

With regard to annual *NEE*, both urban lawn and tallgrass prairie were net sinks for CO_2 in 2011 as well as 2012. Nevertheless, large differences existed between sites and between years. As listed in Tab. 4.5, annual *NEE* at Fort Logan showed about double sink capacity for CO_2 compared to Rocky Flats during both years. Prolonged regional drought conditions in 2012, however, coincided with drastic reductions in sink strength of approximately 85 % at both locations. Moreover, while annual *NEE* is equivalent to the annual carbon budget at Rocky Flats, management activities at Fort Logan led to direct and indirect emissions of CO_2 which needed to be accounted for in the respective annual budget.

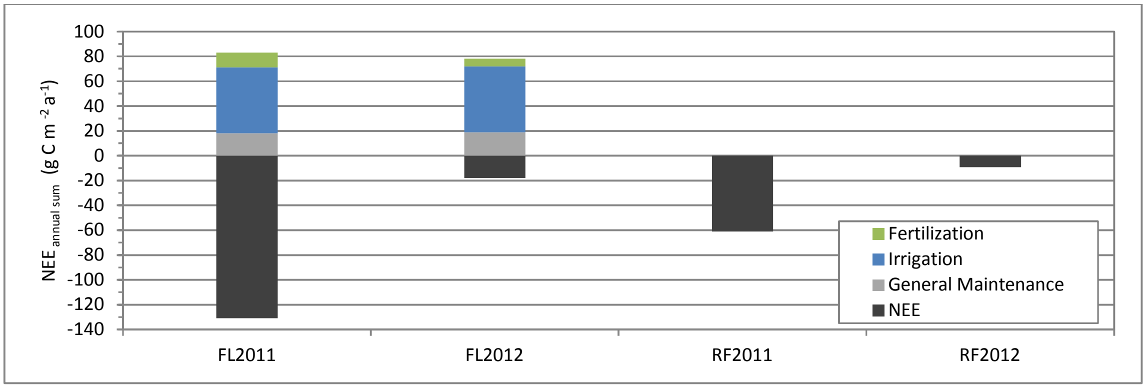

Fig 4.50: Annual sums (g C m^{-2} a^{-1}) of NEE and carbon offsets due to management at Fort Logan and Rocky Flats (2011 + 2012)

	FL 2011	FL 2012	RF 2011	RF 2012
	(g C m^{-2} a^{-1})			
Annual NEE	-131	-18	-61	-9
Carbon Offsets				
General Maintenance	+17	+19	-	-
Irrigation	+53	+53	-	-
Fertilization	+12	+6	-	-
Total Annual Balance	**-49**	**+60**	**-61**	**-9**

Tab 4.5: Budget components and total annual carbon budget (g C m^{-2} a^{-1}) for Fort Logan and Rocky Flats in 2011 and 2012

Based on the results of *Townsend-Small and Czimzcik (2010)*, estimates of monthly emissions due to fossil fuel use (i.e. general maintenance, mowing, aeration, etc.) were adjusted for the aerial extent of Fort Logan and only considered for months of active irrigation (May-Oct 2011; Apr-Oct 2012). This resulted in a monthly carbon offset of approximately +3 g C m^{-2}. Indirect emissions due to irrigation had a considerably stronger impact on the annual carbon budget. Assuming an intermediate scenario for irrigation-related emissions, total management emissions increased by +53 g C m^{-2} annually. Carbon emissions due to the production of fertilizer further added approximately +6 g C m^{-2} per application (2 applications in 2011, 1 in 2012; application rate: 49 kg N ha^{-1}). As a result, management emissions at Fort Logan in 2011 offset annual *NEE* by nearly two-thirds, leading to an annual carbon budget of -49 g C m^{-2} a^{-1}. In 2012, net sequestration of carbon was fully compensated when the annual carbon budget figured to +60 g C m^{-2} a^{-1}.

5. Discussion

5.1. Methods, Instruments, and Site Selection

The EC method employed in this study is widely considered the method of choice to quantify fluxes of carbon and energy at the ecosystem-scale (*Baldocchi et al, 2001*). However, research into this method is still very active and there are a number of studies pointing out the importance of fulfilling the underlying assumptions as well as being aware of potential limitations and biases influencing measurements (e.g. *Fuehrer and Friehe, 2002; Finnigan, 2006+2009; Kowalski, 2008; Acevedo et al., 2009; Mahrt, 2010; Gu et al., 2012; Higgens et al., 2012*). These elements need to be considered when employing the EC method or when analyzing EC data.

Tower Location

Eddy covariance measurements typically involve the setup of an instrument tower as was the case in this study. These towers need to be installed with regard to location and design to minimize potential measurement biases and maintain the ecological integrity of the site. As required by EC theory, the measurement location and height should be chosen to provide an adequate fetch over the spatially homogenous surface of interest (*Munger et al., 2012*). For this study, these requirements were relatively easy to fulfill for the Rocky Flats prairie site which may be described as a large, level tract of land that is nearly treeless with homogenous grassland vegetation. Selecting a suitable turfgrass site within the urban environment was complicated by finding a large, obstacle-free, and well-maintained plot of lawn that would also allow a nearly permanent installation of the measuring equipment and would be of low risk for vandalism. Fort Logan cemetery provided the best conditions for conducting the proposed EC measurements and fulfilling the theoretical assumptions. However, it cannot be completely ruled out that discontinuities and activities within the footprint (infrastructure, trees, management activities) had an impact on flux measurements. Nonetheless, the analysis of fetch indicated that contribution to fluxes originated predominantly or completely within the investigated ecosystems (sections 4.2.1. and 4.2.2.).

Tower and Instrument Design and Setup

The tower and the mounted instruments (e.g. anemometer, IRGA) (Fig. 2.4 and Fig. 2.5) can lead to potential distortions of the natural flow (horizontal and vertical wind velocity) which, in turn, can affect flux measurements (*Wyngaard, 1988*; *Munger et al., 2012*) Thus, the experimental setup at Fort Logan and Rocky Flats aimed to reduce such impact on the wind field by utilizing lattice-structured towers or low-profile tripod designs and mounting measuring equipment on booms that would place them at recommended distances away from the tower. Moreover, anemometers were positioned according to the anticipated predominant wind direction to improve overall data quality and to minimize disturbances caused by wind blowing across/through the tower. To test whether there was a tower influence on data, fluxes from questionable wind sectors were analyzed and compared to data from adjacent sectors but no discernible impact was found. However, anemometer design itself may potentially influence flux measurements. *Kochendorfer et al. (2012)* argue that non-orthogonal sonic anemometer designs (such as the one used in this study) require corrections regarding the measurement of vertical wind speed and found that the magnitude of carbon and heat fluxes increased up to 11 % by implementing the proposed corrections. The results of the mentioned study are still the issue of debate (*Kochendorfer et al., 2013; Mauder, 2013*), but *Nakai and Shimoyama (2012)* as well as *Frank et al. (2013)* have also found issues with regard to sonic anemometer measurements, indicating that more research on this topic is needed.

As mentioned earlier, the calculation of carbon and water fluxes is based on the covariance of vertical wind speed and the scalar of interest and thus requires not only the frequent measurement of wind but also of CO_2 and/or water vapor. For this purpose, an IRGA is usually deployed, either in an open-path (OP) or closed-path (CP) configuration (*Munger et al., 2012*). Both designs have their advantages and disadvantages (*Leuning and Judd, 1996*; *Burba, 2013*) and have been the subject of comparison studies (e.g. *Yasuda and Wanatabe, 2000*; *Haslwanter et al., 2009*).

The tower at Fort Logan was equipped with an OP IRGA (LI-7500, Licor, Inc., USA). This design has two main advantages, i.e. better high-frequency resolution compared to CP designs and low power consumption that suited the conditions at Fort Logan well. Nonetheless, issues concerning the function and design of OP IRGAs have been pointed out in a number of studies. Foremost, fluxes measured with OP IRGAs are subject to the WPL-correction (*Webb et al., 1980*; *Ham and Heilman, 2003*; *Liebethal and Foken, 2003*; *Liu, 2009*; section 3.1.6.), which in the case of CO_2 can become quite large. Furthermore, factors not considered in the WPL-correction such as instrument heat exchange (mostly an issue in colder months) can potentially affect air density in the sensing volume, thereby influencing the CO_2 density measurement (*Ono et al., 2008; Burba et al., 2008; Reverter et al., 2011*). Measurements by OP IRGAs are often affected by precipitation (on the instrument lenses) resulting in bad data (*Heusinkveld et al., 2008*). At Fort Logan, measurements were affected by periods of precipitation and frequent irrigation. Occasionally, thin films of mineral dust on the lens of the OP IRGA led to notably decreased values in CO_2 density without triggering a compensating response in signal gain (AGC). This occurs when optical properties of the dust reduce the detected radiance of the reference wavelength more than the absorbing wavelength. However, the largest impact of this effect is on the absolute accuracy of CO_2 density measurements which is secondary to the correct quantification of turbulent fluctuations.

The experimental setup at Rocky Flats included a closed path IRGA (LI-7200, Licor, Inc., USA) which is fundamentally similar to the OP LI-7500 IRGA. The instrument included a 1m long, 6.4 mm ID stainless steel intake tube and fast-response temperature and pressure sensors upstream, downstream, and within the CP sample cell. This instrument design was first released in 2010 and aimed to combine the advantages of OP and CP IRGAs and reduce their respective weaknesses (*Burba et al., 2012*). The enclosed sample cell and short intake tube were designed to minimize high-frequency signal attenuation in comparison to other CP systems (see *Ibrom et al., 2007; Clement et al., 2009; Fratini et al., 2012*), shorten lag times between the anemometer and IRGA signals and, contrary to OP designs, be less susceptible to data loss during precipitation events. Built-in fast-response temperature and pressure sensors enabled the output of the measured components (CO_2 and water vapor densities) to be computed as mixing ratios, thereby avoiding the need of the more typical WPL-correction (*Webb et al., 1980*) and potentially a large source of error during low CO_2-flux periods (e.g. in winter). These characteristics together with low power consumption led to the choice of this IRGA for year-around deployment at Rocky Flats. However, as later data analysis revealed, precipitation events between April and November were occasionally followed by data loss as water entered the sample cell and led to flawed measurements. Resume of normal operation was also delayed as it took longer for water to exit/evaporate from the enclosed sample cell. Data loss due to precipitation summed up to about 0.3 % in 2011. For unknown reasons, this specific issue became exacerbated in 2012 when losses summed to about 2.3 %.

Gap-filling

As mentioned in section 3.1.8., gaps in the EC data record are due to a number of reasons. *Falge et al. (2001a+2001b)* found that, when comparing 28 annual datasets from the Ameriflux and Euroflux networks, gaps were on average 35 % for *NEE*, 31 % for *LE*, and 25 % for *H*. The percentage of gaps at night was slightly higher than during the day. Similarly, *Moffat et al. (2007)* reviewed 10 datasets from 6 forest sites where gaps for *NEE* ranged between 22-36 % and also showed distinct differences between day and night (day: 10-20 %, night 60-70%). These numbers compare well with the annual datasets for Rocky Flats where gaps were between 33-36 % for *NEE*, 31-34 % for *LE*, and 27-29 % for *H*. Annual EC datasets were not available for Fort Logan but gap percentages were of similar size (*NEE*: 26-33.0 %; *LE*: 24-32 %; *H*: 20-25 %)(Tab. 5.1).

Nonetheless, for a comparison of monthly or annual flux sums between sites, these gaps need to be filled. Currently, there a number of different approaches, primarily for filling *NEE*. Among these are mean diurnal variation (MDV), marginal distribution sampling (MDS), look-up tables (LUT), non-linear regressions (NLR), artificial neural networks (ANN), and semi-parametric models (SPM) (*Falge et al., 2001a; Reichstein et al., 2005; Moffat et al., 2007*). *Falge et al. (2001a)* compared MDV, LUT, and NLR for gap-filling of annual *NEE* and found that the cumulative error sum for these methods ranged between -20 and +20 g C m^{-2}. Moreover, the study revealed that replacing data excluded due to $u*$-filtering increased annual *NEE* on average by +77 g C m^{-2}. *Falge et al. (2001a)* concluded that all three gap-filling methods delivered good results across the test datasets and different gap sizes. Furthermore, errors introduced by gap-filling were small among the methods studied and were directly proportional to the percentage of gaps filled. However, a maximum gap length was not defined due to the varied influence of ecosystem type, time of year, and phenological phases. The authors suggested, though, that the quality of results might be improved by considering additional meteorological parameters or anthropogenic activities. These results were generally confirmed by *Moffat et al. (2007)* reviewing *NEE* gap-filling techniques for different gap scenarios using datasets from European forests. NLR (after *Michaelis and Menten (1913)* and *Lloyd and Taylor (1994)*), LUT, MDS, and SPM showed good performance, slightly exceeded by ANN, whereas MDV produced moderate but consistent results. The impact of gap-filling on annual *NEE* sums was estimated to be within ±25 g C m^{-2}. Similar to *Falge et al. (2001)*, *Moffat et al. (2007)* found that the relative differences between the gap-filling techniques investigated were smaller than anticipated. All methods performed nearly equally well and the best of the techniques left little room for improvement.

Based on these findings, MDS (after *Reichstein et al., 2005*) was chosen as the primary filling method for the datasets of Fort Logan and Rocky Flats. For the estimation of annual carbon budgets at Fort Logan, ecosystem respiration outside the measurement periods (Jan-Feb, Dec) was estimated using NLR as the missing months exceeded maximum gap size for MDS (section 4.10.).

Assessment of the performance of MDS during this study revealed that, similar to *Moffat et al. (2007)*, gap-filling quality was generally higher during the day than at night. Values for r^2, the coefficient of determination between modeled and observed data, were highest for *H* and *LE* during the day (>0.87), while nighttime values were significantly lower (<0.44). *NEE* showed a similar pattern (r^2 day: >0.67, night: <0.39). Varying fill quality between day and night is likely due to generally higher data availability and greater flux magnitude during the day at both sites. Differences in r^2 observed for *NEE* between sites as well as between 2011 and 2012 might also be explained by the amplitude of fluxes at the sites: Fort Logan showed a generally greater span compared to Rocky Flats and a less diminished span during the drought year of 2012 (Tab. 5.1 and Fig. 5.1).

Employing NLR as a method to gap-fill missing data has been shown to deliver good results (*Falge et al., 2001a; Moffat et al., 2007*) and exponential regressions of soil temperature with nighttime *NEE* to estimate ecosystem respiration (section 4.10.) have been successfully implemented in various other studies of ecosystem carbon fluxes (e.g. *Xu and Baldocchi, 2004; Curtis et al., 2005; Verma et al., 2005; Kutzbach, 2006; Dragoni et al., 2007; Nave et al., 2011*). Thus, the NLR approach to help estimate annual carbon budgets for Fort Logan seems reasonable but the assumption of no photosynthetic activity outside the measurement periods (2011: Jan-Feb, Dec; 2012: Jan-Feb) as well as the approximation of soil temperature (as the driving parameter) from Rocky Flats data introduce additional uncertainties to the modeled data. Nonetheless, both gap-filling methods (MDS and NLR) used in the study at hand appear adequate for replacing the missing data.

			FL2011*	FL2012**	RF2011	RF2012
NEE (μmol CO_2 m^{-2} s^{-1})	Day	Gap (%)	21.5	12.7	26.4	24.7
		r^2	0.84	0.78	0.76	0.67
		SE	1.9	2.0	0.9	0.8
		n	4933	5967	6287	6437
	Night	Gap (%)	46.0	40.1	44.5	41.3
		r^2	0.39	0.29	0.36	0.31
		SE	1.2	1.1	0.5	0.4
		n	3007	3809	4980	5292
LE (W m^{-2})	Day	Gap (%)	19.9	9.6	22.7	20.3
		r^2	0.90	0.91	0.91	0.87
		SE	36	29	18	17
		n	5032	6178	6602	6811
	Night	Gap (%)	46.0	38.6	43.9	40.9
		r^2	0.29	0.44	0.25	0.21
		SE	5	5	3	3
		n	3006	3904	5033	5325
H (W m^{-2})	Day	Gap (%)	17.2	10.2	19.9	17.6
		r^2	0.90	0.88	0.91	0.93
		SE	16	17	28	26
		n	5198	6137	6847	7043
	Night	Gap (%)	34.2	30.0	37.1	34.8
		r^2	0.32	0.23	0.35	0.32
		SE	7	6	12	12
		n	3664	4456	5647	5877

Tab. 5.1 Comparison of relative gap size and gap-filling quality parameters. r^2 = coefficient of determination between modeled and observed data. SE = standard error of modeled data. n = number of points. * FL2011 data Mar16 - Nov18 2011; **FL2012 data Mar12 - Dec12 2012

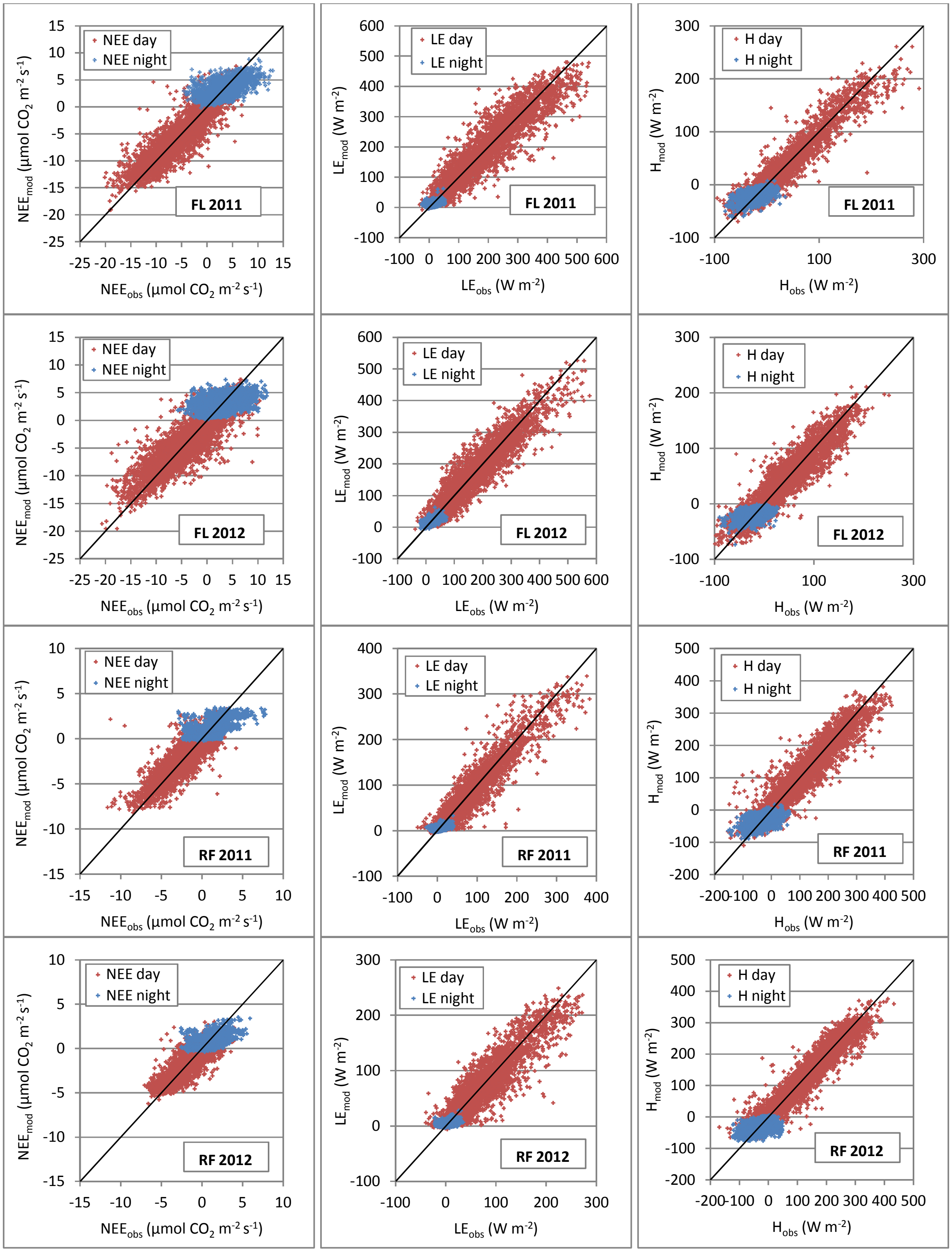

Fig. 5.1: Scatter plots of NEE, LE, and H (observed vs. modeled; separated for day and night (R_s<10 W m^{-2})) at Fort Logan and Rocky Flats (2011+2012); black line = 1:1.

5.2. Temperature and Precipitation

As shown in sections 4.1.1.-4.1.5., meteorological data for Fort Logan and Rocky Flats revealed that climatic conditions differed greatly between 2011 and 2012, especially with regard to temperature and precipitation. These observations are confirmed by other, independent data, for example, from the official Denver climate station:

Here, air temperature in 2011 averaged to 10.4°C, matching the long-term mean of 1981-2010. Nonetheless, monthly deviations from this mean did occur and agree well with variations observed at Fort Logan and Rocky Flats. Among these are most notably a cooler May (-2.5 K) and a warmer August (+2.7 K). With regard to precipitation, 2011 can be regarded as a wet year, thereby confirming the observations made during this study. Although the first 4 months of the year were slightly below normal, above-average precipitation in May, June, and July resulted in total precipitation in Denver summing to 440 mm in 2011, 59 mm more than the long-term mean (*NOAA, 2012*).

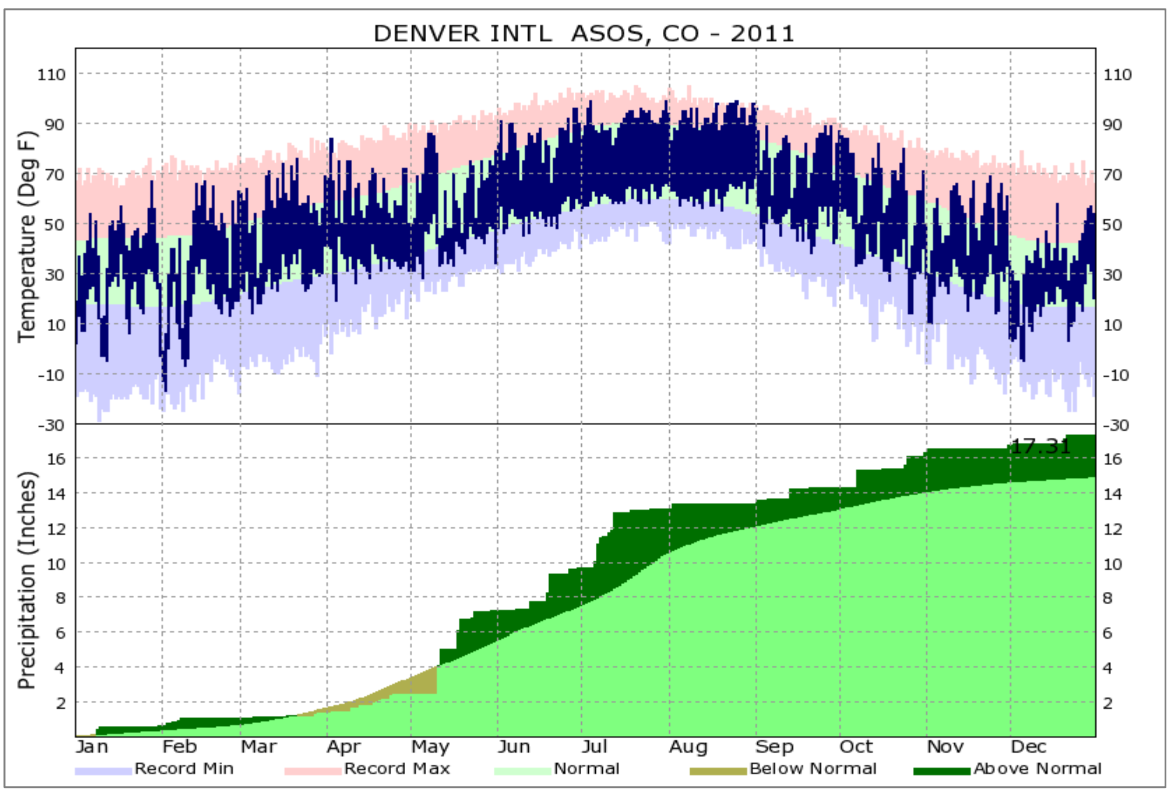

Fig. 5.2: Annual course of air temperature and cumulative precipitation in 2011 in Denver and comparison to long-term means (1981-2010) (*NOAA, 2012a*)

In contrast to 2011, 2012 was characterized by severe drought conditions with above-average temperatures and below-average precipitation. Average air temperature in Denver was 12.2°C, nearly 2 K above the long-term mean. Furthermore, positive monthly deviations occurred for all months except February and October. The most notable examples are March (+4.8 K) and June (+4.2 K), which experienced exceptional heat waves. On 73 days, maximum temperature exceeded 32°C, which is 33 days above average and 23 days more than in 2011. Record-setting temperatures occurred on June 25/26 reaching 40.5°C. Moreover, July proved to be the hottest month in Denver history with an average temperature of 26.1°C (*NOAA, 2013d*).

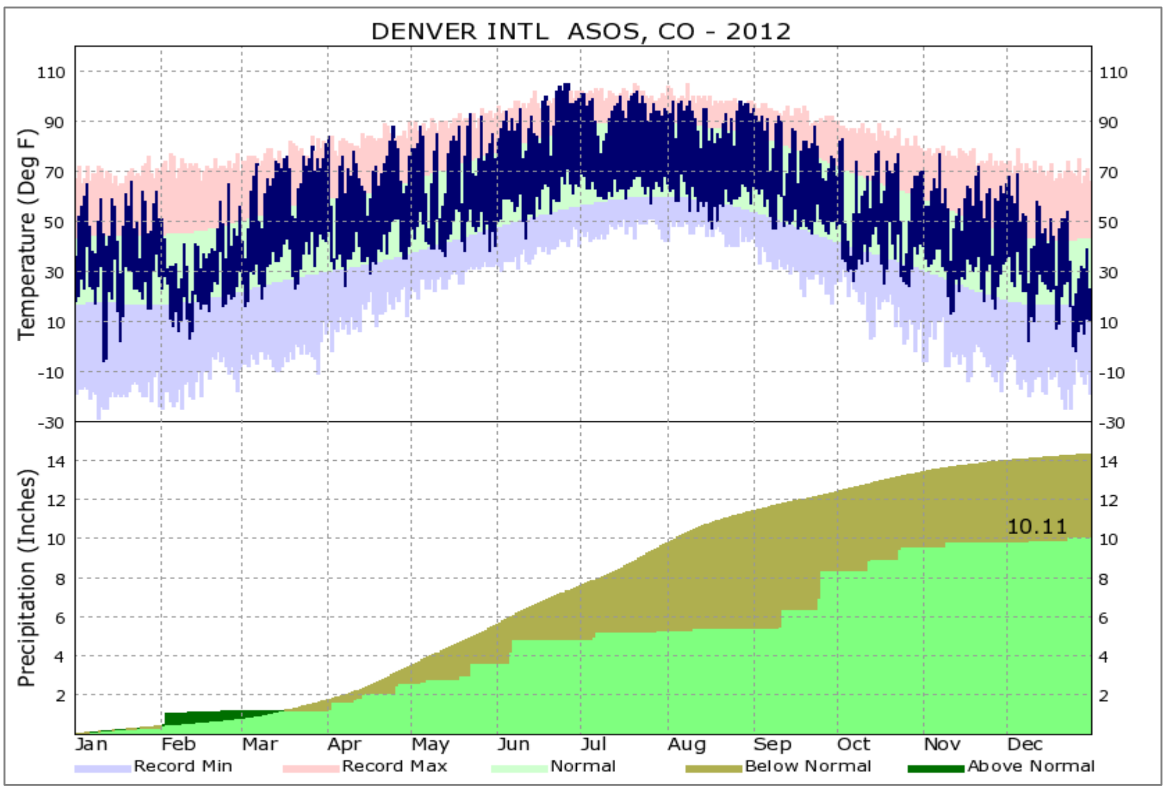

Fig. 5.3: Annual course of air temperature and cumulative precipitation in 2012 in Denver and comparison to long-term means (1981-2010) (*NOAA, 2013e*)

These significant temperature deviations were not limited to Denver or the state of Colorado. Average temperatures for the US showed that the spring of 2012 ranked as the warmest and the summer of 2012 as the third warmest on record (*NIDIS, 2012*). But 2012 was not only one of the warmest years in Denver but also one of the driest. Following good snowfall in early February, March, usually the snowiest month, was the driest on record. Moreover, drought conditions intensified over the summer and between June and August recorded precipitation amounted to only 46 mm, 102 mm below average (*NOAA, 2013d*). By the end of August, more than 60 % of the contiguous US experienced drought conditions (*NIDIS, 2012*). Total precipitation in Denver summed to 257 mm in 2012, 124 mm below average (*NOAA, 2013d*). Overall, these statistics demonstrate that the temperature and precipitation data recorded at Fort Logan and Rocky Flats agree well with other, independently recorded data. Moreover, they show that the meteorological extremes measured in 2012 were not due to local effects but were part of larger climatic conditions affecting Denver as a region, the state of Colorado and beyond. The impact of these climatic conditions on the investigated ecosystem fluxes will be discussed in the following sections.

5.3. Energy Fluxes

Shortwave and Net Radiation

The seasonal sums of R_s (Apr-Oct) at Fort Logan and Rocky Flats showed only small differences between years, amounting to 2.0 % for Fort Logan and 1.1 % for Rocky Flats, indicating that solar input for that time was about the same in 2011 and 2012 (Tab 5.2). However, monthly sums showed more distinct differences, most notably in April, May, and October. Here, both sites showed increased solar input in 2012 (compared to 2011) of 11.1-18.4 %, coinciding with above-average spring temperatures (section 5.2). October on the other had showed decreased solar input in 2012 (compared to 2011) by 10.6-18.7 %, which can be linked to below-average temperatures at both sites during that month. Differences between sites for seasonal and monthly sums in both years revealed a nearly constant offset of -10 % for Rocky Flats, i.e. values at the prairie site were usually lower than at Fort Logan. The most likely cause of this pattern is a mismatch in sensor calibration between sites (*personal communication Dean E. Anderson*).

Relative differences of R_n between years (Apr-Oct) were also small for seasonal sums and amounted to 2.9 % for Fort Logan and 1.6 % for Rocky Flats. Between sites, differences were also small and did not exceed 3.0 % in 2011 and 1.5 % in 2012 (Tab 5.2). Deviations of monthly sums between years usually followed the pattern of R_s. Besides April, May, and October, larger differences between years were most notable in August for Fort Logan and July for Rocky Flats. This may be due to drought conditions in 2012 causing earlier senescence of vegetation and drier soils at these sites and, thus, a change in albedo.

	FL2011		FL2012		RF2011		RF2012	
Month	R_s (mol m^{-2})	R_n (MJ m^{-2})	R_s (mol m^{-2})	R_n (MJ m^{-2})	R_s (mol m^{-2})	R_n (MJ m^{-2})	R_s (mol m^{-2})	R_n (MJ m^{-2})
Apr	596	243	662	290	543	277	612	330
May	634	324	745	353	549	315	650	378
Jun	770	425	785	392	701	398	684	390
Jul	755	398	731	374	683	400	663	365
Aug	691	351	656	296	618	322	602	306
Sep	548	257	551	246	488	238	492	233
Oct	444	168	397	154	421	152	343	134
Total	**4438**	**2167**	**4528**	**2105**	**4002**	**2102**	**4046**	**2136**

Tab. 5.2: Monthly sums of shortwave radiation (R_s; mol m^{-2}) and net radiation (R_n; MJ m^{-2}) between April and October of 2011 and 2012 at Fort Logan and Rocky Flats

Burba et al. (2005) measured annual R_n sums for a tallgrass prairie site in north-central Oklahoma which ranged between 2952-3105 MJ m^{-2} a^{-1}. Compared to the annual sums of Rocky Flats (2011: 2477 MJ m^{-2} a^{-1}; 2012: 2529 MJ m^{-2} a^{-1}), these values are 18-25 % higher, which might be due to differences in latitude affecting solar input as well as vegetation composition and management influencing albedo (e.g. annual burns in spring). On the other hand, daily sums for R_n between June 21 - September 30 at Konza Prairie (tallgrass) averaged to 10.9-11.3 MJ m^{-2} d^{-1} (*Arnold, 2009*), which compares well with averages at Rocky Flats of 10.7 MJ m^{-2} d^{-1} in 2011 and 10.1 MJ m^{-2} d^{-1} in 2012 for the same time frame.

With regard to R_n above turfgrass, *Spronken-Smith et al. (2000)* found average daily sums of R_n in August in Sacramento of 10.5-11.1 MJ m^{-2} d^{-1}. This is comparable to Fort Logan in August 2011 (11.3 MJ m^{-2} d^{-1}) and 2012 (9.6 MJ m^{-2} d^{-1}), albeit the lower value in 2012 might, again, be due to the impact of drought during that year. Measuring energy fluxes above a residential neighborhood dominated by lawns in Kansas City, *Balogun et al. (2009)* found daily averages for R_n in August of 143 W m^{-2} which are similar to daily averages observed in August at Fort Logan (2011: 131 W m^{-2}; 2012: 110 W m^{-2}).

Soil Heat Flux

Energy partitioning (section 4.4.) showed that *G* between April and October at Fort Logan and Rocky Flats only played a minor role in the surface energy balance as the largest share of available energy was consumed by *H* and *LE*. Relative monthly shares of *G* at both sites for

2011 and 2012 ranged from 0.3 to 6.2 % between April and August. With decreasing day length in September and October, soils (on average) became a net source of energy at both sites as reduced R_n caused the soil surface to cool and resulted in the transfer of heat upwards to the soil surface and on towards the atmosphere (Fig. 4.32).

Daily sums of G in August at Fort Logan were similar to the values reported by *Spronken-Smith et al. (2000)* for turfgrass in California. However, they also noted that the contribution of G in comparison to H and LE was insignificant. As shown before (sections 4.3.1. and 4.3.2.), highest values of G were measured in 2011 in mid-May and mid-June coinciding with times of highest R_n. These events were probably enhanced by significant precipitation/irrigation as increasing soil moisture enhances thermal conductivity in soils (*Rosenberg et al., 1983*). The span of values observed in 2012, especially in May and June, was not as high as the year before, possibly due to an earlier start of plant growth in 2012 and generally higher turfgrass density covering the soil surface, as the area around the tower had been reseeded in June 2011.

The impact of G at Rocky Flats on surface energy balance was comparable to Fort Logan. When R_n was highest between April and August, the relative amount consumed by G ranged between 0.6 and 5.3 %. *Krishnan et al. (2012)* found ratios of G/R_n for midday (11:00-14:00 average) from 0.23-0.30 for a semi-arid grassland in Arizona between May and September, similar to what *Aires et al. (2008)* found for a Mediterranean grassland in July. In comparison, ratios at Rocky Flats were noticeably lower, ranging between 0.12-0.16. *Ham and Knapp (1998)* noted for their Konza Prairie site (tallgrass) that G was only a minor component of surface energy balance during daytime, usually amounting to 5-10 % of R_n. Similar to the urban site, G in late summer was, on average, directed from the soils towards the atmosphere. Furthermore, peaks in absolute values coincided with stronger precipitation events as elevated soil moisture affected thermal conductivity. These “outliers” were less pronounced in 2012, likely due to significantly decreased precipitation (as detailed above) and, as a result, longer periods of drier soils. As the study period for Rocky Flats spanned the entire year, data also showed periods of minimal G when snow cover led to increased albedo of the land surface and reduced heat transport from/into the soil. These types of events were rare at Fort Logan.

Sensible and Latent Heat Flux

As indicated by the average daily sums of energy fluxes, the largest share of available energy was partitioned into *H* and *LE* (section 4.4.). Both energy fluxes combined consumed between 59-88 % of available energy at Fort Logan and Rocky Flats (Apr-Oct). However, notable differences with regard to seasonal patterns and flux strength of *H* and *LE* between sites and the investigated years occurred, which clearly showed the influence of climate conditions but also of differences in vegetation and management.

At Fort Logan, *LE* was the dominant partition of available energy between April and October of 2011 and 2012, on average amounting to 71 % and thus by far exceeding the contribution of *H* (Fig. 4.32). This pattern of energy partitioning can be primarily attributed to the impacts of management (especially irrigation) and vegetation (type, LAI). As described above, irrigation input was significant, surpassing precipitation between April and October by a factor of more than 2 in 2011 and nearly 4 in 2012. Moreover, turfgrass at Fort Logan represented a mix of cool-season grasses which show less photosynthetic and water use efficiency than warm-season grasses, e.g. tallgrass prairie (*Romero and Dukes, 2009; Graham, 2011*). Thus, transpiration rates are usually higher in comparison, even under water stress conditions, in order to maintain optimum growth (*Romero and Dukes, 2009*). Furthermore, as transpiration significantly influences water flux from turfgrass sites during the growing season (*Duble, 2006*), the presence of cool-season turfgrass at Fort Logan can be expected to have a considerable impact on *LE*. The seasonal dynamics of *H* and *LE* seem to provide evidence for the combined effect of the mentioned parameters: Prior to the onset of irrigation in 2011, *H* consumed about one third of available energy in April but as irrigation started in May and the site visibly greened (increasing LAI), *H* became markedly weaker and the size of its partition decreased. Simultaneously, the relative amount of *LE* during these months increased and in May *LE* consumed nearly two thirds of available energy. By August, at the time of highest irrigation input (277 mm), highest monthly VPD, and high LAI, *LE* was at maximum while *H* had decreased drastically and even showed negative daily sums (indicating that *H* was a small net source of energy). This relation of *LE* and *H* is similar to the observations made by *Spronken-Smith et al. (2000)* at an irrigated park in Sacramento, California. Throughout the remaining summer and early fall, *LE* generally followed the declining trend of R_n, LAI, and soil moisture (after irrigation had stopped in early October), but little change occurred in the portion consumed by *LE*, which still exceeded 70 %.

In 2012, April and May showed a similar pattern regarding the partitioning of *H* and *LE* as in 2011, albeit accelerated by an earlier start of irrigation and turfgrass growth. *LE* dominated energy partitioning in June, coinciding with the peak in R_n, maximum irrigation input (309 mm), highest monthly average of VPD, and high LAI. However, as drought conditions intensified and irrigation became irregular (most notably in August), daily energy sums revealed an increase in *H* with a decrease in *LE*. This trend was paralleled by declining soil moisture and LAI. With the resumption of irrigation, both parameters recovered and *LE* increased again. This illustrates the dependence of *LE* in urban ecosystems on water input and LAI (*Grimmond and Oke, 1999*). Nonetheless, *LE* consumed about two thirds of available energy while less than 10% was partitioned into *H*.

Peters et al. (2011) found an average evaporative fraction (LE/R_n) for a turfgrass site in mid-summer at midday (11:00-15:00) of 0.45. This is near the lower end of values found for Fort Logan in June-September which figured to 0.59-0.72 in 2011 and 0.49-0.69 in 2012. The site studied by *Peters et al. (2011)* in Minnesota, however, was not irrigated and experienced a cold-temperate climate, which may partially explain the differences in comparison to Fort Logan. *Balogun et al. (2009)* studying surface energy balance in an exurban neighborhood near Kansas City, Missouri, found values in August for LE/R_n and H/R_n of 0.55 and 0.23, respectively. In contrast, Fort Logan showed a higher evaporative fraction and lower fraction for sensible heat during that month, which might be explained by the different land cover characteristics at the site in Kansas City. Here, turfgrass covered only 50 % of the investigated area, which is well within the range reported for US cities (39-54 %; *Dwyer et al., 2000; Milesi et al., 2005*), but the remaining share consisted of buildings and other infrastructure, thereby potentially enhancing *H* at the expense of *LE* (*Bonan, 2000; Spronken-Smith et al., 2000*). *Grimmond and Oke (1999*) found values for LE/R_n of 0.28-0.46 in different North American cities, with higher values linked to higher fractions of vegetation cover. This dependency of LE/R_n on vegetation was also confirmed by *Christen and Vogt (2004)* investigating energy balance along an urban density gradient in Basel, Switzerland. *Moriwaki and Kanda (2004)* observed a ratio of $LE/R_n = 0.38$ for suburban Tokyo. Thus, *LE* in urban ecosystems can be considered an important component of the energy balance as vegetated areas can be extensive and may be heavily irrigated.

In contrast to Fort Logan, Rocky Flats was characterized by a more balanced energy partitioning of *H* and *LE*. Between April and October 2011, daily energy sums revealed that both fluxes consumed on average about one third of available energy, the balance shifting slightly in favor of *H* during the drought year 2012. Similar observations have been reported by *Aires et al. (2008)* for a grassland in Portugal. Furthermore, *LE* seldom dominated surface energy balance at the prairie site, with July 2011 being the only month investigated when, on average, the amplitude of *LE* exceeded that of *H*. The relation between *H* and *LE* was heavily influenced by the semi-arid conditions and the lack of irrigation at Rocky Flats. Nonetheless, the impact of vegetation also appeared to be significant. As previously mentioned, the tallgrass prairie consists of warm-season grasses characterized by several adaptations (e.g. deep root system, high WUE) that help it endure climate extremes of semi-arid environments by reducing water losses through transpiration (*Romero and Dukes, 2009; Graham, 2011*). Thus, energy partitioning showed a clear impact of precipitation and soil moisture but also of LAI and VPD. These dependencies are well reflected in the seasonal course of both fluxes: *LE* strongly increased in June 2011 after strong convective precipitation resulted in a spike in soil moisture, paralleled by increasing LAI and VPD. This rise continued into July, leading to the overall seasonal peak, as more precipitation fell during the first half of the month and LAI increased. August, however, was characterized by lack of precipitation (<10 mm), low soil moisture, high temperatures, highest monthly VPD, and declining LAI. As a result, the share of *H* increased again, while *LE* fell sharply and only recovered partially as individual precipitation events in September led to a temporary rise in soil moisture and a rebound in LAI. Following senescence in early fall (as indicated by the decline in LAI), the diurnal amplitude of *H* as well as its share in energy partitioning further increased while *LE* gradually declined, which is similar to findings reported by *Ham and Knapp (1998)* for their Konza Prairie site.

Similar to Fort Logan, drought conditions in 2012 clearly impacted the patterns of *H* and *LE* at Rocky Flats. Here, not only the reduced total amount but also the changed seasonal distribution of precipitation (especially during the growing season) appears to have played an important role in energy partitioning. Above-average temperatures in spring seem to have aided an earlier greening (LAI) despite overall low precipitation and resulted in an early first peak of *LE* in mid-May. Following this peak, however, soil moisture declined due to a lack of rainfall and *H* dominated energy partitioning during the day. A series of strong precipitation events and high LAI in early July resulted in the second seasonal peak of *LE*. In comparison to 2011, both peaks were noticeably smaller. When drought conditions strengthened again, depleting soil moisture and deficient precipitation caused an early senescence of vegetation. As LAI declined, so did *LE* and for the remaining season *H* consumed the majority of available energy again.

Burba and Verma (2005) found that *LE* was an important consumer of available energy and reported annual evaporative fractions for a native tallgrass prairie in Oklahoma of 0.49-0.59. At Rocky Flats, values varied between 0.29-0.37, which compares better to the range of 0.27-0.46 found by *Ryu et al. (2008)* for a grassland in California. Differences between tallgrass sites (*Burba and Verma (2005)*, Rocky Flats) are most likely due to different climatic conditions (temperature and precipitation) and vegetation characteristics (LAI). Comparing conditions among these studies showed that Rocky Flats was clearly drier, cooler, and characterized by lower vegetation density. Nonetheless, *Burba and Verma (2005*) concluded that variations in *LE* could be primarily explained by variations in soil moisture and vegetation growth, a finding that was confirmed by the observations made during this study. *Krishnan et al. (2012)* found midday (11:00-14:00 average) ratios of H/R_n from 0.37-0.60 and LE/R_n from 0.02-0.25 for a semi-arid grassland in Arizona between May and September. In comparison, the respective ratios at Rocky Flats for H/R_n ranged between 0.23-0.43 in 2011 and 0.37-0.50 in 2012, while LE/R_n varied between 0.17-0.46 (2011) and 0.15-0.30 (2012). Higher similarities between the 2012 Rocky Flats values and the Arizona site are probably due to the encountered drought conditions as above-average temperatures and reduced precipitation at Rocky Flats reduced the differences in general climate between the sites.

5.4. Evapotranspiration and Water Balance

Evapotranspiration, as the water-balance equivalent of *LE*, exhibited similar seasonal trends and distinct differences between sites and years (section 4.7.). The highest daily *ET* sums at Fort Logan and Rocky Flats occurred during the summer months when the impact of influencing parameters (precipitation, irrigation, R_n, VPD, LAI) was generally greatest (Fig. 4.42-4.45). For the urban site, this finding agrees well with the study by *Peters et al. (2011)* who reported highest average daily sums (near 4 mm d^{-1}) for a turfgrass site in Minnesota-St.Paul in June. Average daily sums at Fort Logan during that month were similar at 4.1 mm d^{-1} and 4.5mm d^{-1} in 2011 and 2012, respectively, and also compare well to the *ET* rates of up to 5 mm d^{-1} found by *Zhang et al. (2007)* in their study of turfgrass in Beijing. Higher daily *ET* rates for irrigated lawns (of up to 10 mm d^{-1}) were reported by *Feldhake et al. (1983)* for sites in Colorado and by *Litvak et al. (2013)* for Los Angeles, California. A span of 3-12 mm d^{-1} for different turfgrass species (e.g. fescue, Kentucky bluegrass) was reported by *Romero and Dukes (2009)*.

Rocky Flats, on the other hand, where the mix of warm-season grasses had experienced less precipitation, no irrigation, and lower LAI, had lower daily sums of *ET*. While the timing of *ET* maxima was similar to that of the urban site (i.e. late spring and summer), highest averages (July) were considerably lower (<3 mm d^{-1}) and lower than the average (5 mm d^{-1}) reported by *Bremer et al. (2001)* for tallgrass prairie in Kansas. Daily *ET* rates at Rocky Flats were even smaller during the drought year 2012. This confirms the findings of *Aires et al. (2008)*, who in their study of a Mediterranean grassland recorded peak *ET* rates of 4.5 mm d^{-1} (normal year) and 2.8 mm d^{-1} (dry year), and further emphasizes the importance of soil moisture and canopy growth/LAI for *ET*. At a tallgrass prairie site in Oklahoma, daily *ET* during the growing season ranged between 3.5-5 mm d^{-1} (*Burba and Verma, 2005*), which is higher than the values observed at Rocky Flats in 2011. On the other hand, average *ET* rates of 1.2-2.1 mm d^{-1} between May-October at a shortgrass prairie site in NE Colorado (*Ferretti et al., 2003*) compare well to the values at Rocky Flats (1.3-1.5 mm d^{-1}).

Differences in management (irrigation) and environmental conditions (e.g. soil moisture, type/development of vegetation) between sites did not only affect daily *ET* rates but total seasonal/annual *ET* as well. At Fort Logan, total *ET* summed to 670 mm and 625 mm for the respective investigation periods in 2011 and 2012. These amounts are about 30-40 % higher in comparison to the *annual* sums reported by *Peters et al. (2011)* for a suburban site in Minnesota dominated by turfgrass (74 % of land cover). The total of annual *ET* at Rocky Flats was 350 mm in 2011 and 310 mm in 2012, which is within the span found in the literature for grasslands in North America, for example, by *Krishnan et al. (2012)* (196-284 mm) in Arizona and *Burba and Verma (2005)* (637-807 mm) in Oklahoma.

Furthermore, Fort Logan and Rocky Flats differed with regard to ratios of *ET* and precipitation (*ET/P*), an indicator for how (efficient) ecosystems utilize available water. Urban ecosystems are generally characterized by low *ET/P* as impervious surfaces and sewer systems increase runoff (*Moriwaki and Kanda, 2004*). For urban areas containing large plots of green space, this may also be a sign of excess water use for irrigation. At Fort Logan, *ET/P* figured to 0.63 in 2011 and 0.57 in 2012 and thus showed little difference between seasons as total *ET* and water input over the investigated periods were very similar. *Peters et al. (2011)* in their study of suburban *ET* in Minneapolis-St.Paul found ratios of 0.42-0.61 for a residential area with about one-third turfgrass cover and of 0.62-0.85 for a recreational area with nearly three-quarters covered by turfgrass. In contrast to Fort Logan, *ET/P* for Rocky Flats was clearly higher (2011: 0.78; 2012: 1.15) and displayed notable differences between years. These higher figures at the prairie site are likely due to a thicker and generally drier soil cover (in comparison to Fort Logan) and the lack of impervious surfaces reducing the amount of runoff and enhancing infiltration. Moreover, *ET/P* may have been further increased by better adaptation of Rocky Flats vegetation to water-limited conditions. In the drought year 2012, *ET/P* exceeded unity, possibly due to a higher WUE of the vegetation at Rocky Flats and its ability to access water deeper within the soil that was stored during the previous year. However, an error in the quantification of *ET* and/or precipitation leading to an overestimation of *ET/P* cannot completely be ruled out. Nonetheless, similar patterns of increasing *ET/P* during drought years have been found for a semi-arid grassland in Arizona where values ranged between 0.74-0.84 but peaked at 1.20 during the driest year (*Scott, 2010*). Other studies have also reported increased *ET/P* during drought years, such as *Aires et al. (2008)* (0.64 vs. 0.87) and *Hussain et al. (2011)* (0.55 vs. 0.83) for grasslands in Portugal and Germany, respectively.

5.5. Energy Balance Closure

The analysis of flux data (section 4.5.) revealed an energy imbalance where the sum of turbulent energy fluxes underestimated the available energy by, on average, 22 % for the investigated sites (Fig 4.33). This falls within the range reported by *Twine et al. (2000)* (10-30 %) for grassland sites in the southern Great Plains and is similar to the mean imbalance (20 %) found by *Wilson et al. (2002)* who analyzed data from 22 FLUXNET sites (across different vegetation types and climates). Regression analysis (turbulent fluxes vs. available energy) further showed that coefficients of slope differed between sites and years (FL2011: 0.84; FL2012: 0.73; RF2011: 0.79; RF2012: 0.77) but compared well to other studies. For example, *Wilson et al. (2002)* reported a mean slope of 0.79 (range: 0.53-0.99) whereas *Leuning et al. (2012)* found a median slope for the La Thuile dataset of 0.75. Furthermore, means for the energy balance ratio (EBR = Σ(LE+H) / Σ(Rn+G)) at Fort Logan (2011: 0.82; 2012: 0.76) and Rocky Flats (2011: 0.69; 2012: 0.67) were comparable to the means reported by *Wilson et al. (2002)* (average: 0.84; range: 0.34-1.69) and *Stoy et al. (2013)* (average: 0.84; range: 0.70-0.94) who had investigated 173 datasets from FLUXNET, among them 32 grassland sites.

Energy imbalance is a problem at most EC sites and results from the underestimation of the sum of turbulent fluxes and/or the overestimation of available energy (*Leuning et al., 2012*). Among the numerous reasons that have been discussed in the literature are measurement errors/instrument bias regarding the quantification of turbulent fluxes, net radiation, and storage terms, the influence of advection events due to strong gradients of temperature and humidity, and landscape/footprint heterogeneity (*Wilson et al., 2002; Leuning et al., 2012).*

Related studies have argued that with improved instrument technology and data processing, measurement accuracy and data quality do not contribute significantly to energy imbalance if careful attention is paid to all sources of measurement and data processing errors (*Foken, 2008b; Leuning et al., 2012*). For example, the observed variability in R_n reported in several comparison studies appears unlikely to explain the systematic overestimation of available energy (*Twine et al., 2000; Kohsiek et al., 2007; Blonquist et al., 2009; Leuning et al., 2012*). Also, differences in instrument design, especially with regard to OP vs. CP IRGAs, have been found to have no (*Wilson et al., 2002*) or little impact (*Haslwanter et al., 2009*) on energy imbalance. Thus, these instrument-related issues can be expected to only have a small influence on the energy imbalance found at Fort Logan and Rocky Flats.

Energy storage, however, can be an important component of energy balance. *Wilson et al. (2002)* found that including the storage term for *G* improved energy balance closure, a finding confirmed during this study (data not shown), whereas *Hendricks Franssen et al. (2010)* investigating data from 20 FLUXNET sites found that the overall effect of storage terms on energy balance closure was limited. *Leuning et al. (2012)* reported that energy balance closure might be improved by using 24-hour averages instead of half-hourly data, thereby zeroing diurnal storage terms of soil and biomass. For the La Thuile dataset, sites with energy balance closure increased from 8 % to 45 % while the median slope for the dataset increased from 0.75 to 0.90 (*Leuning et al., 2012*). Using 24-hour averages for the data of this study improved closure slightly, primarily for the urban site (Appendix A3). The effect may have been limited by gaps in the data resulting in distorted daily averages and storage terms.

Other studies have argued that energy imbalance is primarily due to landscape heterogeneity, which results in exchange processes and turbulent motions that affect the land surface at spatial and temporal scales beyond those of typical EC footprints (*Foken et al., 2006+2012b, Stoy et al., 2013*). Furthermore, heterogeneity within the footprint may induce advection events influencing energy balance but requires large gradients of temperature and humidity (*Leuning et al., 2012*). The "oasis effect" is an example of advection in urban ecosystems where areas of different thermal properties (lawns/impervious surfaces) and under different management (irrigated vs. non-irrigated) are often in close proximity. This effect may also explain the occurrence of negative *H* during hot and dry afternoons at Fort Logan. Furthermore, surface heterogeneity may also enhance sampling mismatch, i.e. the influence of sensor source areas on the measured parameters (*Wilson et al., 2002*). Sampling mismatch might serve as an explanation for the differences in energy balance closure observed between years at Fort Logan where spatially differing management (irrigation) likely enhanced this issue.

5.6. Net Ecosystem Exchange of CO_2

Data for cumulative *NEE* (section 4.7.) showed that Fort Logan and Rocky Flats were net sinks for CO_2 over the respective investigation periods in 2011 and 2012. Moreover, Fort Logan proved to be a stronger CO_2 sink than Rocky Flats, sequestering at least twice as much when comparing annual or seasonal sums (Apr-Oct). The seasonal course of cumulative *NEE* as well as the daily sums also illustrated that flux strength and dynamics differed notably between sites and years. As *NEE* represents the relatively small net balance of two larger fluxes, i.e. uptake of CO_2 via photosynthesis and emissions via respiration, small changes regarding these processes can significantly alter the magnitude and the sign of *NEE*. However, complex interactions between the measured ancillary parameters (e.g. precipitation, radiation), which influence photosynthesis and soil respiration, often make analysis of cause-and-effect relations difficult. Nonetheless, data for this comparison study indicated that *NEE* responded notably to leaf area (LAI), climate conditions (temperature, soil moisture, VPD, PAR) and management (irrigation, fertilization) (Fig. 4.42-4.45).

Fort Logan

During the 2011 season, *NEE* at Fort Logan was dominated by sequestration of CO_2 as more than 70 % of daily *NEE* sums indicated net uptake. However, uptake was not continuous throughout the season but varied and reversed (net emission) at times in response to environmental conditions and management. Between the start of measurements and the first week of May, *NEE* was generally weak as low soil temperatures, below-average precipitation, and slow vegetation development likely limited the magnitude of respiration and photosynthetic fluxes. This early phase is followed by a distinct period of net emissions of CO_2 which coincides with a rapid increase in soil temperature (daily average: +8.0 K within 7 days) and the start of irrigation. Data showed a rise in soil temperature preceding the onset of irrigation, but both events are likely to have stimulated soil respiration. The effect of soil temperature on soil CO_2 efflux is well established in science, has been investigated in numerous studies, and remains subject of current research (*Fang and Moncrieff, 2001*; *Risk et al., 2002*; *Hibbard et al., 2005*;*Davidson et al.,* 2006; *Graf et al., 2008; Karhu et al., 2014*). But in most terrestrial ecosystems, including grasslands, soil respiration is also influenced by soil moisture (*Risch and Frank, 2007*; *Balogh et al., 2011*; *Lellei-Kovács et al., 2011*). Short-term pulses of soil CO_2 efflux following the wetting of (dry) soils have been reported in other studies (*Lee et al., 2004b*; *Chowdhury et al., 2011*; *Kim et al., 2012*). Potential explanations for these pulses include increased substrate availability (accumulated dead microbial and plant mass), release of nutrients, and exposure of previously protected organic matter (*Borken and Matzner, 2009*). Furthermore, low LAI and recurring days of low DLI during this period potentially limited photosynthetic activity, thereby contributing to the observed shift towards net release of CO_2. The immediate response of *NEE* at Fort Logan to precipitation/irrigation events, however, was difficult to estimate since data during these events was often incomplete due to instrument design.

When urban lawns at Fort Logan visibly greened during the second half of May, net uptake of CO_2 soon dominated *NEE*. Increased LAI and DLI probably resulted in a stronger photosynthetic flux that met and later exceeded flux from soil respiration. This uptake trend was temporarily interrupted in June by fertilization (and high irrigation input) which, as reported in other studies, can considerably enhance soil respiration (*Fierer et al., 2003*; *Verburg et al., 2004*). Between mid-June and mid-October of 2011, net uptake dominated as favorable environmental conditions (e.g. high DLI, soil moisture levels, and LAI) are likely to have significantly contributed to CO_2 sequestration. Net uptake, though, was not uniform in strength and noticeably slowed in August despite high irrigation input and LAI. High air temperatures as well as high VPD during this month visibly stressed vegetation, probably reducing photosynthetic activity and weakening uptake (*Mathur et al., 2014*). Small, positive daily sums of *NEE* (net emission) during some of the warmest days in July and August as well as the strengthening of net uptake as air temperatures cooled and VPD decreased again seem to support this analysis. In contrast, events of net release in September coincided with drastic drops in DLI.

A second fertilization event in early October did not result in net emissions again but data showed reduced daily net uptake of CO_2. Whether a stronger response was dampened by temperature drops at the time or the observed reduction in net uptake was due to a decrease in DLI and, thus, reduced photosynthetic flux (or a combination of both) is uncertain. Sequestration continued until the end of the investigation period, but as soil moisture became increasingly depleted in mid-October, uptake decreased as well. Furthermore, uptake was twice interrupted by snowfall events which brought below-freezing air temperatures, reduced DLI, and partially snow-covered vegetation. This temporarily reduced photosynthetic uptake and resulted in the observed net emission of CO_2 in late October and early November. Although uptake partially recovered, data for the last week of measurements indicated that *NEE* increasingly weakened as LAI, soil moisture, DLI, and temperatures decreased.

In 2012, *NEE* was characterized by a more variable seasonal course as days/periods of net uptake and net release alternated, reflecting the impact of drought conditions and related management decisions (i.e. irrigation). However, the resilience of turfgrass to intervals of limited irrigation and (heat) stress dampened the negative impact on carbon sequestration. Research indicates that this property of turfgrass may be further improved by adapted management (*Trudgill et al., 2010*).

Differences to the previous year became apparent soon after the start of measurements. Above-average temperatures and early vegetation development (LAI) led to increased soil respiration and photosynthetic fluxes, resulting in greater diurnal amplitudes of *NEE* in 2012 than in 2011. Following the first significant period of sequestration in April 2012, net uptake was temporarily paused by the start of irrigation when daily *NEE* sums became close to zero or positive. The reaction of *NEE* in response to the start of irrigation in 2012 was muted in comparison to 2011, possibly due to a lesser effect on soil moisture or the lack of a strong increase in soil temperature (as in 2011). Also, photosynthetic flux may have balanced enhanced soil respiration and thus prevented a more distinct shift towards net emissions. Nonetheless, as LAI, soil moisture, and temperature increased in May, net uptake resumed and became progressively stronger, resulting in the highest monthly net uptake of 2012. This trend of sequestration soon ended as the outlook of worsening drought conditions (*NIDIS, 2012*) impacted irrigation patterns at Fort Logan.

Irrigation proved to be a major influence on *NEE* through feedbacks via soil moisture and LAI. Along with record high air temperatures and high VPD, these factors primarily determined the seasonal course of *NEE* until early September. The effect of limited irrigation already became apparent during the last week of May: As irrigation stopped for one week, soil moisture and LAI declined while, simultaneously, air and soil temperatures increased. As a result, daily sums of *NEE* became positive towards the end of the month leading to a net loss of carbon. Irrigation resumed in June, the month of highest water input in 2012, witnessing a sharp increase in soil moisture and a recovery of LAI. Thereafter, sequestration of CO_2 was moderate as daily *NEE* sums alternated between uptake and loss. This was probably due to high air temperatures (record heat days) and high values of VPD impacting photosynthetic activity and seems confirmed by the fact that uptake temporarily accelerated in early July during a brief period when both parameters were notably lower.

Fertilization in mid-July coincided with positive daily *NEE* sums, similar to 2011. However, decreasing soil moisture and LAI preceding fertilizer application might have contributed to this shift towards net release of CO_2. The most significant impact of management, however, was the halt of irrigation for 2 weeks at the peak of drought conditions in late July and early August. This resulted in a rapid decline in soil moisture and LAI and soon in net losses of CO_2 as photosynthetic flux was reduced. The resumption of irrigation did not immediately result in net uptake again but rather increased daily positive sums of *NEE*, thus accelerating net CO_2 losses. Higher soil moisture likely caused soil respiration to increase, possibly further enhanced by the availability of carbon substrates derived from the photo-degradation of dead biomass during the pause in irrigation (*Ma et al., 2012*). Over time, LAI recovered and net uptake resumed but minimal irrigation in late August led again to a period of net CO_2 losses. Sequestration started again as high soil moisture and LAI stabilized and temperatures cooled. This period lasted from mid-September to mid-November after which vegetation went into senescence.

The effect of lawn-mowing on *NEE* at Fort Logan could not be clearly identified as mowing times were variable and differed from plot to plot. Reduced LAI may have contributed to decreased net uptake of CO_2, but other variables such as soil moisture, temperature, and PAR may have equally impacted *NEE*. The collected data included days of net release or distinctly reduced net uptake of CO_2 that coincided with or followed lawn-mowing, but other influencing factors (e.g. high temperature, lower soil moisture, low PAR) were usually present as well and confounded interpretation. The effect of leaving grass clippings on lawns is also difficult to estimate but may have impacted drought resilience (*Trudgill et al., 2010*) as well as carbon and nitrogen cycling (*Byrne et al., 2008; Qian and Follet, 2012*).

Investigating *NEE* of CO_2 at turfgrass sites is still relatively rare and few studies have been published (e.g. for Denver *Thienelt, 2007;* for Minneapolis-St.Paul *Hiller et al., 2011*). Thus, data drawn for comparison also included urban studies that contained a significant portion of lawns (e.g. suburban neighborhoods, park landscapes) in order to evaluate the magnitude of measured fluxes and annual/seasonal sequestration at Fort Logan.

Bergeron and Strachan (2011) studied *NEE* in Montreal, Canada, including one suburban site with 30 % lawn cover (50 % vegetation cover in total). Fluxes in spring (Apr-May) and fall (Sep-Nov) at midday were generally close to zero. In summer (Jun-Aug), midday *NEE* showed an average uptake of -7 μmol CO_2 m^{-2} s^{-1} and diurnal amplitudes were notably influenced by air temperature and incoming light levels. In comparison, diurnal averages observed at Fort Logan were usually stronger reaching up to -10.6 (spring 2012), -11.8 (fall 2011), and -13.3 μmol CO_2 m^{-2} s^{-1} (summer 2011). *Kordowski and Kuttler* (2010) reported average summer *NEE* maxima of up to -10 μmol CO_2 m^{-2} s^{-1} for a suburban site in Essen, Germany, while *Buckley et al. (2014)* in their study of suburban Syracuse, New York, found a midday average CO_2 flux of -11 μmol CO_2 m^{-2} s^{-1}, but also reported that absolute values varied between -20 and +10 μmol CO_2 m^{-2} s^{-1} during the summer months, which compares well to the data of Fort Logan. For a 5-year study at a suburban site near Baltimore, Maryland (65 % vegetation cover), average *NEE* during the summer months (Jun-Aug) ranged between -14 and +10 μmol CO_2 m^{-2} s^{-1} and diurnal amplitudes showed a sensitivity to PAR and soil temperature (*Crawford et al., 2011*). Results from these studies compare well to the data of

Fort Logan. However, *NEE* measured at suburban/residential sites was most likely also influenced by anthropogenic emissions (e.g. traffic, heating) which could have significantly skewed results.

Most studies that aim to quantify annual carbon sequestration of turfgrass are based on the analysis of changes in soil carbon stocks (chronosequences) as the sequestered carbon is mostly stored in the soil and not in shoots or roots (*Guertal, 2012*). *Qian and Follett (2002)* investigated golf courses of different age (mainly in Colorado) and found that these turfgrass sites showed average sequestration rates of -90 to -100 g C m^{-2} a^{-1} during the first 30 years following establishment. During a later study, *Qian at al. (2010)* reported a narrower range of -34 to -78 g C m^{-2} a^{-1}. Furthermore, *Milesi et al. (2005)* estimated that turfgrass in the United States could sequester between -36 to -100 g C m^{-2} a^{-1} annually while annual carbon sequestration for ornamental lawns in Irvine, California, was -140 g C m^{-2} a^{-1} (*Townsend-Small and Czimczik; 2010*). The estimated annual sequestration for Fort Logan in 2011 (-131 g C m^{-2} a^{-1}) compares well to the range reported in the literature but also highlights that summer drought conditions can severely impact the potential for carbon sequestration. During such conditions at Fort Logan, annual sequestration fell to -18 g C m^{-2} a^{-1}.

	Reference	**Location**	**Annual Carbon Balance (g C m^{-2} a^{-1})**	
Turfgrass studies	*Qian and Follett, 2002*	Colorado	-100 to -90	FL 2011: -131 FL 2012 -18
	Milesi et al, 2005	USA	-100 to -36	
	Townsend-Small and Czimczik, 2010	California	-140	
	Qian et al., 2010	Nebraska	-78 to -34	
Grassland studies	*Sims and Bradford, 2001*	Oklahoma	-159 to +46 (avg: -70)	RF 2011: -61 RF 2012: -9
	Suyker et al., 2003	Oklahoma	-274 to -46 (avg: -148)	
	Xu and Baldocchi, 2004	California	-132 / +29	
	Ma et al., 2007	California	-88 to +189 (avg: +38)	
			Seasonal Carbon Balance (g C m^{-2})	
	*Frank and Dugas, 2001**	North Dakota	-130 to -50 (avg: -95)	RF 2011: -85 RF 2012: -24
	*Meyers, 2001***	Oklahoma	-196 to +155 (avg: -50)	RF 2011: -77 RF 2012: -27

Tab. 5.3: Carbon balance reported by other studies for turfgrass and grassland ecosystems (negative values indicate carbon sequestration, positive values carbon loss) (*only DOY 114-299; **only DOY 150-240)

Rocky Flats

Measurements of *NEE* in 2011 spanned the entire year, but fluxes outside the growing season were mostly small and had less impact on the annual carbon balance. For example, during winter dormancy in January and February, there were negligible diurnal variation and small positive daily sums of *NEE*. Soil respiration, albeit weak, was mainly determining CO_2 exchange. Wintertime fluxes in steppe/prairie ecosystems have been found to be generally low and contribute only about 10 % or less to total annual respiration (*Gilmanov et al., 2004; Wang et al., 2010*). In March and April, *NEE* started to display a weak diurnal cycle, evidence that rising soil temperatures stimulated soil respiration while beginning vegetation growth initiated uptake of CO_2. Further into the growing season, photosynthetic flux was apparent in May and became stronger through the month. However, following a rapid increase in soil temperature and significant precipitation, comparable to Fort Logan at the time, this trend stopped and even reversed. Similar to the urban site, higher temperatures and soil moisture can be expected to have increased soil respiration while low DLI reduced photosynthetic flux resulting in the observed net emissions of CO_2. Estimating the individual impact of temperature and moisture on soil respiration is difficult as both parameters have been shown to influence soil CO_2 efflux in prairie ecosystems (*Mielnick and Dugas, 2000*; *Frank and Dugas, 2001*; *Chimner and Welker, 2005*). Daily uptake became stronger during the second half of May as the prairie site noticeably greened and temperature and DLI rapidly increased. The continuing increase of net uptake until late July/early August can be attributed to the rise in LAI and significant precipitation input in June and July. In mid-August, net uptake slowed abruptly, likely due to stress conditions (high temperatures and VPD, depleted soil moisture) impacting photosynthetic activity and LAI. Cooling temperatures, declining VPD, and moderate precipitation in early September led to a partial recovery of net uptake which continued until early October. Senescence of vegetation, however, soon ended sequestration and net emission characterized *NEE* for the remainder of the year.

Comparable to the urban site, *NEE* in 2012 at Rocky Flats was impacted by anomalous climate conditions in spring and summer. The amount of precipitation and, particularly, its timing appeared as important parameters affecting strength and direction of CO_2 flux (uptake/emission) and, as a result, the annual carbon balance, a finding in-line with previous studies (e.g. *Frank and Dugas, 2001*; *Sims and Bradford, 2001*; *Huxman et al., 2004*; *Harper et al., 2005*; *St.Clair et al., 2009*). During the first months of 2012, however, winter dormancy resulted in very similar *NEE* as in the previous year, characterized by weak respiration and practically no diurnal variation until the end of February. Although March witnessed strong increases in soil temperature over the course of the month (~15 K), *NEE* showed little response, possibly due to the fact that warming did not reach deep enough yet into the soil (preventing a stronger response from soil respiration) or due to limited substrate availability and soil moisture. But above-average temperatures led to an earlier and more rapid development of vegetation. Increasing LAI and DLI strengthened photosynthetic flux and caused net uptake to dominate *NEE* by mid-April. Daily uptake clearly increased in May, enhanced by nearly regular precipitation and a further rise in LAI. However, towards the end of the month and into June, changing environmental conditions increasingly impacted vegetation vitality. As soil moisture became depleted and air temperature as well as VPD trended towards annual maxima, net uptake declined drastically. Precipitation in early July temporarily replenished soil moisture and as a result uptake resumed. But as air temperatures and VPD remained high throughout July and August and soil moisture quickly dropped to very low values for a second time, daily uptake sums became gradually smaller again. By the end of August, drought conditions had weakened photosynthetic flux to the extent that net emissions characterized *NEE*. As vegetation went into senescence, Rocky Flats became a considerable net source of CO_2 until the end of October. Warm soils and episodical precipitation events fuelled respiration before declining temperatures moderated CO_2 fluxes and *NEE* became minimal.

During both years of this study, *NEE* at Rocky Flats displayed a distinct sensitivity in summer to strong precipitation events after periods of low or no precipitation. Typically, net uptake ceased after these precipitation pulses, followed by a peak of net release of CO_2 (up to 10 g C m^{-2} within one week) before uptake usually resumed. The magnitude of net emissions seemed to be mainly influenced by the amount of precipitation and the length of time between precipitation pulses. The most notable events occurred around the same time in both years, i.e. early July and early-mid September; although during the drought year 2012 resultant net emissions appeared stronger. The response of semiarid ecosystems to precipitation pulses after dry periods is known as the "Birch effect" (*Birch, 1958*) and remains subject of various studies (e.g. *Huxman et al., 2004*; *Parton et al., 2012*) including in shortgrass (*Munson et al., 2010*) and tallgrass prairie (*Liu et al., 2002*). Interest in these precipitation-induced carbon losses is due to the fact that the events, as observed for Rocky

Flats, can lead to very large CO_2 effluxes and can amount to a considerable portion of annual respiration and, thus, potentially represent an important component of carbon budgets (*Ma et al., 2012*).

The described peaks in net emissions at Rocky Flats following precipitation pulses can be explained as the result of multiple processes (*Ma et al., 2012*): Firstly, the infiltration of rain into the soil causes the physical displacement of air from soil pores where CO_2 concentrations can be up to one magnitude higher than above ground. The resulting flux, however, is estimated to be small due to the small effective volume occupied by soil air. Secondly, as pulse precipitation leads to a sudden increase in soil moisture, soil microbial activity becomes strongly stimulated. This is due to the re-hydration of dormant microbes and the availability of new carbon substrates (break-up of soil aggregates, microbial cell lysis) which stimulates growth, metabolic activity, and reproduction of surviving microbes. As a result, soil respiration quickly increases and high efflux rates may continue for days as the soils dry. Thirdly, photo-degradation, i.e. the breakdown of dead biomass by direct sunlight, could increase the amount of carbon available to microbes for consumption. This process has been shown to cause direct CO_2 emissions from litter (*Rutledge et al., 2010*), but rain could also move carbon substrates from photo-degraded litter into the soil, thereby enhancing precipitation-induced respiration. Additionally, parameters such as timing and magnitude of precipitation pulses also exert an influence on respiration response (*Harper et al., 2005*; *Munson et al., 2010*; *Ma et al., 2012*).

As the data from Rocky Flats has shown, variability of *NEE* can be substantial not only from day-to-day but through the course of a season and also between years. This variability has been observed in various other (multi-year) studies in the Great Plains, including changes in ecosystem function from carbon sink to source (*Frank and Dugas, 2001*; *Sims and Bradford, 2001*; *Polley et al., 2008*; *Parton et al., 2012*). Differences in (annual) carbon budgets are often attributed to climatic variability which can directly and indirectly impact the magnitude of *NEE*, for example, by influencing aboveground-NPP in grasslands (*Knapp and Smith, 2001*; *Flanagan et al., 2002*; *Xu and Baldocchi, 2004*).

Frank and Dugas (2001), measuring *NEE* over 4 years at a mixed prairie site in North Dakota, found that cumulative sequestration ranged between -50 to -130 g C m^{-2} for a period of April-October (DOY 114-299) with an average of -95 g C m^{-2} for all years. This illustrates that the span in uptake observed between years at Rocky Flats for this period (2011: -85 g C m^{-2}; 2012: -24 g C m^{-2}) is not atypical. Furthermore, *Frank and Dugas (2001)* noted that, similar to Rocky Flats, seasonal variability in *NEE* was clearly related to LAI/biomass responding to moisture and temperature stress and that maximum CO_2 flux occurred at the time of maximum LAI. For a prairie site in Oklahoma, *Sims and Bradford (2001)* reported an average annual uptake of -70 g C m^{-2} a^{-1}, comparable to Rocky Flats in 2011 (-61 g C m^{-2} a^{-1}). However, annual variability, as reflected by the individual annual sums, showed the importance of the timing of precipitation. In years with 80 % and 140 % of average precipitation, annual sequestration estimates were -97 and -159 g C m^{-2} a^{-1}, respectively. But in another year with below-normal precipitation in January-May (despite annual precipitation being 130 % of average), the site became a carbon source with an annual *NEE* showing a *loss* of +46 g C m^{-2} a^{-1}. *Xu and Baldocchi (2004)* also emphasized the importance of precipitation timing when reporting annual *NEE* for a California grassland which first showed net sequestration of -132 g C m^{-2} a^{-1}, but as precipitation patterns shifted (shortening the growing season) observed a net loss of +29 g C m^{-2} a^{-1}. Similar observations regarding the change of grasslands from carbon sink to source in response to precipitation patterns have been made by *Meyers (2001)* and *Ma et al. (2007)*.

In another study, interannual variability of sequestration was clearly reflected in daily *NEE* averages during the growing season which varied by more than a factor of 3 (*Polley et al., 2008*), comparable to the ratio found for Rocky Flats. Measurements of *NEE* by *Suyker and Verma (2001)* in a tallgrass prairie in Oklahoma revealed daily *NEE* sums in July and August ranging between -1.8 g C m^{-2} d^{-1} (uptake) and +2.2 g C m^{-2} d^{-1} (emission). A similar range was found at Rocky Flats in 2011 between May and July (-2.6 to +2.1 g C m^{-2} d^{-1}) and in 2012 between July and September (-1.9 to +2.8 g C m^{-2} d^{-1}). However, peaks in daily uptake of up to -8.4 g C m^{-2} d^{-1} clearly exceeded daily sequestration maxima at Rocky Flats, likely due to significantly higher LAI (maximum: 2.8) at the Oklahoma site (Rocky Flats < 0.8). Results of annual *NEE* for the same tallgrass site (*Suyker et al., 2003*) confirmed that sequestration was stronger in comparison to Rocky Flats (maximum annual NEE: -274 vs. -61 g C m^{-2} a^{-1}). The occurrence of severe drought conditions, however, also showed that moisture stress can reduce annual *NEE* by more than 80 %, similar to what Rocky Flats experienced in 2012. Furthermore, management at the Oklahoma tallgrass site (i.e. prescribed burns) shifted annual *NEE* either towards equilibrium or net source.

As the studies cited above have revealed, the observed year-to-year differences in *NEE* at Rocky Flats appear to be typical for grasslands in North America, resulting largely from climatic variability inherent to semiarid ecosystems. Future developments in climate will therefore determine the role of these ecosystems with regard to carbon sequestration.

5.7. The Impact of Lawns in Urban Ecosystems

Quantifying *NEE* of CO_2 and energy fluxes for turfgrass and tallgrass prairie in the Denver metropolitan area has provided a unique opportunity for identifying differences in these fluxes and the parameters that appear to determine their characteristics (such as climate and management). The obtained results, however, also need to be viewed within the context of land use change (urban sprawl) and resource allocation as well as potential feedbacks on climate and carbon sequestration.

Data from this study showed that available energy was more strongly partitioned into *LE* over irrigated lawns than over tallgrass prairie, indicating increased *ET* and enhanced evaporative cooling at the turfgrass site. Between April and October, cumulative *ET* at Rocky Flats amounted to 302 mm and 265 mm in 2011 and 2012, respectively. In contrast, *ET* at Fort Logan during those months summed to 639 mm (2011) and 584 mm (2012), thereby exceeding *ET* at the prairie site by more than factor of 2. Considering these distinct differences in *ET* sums and the estimates for the land cover fraction of turf in Denver (~ 40 %; *Thienelt, 2007*), a substantial influence of watered lawns on urban microclimate can be assumed. The cooling effect of urban green space/vegetation on air and surface temperatures has been measured in other urban studies and may help alleviate the urban heat island effect (*Taha, 1991; Ca et al., 1998; Bonan, 2000; Kong et al., 2014*). Moreover, cooling facilitated through energy balance partitioning by vegetation may also lead to reduced carbon emissions with lower demand for air conditioning (*Ca et al., 1998; Pataki et al., 2006; Salamanca et al., 2014*). The potential of both effects should be considered in urban planning when trying to adapt urban areas to climate change, i.e. rising temperatures (*Kong et al., 2014*). However, establishing and maintaining urban vegetation, specifically lawns, is also associated with energy and resource inputs, as has been observed during this study. For example, lawns in urban areas will typically experience regular maintenance (mowing, aerating, thatching) as well as application of synthetic inputs (fertilizer/ pesticides) which can equal or even surpass that of agricultural ecosystems on a per-area basis (*Robbins and Birkenholtz, 2003*; *Alumai et al., 2009*). Moreover, frequent irrigation of lawns can put enormous pressure on water resources, especially in arid and semi-arid climates (*Milesi et al., 2005*). Water input between April and October at Fort Logan summed to 1059 mm and 1107 mm in 2011 and 2012, respectively. However, only 31 % (2011) and 20 % (2012) of this water was precipitation and, thus, irrigation for these months exceeded precipitation by a factor of more than 2 in 2011 and nearly 4 in 2012. Other studies have shown that water use in urban areas increased 3-4 fold during the growing season and irrigation amounted to nearly half of annual municipal water use (*Kjelgren et al., 2000*). Also, on a household level, irrigation was estimated to account for 40-70 % of water use depending on regional climate, often showing considerable potential for water conservation (*Hilaire et al., 2008*). Strategies for water conservation may include deficit irrigation (i.e. applying less water than fully required by vegetation) and shading (by trees) (*Bastug and Buyuktas, 2003*; *Litvak et al., 2013*). Especially deficit irrigation might be an ecologically and economically valuable tool for (commercial) turfgrass sites facing the problem of restrictions on water use and maintaining acceptable turfgrass quality (*Wherley, 2011*): Besides lowering *ET*, deficit irrigation also leads to reduced photosynthesis and shoot growth, possibly resulting in less need for maintenance (mowing) and thus reduced fossil fuel consumption and emissions. However, increasing irrigation deficits can lead to rising canopy temperatures, thereby diminishing the cooling effect of vegetation in urban areas. Thus, it appears that more data is needed to assess the potential benefits of evaporative cooling against those of resource conservation by reducing energy and water consumption.

Urban lawns not only impact urban energy balance, but also function as sinks and sources for greenhouse gases such as CH_4 and N_2O. For example, fertilization of turf can lead to sharp, temporary increases in N_2O emissions (*Bremer, 2006*; *Bijoor et al., 2008*). Along the northern Colorado Front Range, enhanced N_2O fluxes and reduced CH_4 uptake were observed for urban lawns by *Kaye et al. (2004)* in comparison to nearby agricultural and steppe soils. Similar results have been reported for lawns at and near Fort Logan (*Thienelt, 2007*). The importance of these findings stems from the fact that both gases, N_2O and CH_4, can significantly contribute to climate change due to their increased warming potential per molecule in comparison to CO_2 and that emissions from urban lawns can make a notable contribution to regional greenhouse gas budgets (*Kaye et al., 2004*).

This study has also shown that urban lawns can act as stronger sinks than tallgrass prairie for the most important greenhouse gas, CO_2, although year-to-year climatic variability can notably impact annual carbon sequestration. Cumulative *NEE* (Apr-Oct) at Fort Logan was -173 g C m^{-2} in 2011 and -73 g C m^{-2} in 2012. Thus, net uptake was reduced by nearly 60 % during the drought year 2012 in comparison to the previous year. However, seasonal *NEE* sums of Fort Logan still exceeded those of Rocky Flats (2011: -81 g C m^{-2}; 2012: -21 g C m^{-2}) by factors of more than 2 and 3 for the respective years.

The observed sequestration of CO_2 by urban lawns in this study supports other findings of substantial carbon storage in urban vegetation and soils. For example, *Churkina et al. (2010)* estimated that urban ecosystems in the US contain up to 10 % of total US land carbon with 64 % of this share stored in soils and a further 20 % in vegetation. Studying carbon storage in the Colorado Front Range, *Golubiewski (2006)* found that urban lawns had more biomass and higher carbon storage on a per-area basis than native grassland or agricultural land. Turf in Denver, two decades after establishment, showed SOC values that in some cases were more than double in comparison to shortgrass prairie (*Pouyat et al., 2009*). Furthermore, *Golubiewski (2006)* found that woody vegetation can become a substantial carbon pool in urban green spaces, increasing aboveground carbon storage up to 30 % whereas native grasslands typically stored 90 % of carbon belowground. This also confirms the findings of *Nowak et al. (2002)* regarding the importance of trees in urban areas for carbon storage. Thus, carbon sequestration and carbon storage can be enhanced as a result of urbanization. In drier climates (such as Denver), urban vegetation can be substantially more productive than vegetation of natural ecosystems and management as well as the lack of disturbance can boost carbon storage in soils (*Pataki et al., 2006*; *Pouyat et al., 2006*; *Townsend-Small and Czimczik, 2010*).

Despite the fact that urban lawns can act as sinks for CO_2, accounting for direct and indirect carbon emissions due to maintenance, can lead to offsets in net uptake (*Towsend-Small and Czimczik, 2010*; *Zirkle et al., 2011*). For example, estimated annual *NEE* for Fort Logan in 2011 was reduced by more than 60 % to -49 g C m^{-2} a^{-1} when accounting for maintenance emissions, indicating that Fort Logan had become a slightly weaker carbon sink that year than Rocky Flats (2011: -61 g C m^{-2} a^{-1}). In the drought year 2012, maintenance emissions shifted Fort Logan from sink to source (+60 g C m^{-2} a^{-1}) while Rocky Flats remained a (weak) net carbon sink (-9 g C m^{-2} a^{-1}). Besides emissions related to maintenance, the strength of numerous other sources of CO_2 and greenhouse gases in urban areas (e.g. traffic, industrial activities) can also be assumed to considerably offset potential carbon gains by urban lawns. Unless significant decreases in general energy use and carbon intensity will be realized, urban ecosystems are unlikely to become net carbon sinks despite harboring large carbon pools (*Golubiewski ,2006; Pataki et al., 2006*; *Churkina et al., 2010*; *Hutyra et al., 2010*).

Lastly, the contribution of lawns to carbon sequestration in urban ecosystems may be weakened by future climate change. Temperature and precipitation anomalies, as were observed in 2012, require more management of turfgrass that may include higher input of water and chemicals to maintain desired turfgrass quality, leading to more carbon emissions and increased resource consumption. Sequestration may also be affected by higher temperatures that may enhance respiration and/or suppress photosynthesis (as a consequence of heat stress) as has been shown for tallgrass prairie (*Arnone et al., 2008*; *Niu et al., 2013*). A warming climate could therefore have strong implications for carbon sequestration in tallgrass prairie as well as in urban lawns.

6. Conclusion

The main objective of this study was to quantify carbon and energy exchange of turfgrass and a xeric tallgrass prairie in the Denver metropolitan area (Colorado, USA), identify important drivers regarding the diurnal and seasonal courses of these exchanges, and assess the impact of land use change in a semi-arid climate on carbon and water budgets. The following section presents the main conclusions based on the results of this study:

- The EC method was shown to be a suitable approach to assess *NEE* of CO_2 and energy fluxes in the turfgrass and tallgrass ecosystems chosen for this study. Data quality control and analysis of energy balance closure indicated that measurement setups at both sites regularly fulfilled the basic requirements of the EC method and that data coverage was similar to other FLUXNET sites. These qualities enabled the comparison of simultaneously measured fluxes over various time scales between turfgrass or prairie and the atmosphere. Furthermore, the results confirmed that the EC method, with careful site selection, can be successfully applied within the often heterogeneous urban landscape to quantify carbon and energy fluxes of individual landscape components such as urban lawns.
- Vegetation acted as an important modifier for the partition of the surface energy balance and largely determined the rates and direction of carbon exchange. This investigation found close links between seasonal vegetation development, energy fluxes, and *NEE* of CO_2. Results of data analysis also indicated the importance and complexity of interacting factors and processes that determine the magnitude of energy and carbon exchange, which made it difficult to identify individual driving parameters. Nonetheless, results from both sites showed that meteorological parameters (e.g. radiation, temperature, VPD, soil moisture) as well as vegetation characteristics (e.g. LAI) clearly had a large impact on energy and carbon fluxes.
- Water availability was one of the most important influences on carbon and energy exchange in the semi-arid climate of the investigation area. Management represented an additional influence in this regard. Irrigation at the urban site, which clearly surpassed precipitation in quantity, led to discernible consequences for energy partitioning and carbon flux, and greatly contributed to the diurnal and seasonal differences observed between turfgrass and tallgrass prairie.

- Energy partitioning at the turfgrass site was characterized by a distinct shift from *H* to *LE* in comparison to the tallgrass prairie. This affected diurnal patterns as well as seasonal sums. Irrigation, which greatly enhanced water availability, resulted in *LE* consuming, on average, more than 70 % of available energy at the urban site between April and October.
- As a result of *LE* dominating energy partitioning at the urban site in both years, 2011 and the drought year 2012, *ET* was considerably larger in comparison to the prairie site. Greater water availability allowed for a longer period of high daily *ET* sums and resulted in considerably higher seasonal totals over turfgrass in comparison with the tallgrass prairie. Between April and October, cumulative *ET* of turfgrass exceeded that of tallgrass prairie by a factor of more than 2 (2011: 639 mm vs. 302 mm; 2012: 584 mm vs. 265 mm).
- Higher productivity and vegetation density of turfgrass in comparison to tallgrass prairie as well as management at the urban site (e.g. irrigation and fertilization) led to large differences regarding diurnal and seasonal carbon fluxes. *NEE* at the turfgrass site was characterized by a longer growing season showing higher daily net uptake and, hence, higher seasonal sums of sequestered CO_2. Data for cumulative *NEE* between April and October indicated that net uptake by turfgrass exceeded that of tallgrass prairie by a factor of more than 2 in 2011 and 3 in 2012. The comparative sums of the turfgrass vs. tallgrass prairie sites were -173 g C m^{-2} vs. -81 g C m^{-2} in 2011 and -73 g C m^{-2} vs. -21 g C m^{-2} in 2012.
- Annual *NEE* at the urban site considerably changed when including carbon emissions due to turfgrass management (e.g. from irrigation, fertilization, and fossil fuel use). In 2011, the carbon offset introduced by management reduced the estimated annual *NEE* from -131 g C m^{-2} a^{-1} to -49 g C m^{-2} a^{-1}, resulting in a smaller net sink for CO_2 than the tallgrass prairie (2011: -61 g C m^{-2} a^{-1}). In 2012, management emissions shifted the urban site from sink to source, a change from -18 g C m^{-2} a^{-1} to +60 g C m^{-2} a^{-1}, whereas the prairie site functioned as a small net CO_2 sink (-9 g C m^{-2} a^{-1}).
- In 2012, above-average temperatures (+1.8 K) and reduced precipitation (-30 %) in Denver (with respect to 1981-2010) influenced diurnal and seasonal *NEE* at both research sites. Temperature and water stress during the summer months affected

vegetation vitality and greatly influenced the direction and magnitude of CO_2 flux, i.e. net uptake or net loss. Cumulative *NEE* at the prairie site was reduced in 2012 by more than 70 % in comparison to 2011 (Apr-Oct). The relative loss in sink strength at the urban site was temporarily of similar size, but was lessened to approximately 55 % following the recovery of turfgrass in late summer and fall (after peak drought).

- Observed sequestration of CO_2 by turfgrass and the spatial extent of urban lawns in Denver suggest that lawns can function as important carbon sinks and large carbon pools within urban ecosystems but require considerable amounts of irrigation, particularly in semi-arid climates. Transformation of natural grasslands to urban land uses could therefore increase carbon storage on a per-area basis but simultaneously strain water resources.
- The establishment of urban vegetation may contribute to the mitigation of carbon emissions in urban areas to a certain degree, directly by CO_2 sequestration, indirectly through effects of evaporative cooling on microclimate and energy use. An assessment of the magnitude of these effects regarding urban carbon budget and climate needs to integrate emissions from maintenance and costs of resource allocation.

Data presented in this thesis has demonstrated that urban lawns and tallgrass prairie differ notably with regard to *NEE* of CO_2, energy fluxes, and *ET*. This finding appears most relevant considering the present rapid expansion of Denver and predicted future urban growth in the Rocky Mountain West, as the results indicate that urbanization/urban sprawl is not only a process of land cover change, but can also lead to distinct modifications of the partitioning of the surface energy budget, carbon fluxes, and water budgets. These implications demand further scrutiny to improve our understanding of the interactions of ecosystems and the atmosphere and the impact of anthropogenic activity on biogeochemical cycles.

7. References

Acevedo, O. C.; Moraes, O. L.L.; Degrazia, G. A.; Fitzjarrald, D. R.; Manzi, A. O.; Campos, J. G. (2009): Is friction velocity the most appropriate scale for correcting nocturnal carbon dioxide fluxes? In *Agricultural and Forest Meteorology* 149 (1), pp. 1–10. DOI: 10.1016/j.agrformet.2008.06.014.

Aires, L. M.; Pio, C. A.; Pereira, J. S. (2008): The effect of drought on energy and water vapour exchange above a mediterranean C3/C4 grassland in Southern Portugal. In *Agricultural and Forest Meteorology* 148 (4), pp. 565–579. DOI: 10.1016/j.agrformet.2007.11.001.

Alig, R. J.; Kline, J. D.; Lichtenstein, M. (2004): Urbanization on the US landscape: looking ahead in the 21st century. In *Landscape and Urban Planning* 69 (2-3), pp. 219–234. DOI: 10.1016/j.landurbplan.2003.07.004.

Allen, M. R.; Gillett, N. P.; Kettleborough, J. A.; Hegerl, G.; Schnur, R.; Stott, P. A. et al. (2006): Quantifying anthropogenic influence on recent near-surface temperature change. In *Surv Geophys* 27 (5), pp. 491–544. DOI: 10.1007/s10712-006-9011-6.

Alumai, A.; Salminen, S. O.; Richmond, D. S.; Cardina, J.; Grewal, P. S. (2009): Comparative evaluation of aesthetic, biological, and economic effectiveness of different lawn management programs. In *Urban Ecosyst* 12 (2), pp. 127–144. DOI: 10.1007/s11252-008-0073-8.

Arneth, A.; Harrison, S. P.; Zaehle, S.; Tsigaridis, K.; Menon, S.; Bartlein, P. J. et al. (2010): Terrestrial biogeochemical feedbacks in the climate system. In *Nature Geosci* 3 (8), pp. 525–532. DOI: 10.1038/ngeo905.

Arnold, K. B. (2009): Eddy Covariance in a Tallgrass Prairie: Energy Balance Closure, Water and Carbon Budgets, and Shrub Expansion. Master Thesis. Kansas State University.

Arnone, J. A.; Verburg, P. S. J.; Johnson, D. W.; Larsen, J. D.; Jasoni, R. L.; Lucchesi, A. J. et al. (2008): Prolonged suppression of ecosystem carbon dioxide uptake after an anomalously warm year. In *Nature* 455 (7211), pp. 383–386. DOI: 10.1038/nature07296.

Aubinet, M.; Vesala, T.; Papale, D. (2012): Eddy covariance. A practical guide to measurement and data analysis. Dordrecht, New York: Springer.

Baldocchi, D. D. (2003): Assessing the eddy covariance technique for evaluating carbon dioxide exchange rates of ecosystems: past, present and future. In *Global Change Biol* 9 (4), pp. 479–492. DOI: 10.1046/j.1365-2486.2003.00629.x.

Baldocchi, D. (2008): Turner Review No. 15. 'Breathing' of the terrestrial biosphere: lessons learned from a global network of carbon dioxide flux measurement systems. In *Aust. J. Bot.* 56 (1), p. 1. DOI: 10.1071/BT07151.

Baldocchi, D.; Falge, E.; Gu, L.; Olson, R.; Hollinger, D.; Running, S. et al. (2001): FLUXNET: A New Tool to Study the Temporal and Spatial Variability of Ecosystem–Scale Carbon Dioxide, Water Vapor, and Energy Flux Densities. In *Bull. Amer. Meteor. Soc.* 82 (11), pp. 2415–2434. DOI: 10.1175/1520-0477(2001)082<2415:FANTTS>2.3.CO;2.

Balogh, J.; Pintér, K.; Fóti, Sz.; Cserhalmi, D.; Papp, M.; Nagy, Z. (2011): Dependence of soil respiration on soil moisture, clay content, soil organic matter, and CO2 uptake in dry grasslands. In *Soil Biology and Biochemistry* 43 (5), pp. 1006–1013. DOI: 10.1016/j.soilbio.2011.01.017.

Balogun, A. A.; Adegoke, J. O.; Vezhapparambu, S.; Mauder, M.; McFadden, J. P.; Gallo, K. (2009): Surface Energy Balance Measurements Above an Exurban Residential Neighbourhood of Kansas City, Missouri. In *Boundary-Layer Meteorol* 133 (3), pp. 299–321. DOI: 10.1007/s10546-009-9421-3.

Bastug, R.; Buyuktas, D. (2003): The effects of different irrigation levels applied in golf courses on some quality characteristics of turfgrass. In *Irrigation Science* 22 (2), pp. 87–93. DOI: 10.1007/s00271-003-0073-7.

Bergeron, O.; Strachan, I. B. (2011): CO2 sources and sinks in urban and suburban areas of a northern mid-latitude city. In *Atmospheric Environment* 45 (8), pp. 1564–1573. DOI: 10.1016/j.atmosenv.2010.12.043.

Bijoor, N. S.; Czimczik, C. I.; Pataki, D. E.; Billings, S. A. (2008): Effects of temperature and fertilization on nitrogen cycling and community composition of an urban lawn. In *Global Change Biology* 14 (9), pp. 2119–2131. DOI: 10.1111/j.1365-2486.2008.01617.x.

Birch, H. F. (1958): Pattern of Humus Decomposition in East African Soils. In *Nature* 181 (4611), p. 788. DOI: 10.1038/181788a0.

Blonquist, J. M.; Tanner, B. D.; Bugbee, B. (2009): Evaluation of measurement accuracy and comparison of two new and three traditional net radiometers. In *Agricultural and Forest Meteorology* 149 (10), pp. 1709–1721. DOI: 10.1016/j.agrformet.2009.05.015.

Bonan, G. B. (2000): The microclimates of a suburban Colorado (USA) landscape and implications for planning and design. In *Landscape and Urban Planning* 49 (3-4), pp. 97–114. DOI: 10.1016/S0169-2046(00)00071-2.

Bond, T. C. (2013): Bounding the role of black carbon in the climate system: A scientific assessment†. In *Journal of Geophysical Research: Atmospheres*.

Borken, W.; Matzner, E. (2009): Reappraisal of drying and wetting effects on C and N mineralization and fluxes in soils. In *Global Change Biology* 15 (4), pp. 808–824. DOI: 10.1111/j.1365-2486.2008.01681.x.

Brady, N. C.; Weil, R. R. (1999): The nature and properties of soils. 12^{th} ed. Upper Saddle River, NJ: Prentice Hall.

Bremer, D. J. (2006): Nitrous oxide fluxes in turfgrass: effects of nitrogen fertilization rates and types. In *J. Environ. Qual.* 35 (5), pp. 1678–1685. DOI: 10.2134/jeq2005.0387.

Bremer, D. J.; Auen, L. M.; Ham, J. M.; Owensby, C. E. (2001): Evapotranspiration in a Prairie Ecosystem. In *Agronomy Journal* 93 (2), p. 338. DOI: 10.2134/agronj2001.932338x.

Bremer, D. J.; Ham, J. M. (1999): Effect of spring burning on the surface energy balance in a tallgrass prairie. In *Agricultural and Forest Meteorology* 97 (1), pp. 43–54. DOI: 10.1016/S0168-1923(99)00034-9.

Bremer, D. J.; Ham, J. M. (2010): Net Carbon Fluxes Over Burned and Unburned Native Tallgrass Prairie. In *Rangeland Ecology & Management* 63 (1), pp. 72–81. DOI: 10.2111/REM-D-09-00010.1.

Buckley, S. M.; Mitchell, M. J.; McHale, P. J.; Millard, G. D. (2014): Variations in carbon dioxide fluxes within a city landscape: Identifying a vehicular influence. In *Urban Ecosyst. DOI:* 10.1007/s11252-013-0341-0.

Bulkeley, H. (2013): Cities and climate changes. London: Routledge.

Burba, G. (2013): Eddy covariance method for scientific, industrial, agricultural, and regulatory applications. A field book on measuring ecosystem gas exchange and areal emission rates.

Burba, G.; Anderson, D. (2010): A brief practical guide to eddy covariance flux measurements. Principles and workflow examples for scientific and industrial applications. Lincoln, Neb: LI-COR.

Burba, G.; McDermitt, D. K.; Grelle, A.; Anderson, D. J.; Xu, L. (2008): Addressing the influence of instrument surface heat exchange on the measurements of CO 2 flux from open-path gas analyzers. In *Global Change Biology* 14 (8), pp. 1854–1876. DOI: 10.1111/j.1365-2486.2008.01606.x.

Burba, G.; Schmidt, A.; Scott, R. L.; Nakai, T.; Kathilankal, J.; Fratini, G. et al. (2012): Calculating CO2 and H2O eddy covariance fluxes from an enclosed gas analyzer using an instantaneous mixing ratio. In *Glob Change Biol* 18 (1), pp. 385–399. DOI: 10.1111/j.1365-2486.2011.02536.x.

Burba, G.; Verma, S. B. (2005): Seasonal and interannual variability in evapotranspiration of native tallgrass prairie and cultivated wheat ecosystems. In *Agricultural and Forest Meteorology* 135 (1-4), pp. 190–201. DOI: 10.1016/j.agrformet.2005.11.017.

Byrne, L. B.; Bruns, M. A.; Kim, K. C. (2008): Ecosystem Properties of Urban Land Covers at the Aboveground–Belowground Interface. In *Ecosystems* 11 (7), pp. 1065–1077. DOI: 10.1007/s10021-008-9179-3.

Ca, V. T.; Asaeda, T.; Abu, E. M. (1998): Reductions in air conditioning energy caused by a nearby park. In *Energy and Buildings* 29 (1), pp. 83–92. DOI: 10.1016/S0378-7788(98)00032-2.

Campbell Scientific, Inc. (2012): Soil Heat Flux Plate Model HFP01. Instruction Manual. Available online at http://www.campbellsci.com/hfp01sc-l.

Canadell, J. G.; Pataki, D. E.; Pitelka, L. F. (Eds.) (2007): Terrestrial Ecosystems in a Changing World. Berlin, Heidelberg: Springer Berlin Heidelberg (Global Change — The IGBP Series).

Canadell, J. G.; Pataki, D. E.; Gifford, R.; Houghton, R. A.; Luo, Y.; Raupach, M. R. et al. (2007): Saturation of the Terrestrial Carbon Sink. In J. G. Canadell, D. E. Pataki, L. F. Pitelka (Eds.): Terrestrial Ecosystems in a Changing World. Berlin, Heidelberg: Springer Berlin Heidelberg (Global Change — The IGBP Series), pp. 59–78.

Chimner, R. A.; Welker, J. M. (2005): Ecosystem respiration responses to experimental manipulations of winter and summer precipitation in a Mixedgrass Prairie, WY, USA. In *Biogeochemistry* 73 (1), pp. 257–270. DOI: 10.1007/s10533-004-1989-6.

Chowdhury, N.; Burns, R. G.; Marschner, P. (2011): Recovery of soil respiration after drying. In *Plant Soil* 348 (1-2), pp. 269–279. DOI: 10.1007/s11104-011-0871-2.

Christen, A.; Vogt, R. (2004): Energy and radiation balance of a central European city. In *Int. J. Climatol.* 24 (11), pp. 1395–1421. DOI: 10.1002/joc.1074.

Chronic, H. (1980): Roadside geology of Colorado. Missoula, Mont: Mountain Press Pub. Co.

Churkina, G.; Brown, D. G.; Keoleian, G. (2010): Carbon stored in human settlements: the conterminous United States. In *Global Change Biology* 16 (1), pp. 135–143. DOI: 10.1111/j.1365-2486.2009.02002.x.

Clement, R. J. (2004): Mass and energy exchange of a plantation forest in Scotland using micrometeorological methods. Thesis.

Clement, R. J.; Burba, G. G.; Grelle, A.; Anderson, D. J.; Moncrieff, J. B. (2009): Improved trace gas flux estimation through IRGA sampling optimization. In *Agricultural and Forest Meteorology* 149 (3-4), pp. 623–638. DOI: 10.1016/j.agrformet.2008.10.008.

Conant, R. T. (2010): Challenges and opportunities for carbon sequestration in grassland systems. A technical report on grassland management and climate mitigation. Rome: Food and Agriculture Organization of the United Nations (Integrated crop management, vol. 9-2010).

Crawford, B.; Grimmond, C.S.B.; Christen, A. (2011): Five years of carbon dioxide fluxes measurements in a highly vegetated suburban area. In *Atmospheric Environment* 45 (4), pp. 896–905. DOI: 10.1016/j.atmosenv.2010.11.017.

Curtis, P. S.; Vogel, C. S.; Gough, C. M.; Schmid, H. P.; Su, H.-B.; Bovard, B. D. (2005): Respiratory carbon losses and the carbon-use efficiency of a northern hardwood forest, 1999-2003. In *New Phytologist* 167 (2), pp. 437–456. DOI: 10.1111/j.1469-8137.2005.01438.x.

Davidson, E. A.; Janssens, I. A.; Luo, Y. (2006): On the variability of respiration in terrestrial ecosystems: moving beyond Q10. In *Global Change Biol* 12 (2), pp. 154–164. DOI: 10.1111/j.1365-2486.2005.01065.x.

Davis, P. A.; Brown, J. C.; Saunders, M.; Lanigan, G.; Wright, E.; Fortune, T. et al. (2010): Assessing the effects of agricultural management practices on carbon fluxes: Spatial variation and the need for replicated estimates of Net Ecosystem Exchange. In *Agricultural and Forest Meteorology* 150 (4), pp. 564–574. DOI: 10.1016/j.agrformet.2010.01.021.

DOE. Department of Energy (2010): Rocky Flats, Colorado, Site Operations Guide.

Doesken, N. J.; Pielke, R. A.; Bliss, O. A. P. (2003): Climate of Colorado. Fort Collins, Colo: Colorado Climate Center, Colorado State University.

Dragoni, D.; Schmid, H. P.; Grimmond, C. S. B.; Loescher, H. W. (2007): Uncertainty of annual net ecosystem productivity estimated using eddy covariance flux measurements. In *J. Geophys. Res.* 112 (D17). DOI: 10.1029/2006JD008149.

Duble, R. L. (2006): Water Management on Turfgrasses. Available online at http://aggie-horticulture.tamu.edu/archives/parsons/turf/publications/water.html.

Dwyer, J.F.; Nowak, D.J.; Noble, M.H.; Sisinni, S.M. (2000): Connecting People with Ecosystems in the 21st Century: An Assessment of our Nation's Urban Forests. USDA.

Elvidge, C. D.; Milesi, C.; Dietz, J. B.; Tuttle, B. T.; Sutton, P. C.; Nemani, R.; Vogelmann, J. E. (2004): U.S. constructed area approaches the size of Ohio. In *Eos Trans. AGU* 85 (24), p. 233. DOI: 10.1029/2004EO240001.

Elvidge, C. D.; Tuttle, B. T.; Sutton, P. C.; Baugh, K. E.; Howard, A. T.; Milesi, C. et al. (2007): Global Distribution and Density of Constructed Impervious Surfaces. In *Sensors* 7 (9), pp. 1962–1979. DOI: 10.3390/s7091962.

Eugster, W.; Moffat, A. M.; Ceschia, E.; Aubinet, M.; Ammann, C.; Osborne, B. et al. (2010): Management effects on European cropland respiration. In *Agriculture, Ecosystems & Environment* 139 (3), pp. 346–362. DOI: 10.1016/j.agee.2010.09.001.

Falge, E.; Baldocchi, D.; Olson, R.; Anthoni, P.; Aubinet, M.; Bernhofer, C. et al. (2001a): Gap filling strategies for defensible annual sums of net ecosystem exchange. In *Agricultural and Forest Meteorology* 107 (1), pp. 43–69. DOI: 10.1016/S0168-1923(00)00225-2.

Falge, E.; Baldocchi, D.; Olson, R.; Anthoni, P.; Aubinet, M.; Bernhofer, C. et al. (2001b): Gap filling strategies for long term energy flux data sets. In *Agricultural and Forest Meteorology* 107 (1), pp. 71–77. DOI: 10.1016/S0168-1923(00)00235-5.

Fang, C.; Moncrieff, J.B (2001): The dependence of soil CO2 efflux on temperature. In *Soil Biology and Biochemistry* 33 (2), pp. 155–165. DOI: 10.1016/S0038-0717(00)00125-5.

Feldhake, C. M.; Danielson, R. E.; Butler, J. D. (1983): Turfgrass Evapotranspiration. I. Factors Influencing Rate in Urban Environments1. In *Agronomy Journal* 75 (5), p. 824. DOI: 10.2134/agronj1983.00021962007500050022x.

Ferretti, D. F.; Pendall, E.; Morgan, J. A.; Nelson, J. A.; LeCain, D.; Mosier, A. R. (2003): Partitioning evapotranspiration fluxes from a Colorado grassland using stable isotopes: Seasonal variations and ecosystem implications of elevated atmospheric CO2. In *Plant and Soil* 254 (2), pp. 291–303. DOI: 10.1023/A:1025511618571.

Fierer, N.; Allen, A. S.; Schimel, J. P.; Holden, P. A. (2003): Controls on microbial CO2 production: a comparison of surface and subsurface soil horizons. In *Global Change Biol* 9 (9), pp. 1322–1332. DOI: 10.1046/j.1365-2486.2003.00663.x.

Finnigan, J. (2006): The storage term in eddy flux calculations. In *Agricultural and Forest Meteorology* 136 (3-4), pp. 108–113. DOI: 10.1016/j.agrformet.2004.12.010.

Finnigan, J. J. (2009): Response to comment by Dr. A.S. Kowalski on “The storage term in eddy flux calculations”. In *Agricultural and Forest Meteorology* 149 (3-4), pp. 725–729. DOI: 10.1016/j.agrformet.2008.10.012.

Flanagan, L. B.; Wever, L. A.; Carlson, P. J. (2002): Seasonal and interannual variation in carbon dioxide exchange and carbon balance in a northern temperate grassland. In *Global Change Biol* 8 (7), pp. 599–615. DOI: 10.1046/j.1365-2486.2002.00491.x.

FLUXNET. Available online at http://fluxnet.ornl.gov/, checked on 1/16/2013.

Foken, T. (2008a): Micrometeorology. Berlin: Springer.

Foken, T. (2008b): The Energy Balance Closure Problem: an Overview. In *Ecological Applications* 18 (6), pp. 1351–1367. DOI: 10.1890/06-0922.1.

Foken, T.; Wichura, B. (1996): Tools for quality assessment of surface-based flux measurements. In *Agricultural and Forest Meteorology* 78 (1-2), pp. 83–105. DOI: 10.1016/0168-1923(95)02248-1.

Foken, T.; Göckede, M.; Mauder, M.; Mahrt, L.; Amiro, B.; Munger, W. (2004): Post-field Data Quality Control. In: Handbook of micrometeorology. A guide for surface flux measurement and analysis. 2004. (eds. Lee, X.; Massman, W. J.; Law, B. E.). Dordrecht. Kluwer Academic Publishers.

Foken, T.; Wimmer, F.; Mauder, M.; Thomas, C.; Liebethal, C. (2006): Some aspects of the energy balance closure problem. In *Atmos. Chem. Phys.* 6 (12), pp. 4395–4402. DOI: 10.5194/acp-6-4395-2006.

Foken, T. W.; Aubinet, M.; Leuning, R. (2012a): The Eddy Covariance Method - Chapter 1. In: Eddy Covariance: A practical guide to measurement and data analysis (eds. Aubinet, M.; Vesala, T.; Papale, D.). Dordrecht, New York: Springer.

Foken, T.; Leuning R.; Oncley, S. R.; Mauder, M.; Aubinet, M. (2012b): Corrections and Data Quality Control – Chapter 4. In: Eddy covariance - A practical guide to measurement and data analysis (eds. Aubinet, M.; Vesala, T.; Papale, D.). Dordrecht, New York: Springer.

Frank, A.B; Dugas, W.A (2001): Carbon dioxide fluxes over a northern, semiarid, mixed-grass prairie. In *Agricultural and Forest Meteorology* 108 (4), pp. 317–326. DOI: 10.1016/S0168-1923(01)00238-6.

Frank, J. M.; Massman, W. J.; Ewers, B. E. (2013): Underestimates of sensible heat flux due to vertical velocity measurement errors in non-orthogonal sonic anemometers. In *Agricultural and Forest Meteorology* 171-172, pp. 72–81. DOI: 10.1016/j.agrformet.2012.11.005.

Fratini, G.; Ibrom, A.; Arriga, N.; Burba, G.; Papale, D. (2012): Relative humidity effects on water vapour fluxes measured with closed-path eddy-covariance systems with short sampling lines. In *Agricultural and Forest Meteorology* 165, pp. 53–63. DOI: 10.1016/j.agrformet.2012.05.018.

Friend, A. D.; Arneth, A.; Kiang, N. Y.; Lomas, M.; Ogee, J.; Rodenbeck, C. et al. (2007): FLUXNET and modelling the global carbon cycle. In *Global Change Biol* 13 (3), pp. 610–633. DOI: 10.1111/j.1365-2486.2006.01223.x.

Fuehrer, P. L.; Friehe, C. A. (2002): Flux Corrections Revisited. In *Boundary-Layer Meteorology* 102 (3), pp. 415–458. DOI: 10.1023/A:1013826900579.

Gilmanov, T. G.; Johnson, D. A.; Saliendra, N. Z.; Svejcar, T. J.; Angell, R. F.; Clawson, K. L. (2004): Winter CO2 fluxes above sagebrush-steppe ecosystems in Idaho and Oregon. In *Agricultural and Forest Meteorology* 126 (1-2), pp. 73–88. DOI: 10.1016/j.agrformet.2004.05.007.

Golubiewski, N. E. (2006): Urbanization Increases Grassland Carbon Pools: Effects Of Landscaping In Colorado's Front Range. In *Ecological Applications* 16 (2), pp. 555–571. DOI: 10.1890/1051-0761(2006)016[0555:UIGCPE]2.0.CO;2.

Graf, A.; Weihermüller, L.; Huisman, J. A.; Herbst, M.; Bauer, J.; Vereecken, H. (2008): Measurement depth effects on the apparent temperature sensitivity of soil respiration in field studies. In *Biogeosciences* 5 (4), pp. 1175–1188. DOI: 10.5194/bg-5-1175-2008.

Graham, P. (2011): The Tallgrass Prairie: An Endangered Landscape. Available online at http://www.csa.com/discoveryguides/prairie/review.pdf.

Grimmond, C. S. B., and T. R. Oke (1999): Evapotranspiration rates in urban areas. Impacts of Urban Growth on Surface Water and Groundwater Quality. In *Proceedings of IUGG 99 Symposium HS5, IAHS Publ., 259*.

Gu, L.; Massman, W. J.; Leuning, R.; Pallardy, S. G.; Meyers, T.; Hanson, P. J. et al. (2012): The fundamental equation of eddy covariance and its application in flux measurements. In *Agricultural and Forest Meteorology* 152, pp. 135–148. DOI: 10.1016/j.agrformet.2011.09.014.

Guertal, E. A. (2012): Carbon Sequestration in Turfed Landscapes: A Review. In R. Lal, B. Augustin (Eds.): Carbon Sequestration in Urban Ecosystems. Dordrecht: Springer Netherlands, pp. 197–213.

Ham, J. M.; Heilman, J. L. (2003): Experimental Test of Density and Energy-Balance Corrections on Carbon Dioxide Flux as Measured Using Open-Path Eddy Covariance. In *Agronomy Journal* 95 (6), p. 1393. DOI: 10.2134/agronj2003.1393.

Ham, J. M.; Knapp, A. K. (1998): Fluxes of CO2, water vapor, and energy from a prairie ecosystem during the seasonal transition from carbon sink to carbon source. In *Agricultural and Forest Meteorology* 89 (1), pp. 1–14. DOI: 10.1016/S0168-1923(97)00062-2.

Harper, C. W.; Blair, J. M.; Fay, P. A.; Knapp, A. K.; Carlisle, J. D. (2005): Increased rainfall variability and reduced rainfall amount decreases soil CO2 flux in a grassland ecosystem. In *Global Change Biol* 11 (2), pp. 322–334. DOI: 10.1111/j.1365-2486.2005.00899.x.

Haslwanter, A.; Hammerle, A.; Wohlfahrt, G. (2009): Open-path vs. closed-path eddy covariance measurements of the net ecosystem carbon dioxide and water vapour exchange: A long-term perspective. In *Agricultural and Forest Meteorology* 149 (2), pp. 291–302. DOI: 10.1016/j.agrformet.2008.08.011.

Heimann, M.; Reichstein, M. (2008): Terrestrial ecosystem carbon dynamics and climate feedbacks. In *Nature* 451 (7176), pp. 289–292. DOI: 10.1038/nature06591.

Hendricks Franssen, H. J.; Stöckli, R.; Lehner, I.; Rotenberg, E.; Seneviratne, S. I. (2010): Energy balance closure of eddy-covariance data: A multisite analysis for European FLUXNET stations. In *Agricultural and Forest Meteorology* 150 (12), pp. 1553–1567. DOI: 10.1016/j.agrformet.2010.08.005.

Heusinkveld, B. G.; Jacobs, A. F.G.; Holtslag, A. A.M. (2008): Effect of open-path gas analyzer wetness on eddy covariance flux measurements: A proposed solution. In *Agricultural and Forest Meteorology* 148 (10), pp. 1563–1573. DOI: 10.1016/j.agrformet.2008.05.010.

Hibbard, K. A.; Law, B. E.; Reichstein, M.; Sulzman, J. (2005): An analysis of soil respiration across northern hemisphere temperate ecosystems. In *Biogeochemistry* 73 (1), pp. 29–70. DOI: 10.1007/s10533-004-2946-0.

Higgins, C. W.; Froidevaux, M.; Simeonov, V.; Vercauteren, N.; Barry, C.; Parlange, M. B. (2012): The Effect of Scale on the Applicability of Taylor's Frozen Turbulence Hypothesis in the Atmospheric Boundary Layer. In *Boundary-Layer Meteorol* 143 (2), pp. 379–391. DOI: 10.1007/s10546-012-9701-1.

Hilaire, R. S.; Arnold, M. A.; Wilkerson, D. C.; Devitt, D. A.; Hurd, B. H.; Lesikar, B. J. et al. (2008): Efficient Water Use in Residential Urban Landscapes. In *HortScience* 43 (7), pp. 2081–2092.

Hiller, R. V.; McFadden, J. P.; Kljun, N. (2011): Interpreting CO2 Fluxes Over a Suburban Lawn: The Influence of Traffic Emissions. In *Boundary-Layer Meteorol* 138 (2), pp. 215–230. DOI: 10.1007/s10546-010-9558-0.

Houghton, J. (2009): Global Warming 4ed. 4th ed. Cambridge [England],, New York: Cambridge University Press Textbooks.

Hunt, B. G. (2011): The role of natural climatic variation in perturbing the observed global mean temperature trend. In *Clim Dyn* 36 (3-4), pp. 509–521. DOI: 10.1007/s00382-010-0799-x.

Hussain, M. Z.; Grünwald, T.; Tenhunen, J. D.; Li, Y. L.; Mirzae, H.; Bernhofer, C. et al. (2011): Summer drought influence on CO2 and water fluxes of extensively managed grassland in Germany. In *Agriculture, Ecosystems & Environment* 141 (1-2), pp. 67–76. DOI: 10.1016/j.agee.2011.02.013.

Hutyra, L. R.; Yoon, B.; Alberti, M. (2011): Terrestrial carbon stocks across a gradient of urbanization: a study of the Seattle, WA region. In *Global Change Biology* 17 (2), pp. 783–797. DOI: 10.1111/j.1365-2486.2010.02238.x.

Huxman, T. E.; Cable, J. M.; Ignace, D. D.; Eilts, J. A.; English, N. B.; Weltzin, J.; Williams, D. G. (2004): Response of net ecosystem gas exchange to a simulated precipitation pulse in a semi-arid grassland: the role of native versus non-native grasses and soil texture. In *Oecologia* 141 (2), pp. 295–305. DOI: 10.1007/s00442-003-1389-y.

Ibrom, A.; Dellwik, E.; Flyvbjerg, H.; Jensen, N. O.; Pilegaard, K. (2007): Strong low-pass filtering effects on water vapour flux measurements with closed-path eddy correlation systems. In *Agricultural and Forest Meteorology* 147 (3-4), pp. 140–156. DOI: 10.1016/j.agrformet.2007.07.007.

Imhoff, M. L.; Bounoua, L.; DeFries, R.; Lawrence, W. T.; Stutzer, D.; Tucker, C. J.; Ricketts, T. (2004): The consequences of urban land transformation on net primary productivity in the United States. In *Remote Sensing of Environment* 89 (4), pp. 434–443. DOI: 10.1016/j.rse.2003.10.015.

IPCC 2013: Climate change 2013. The physical science basis : Working Group I contribution to the fifth assessment report of the Intergovernmental Panel on Climate Change. With assistance of Stocker, T.F., D. Qin, G.-K. Plattner, M. Tignor, S.K. Allen, J. Boschung, A. Nauels, Y. Xia, V. Bex and P.M. Midgley. 2013.

Karhu, K.; Auffret, M. D.; Dungait, J. A. J.; Hopkins, D. W.; Prosser, J. I.; Singh, B. K. et al. (2014): Temperature sensitivity of soil respiration rates enhanced by microbial community response. In *Nature* 513 (7516), pp. 81–84. DOI: 10.1038/nature13604.

Karl, T. R.; Trenberth, K. E. (2003): Modern Global Climate Change. In *Science* 302 (5651), pp. 1719–1723. DOI: 10.1126/science.1090228.

Katul, G.; Lai, C.-T.; Schäfer, K.; Vidakovic, B.; Albertson, J.; Ellsworth, D.; Oren, R. (2001): Multiscale analysis of vegetation surface fluxes: from seconds to years. In *Advances in Water Resources* 24 (9-10), pp. 1119–1132. DOI: 10.1016/S0309-1708(01)00029-X.

Kaye, J. P.; Burke, I. C.; Mosier, A. R.; Pablo Guerschman, J. (2004): Methane and Nitrous Oxide Fluxes from Urban Soils to the Atmosphere. In *Ecological Applications* 14 (4), pp. 975–981. DOI: 10.1890/03-5115.

Kim, D.-G.; Vargas, R.; Bond-Lamberty, B.; Turetsky, M. R. (2012): Effects of soil rewetting and thawing on soil gas fluxes: a review of current literature and suggestions for future research. In *Biogeosciences* 9 (7), pp. 2459–2483. DOI: 10.5194/bg-9-2459-2012.

King, D. A. (2004): ENVIRONMENT: Climate Change Science: Adapt, Mitigate, or Ignore? In *Science* 303 (5655), pp. 176–177. DOI: 10.1126/science.1094329.

Kjelgren, R.; Rupp, L.; Kilgren, D. (2000): Water Conservation in Urban Landscapes. In *HortScience* 35 (6), pp. 1037–1040.

Klein Tank, A. M. G.; Können, G. P.; Selten, F. M. (2005): Signals of anthropogenic influence on European warming as seen in the trend patterns of daily temperature variance. In *Int. J. Climatol.* 25 (1), pp. 1–16. DOI: 10.1002/joc.1087.

Knapp, A. K.; Smith, M. D. (2001): Variation among biomes in temporal dynamics of aboveground primary production. In *Science* 291 (5503), pp. 481–484. DOI: 10.1126/science.291.5503.481.

Kochendorfer, J.; Meyers, T. P.; Frank, J.; Massman, W. J.; Heuer, M. W. (2012): How Well Can We Measure the Vertical Wind Speed? Implications for Fluxes of Energy and Mass. In *Boundary-Layer Meteorol* 145 (2), pp. 383–398. DOI: 10.1007/s10546-012-9738-1.

Kochendorfer, J.; Meyers, T. P.; Frank, J. M.; Massman, W. J.; Heuer, M. W. (2013): Reply to the Comment by Mauder on "How Well Can We Measure the Vertical Wind Speed? Implications for Fluxes of Energy and Mass". In *Boundary-Layer Meteorol* 147 (2), pp. 337–345. DOI: 10.1007/s10546-012-9792-8.

Kohsiek, W.; Liebethal, C.; Foken, T.; Vogt, R.; Oncley, S. P.; Bernhofer, C.; Debruin, H. A. R. (2007): The Energy Balance Experiment EBEX-2000. Part III: Behaviour and quality of the radiation measurements. In *Boundary-Layer Meteorol* 123 (1), pp. 55–75. DOI: 10.1007/s10546-006-9135-8.

Kong, F.; Yin, H.; James, P.; Hutyra, L. R.; He, H. S. (2014): Effects of spatial pattern of greenspace on urban cooling in a large metropolitan area of eastern China. In *Landscape and Urban Planning* 128, pp. 35–47. DOI: 10.1016/j.landurbplan.2014.04.018.

Kordowski, K. (2009): Turbulenter Austausch von Kohlendioxid in der urbanen Grenzschicht über einer Parkfläche. Hohenwarsleben: Westarp-Wiss. (Essener ökologische Schriften, 29).

Kordowski, K.; Kuttler, W. (2010): Carbon dioxide fluxes over an urban park area. In *Atmospheric Environment* 44 (23), pp. 2722–2730. DOI: 10.1016/j.atmosenv.2010.04.039.

Kormann, R., Meixner, F. X. (2001): An analytical footprint model for non-neutral stratification. In *Boundary-Layer Meteorology*, 99:207–224. DOI: 10.1023/A:1018991015119.

Kowalski, A. S. (2008): Comment on "the storage term in eddy flux calculations". In *Agricultural and Forest Meteorology* 148 (4), pp. 691–692. DOI: 10.1016/j.agrformet.2007.10.010.

Krishnan, P.; Meyers, T. P.; Scott, R. L.; Kennedy, L.; Heuer, M. (2012): Energy exchange and evapotranspiration over two temperate semi-arid grasslands in North America. In *Agricultural and Forest Meteorology* 153, pp. 31–44. DOI: 10.1016/j.agrformet.2011.09.017.

Kutzbach, L. (2006): The exchange of energy, water and carbon dioxide between wet arctic tundra and the atmosphere at the Lena River Delta, Northern Siberia. Univ, Bremerhaven, Hamburg.

Labedzki, L. (Ed.) (2011): Evapotranspiration: InTech.

Lal, R.; Augustin, B. (Eds.) (2012): Carbon Sequestration in Urban Ecosystems. Dordrecht: Springer Netherlands.

Lee, X; Finnigan, J.; U, K.T.P. (2004a): Coordinate Systems and Flux Bias Error. In: Handbook of micrometeorology. A guide for surface flux measurement and analysis. 2004. (eds. Lee, X.; Massman, W. J.; Law, B. E.). Dordrecht. Kluwer Academic Publishers.

Lee, X.; Wu, H.-J.; Sigler, J.; Oishi, C.; Siccama, T. (2004b): Rapid and transient response of soil respiration to rain. In *Global Change Biology* 10 (6), pp. 1017–1026. DOI: 10.1111/j.1529-8817.2003.00787.x.

Lellei-Kovács, E.; Kovács-Láng, E.; Botta-Dukát, Z.; Kalapos, T.; Emmett, B.; Beier, C. (2011): Thresholds and interactive effects of soil moisture on the temperature response of soil respiration. In *European Journal of Soil Biology* 47 (4), pp. 247–255. DOI: 10.1016/j.ejsobi.2011.05.004.

Leuning, R.; Judd, M. J. (1996): The relative merits of open- and closed-path analysers for measurement of eddy fluxes. In *Global Change Biol* 2 (3), pp. 241–253. DOI: 10.1111/j.1365-2486.1996.tb00076.x.

Leuning, R.; Raupach, M. R.; Coppin, P. A.; Cleugh, H. A.; Isaac, P.; Denmead, O. T. et al. (2004): Spatial and Temporal Variations in Fluxes of Energy, Water Vapour and Carbon Dioxide During OASIS 1994 and 1995. In *Boundary-Layer Meteorology* 110 (1), pp. 3–38. DOI: 10.1023/A:1026028217081.

Leuning, R.; van Gorsel, E.; Massman, W. J.; Isaac, P. R. (2012): Reflections on the surface energy imbalance problem. In *Agricultural and Forest Meteorology* 156, pp. 65–74. DOI: 10.1016/j.agrformet.2011.12.002.

Liebethal, C.; Foken, T. (2003): On the significance of the Webb correction to fluxes. In *Boundary-Layer Meteorology* 109 (1), pp. 99–106. DOI: 10.1023/A:1025421903542.

Litvak, E.; Bijoor, N. S.; Pataki, D. E. (2013): Adding trees to irrigated turfgrass lawns may be a water-saving measure in semi-arid environments. In *Ecohydrol.*, pp. n/a. DOI: 10.1002/eco.1458.

Liu, H. (2009): A re-examination of density effects in eddy covariance measurements of CO2 fluxes. In *Adv. Atmos. Sci.* 26 (1), pp. 9–16. DOI: 10.1007/s00376-009-0009-0.

Liu, X.; Wan, S.; Su, B.; Hui, D.; Luo, Y. (2002): Response of soil CO2 efflux to water manipulation in a tallgrass prairie ecosystem. In *Plant and Soil* 240 (2), pp. 213–223. DOI: 10.1023/A:1015744126533.

Lloyd, J.; Taylor, J. A. (1994): On the Temperature Dependence of Soil Respiration. In *Functional Ecology* 8 (3), p. 315. DOI: 10.2307/2389824.

Ma, S.; Baldocchi, D. D.; Xu, L.; Hehn, T. (2007): Inter-annual variability in carbon dioxide exchange of an oak/grass savanna and open grassland in California. In *Agricultural and Forest Meteorology* 147 (3-4), pp. 157–171. DOI: 10.1016/j.agrformet.2007.07.008.

Ma, S.; Baldocchi, D. D.; Hatala, J. A.; Detto, M.; Curiel Yuste, J. (2012): Are rain-induced ecosystem respiration pulses enhanced by legacies of antecedent photodegradation in semi-arid environments? In *Agricultural and Forest Meteorology* 154-155, pp. 203–213. DOI: 10.1016/j.agrformet.2011.11.007.

Mahrt, L. (2010): Computing turbulent fluxes near the surface: Needed improvements. In *Agricultural and Forest Meteorology* 150 (4), pp. 501–509. DOI: 10.1016/j.agrformet.2010.01.015.

Mann, M. E.; Zhang, Z.; Hughes, M. K.; Bradley, R. S.; Miller, S. K.; Rutherford, S.; Ni, F. (2008): Proxy-based reconstructions of hemispheric and global surface temperature variations over the past two millennia. In *Proceedings of the National Academy of Sciences* 105 (36), pp. 13252–13257. DOI: 10.1073/pnas.0805721105.

Mathur, S.; Agrawal, D.; Jajoo, A. (2014): Photosynthesis: response to high temperature stress. In *J. Photochem. Photobiol. B, Biol.* 137, pp. 116–126. DOI: 10.1016/j.jphotobiol.2014.01.010.

Mauder, M. (2013): A Comment on “How Well Can We Measure the Vertical Wind Speed? Implications for Fluxes of Energy and Mass” by Kochendorfer et al. In *Boundary-Layer Meteorol* 147 (2), pp. 329–335. DOI: 10.1007/s10546-012-9794-6.

Mauder, M.; Foken, T. (2006): Impact of post-field data processing on eddy covariance flux estimates and energy balance closure. In *Meteorol. Z.* 15 (6), pp. 597–609. DOI: 10.1127/0941-2948/2006/0167.

Metro Denver: Metro Denver Economic Development Corporation. Available online at http://www.metrodenver.org/, checked on 2/5/2013.

Meyers, T. P. (2001): A comparison of summertime water and CO2 fluxes over rangeland for well watered and drought conditions. In *Agricultural and Forest Meteorology* 106 (3), pp. 205–214. DOI: 10.1016/S0168-1923(00)00213-6.

Michaelis, L.; Menten, M. L. (1913): Die Kinetik der Invertinwirkung. In *Biochemische Zeitschrift* 49, pp. 333–369.

Mielnick, P.; Dugas, W. A. (2000): Soil CO2 flux in a tallgrass prairie. In *Soil Biology and Biochemistry* 32 (2), pp. 221–228. DOI: 10.1016/S0038-0717(99)00150-9.

Milesi, C.; Running, S. W.; Elvidge, C. D.; Dietz, J. B.; Tuttle, B. T.; Nemani, R. R. (2005): Mapping and Modeling the Biogeochemical Cycling of Turf Grasses in the United States. In *Environmental Management* 36 (3), pp. 426–438. DOI: 10.1007/s00267-004-0316-2.

Moberg, A.; Sonechkin, D. M.; Holmgren, K.; Datsenko, N. M.; Karlén, W. (2005): Highly variable Northern Hemisphere temperatures reconstructed from low- and high-resolution proxy data. In *Nature* 433 (7026), pp. 613–617. DOI: 10.1038/nature03265.

Moffat, A. M.; Papale, D.; Reichstein, M.; Hollinger, D. Y.; Richardson, A. D.; Barr, A. G. et al. (2007): Comprehensive comparison of gap-filling techniques for eddy covariance net carbon fluxes. In *Agricultural and Forest Meteorology* 147 (3-4), pp. 209–232. DOI: 10.1016/j.agrformet.2007.08.011.

Moncrieff, J. B.; Massheder, J. M.; Bruin, H. de; Elbers, J.; Friborg, T.; Heusinkveld, B. et al. (1997): A system to measure surface fluxes of momentum, sensible heat, water vapour and carbon dioxide. In *Journal of Hydrology* 188-189, pp. 589–611. DOI: 10.1016/S0022-1694(96)03194-0.

Moncrieff, J.; Clement, R.; Finnigan, J.; Meyers, T.: Averaging, Detrending, and Filtering of Eddy Covariance Time Series. In : Handbook of micrometeorology. A guide for surface flux measurement and analysis. 2004. (eds. Lee, X.; Massman, W. J.; Law, B. E.). Dordrecht. Kluwer Academic Publishers.

Montgomery, R. B. (1948): Vertical Eddy Flux of Heat in the Atmosphere. In *J. Meteor.* 5 (6), pp. 265–274. DOI: 10.1175/1520-0469(1948)005<0265:VEFOHI>2.0.CO;2.

Moore, C. J. (1986): Frequency response corrections for eddy correlation systems. In *Boundary-Layer Meteorol* 37 (1-2), pp. 17–35. DOI: 10.1007/BF00122754.

Moriwaki, R.; Kanda, M. (2004): Seasonal and Diurnal Fluxes of Radiation, Heat, Water Vapor, and Carbon Dioxide over a Suburban Area. In *J. Appl. Meteor.* 43 (11), pp. 1700–1710. DOI: 10.1175/JAM2153.1.

MPI (2013): Eddy covariance gap-filling & flux-partitioning tool. Available online at http://www.bgc-jena.mpg.de/~MDIwork/eddyproc/.

Mu, Q.; Zhao, M.; Running, S. W. (2011): Evolution of hydrological and carbon cycles under a changing climate. In *Hydrol. Process.* 25 (26), pp. 4093–4102. DOI: 10.1002/hyp.8367.

Munger, J. W.; Loescher, H. W.; Luo, H. (2012): Measurement, Tower, and Site Design Considerations - Chapter 2. In: Eddy Covariance: A practical guide to measurement and data analysis (eds. Aubinet, M.; Vesala, T.; Papale, D.). Dordrecht, New York: Springer.

Munson, S. M.; Benton, T. J.; Lauenroth, W. K.; Burke, I. C. (2010): Soil carbon flux following pulse precipitation events in the shortgrass steppe. In *Ecol Res* 25 (1), pp. 205–211. DOI: 10.1007/s11284-009-0651-0.

Nakai, T.; Shimoyama, K. (2012): Ultrasonic anemometer angle of attack errors under turbulent conditions. In *Agricultural and Forest Meteorology* 162-163, pp. 14–26. DOI: 10.1016/j.agrformet.2012.04.004.

Nave, L. E.; Gough, C. M.; Maurer, K. D.; Bohrer, G.; Hardiman, B. S.; Le Moine, J. et al. (2011): Disturbance and the resilience of coupled carbon and nitrogen cycling in a north temperate forest. In *J. Geophys. Res.* 116 (G4). DOI: 10.1029/2011JG001758.

NIDIS (2012): Quarterly Climate Impacts and Outlook. Western Region, June and September 2012. Available online at http://www.drought.gov/drought/content/resources/reports.

Niu, S.; Sherry, R. A.; Zhou, X.; Luo, Y. (2013): Ecosystem Carbon Fluxes in Response to Warming and Clipping in a Tallgrass Prairie. In *Ecosystems* 16 (6), pp. 948–961. DOI: 10.1007/s10021-013-9661-4.

NOAA. National Weather Service Forecast Office (2012): The Denver CO Climate Summary of the year of 2011. Available online at http://www.crh.noaa.gov/bou/include/showProduct.php?product=denclm_2011.txt.

NOAA. National Weather Service Forecast Office (2012a): Denver's Annual Temperature & Precipitation Profile - 2011 Available online at http://www.crh.noaa.gov/bou/?n=denver_climategraphs_2011

NOAA. National Weather Service Forecast Office (2013a). Available online at http://www.nws.noaa.gov/climate/xmacis.php?wfo=bou, checked on 2/14/2013.

NOAA. National Weather Service Forecast Office (2013b). Available online at http://www.crh.noaa.gov/bou/cli/normals.php.

NOAA. National Climatic Data Center (2013c). Available online at http://www.ncdc.noaa.gov/oa/climate/online/ccd/clpcdy.txt.

NOAA. National Weather Service Forecast Office (2013d): The Denver CO Climate Summary for the year of 2012. Available online at http://www.crh.noaa.gov/bou/include/showProduct.php?product=denclm_2012.txt.

NOAA. National Weather Service Forecast Office (2013e): Denver's Annual Temperature & Precipitation Profile - 2012 Available online at http://www.crh.noaa.gov/bou/?n=denver_climategraphs_2012

Nowak, D.; Crane, D. E. (2002): Carbon storage and sequestration by urban trees in the USA. In *Environmental Pollution* 116 (3), pp. 381–389. DOI: 10.1016/S0269-7491(01)00214-7.

Nowak, D. J.; Greenfield, E. J. (2012): Tree and impervious cover in the United States. In *Landscape and Urban Planning* 107 (1), pp. 21–30. DOI: 10.1016/j.landurbplan.2012.04.005.

NREL. National Renewable Energy Laboratory (2013): NWTC M2 Tower. NREL. Available online at http://www.nrel.gov/midc/nwtc_m2/.

Obukhov, A. M.: Charakteristiki mikrostruktury vetra v prizemnom sloje atmosfery. (Characteristics of the micro-structure of the wind in the surface layer of the atmosphere). In *Izv AN SSSR ser Geofiz* 3, pp. 49–68.

Oncley, S. P.; Lenschow, D. H.; Campos, T. L.; Davis, K. J.; Mann, J. (1997): Regional-scale surface flux observations across the boreal forest during BOREAS. In *J. Geophys. Res.* 102 (D24), p. 29147. DOI: 10.1029/97JD00242.

Ono, K.; Miyata, A.; Yamada, T. (2008): Apparent downward CO2 flux observed with open-path eddy covariance over a non-vegetated surface. In *Theor Appl Climatol* 92 (3-4), pp. 195–208. DOI: 10.1007/s00704-007-0323-3.

Owensby, C. E.; Ham, J. M.; Auen, L. M. (2006): Fluxes of CO2 From Grazed and Ungrazed Tallgrass Prairie. In *Rangeland Ecology & Management* 59 (2), pp. 111–127. DOI: 10.2111/05-116R2.1.

Pacala, S. W. (2001): Consistent Land- and Atmosphere-Based U.S. Carbon Sink Estimates. In *Science* 292 (5525), pp. 2316–2320. DOI: 10.1126/science.1057320.

Parton, W.; Morgan, J.; Smith, D.; Del Grosso, S.; Prihodko, L.; LeCain, D. et al. (2012): Impact of precipitation dynamics on net ecosystem productivity. In *Glob Change Biol* 18 (3), pp. 915–927. DOI: 10.1111/j.1365-2486.2011.02611.x.

Paschke, S. S. (2011): Groundwater availability of the Denver Basin aquifer system, Colorado. Reston, Va: U.S. Dept. of the Interior, U.S. Geological Survey.

Pataki, D. E.; Alig, R. J.; Fung, A. S.; Golubiewski, N. E.; Kennedy, C. A.; McPherson, E. G. et al. (2006): Urban ecosystems and the North American carbon cycle. In *Global Change Biol* 12 (11), pp. 2092–2102. DOI: 10.1111/j.1365-2486.2006.01242.x.

Peters, E. B.; Hiller, R. V.; McFadden, J. P. (2011): Seasonal contributions of vegetation types to suburban evapotranspiration. In *J. Geophys. Res.* 116 (G1). DOI: 10.1029/2010JG001463.

Peters, E. B.; McFadden, J. P. (2012): Continuous measurements of net CO_2 exchange by vegetation and soils in a suburban landscape. In *J. Geophys. Res.* 117 (G3). DOI: 10.1029/2011JG001933.

Pickett, S.T.A; Cadenasso, M.L; Grove, J.M; Boone, Christopher G.; Groffman, Peter M.; Irwin, Elena et al. (2011): Urban ecological systems: Scientific foundations and a decade of progress. In *Journal of Environmental Management* 92 (3), pp. 331–362. DOI: 10.1016/j.jenvman.2010.08.022.

Polley, H. W.; Frank, A. B.; Sanabria, J.; Phillips, R. L. (2008): Interannual variability in carbon dioxide fluxes and flux–climate relationships on grazed and ungrazed northern mixed-grass prairie. In *Global Change Biol* 14 (7), pp. 1620–1632. DOI: 10.1111/j.1365-2486.2008.01599.x.

Potere, D.; Schneider, A. (2007): A critical look at representations of urban areas in global maps. In *GeoJournal* 69 (1-2), pp. 55–80. DOI: 10.1007/s10708-007-9102-z.

Pouyat, R. V.; Yesilonis, I. D.; NOWAK, D. J. (2006): Carbon storage by urban soils in the United States. In *J. Environ. Qual.* 35 (4), pp. 1566–1575. DOI: 10.2134/jeq2005.0215.

Pouyat, R. V.; Yesilonis, I. D.; Golubiewski, N. E. (2009): A comparison of soil organic carbon stocks between residential turf grass and native soil. In *Urban Ecosyst* 12 (1), pp. 45–62. DOI: 10.1007/s11252-008-0059-6.

Powell, K. M.; Anderson, D. E.; Stannard, D. I.; Mladinich, C. S.; Thienelt, T. S.; Blanken, P. (2011): Soil Water Cycling Links to Carbon Content between Ecosystems in the Colorado Front Range. AGU Fall Meeting. Poster.

Qian, Y.; Follett, R. F. (2002): Assessing Soil Carbon Sequestration in Turfgrass Systems Using Long-Term Soil Testing Data. In *Agronomy Journal* 94 (4), p. 930. DOI: 10.2134/agronj2002.9300.

Qian, Y.; Follett, R. (2012): Carbon Dynamics and Sequestration in Urban Turfgrass Ecosystems. In R. Lal, B. Augustin (Eds.): Carbon Sequestration in Urban Ecosystems. Dordrecht: Springer Netherlands, pp. 161–172.

Qian, Y.; Follett, R. F.; Kimble, J. M. (2010): Soil Organic Carbon Input from Urban Turfgrasses. In *Soil Science Society of America Journal* 74 (2), p. 366. DOI: 10.2136/sssaj2009.0075.

Rebmann, C.; Kolle, O.; Heinesch, B.; Queck, R.; Ibrom, A.; Aubinet, M. (2012): Data Acquisition and Flux Calculations - Chapter 3. In: Eddy Covariance: A practical guide to measurement and data analysis (eds. Aubinet, M.; Vesala, T.; Papale, D.). Dordrecht, New York: Springer.

Reichstein, M.; Falge, E.; Baldocchi, D.; Papale, D.; Aubinet, M.; Berbigier, P. et al. (2005): On the separation of net ecosystem exchange into assimilation and ecosystem respiration: review and improved algorithm. In *Global Change Biol* 11 (9), pp. 1424–1439. DOI: 10.1111/j.1365-2486.2005.001002.x.

Reverter, B. R.; Carrara, A.; Fernández, A.; Gimeno, C.; Sanz, M. J.; Serrano-Ortiz, P. et al. (2011): Adjustment of annual NEE and ET for the open-path IRGA self-heating correction: Magnitude and approximation over a range of climate. In *Agricultural and Forest Meteorology* 151 (12), pp. 1856–1861. DOI: 10.1016/j.agrformet.2011.06.001.

Risch, A. C.; Frank, D. A. (2007): Effects of increased soil water availability on grassland ecosystem carbon dioxide fluxes. In *Biogeochemistry* 86 (1), pp. 91–103. DOI: 10.1007/s10533-007-9148-5.

Risk, D.; Kellman, L.; Beltrami, H. (2002): Carbon dioxide in soil profiles: Production and temperature dependence. In *Geophys. Res. Lett.* 29 (6). DOI: 10.1029/2001GL014002.

Robbins, P.; Birkenholtz, T. (2003): Turfgrass revolution: measuring the expansion of the American lawn. In *Land Use Policy* 20 (2), pp. 181–194. DOI: 10.1016/S0264-8377(03)00006-1.

Rohde, R.; Muller, R. A.; Jacobsen, R.; Muller, E.; Perlmutter, S.; Rosenfeld, A. et al. (2012): A New Estimate of the Average Earth Surface Land Temperature Spanning 1753 to 2011. In *Geoinfor Geostat: An Overview*.

Romero, C. C.; Dukes, M. D. (2009): Turfgrass and Ornamental Plant Evapotranspiration and Crop Coefficient. Literature Review. Agricultural and Biological Engineering Department University of Florida.

Rosenberg, N. J.; Blad, B. L.; Verma, S. B. (1983): Microclimate. The biological environment. 2nd ed. New York: Wiley.

Rutledge, S.; Campbell, D. I.; Baldocchi, D.; Schipper, L. A. (2010): Photodegradation leads to increased carbon dioxide losses from terrestrial organic matter. In *Global Change Biology*, pp. no. DOI: 10.1111/j.1365-2486.2009.02149.x.

Ryu, Y.; Baldocchi, D. D.; Ma, S.; Hehn, T. (2008): Interannual variability of evapotranspiration and energy exchange over an annual grassland in California. In *J. Geophys. Res.* 113 (D9). DOI: 10.1029/2007JD009263.

Salamanca, F.; Georgescu, M.; Mahalov, A.; Moustaoui, M.; Wang, M. (2014): Anthropogenic heating of the urban environment due to air conditioning. In *J. Geophys. Res. Atmos.* 119 (10), pp. 5949–5965. DOI: 10.1002/2013JD021225.

Schmid, H. P. (1994): Source areas for scalars and scalar fluxes. In *Boundary-Layer Meteorol* 67 (3), pp. 293–318. DOI: 10.1007/BF00713146.

Scholes, R.J; Monteiro, P.M.S; Sabine, C.L; Canadell, J.G (2009): Systematic long-term observations of the global carbon cycle. In *Trends in Ecology & Evolution* 24 (8), pp. 427–430. DOI: 10.1016/j.tree.2009.03.006.

Scott, R. L. (2010): Using watershed water balance to evaluate the accuracy of eddy covariance evaporation measurements for three semiarid ecosystems. In *Agricultural and Forest Meteorology* 150 (2), pp. 219–225. DOI: 10.1016/j.agrformet.2009.11.002.

Shakun, J. D.; Clark, P. U.; He, F.; Marcott, S. A.; Mix, A. C.; Liu, Z. et al. (2012): Global warming preceded by increasing carbon dioxide concentrations during the last deglaciation. In *Nature* 484 (7392), pp. 49–54. DOI: 10.1038/nature10915.

Sims, P. L.; Bradford, J.A (2001): Carbon dioxide fluxes in a southern plains prairie. In *Agricultural and Forest Meteorology* 109 (2), pp. 117–134. DOI: 10.1016/S0168-1923(01)00264-7.

Spronken-Smith, R. A.; Oke, T. R.; Lowry, W. P. (2000): Advection and the surface energy balance across an irrigated urban park. In *International Journal of Climatology* 20 (9), pp. 1033–1047.

St. Clair, S. B.; Sudderth, E. A.; Fischer, M. L.; Torn, M. S.; Stuart, S. A.; Salve, R. et al. (2009): Soil drying and nitrogen availability modulate carbon and water exchange over a range of annual precipitation totals and grassland vegetation types. In *Global Change Biology* 15 (12), pp. 3018–3030. DOI: 10.1111/j.1365-2486.2009.01862.x.

Stern, N. (2007): The economics of climate change. The Stern review. Reprint. Cambridge: Cambridge Univ. Press.

Stoy, P. C.; Mauder, M.; Foken, T.; Marcolla, B.; Boegh, E.; Ibrom, A. et al. (2013): A data-driven analysis of energy balance closure across FLUXNET research sites: The role of landscape scale heterogeneity. In *Agricultural and Forest Meteorology* 171-172, pp. 137–152. DOI: 10.1016/j.agrformet.2012.11.004.

Stull, R. B. (1988): An introduction to boundary layer meteorology. Dordrecht, Kluwer Acad. Publ (Atmospheric sciences library, 13).

Suttie, J. M.; Reynolds, S. G.; Batello, C. (2005): Grasslands of the world. Rome: Food and Agricultural Organization of the United Nations.

Suyker, A. E.; Verma, S. B. (2001): Year-round observations of the net ecosystem exchange of carbon dioxide in a native tallgrass prairie. In *Global Change Biol* 7 (3), pp. 279–289. DOI: 10.1046/j.1365-2486.2001.00407.x.

Suyker, A. E.; Verma, S. B.; Burba, G. G. (2003): Interannual variability in net CO2 exchange of a native tallgrass prairie. In *Global Change Biol* 9 (2), pp. 255–265. DOI: 10.1046/j.1365-2486.2003.00567.x.

Swanson, K. L.; Sugihara, G.; Tsonis, A. A. (2009): Long-term natural variability and 20th century climate change. In *Proceedings of the National Academy of Sciences* 106 (38), pp. 16120–16123. DOI: 10.1073/pnas.0908699106.

Swinbank, W. C. (1951): The measurement of vertical transfer of heat and water vapor by eddies in the lower atmosphere. In *J. Meteor.* 8 (3), pp. 135–145. DOI: 10.1175/1520-0469(1951)008<0135:TMOVTO>2.0.CO;2.

Taha, H.; Akbari, H.; Rosenfeld, A. (1991): Heat island and oasis effects of vegetative canopies: Micro-meteorological field-measurements. In *Theor Appl Climatol* 44 (2), pp. 123–138. DOI: 10.1007/BF00867999.

Thienelt, T. S. (2007): Greenhouse Gas Fluxes from Urban Lawns to the Atmosphere in Denver, Colorado. Diploma thesis. Martin-Luther-University, Halle, Germany.

Townsend-Small, A.; Czimczik, C. I. (2010): Carbon sequestration and greenhouse gas emissions in urban turf. In *Geophys. Res. Lett.* 37 (2), pp. n/a. DOI: 10.1029/2009GL041675.

Trudgill, S.; Jeffery, A.; Parker, J. (2010): Climate change and the resilience of the domestic lawn. In *Applied Geography* 30 (1), pp. 177–190. DOI: 10.1016/j.apgeog.2009.08.002.

Twine, T. E.; Kustas, W. P.; Norman, J. M.; Cook, D. R.; Houser, P. R.; Meyers, T. P. et al. (2000): Correcting eddy-covariance flux underestimates over a grassland. In *Agricultural and Forest Meteorology* 103 (3), pp. 279–300. DOI: 10.1016/S0168-1923(00)00123-4.

US Census: Census Bureau Homepage. Available online at http://www.census.gov/, checked on 1/14/2013.

USDA. U.S. Department of Agriculture (1971): Soil Survey of Arapahoe County Colorado. Available online at http://www.co.nrcs.usda.gov/technical/soil/soil-surveys/colorado-surveys/ArapahoeCty/ArapahoeCOweb.html.

USGS. U.S. Geological Survey (2014): The National Map. Available online at http:// http://nationalmap.gov/.

FWS. U.S. Fish and Wildlife Service (2013): Rocky Flats National Wildlife Refuge. Available online at http://www.fws.gov/rockyflats/, checked on 2/20/2013.

FWS. U.S. Fish and Wildlife Service (2005): Comprehensive Conservation Plan. Rocky Flats National Wildlife Refuge. Available online at http://www.fws.gov/rockyflats/overview.htm.

United Nations (2012): World Urbanization Prospects. The 2011 Revision: United Nations Pubns.

VA. Department of Veteran Affairs: Fort Logan National Cemetery. Available online at http://www.cem.va.gov/cems/nchp/ftlogan.asp, checked on 2/19/2013.

Verburg, P. S. J.; Arnone, J. A.; Obrist, D.; Schorran, D. E.; Evans, R. D.; Leroux-Swarthout, D. et al. (2004): Net ecosystem carbon exchange in two experimental grassland ecosystems. In *Global Change Biol* 10 (4), pp. 498–508. DOI: 10.1111/j.1529-8817.2003.00744.x.

Verma, S. B.; Dobermann, A.; Cassman, K. G.; Walters, D. T.; Knops, J. M.; Arkebauer, T. J. et al. (2005): Annual carbon dioxide exchange in irrigated and rainfed maize-based agroecosystems. In *Agricultural and Forest Meteorology* 131 (1-2), pp. 77–96. DOI: 10.1016/j.agrformet.2005.05.003.

Verma, S. B.; Kim, J.; Clement, R. J. (1992): Momentum, water vapor, and carbon dioxide exchange at a centrally located prairie site during FIFE. In *J. Geophys. Res.* 97 (D17), p. 18629. DOI: 10.1029/91JD03045.

Vickers, D.; Mahrt, L. (1997): Quality Control and Flux Sampling Problems for Tower and Aircraft Data. In *J. Atmos. Oceanic Technol.* 14 (3), pp. 512–526. DOI: 10.1175/1520-0426(1997)014%3C0512%3AQCAFSP%3E2.0.CO%3B2.

Wang, W.; Peng, S.; Wang, T.; Fang, J. (2010): Winter soil CO2 efflux and its contribution to annual soil respiration in different ecosystems of a forest-steppe ecotone, north China. In *Soil Biology and Biochemistry* 42 (3), pp. 451–458. DOI: 10.1016/j.soilbio.2009.11.028.

Warren, R.; Price, J.; Fischlin, A.; Nava Santos, S.; Midgley, G. (2011): Increasing impacts of climate change upon ecosystems with increasing global mean temperature rise. In *Climatic Change* 106 (2), pp. 141–177. DOI: 10.1007/s10584-010-9923-5.

Webb, E. K.; Pearman, G. I.; Leuning, R. (1980): Correction of flux measurements for density effects due to heat and water vapour transfer. In *Q.J Royal Met. Soc.* 106 (447), pp. 85–100. DOI: 10.1002/qj.49710644707.

Wherley, B. (2011): Turfgrass Growth, Quality, and Reflective Heat Load in Response to Deficit Irrigation Practices. In L. Labedzki (Ed.): Evapotranspiration: InTech.

Wilson, K.; Goldstein, A.; Falge, E.; Aubinet, M.; Baldocchi, D.; Berbigier, P. et al. (2002): Energy balance closure at FLUXNET sites. In *Agricultural and Forest Meteorology* 113 (1-4), pp. 223–243. DOI: 10.1016/S0168-1923(02)00109-0.

Wyngaard, J. C. (1988): Flow-distortion effects on scalar flux measurements in the surface layer: Implications for sensor design. In *Boundary-Layer Meteorol* 42 (1-2), pp. 19–26. DOI: 10.1007/BF00119872.

Xu, L.; Baldocchi, D. D. (2004): Seasonal variation in carbon dioxide exchange over a Mediterranean annual grassland in California. In *Agricultural and Forest Meteorology* 123 (1-2), pp. 79–96. DOI: 10.1016/j.agrformet.2003.10.004.

Yasuda, Y.; Watanabe, T. (2001): Comparative measurements of CO2 flux over a forest using closed-path and open-path CO2 analysers. In *Boundary-Layer Meteorology* 100 (2), pp. 191–208. DOI: 10.1023/A:1019277003979.

Zhang, X.; Hu, L.; Bian, X.; Zhao, B.; Chai, F.; Sun, X. (2007): The most economical irrigation amount and evapotranspiration of the turfgrasses in Beijing City, China. In *Agricultural Water Management* 89 (1-2), pp. 98–104. DOI: 10.1016/j.agwat.2006.11.006.

Zirkle, G.; Lal, R.; Augustin, B. (2011): Modeling Carbon Sequestration in Home Lawns. In *HortScience* 46 (5), pp. 808–814.

Zorita, E.; Stocker, T. F.; Storch, H. von (2008): How unusual is the recent series of warm years? In *Geophys. Res. Lett.* 35 (24). DOI: 10.1029/2008GL036228.

Appendix

A1 – Calculation of soil heat flux at the soil surface (after *Campbell Scientific, Inc., 2012*)

Soil heat flux at the surface is calculated by adding the measured soil heat flux (at depth *d*) to the energy stored in the soil layer above the soil heat flux plates. This calculation requires knowledge of the heat capacity of the soil and the change in soil temperature over the output interval.

$$C_s = \rho_b C_d + \theta_v \rho_w C_w$$

Eq. (A.1) – (C_s) heat capacity of moist soil, (ρ_b; 1.4 g cm^{-3}) bulk density, (C_d; 840 J kg^{-1} K^{-1}) heat capacity of dry mineral soil, (θ_v) volumetric water content, (ρ_w) density of water, (C_w; 4190 J kg^{-1} K^{-1}) heat capacity of water.

$$S = \frac{\Delta T_s C_s d}{t}$$

Eq. (A.2) – (S) storage term of soil heat flux, (ΔT_s) change in soil temperature over output interval, (C_s) heat capacity of moist soil, (d) depth of soil heat flux plate, (t) output interval

$$G_{sfc} = G_d + S$$

Eq. (A.3) – (G_{sfc}) soil heat flux at the soil surface, (G_d) soil heat flux at measurement depth, (S) storage term

A2 – Calculation of *NEE* outside the measurement period at Fort Logan (2011+2012)

The calculation of *NEE* outside the measurement periods at Fort Logan (Jan-Feb 2011+2012; Dec 2011) is based on the relation of soil temperature and nighttime *NEE* at Fort Logan in 2011 (Fig. A.1). Nighttime *NEE* was defined by shortwave radiation (R_s< 10 W/m2) and Foken QC criteria (only QC=1). Soil temperature for the missing months was calculated based on a regression between soil temperatures at Fort Logan and Rocky Flats in 2011.

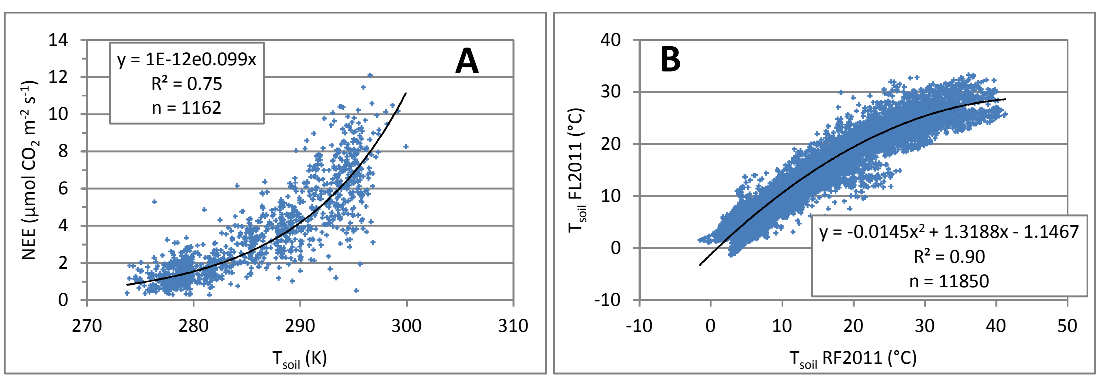

Fig. A.1: (**A**) Relation between soil temperature and nighttime NEE at Fort Logan in 2011 (data: FL 2011; nighttime NEE when Rs<10 W m^{-2}; only Foken QC =1 (Foken et al., 2004)) and (**B**) Relation between soil temperature at Rocky Flats (2011) and soil temperature at Fort Logan (2011)

A3 – Comparison of energy balance closure at Fort Logan and Rocky Flats using 24-hour averages

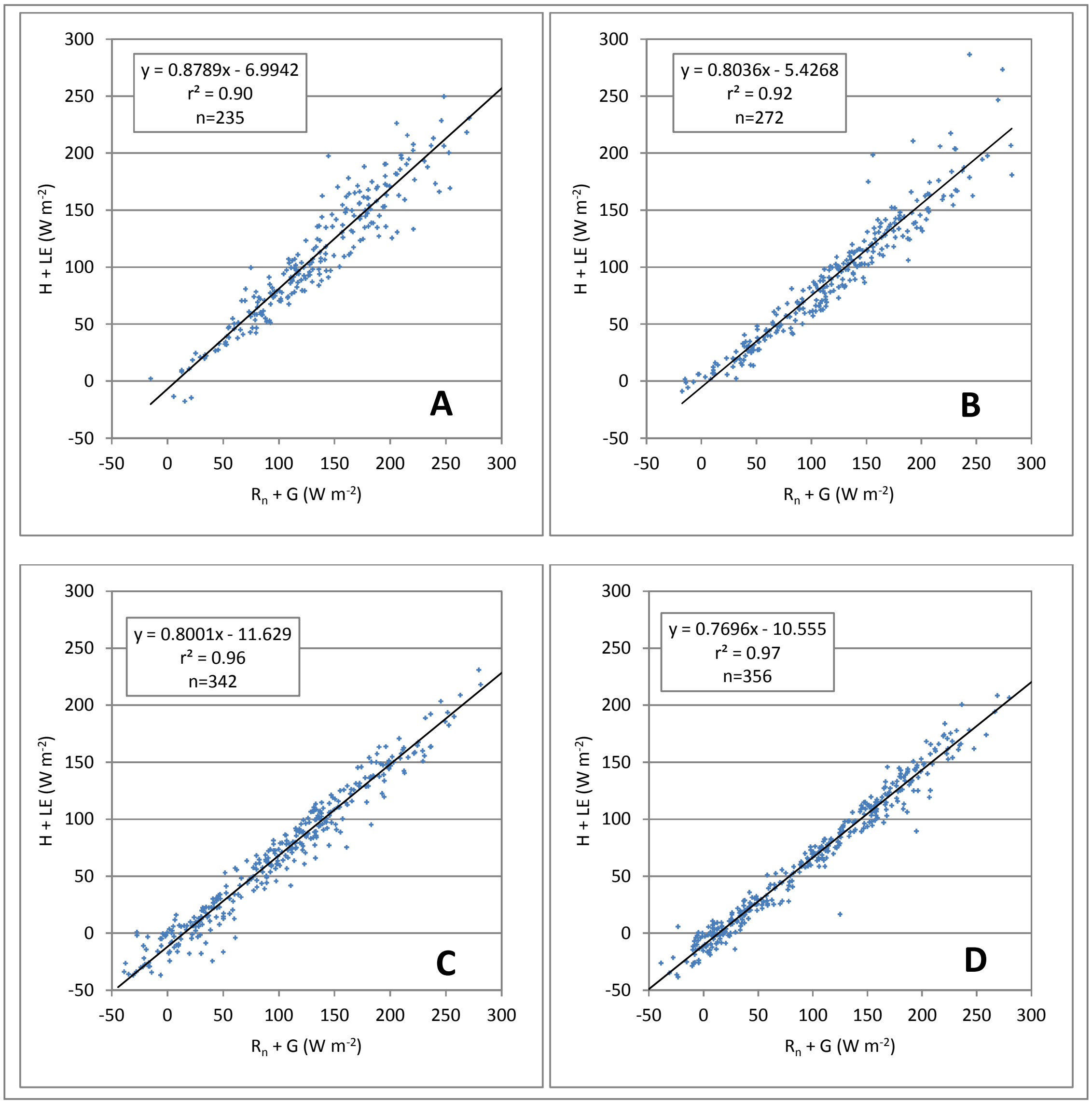

Fig. A.2: Comparison of energy balance closure for Fort Logan and Rocky Flats (2011 + 2012). Valid data (24 hour averages) of net radiation (Rn; W m^{-2}) and soil heat flux at the soil surface (G; W m^{-2}) is plotted against latent (LE; W m^{-2}) and sensible heat (H; W m^{-2}) flux. Black line represents the regression line (OLS). (**A**) Fort Logan 2011, (**B**) Fort Logan 2012, (**C**) Rocky Flats 2011, (**D**) Rocky Flats 2012

LEBENSLAUF

Persönliche Daten:

Thomas Sebastian Thienelt
geb. am 20.04. 1979 in Halle/Saale

Ausbildungsgang:

01/2013-12/2014	Hilfswissenschaftler am Institut für Geowissenschaften und Geographie, Martin-Luther-Universität Halle-Wittenberg
09/2010- 12/2012	Forschungsaufenthalt beim USGS in Denver (USA) (Förderung durch ein Promotionsstipendium des DAAD)
09/2007-07/2010	Hilfswissenschaftler/Projektmitarbeiter am Institut für Geowissenschaften und Geographie, Martin-Luther-Universität Halle-Wittenberg
07/2007	Verteidigung der Diplomarbeit – „Greenhouse Gas Fluxes from Urban Lawns to the Atmosphere in Denver, Colorado“
08-12/2005	Austauschsemester an der Humboldt State University (Kalifornien/USA)
2004/2005	Praktika (April-Juli) beim USGS in Denver (USA)
1999-2007	Geographie-Studium an der Martin-Luther-Universität Halle-Wittenberg, Spezialisierung Physische Geographie/Geoökologie
1998	Abitur am Albert-Schweitzer-Gymnasium (Halle/Saale)

Halle/Saale, den 5.12. 2014

Eidesstattliche Erklärung

Ich erkläre an Eides statt, dass ich die Arbeit selbstständig und ohne fremde Hilfe verfasst, keine anderen als die von mir angegebenen Quellen und Hilfsmittel benutzt und die den benutzten Werken wörtlich oder inhaltlich entnommenen Stellen als solche kenntlich gemacht habe.

Datum Unterschrift des Antragstellers